SYNTHESIS AND CHARACTERISATION OF VINYL BLOCK COPOLYMERS

MONALI ROY

Doctor of Philosophy

THE UNIVERSITY OF ASTON IN BIRMINGHAM

December 1995

THE UNIVERSITY OF ASTON IN BIRMINGHAM

SYNTHESIS AND CHARACTERISATION OF VINYL BLOCK COPOLYMERS

MONALI ROY

DOCTOR OF PHILOSOPHY

1995

SUMMARY

A study has been made of the anionic polymerization of methyl methacrylate using butyllithium and polystyryl lithium as initiators and the effects of lithium chloride and aluminium alkyls on the molecular weight and molecular weight distributions. Diblock copolymers of styrene-*b*-methyl methacrylate were synthesized at -78°C in THF in the presence of lithium chloride, and at ambient temperatures in toluene in the presence of aluminium alkyls.

Studies in the presence of lithium chloride showed that the polymerization was difficult to control; there was no conclusive evidence of a living system and the polydispersity indices were between 1.5 and 3. However, using relatively apolar solvents, in the presence of aluminium alkyls, homopolymerization of methyl methacrylate showed characteristics of a living polymerization. An investigation of the effects of the structures of the lithium and aluminium alkyls on the efficiency of initiation showed that a *t*-butyllithium/triisobutylaluminium initiating system exhibited an efficiency of 80%, compared with lower efficiencies (typically 30%) for systems based on butyllithium/triethylaluminium. The polydispersity index was found to decrease from ~2.2 to ~1.5 when butyllithium was replaced by *t*-butyllithium. The efficiency of the initiator was found to be solely dependent on the size of the alkyl group on the aluminium component, whereas the polydispersity index was found to be solely dependent on the size of the alkyl group on the lithium component. The aluminium alkyl is thought to be coordinated to the ester carbonyl groups of both the monomer and polymer. There is a critical degree of polymerization, at which point the rate of polymerization decreases, which probably relates to a change in structure of the active chain end.

Characterisation of poly(styrene)-*b*-poly(4-vinylpyridine) and poly(styrene)-*b*-poly(4-vinylpyridine methyl iodide) diblock copolymers using static light scattering techniques, showed the formation of star-shaped 'reverse' micelles when placed in toluene. Temperature effects on micellization behaviour are only exhibited for the unquaternised micelles, which showed characterisically lower aggregation numbers than their quaternised counterparts. A suitable solvent was not obtained for characterisation of the styrene-*b*-methyl methacrylate diblock copolymers synthesized.

Key words: Living anionic polymerization, Lithium alkyls, Aluminium alkyls, Methyl methacrylate, Styrene

To my parents, with love

ACKNOWLEDGEMENTS

I wish to thank Dr. Allan Amass most sincerely for his guidance, patient supervision and continuous support and encouragement for the duration of this project.

I would like to extend my gratitude to Dr. Adi Eisenberg of McGill University, for inviting me to his laboratory and for the supervision of the work concerning the light scattering studies of diblock copolymer micelles.

Thanks are also due to Miss Karine Khoughaz of McGill University, for all her assistance regarding the project and Dr. Xing-Fu Zhong of McGill University, for the synthesis of the block copolymer samples used in the light scattering studies. I also wish to thank all members of Dr. Eisenberg's research group for welcoming me into their lab and making my visit such a pleasant and memorable one.

I wish to thank EPSRC for providing me with financial support for the research carried out and also Aston University, for awarding me the James Watt Travelling Fellowship which funded my visit to McGill University in Montreal.

I am eternally grateful to all the technical and support staff at Aston University : namely Dr. Mike Perry, for running those never-ending NMR samples; Steve Ludlow, for ordering the chemicals; Mike and Denise, for their assistance in the analytical laboratory and Roger, for fixing all the vacuum pumps!

I wish to say a big "thank-you" to my friends and colleagues for all their support and for "putting up" with me over the last few years : Val, Luke, Wendy, Fred, Karine Robert, Monique, Babs, Mike, Mark, Phil and Andy.

I would like to thank my friends and flatmates Syrah, Sarah, Udkhar and Louise for keeping me sane during the writing-up period of this thesis!

I wish to thank Sujoy for his love, understanding and words of encouragement.

Last, but by no means least, I wish to thank my parents for always being there and for all their support and advice over the last few years.

LIST OF CONTENTS

LIST OF FIGURES

CHAPTER THREE

CHAPTER FOUR

CHAPTER SIX

LIST OF TABLES

CHAPTER FIVE

CHAPTER SIX

LIST OF SCHEMES

CHAPTER FOUR

CHAPTER SIX

LIST OF ABBREVIATIONS

MMA	Methyl Methacrylate
PMMA	Poly(Methyl Methacrylate)
TBA	*tert*-Butyl Acrylate
TBMA	*tert*-Butyl Methacrylate
Sty	Styrene
PS	Poly(styrene)
VP	Vinyl Pyridine
P4VP	Poly(4-Vinyl Pyridine)
P4VPMeI	Poly(4-Vinyl Pyridine Methyl Iodide)
PTFE	Poly(Tetrafluoroethylene)
PS^-Li^+	Polystyryl Lithium
BuLi	Butyllithium
s-BuLi	*sec*-Butyllithium
t-BuLi	*tert*-Butyllithium
RLi	Lithium Alkyls
LiCl	Lithium Chloride
DPE	Diphenylethylene
$AlEt_3$	Triethylaluminium
$Al(^iBu)_3$	Triisobutylaluminium
THF	Tetrahydrofuran
DMF	N,N Dimethylformamide
Hg	Mercury
$\overline{DP}_n$, $(\overline{DP})$	Number Average Degree of Polymerization
R_p	Rate of Polymerization
k_i	Rate Constant for Initiation
k_p	Rate Constant for Propagation

$\overline{M}_n$	Number Average Molecular Weight
$\overline{M}_w$	Weight Average Molecular Weight
MW	Molecular Weight
MWD	Molecular Weight Distribution
PDI	Polydispersity Index
LE	Living Ends
N_{agg}	Aggregation Number
R_g	Radius of Gyration
A_2	Second Virial Coefficient
dn/dc	Specific Refractive Index Increment
$R(\theta)$	Rayleigh Ratio
$P(\theta)$	Particle Scattering Function
Zd	Dissymmetry Ratio
cmc	Critical Micelle Concentration
SEC	Size Exclusion Chromatography
GPC	Gel Permeation Chromatography
SLS	Static Light Scattering
DLS	Dynamic Light Scattering
SAXS	Small Angle X-ray Scattering
TEM	Transmission Electron Microscopy
R.I	Refractive Index
UV	Ultraviolet
GC	Gas Chromatography
IR	Infrared Spectroscopy
NMR	Nuclear Magnetic Resonance Spectroscopy
(w)	Weak
(m)	Medium
(s)	Strong
δ	Chemical Shift

CHAPTER ONE

INTRODUCTION

1.1 Scope of the Work

The anionic polymerization of vinyl monomers has been well documented since the 1950's[1-12]. The vast interest in this area is largely attributable to the fact that polymers with well defined molecular architectures and narrow molecular weight distributions can be obtained. Anionic polymerization differs from other polymerization systems in that, under suitable conditions it lacks a termination or transfer step. This type of polymerization was first described by Szwarc[1-4] as a "living" system and can give rise to the synthesis of functionally terminated polymers, branched polymers and block copolymers.

Living anionic polymerization is a powerful pathway to the formation of block copolymers, whereby the length of the blocks can be controlled in a predictable way. These copolymers are one of the most important industrial products synthesised using anionic polymerization techniques. Block copolymers can be used for the production of thermoplastic elastomers, which depend for their behaviour on the separation of islands of the plastic, in a continous elastomeric phase. e.g. styrene-butadiene block copolymers are used as hot melt adhesives. These materials are also largely used for the production of paints, sponges, films, surgical sutures, dialysis membranes and prosthetic materials as well as for structural applications[7]. The optical qualities of poly(styrene) and the poly(methacrylates) make these materials particularly invaluable in the contact lens industry, where transparency is a premium. Biomedical and pharmaceutical applications of amphiphilic block copolymers in solution are particularly useful in drug delivery systems whereby they act as solubilisers, dispersants and emulsifying agents.

This chapter aims to discuss the principles of anionic polymerization, and review some of the previous work carried out in the area, particularly with regard to styrene and methyl methacrylate. There are numerous problems encountered when generating 'living'

polymers of methacrylates and acrylates, which are tackled during the course of this investigation.

1.2 General Principles of Polymerization

The modern concept of linear polymers was introduced in 1920 by Staudinger[13] , who fully recognised the idea of chain addition reaction yielding long molecules composed of monomeric units linked by covalent bonds. He was also the first to understand the anionic character of formaldehyde polymerization initiated by bases such as sodium methoxide.

In 1929, Carothers[14] subdivided polymers into two main groups :-

(i) Polymers prepared by the stepwise reaction of monomers ie Condensation Polymers, characteristically formed by reactions involving the elimination of a small molecule such as water at each step.

(ii) Polymers prepared from chain reactions, i.e. Addition Polymers, where no such loss of a molecule occurred.

In later years, it became apparent that a more adequate definition would be based on a description of the chain growth mechanism, thus the term 'Condensation Polymerization' was replaced by 'Step Growth Polymerization'. Whereas in step growth polymerization reactions it is often necessary to use multifunctional monomers if polymers with high molecular weights are to be formed, in addition reactions, long chains are readily obtained from monomers such as vinylidine compounds with the general structure $CH_2=CR_1R_2$. These monomers are such that the reactivity of π bonds in the carbon-carbon double bond makes them susceptible to rearrangement if activated by free radical or ionic initiators. The active centre created by this reaction then propagates in a kinetic chain, leading to the formation of a single macromolecule, where growth is stopped when the active centre is neutralised by a termination reaction. The polymerization proceeds in three stages :-

(i) Initiation , where the active centre which acts as a chain carrier is created.

(ii) Propagation, whereby the macromolecular chain grows by a kinetic chain mechanism involving the repeated addition of a monomer to a growing chain.

(iii) Termination, where the kinetic chain is brought to a halt by neutralisation or transfer of the active centre.

Typically, the polymer formed has the same chemical composition as the monomer i.e. each unit in the chain is a complete monomer and not a residue as in most step growth reactions, except for the presence of any end groups introduced during initiation or transfer.

1.2.1 Nature of the Monomer and Choice of Initiator

There are a variety of initiators available which fall into the general categories: free radical, cationic and anionic. The choice of the one used depends on the groups R_1 and R_2 in the monomer and their effect on the double bond, ie the π-bond reacts differently with each initiator species to produce either heterolytic (a), or homolytic (b) fission :

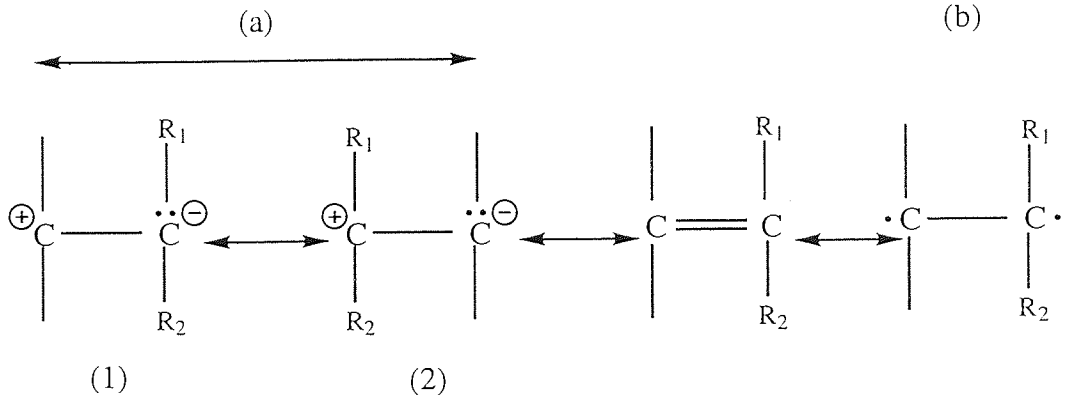

In most monomers either R_1 or R_2 is classified as an electron withdrawing (1) or an electron donating (2) group. The negativity of the π electron cloud is altered which determines whether or not a radical, an anion or cation will be stabilised preferentially.

Electron withdrawing substituents e.g. -COOR, -CN reduce the electron density in the double bond and favour propagation by an anionic species. Electron donating substituents, which increase the nucleophilicity of the double bond, encourage attack by cationic initiators. In addition the active centres that are formed are stabilised, by either inductive or resonance effects. Monomers such as styrene and 1,3 butadiene can undergo

polymerization by both types of ionic method since both the anionic and cationic species is resonance stabilised. Because of its electrical neutrality, the free radical is a less selective initiator since most substituents can provide some (resonance) stabilisation for this propagating species.

1.3 An Introduction to Anionic Polymerization

Anionic polymerization occurs amongst monomers with electron withdrawing substituents e.g. -CN, -COOH, -CH=CH_2 etc. to promote the formation of a stable carbanion which is enhanced when there is a combination of inductive and mesomeric effects.

The polymerization of monomers with strongly electronegative groups e.g. methyl methacrylate and styrene, can be initiated by either of the following mechanisms :-

$$M + I^{\ominus} \longrightarrow M^{\ominus} I \qquad (1) \text{ anionic}$$

$$M + e^{\ominus} \longrightarrow \cdot M^{\ominus} \qquad (2) \text{ radical anionic}$$

where M is the monomer

and $I^{\ominus}$ is the initiator

In (1) an ionic or ionogenic molecule is required, capable of adding the anion to a vinyl double bond and creating a carbanion :-

$$CX \longrightarrow C^{\oplus} + X^{\ominus} \qquad (3)$$

$$X^{\ominus} + M \longrightarrow M^{\ominus} X \qquad (4)$$

where CX is ionic molecule e.g.BuLi

and $C^{\oplus}$ is the counterion e.g. $Li^{\oplus}$

The counterion may be inorganic or organic and typical initiators include butyllithium, KNH_2 and Grignard reagents. If the monomer has a strong electron withdrawing group, only a weakly electropositive initiator e.g. a Grignard will be required for polymerization

but when the side group is phenyl or the electronegativity is low, a highly electropositive metal initiator such as a lithium compound is required. For example, the initiation of styrene using butyllithium takes place via the mechanism shown in scheme 1.1.

Scheme 1.1 Initiation of Styrene Polymerization by Butyllithium.

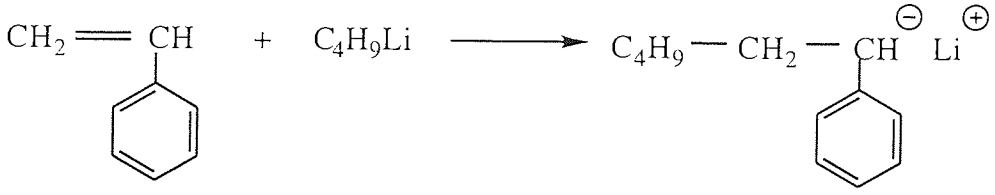

delocalisation of negative charge around benzene ring

In (2), an electron is transferred directly from a donor (such as an alkali metal) to the monomer to form a radical anion. For example, sodium or potassium can initiate the polymerization of methacrylonitrile in liquid ammonia at 198K[6] (as shown in scheme 1.2).

Scheme 1.2 Initiation of Methacrylonitrile Polymerization by Sodium

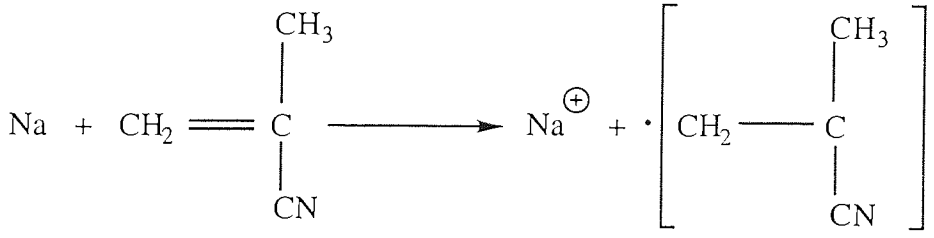

The polymerization of styrene initiated by potassium amide was one of the first anionic polymerizations to be studied in detail (see reaction scheme 1.3)[14]. The reaction is conducted at low temperature in liquid ammonia, which is a highly polar solvent. Potassium amide dissociates into its constituent ions and the anion formed adds to the carbon-carbon double bond, creating an propagating chain.

Scheme 1.3 Initiation of Styrene Polymerization by Potassium Amide.

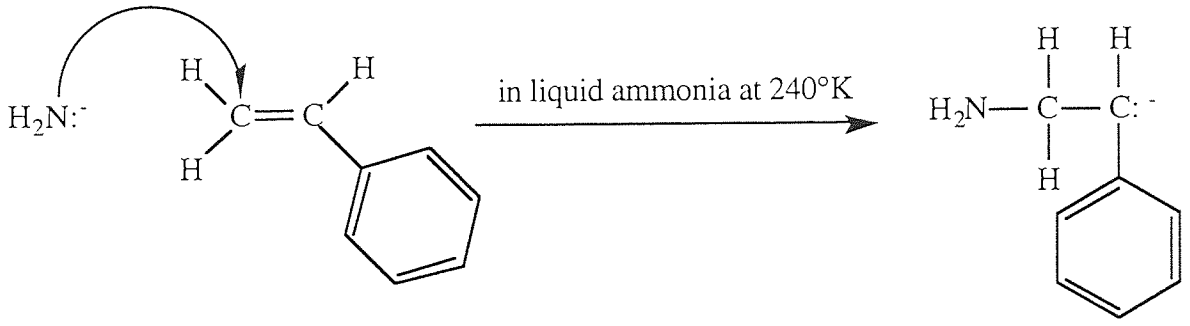

Anionic polymerizations generally proceed rapidly at low temperatures. Reaction rates depend on the dielectric constant of the solvent, the resonance stability of the carbanion, the electronegativity of the initiator and degree of solvation of the counterion. Many anionic polymerizations are devoid of termination reactions, but are sensitive to traces of impurities of water, alcohol, carbon dioxide and oxygen, which are effective terminating agents. Termination can also occur by transfer of a positive fragment, usually a proton from the solvent or some other transfer agent. Exclusion of these impurities from the system imposes the need for rigorous experimental conditions.

1.4 'Living' Polymerization Systems

Ziegler[15] first identified that anionic polymerizations have no intrinsic termination step. The absence of this stage in a polymerization mechanism has significant implications for the synthetic utility of such reactions. In 1956, Szwarc[4] conclusively demonstrated the lack of a termination step in anionic polymerization of vinyl monomers in the absence of impurities. The term "living polymers" was proposed for those macromolecules which may spontaneously resume their growth whenever fresh monomer is supplied to the system[1-3].

Szwarc and his associates investigated the polymerization of styrene initiated by sodium naphthalide. The initiator, a green solution, was formed by addition of sodium to naphthalene in 50 cm^3 of tetrahydrofuran.

Scheme 1.4 Formation of Sodium Naphthalide Initiator

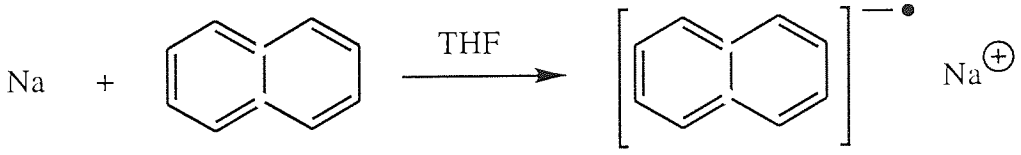

Highly delocalised radical anion
can react with monomer

The sodium dissolves to form a charge transfer complex, and, by transfer of an electron, produces the green naphthalide radical anion. Addition of styrene to the system leads to electron transfer from the naphthalide radical anion to the monomer to form a red styryl radical anion. The colour is produced as a result of delocalisation of π electrons around the benzene ring of the styryl anion, which absorb electromagnetic radiation in the visible range of the spectrum.

Scheme 1.5 Initiation of Styrene Polymerization by Sodium Naphthalide

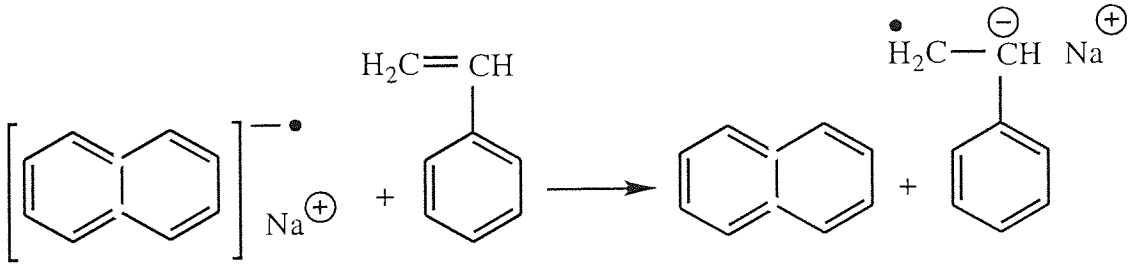

A dianion, which can propagate from both ends, is formed by combination of two styryl radicals (see scheme 1.6).

Scheme 1.6 Propagation of Styrene Polymerization Initiated by Sodium Naphthalide

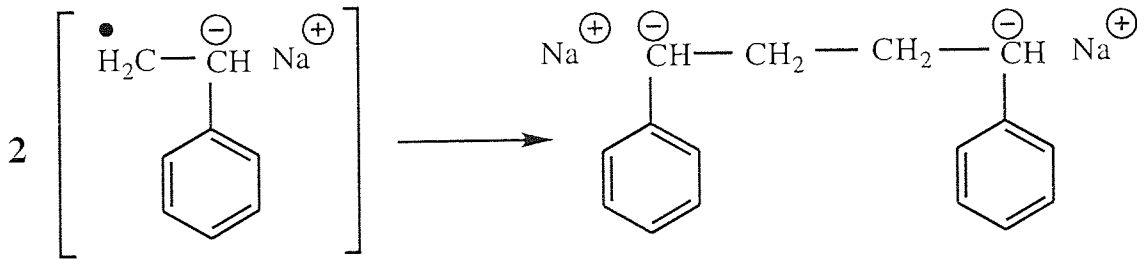

The reaction scheme has no formal termination step and, if all the impurities which can react with the carbanions are excluded from the system, propagation continues until the monomer concentration reaches its equilibrium value, leaving the carbanion intact and still active; this can be seen from the red colour which remains as an indication of the living polystyryl ends. Then if more monomer is introduced, the active centre would continue growing unless inadvertently terminated. Szwarc conclusively demonstrated that the molecular weight of the polymer formed in the first stage of the experiment increased upon addition of fresh styrene. Szwarc also demonstrated the ability to form block copolymers in such systems by addition of isoprene to the living polystyryl ends, resulting in the formation of poly(styrene)-*b*-poly(isoprene). The absence of termination and transfer reactions means that if no accidental termination by impurity occurs the chains will remain active indefinitely.

Living polymers do not become infinitely long because the system contains a specified concentration of active centres, or living polymers, and consequently all of the available monomer becomes partitioned among them. Hence, the number average degree of polymerization ($\overline{DP_n}$), is given by the ratio :

$$\overline{DP_n} = \frac{[M]_o - [M]_t}{[I]_o}$$

where $[M]_o$ = Initial concentration of monomer

$[M]_t$ = Concentration of monomer at time t

and $[I]_o$ = Initial concentration of initiator

The resulting polymers have a Poisson molecular weight distribution provided that propagation is irreversible, the polymerized solution, or melt, remains homogeneous during the whole course of the polymerization, the termination and transfer reactions are rigorously excluded and the rate of initiation is faster than, or at least equal to the rate of

propagation. Although all these conditions are beneficial and desired, they are not necessarily demanded for achieving a living system.

The lack of spontaneous termination in living systems does not imply immortality, since the reactive end groups of living polymers may be annihilated by suitable reagents, known as "killing" of living polymers. This technique enables the introduction of valuable functional end-groups e.g. -OH and -COOH groups into macromolecules to give novel and interesting products for a wider range of applications.

Ideally, living polymers should retain their activities forever provided they are not terminated by addition of terminating reagents. However, in any real system this is not the case. Some feasible slow side reactions which annihilate the growing ends are unavoidable and set an upper limit on the durability of living polymers. Nevertheless, if the rates of these reactions are sufficiently slow to permit successful completion of an intended synthesis or desired task, the system may be classified as a living system.

The shelftime of living polymers is believed to be very long. Further studies of ionic polymerization have revealed that several interconvertible species participate in most of the ionic reactions e.g. free ions, ion-pairs and their aggregates[16] . These species co-exist in equilibrium with each other and if their interconversion is fast, their equilibria is not perturbed by propagation. Some of these species are dormant and may not propagate the polymerization but their interconversion with the active species allows them to grow. This type of polymerization is said to be living when none of the participating species induces termination or chain transfer.

Hence, the nature of the monomer, the conditions prevailing in the polymerization system and the presence of impurities determine the lifetime of living polymers. Living polymers tend to decay more slowly at lower temperatures and indeed some living polymers have to be kept at low temperatures all the time to prevent their decomposition during preparation and storage. For most systems dilution of living polymers is detrimental to their stability since the ratio of concentrations of the damaging impurities present in the solvent, to the concentration of living polymer ends increases on dilution[11]. Dilution also affects the

degree of aggregation and species of lower degrees of aggregation are more reactive and therefore more susceptible to destruction by solvent, impurities or side reactions.

The proportionality of the number-average molecular weight, $\overline{M}_n$, to the degree of conversion was generally thought of as sufficient evidence for the "livingness" of a polymerization[16] . However, Penczek *et al*[17] stated that this, whilst proving the absence of chain transfer during propagation, does not exclude the occurrence of termination. Nevertheless, such behaviour taken together with narrowness of molecular weight distribution of these polymers, is generally regarded as satisfactory evidence for the living character of a polymerization, especially when the polydispersity decreases with conversion.

1.5 Solvent and Counterion Effects

Both the solvent and the counterion have a pronounced influence on the rates of anionic polymerizations[1-3,5,6]. Unlike free-radical polymerizations, when the dielectric constant of the solvent has little effect on the structure of the chain end and hence the rate of propagation, in an anionic polymerization, the propagating chains may exist in a number of forms, ranging from aggregated molecules to free solvated ions, (see figure 1.1). In a polar solvent (e.g. tetrahydrofuran, dielectric constant = 7.6) the equilibrium is shifted toward the right, favouring dissociated species. In a non-polar solvent (e.g. hexane, dielectric constant = 1.9) the formation of close contact ion pairs and aggregates of covalent structures is favoured (e.g. butyllithium is thought to be hexameric in hexane)[1].

Figure 1.1 Effect of Solvent Polarity on Nature of Propagating Species.

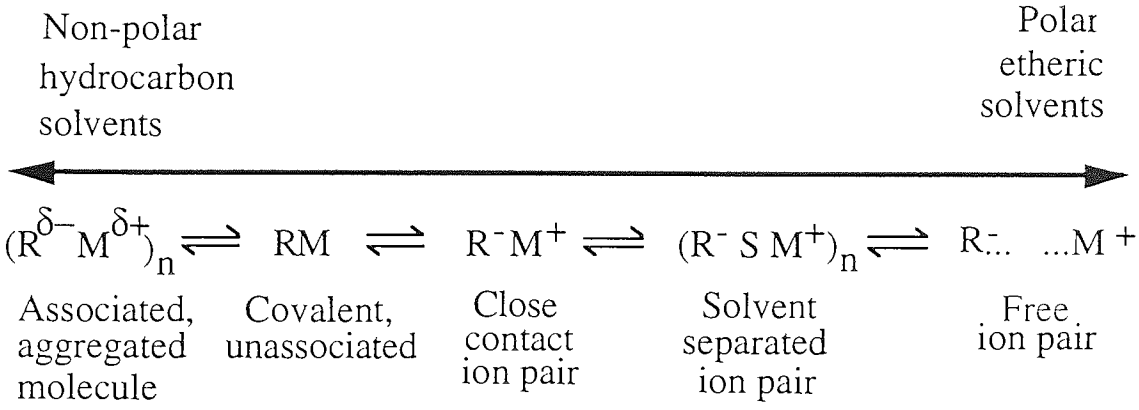

Free ions tend to react with the monomer much faster than the corresponding ion pairs and covalent structures, so that the rate of propagation depends upon the nature of the solvent used. When interconversion between the contact ion pairs, solvent-separated ion pairs and free ions is very rapid, each propagating chain exists in all forms at different times during the polymerizaton, which results in an 'averaging-out' of the rate of propagation for each species and the production of narrow molecular weight distribution polymer.

Generally, if non-polar hydrocarbon solvents are used, solvation does not occur, the equilibrium lies towards contact ion pairs and in some cases the bonding may even be covalent, with the initiator species and/or propagating ends existing as aggregates. Initiation may be very slow in these cases resulting in a steady increase in the concentration of living ends. The polymer product may exhibit a fairly broad molecular weight distribution. With solvents of low dielectric constant containing donor molecules, e.g. ethers and amines, the equilibrium lies towards solvent separated ion pairs which are still in close proximity even though the cation or anion can be solvated. In this case initiation is faster than that for hydrocarbon solvents and polymers with narrower molecular weight distributions are produced. With solvents of high dielectric constant containing donor molecules, e.g. THF, the equilibrium lies between solvent separated ion pairs and free ions. Initiation is rapid in this case, and polymers with narrow molecular weight distributions are produced.

The influence of the counterion on the polymerization of styrene in THF at 298 K[1,2] is shown in figure 1.2. The smaller Li^+ ions can be solvated to a greater extent than the larger ions (K^+ and Cs^+), and the decreasing rate with increase in counterion size reflects the increasing tendency for ion pairs to be the active species, rather than free ions, since the solvating power of the solvent deteriorates.

Figure 1.2 Effect of Change in Counterion on the Polymerization of Styrene in THF at 298K

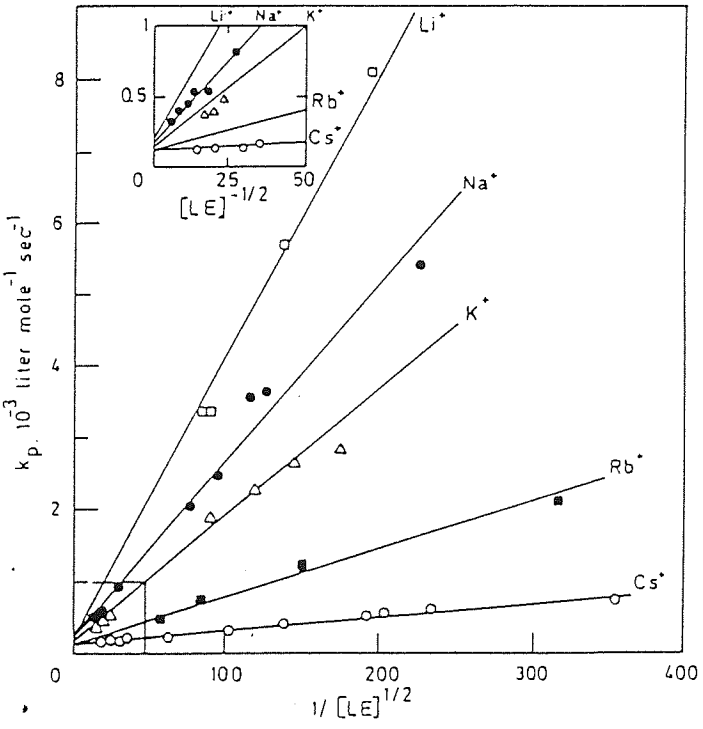

The nature of the solvent has a great effect on the structure of the propagating centre and thus has an effect on k_p. The polymerization rate increases with increasing polarity of solvent eg. k_p = 2.0 $dm^3\ mol^{-1}\ s^{-1}$ for the anionic polymerization of styrene in benzene, but, k_p = 3800 $dm^3\ mol^{-1}\ s^{-1}$ when the solvent is 1,2, dimethoxyethane. In solvents of higher dielectric constant, only an apparent propagation constant (k_p^{app}), which increases as the active centre concentration is decreased, can be obtained. This effect is caused by the increasing importance of the dissociation of ion pairs to the more reactive free ions upon dilution. The apparent k_p for low degrees of ionization is given by :

$$k_p^{app} = k_p^{\pm} + \frac{k_p^{-}\ K_{diss}^{1/2}}{[\text{active centres}]^{1/2}}$$

where $k_p^{\pm}$ = propagation rate constant of ion pairs

and k_p^{-} = propagation rate constant of free ions

If k_p^{app} is plotted against [active centres]$^{1/2}$ the intercept gives $k_p^{\pm}$ directly and the slope gives $k_p^{-}\ K_{diss}^{1/2}$. If the ionic dissociation constant (K_{diss}) is known, then k_p^{-} can be evaluated. Some representative values[1,18] are shown in table 1.1

Table 1.1. Typical Ion Pair ($k_p^{\pm}$) and Free Anion (k_p^{-}) Propagation Constants of Some Vinyl Monomers ($M^{-1}S^{-1}$)

	$k_p^{\pm}$ For Counter-ion				k_p^{-}
Monomer-Solvent	Li^+	Na^+	K^+	Cs^+	Free Anion
styrene-THF, 25°C	160	180	~60	22	6.5×10^4
styrene-dioxane, 25°C	0.9	3.4	20	24.5	
2-vinylpyridine-THF, 25°C		2.1×10^3		1.5×10^3 (15°C)	~10^5
methyl methacrylate-THF, -98°C	~1	32	~30	33	2×10^3

For comparitive purposes, $k_p^{+/-}$ of methyl methacrylate would be approximately 1700 (Li^+), 5600 (Na^+), and 7600 (Cs^+) at 25°C if the polymerizations were to be carried out at this temperature.

Although the degree of ionization is very low in all cases, the presence of very small quantities of free anions is very important because of their extremely high reactivity. However, increased polymerization rate is caused not only by free anions. In solvents such as THF, $k_p^{+/-}$ is much higher than in dioxane, because a fraction of the ion pairs (at least for Li^+ and Na^+) is converted into solvent separated ion pairs, which have a reactivity approaching that of free anions. Curious increases in rate can also occur under certain conditions as the temperature is decreased. These changes require the presence of different types of ion pairs; their proportions changing with temperature.

1.6 The Polymerization of Styrene Initiated by Lithium Alkyls

The simplest of all the anionic initiators are the alkali-metal alkyls. The properties of lithium alkyls have been studied extensively and indicate a rather complex behaviour[1,2]. Some of the other initiators include fluorenyl, cyclopentadienyl and benzylic derivatives of the alkali metals. Grignard reagents have been used for the initiation of monomers containing a strong electron withdrawing group.

1.6.1 The Structure of Lithium Alkyls

Lithium alkyls are an important and frequently used class of anionic initiators. They exhibit rather unusual features which arise from the small size of the lithium cation, its high electronegativity, and the availability of empty, low-energy *p*-orbitals[1,2] . Lithium alkyls exist as aggregates in the solid and liquid state, mostly as tetramers or hexamers, in even the most dilute solutions or highly rarified vapour. This high degree of aggregation accounts for their high volatility, e.g. the vapour pressure of butyllithium is 10^{-4} Torr at 60°C. The lithium atoms form the kernels of the aggregates, while the shell surrounding

them consist of alkyl moieties. This structure enables them to be soluble in hydrocarbon solvents.

Colligative properties of solutions of alkyl lithiums show that aggregates of butyllithium and ethyllithium are hexameric in hydrocarbons, but tetrameric in diethyl ether[19-21], whereas a mixture of dimers and tetramers of BuLi is formed in THF. In hydrocarbon solvents and ethers, both *sec*-BuLi and *tert*-BuLi are found to be tetrameric[22,23]. Hence, the degree of aggregation varies with the nature of the alkyl group and the solvent. As a general rule, the degree of aggregation decreases with increasing bulkiness of the alkyl group and increasing polarity of the solvent. Dilution of hydrocarbon solutions of alkyl lithiums has no effect on their degree of aggregation, implying that each alkyl lithium forms one kind of aggregate only in this medium.

Arylmethyl lithiums exhibit lower degrees of aggregation e.g. polystyryl lithium is dimeric in hydrocarbons. It would appear that the C-Li bond is more ionic than that of the alkyl lithiums, although the ^{13}C NMR spectrum indicates sp^3 hybridization of the benzylic carbon atom.

The Li-C bonds of the monomeric gaseous alkyl lithium molecules are thought to be ionic in nature. The structures of the aggregates are governed by their electron deficiency, whereby the number of bonding orbitals exceeds that of the available valence electrons. The X-ray crystallography studies of methyllithium tetramers investigated by Weis[24] show the structure to be tetrahedral in shape (see figure 1.3). The four lithium atoms form a tight tetrahedrally shaped core with the methyl groups placed above the respective faces of a tetrahedron.

Figure 1.3 Tetrahedral Structure of Methyllithium

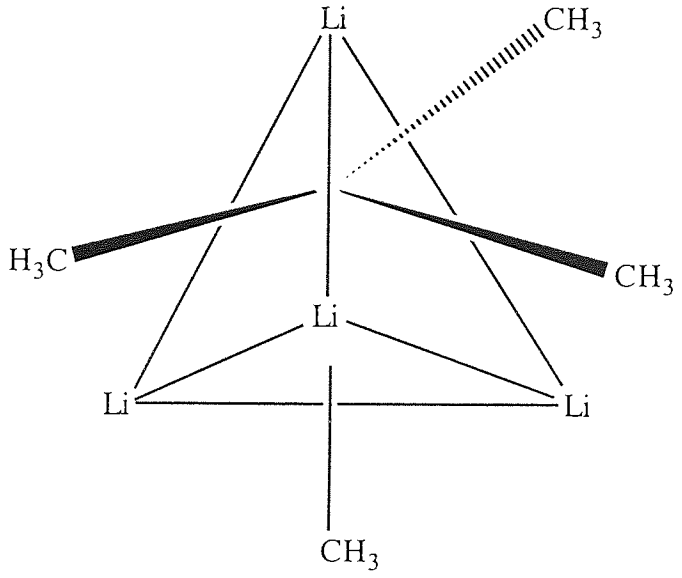

The Li-Li bond length of 2.5 Å, is shorter than the length of the Li-Li bond of the Li_2 molecule (2.67 Å). Each lithium atom donates 3 *p*-orbitals to the binding of the aggregate and is associated with the carbon atoms of three methyl groups; each methyl group contributing a single sp^3 orbital is linked to three Li atoms. A similar structure is attributed to tetrameric ethyllithium and *t*-butyllithium, whereas a more complex structure involving Li-C bonds as well as hydrogen bridges was proposed for the hexamers (see figure 1.4).

Figure 1.4. Hexameric Structure of Butyllithium

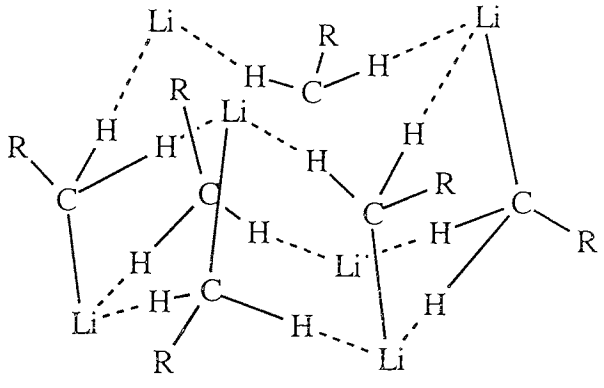

The higher aggregates of lithium alkyls can dissociate in certain solvents to form mixed aggregates.

1.6.2 Initiation

Lithium alkyls are extremely reactive and versatile reagents. They react rapidly with oxygen, carbon dioxide, water, alcohols etc.[1,2,7].

Scheme 1.7 Some Reactions of Lithium Alkyls

$$RLi + O_2 \longrightarrow ROOLi \xrightarrow{RLi} 2ROLi$$

$$RLi + CO_2 \longrightarrow RC(O)OLi$$

$$RLi + H_2O \longrightarrow RH + LiOH$$

$$RLi + R'OH \longrightarrow RH + R'OLi$$

Alkyl lithiums also readily react with C=C double bonds, especially those of styrene, the conjugated dienes and their derivatives, to initiate their anionic polymerization. However, such addition is slow compared to the rates of the reactions of alkyl lithiums described in scheme 1.7 ; hence the monomers and solvents have to be purged from all traces of these compounds when alkyl lithiums are used as their initiators.

The lithium alkyl-initiated polymerization of styrene in hydrocarbon solvents has received much attention[12,25]. This system shows the simplest behaviour, whereby only chain initiation and propagation is important at ambient temperatures. Rates of chain initiation depend on the type of solvent employed i.e. aliphatic or aromatic, and on the nature of the alkyl group attached to the lithium.

Anionic polymerization of styrene, the dienes and their derivatives initiated by alkyl lithiums in hydrocarbon solvents was first studied by Ziegler[15] and subsequently by many other investigators. Worsfold and Bywater[23] , investigated the initiation and propagation of the polymerization by studying spectroscopically the polymerization of styrene initiated by butyllithium in benzene. Initiation produces the lithium salt of polystyryl carbanions that absorb light at λ_{max} = 334 nm. The polymers produced were found to be living; the absorbance at 334-nm increasing monotonically as the reaction proceeded, and asymptotically reached a constant value as shown by curve B figure 1.5. The

consumption of styrene was monitored by its absorbance at 291nm, which decays continuously to zero as shown by curve A figure 1.5.

The initial slope of curve B shown in figure 1.5 measures the early rate of initiation (R_i). The plot of $\log(R_i / [\text{styrene}]_0)$ as a function of $\log[\text{BuLi}]_0$, given in figure 1.6, is linear for $[\text{BuLi}]_0 > \sim 10^{-4}$ M, implying that the concentration of active species at the early stages of the reaction is proportional to $[\text{BuLi}]^{\alpha}$, α being the slope of the line shown in figure 1.6. α was found to be 1/6 and since BuLi was found to be hexameric in benzene, it was proposed that the monomeric BuLi, present at equilibrium with the hexamers, was the initiating species. The rate of polymerization was then given by :

$$-d[\text{styrene}]/dt = k_p.(K_{diss} / 6)^{1/6} [\text{styrene}].[\text{BuLi}]^{1/6}$$

where k_p = rate constant of addition of monomeric BuLi to styrene

K_{diss} = Equilibrium constant of dissocation of hexamers into monomers.

The experimental results provide the constant $k_p.K_{diss}^{1/6}$. The proposed mechanism gains support from the results obtained with other alkyl lithium initiators. The polymerization of styrene or isoprene initiated by *sec*-butyllithium in benzene, is ten times faster than that of BuLi[26,27]. The initial rates of polymerization by *sec*-butyllithium are proportional to ~1/4 power of the initiator concentration, which can be attributable to the tetrameric aggregation of *sec*-butyllithium. Hence secondary or tertiary butyllithiums are used in preference to butyllithium or ethyllithiuim to achieve rapid initiation.

Figure 1.5 Typical Conversion Curves Recorded Spectrophotometrically for the Initiation of Styrene Polymerization in Benzene by Butyllithium

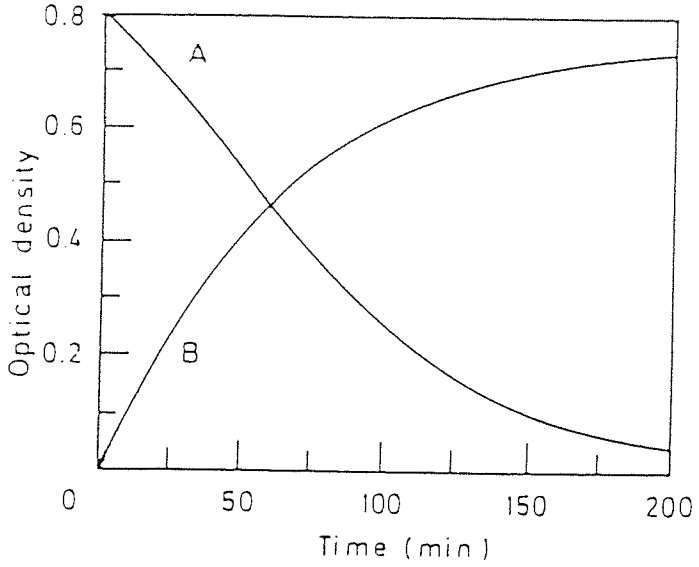

[styrene] = 1.4 x 10^{-2} M [BuLi] = 1.1 x 10^{-3}M

Figure 1.6 The Dependence of the Initial Rate of Styrene Polymerization in Benzene. Plot of $\log(R_i/[\text{styrene}]_0)$ as a Function of $\log([\text{BuLi}]_0)$

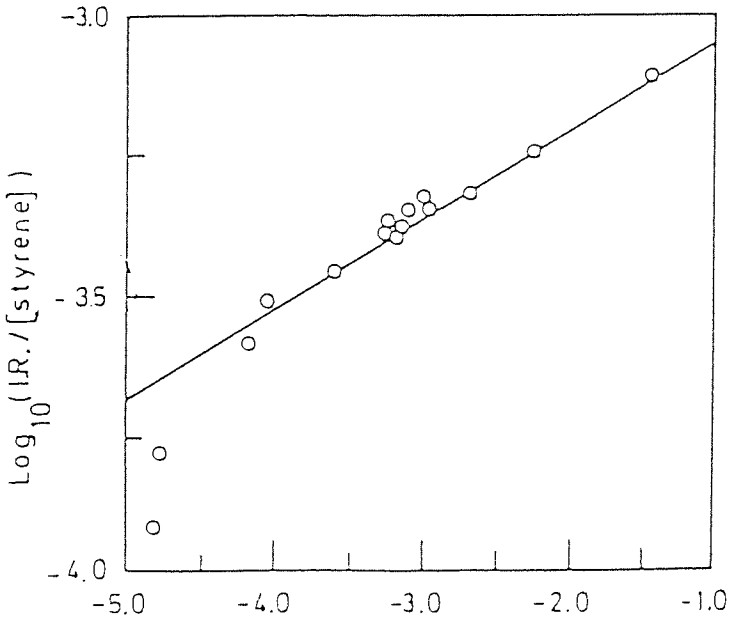

$\log[\text{BuLi}]_0$

The straight-chain lithium alkyls exhibit poor initiation under certain conditions in aliphatic solvents e.g. cyclohexane, leaving appreciable unreacted quantities of initiator after all the monomer has been consumed (see figure 1.7). There may be some contribution to this effect from intrinsic differences in reactivity, but it is likely that the steric factors are most important. The *sec.* and *tert.* isomers of butyllithiun are more bulky than the straight *n*-isomer, so aggregation of initiator molecules is inhibited and the equilibrium concentration of monomeric initiator increased. These straight chain alkyls can become efficient initiators in the presence of small amounts of polar materials e.g. ethers or lithium alkoxides[28]. This is because mixed aggregates formed in the presence of lithium alkoxides are more readily dissociated than the homoaggregates.

The initiation of styrene polymerization in benzene using *tert*-butyl lithium is unconventional. The rate was found to be proportional to the first power of *tert*-BuLi but independent of monomer concentration[29] . An explanation was later proposed whereby a rapid formation of the monomer-BuLi complex [(*t*-BuLi)$_4$ • M], undergoes an intramolecular rearrangement resulting in the formation of t-Bu • M$^-$Li$^+$ adduct :

$$(t\text{-BuLi})_4 \bullet M \longrightarrow (t\text{-Bu} \bullet M^-, Li^+) \bullet (t\text{-BuLi})_3$$

Hence the most convenient and preferred initiator for the polymerization of styrene and the dienes is *sec*-BuLi.

Figure 1.7 Percentage Conversion of the Different Structural Isomers of Butyllithium in the Initiation of Styrene Polymerization in Cyclohexane at 40°C

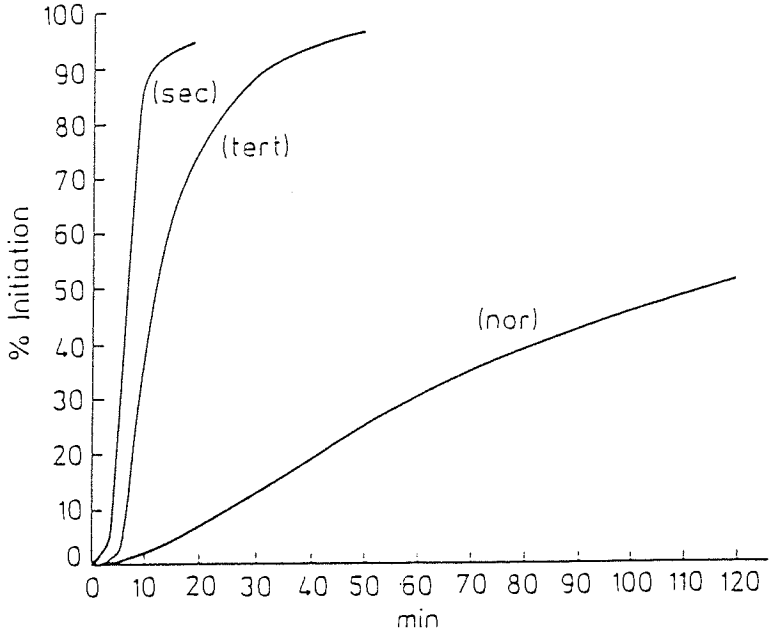

Figure 1.8 Rate of Formation of Polystyryl Anions as a Function of Time, Initiated by *sec*-Butyllithium

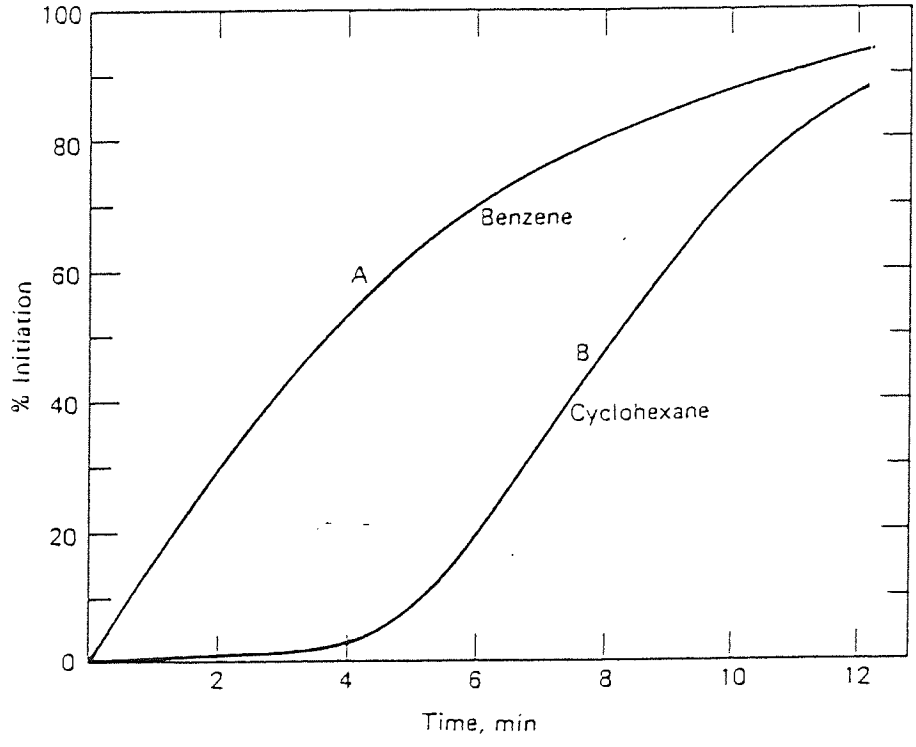

Curve A: [*s*-BuLi] = 1.1 x 10^{-3} M [styrene] = 5.3 x 10^{-4} M solvent benzene at 30°C

Curve B: [*s*-BuLi] = 1.3 x 10^{-3} M [styrene] = 8.7 x 10^{-2} M solvent cyclohexane at 40°C

Whereas in benzene the rate of polymerization decreases as the reactants are consumed, in cyclohexane or hexane the rate is slow initially and then rapidly accelerates, before the final concentration-induced decay occurs (see figure 1.8). Both types of behaviour appear to be connected to the fact that both the initiator and the growing chains are aggregated in hydrocarbon solvents. This fact adds to the complexity of the mechanism , because at various times mixed aggregates containing initiator and polymeric-lithium species exist, and the composition changes as the initiator is gradually depleted. These differently aggregated species can produce different initiation rates, and it can be shown by adding some preformed polymeric-initiator species to a monomer initiating system in cyclohexane that it is, in fact, mixed aggregates that produce the acceleration in rates after a period of time has elapsed. Whereas lithium alkyls $(RLi)_n$ on their own are thought not to be very reactive, their solvation in benzene causes an increase in reactivity possibly because of the dissociative mechanism :

$$(RLi)_n \rightleftharpoons n\,RLi \xrightarrow{+M} RMLi$$

where M = Monomer

Hence, the negligible dependence of the rate of polymerization on the concentration of initiator i.e.$[RLi]^{1/n}$, is in agreement with this hypothesis, which requires that aromatic solvents promote the dissociation process to more reactive forms by solvation.

At the beginning of polymerization, both initiation of new chains,and their propagation occur simultaneously. For a system which exhibits efficient initiation, initiation is complete at about 10-15% conversion of monomer to polymer. At this point the polymerization rate is equal to the rate of propagation. The chain propagation process is also dominated by the association phenomenon; the dependence on rate is quite insensitive to the concentration of growing chains, which is proportional to the concentration of initiator added.

1.6.3 Propagation

Early studies of the propagation of polystyryl lithium were confused by the lack of differentiation between initiation and propagation steps. The kinetics of propagation could only be perceived clearly in hydrocarbon solvents after complete depletion of the initiator; otherwise the formation of various mixed alkyl-lithium-polystyryl-lithium aggregates, as well as the initiation, distort the kinetics of propagation.

The kinetics of polymerization was first reported by Bywater and Worsfold[23,26]. The propagation was found to be first order in monomer, but 1/2 order with respect to active centres. In hydrocarbon solvents polystyryl lithium is present as inactive dormant dimers in equilibrium with a very small amount of active unassociated species :

$$(PS^- Li^+)_2 \rightleftharpoons 2\ PS^- Li^+$$

$$PS_n^- Li^+ + M \longrightarrow PS_{(n+1)}^- Li^+$$

For rapid equilibrium between monomeric and dimeric species, the concentration of the active centres, i.e. those unassociated, is proportional to the square root of the concentration of dimeric species. The supposition that virtually all the polymer chains are associated into dimers was confirmed by viscosity measurements of Morton *et al* [30]. The viscosity of a solution of living polystyryl lithium was found to decrease by a factor of ~10 on addition of a drop of methanol, which converts the dimeric polymers associated through the $-CH_2CH^-Ph$, Li^+ end-groups into the "dead" unassociated polymers terminated by the inactive $-CH_2CH_2Ph$ groups without seriously affecting the nature of the solvent. The decrease in viscosity corresponded to a decrease in molecular weight, confirming the dimeric nature of polystyryl lithium in hydrocarbons.

The rate of propagation is said to be proportional to the square root of the active centre concentration so that :

$$-\left(\frac{1}{[Sty]}\cdot\frac{d[Sty]}{dt}\right) = k_p(K_{diss}/2)^{1/2}\cdot[LP]^{1/2}$$

where [Sty] = concentration of styrene at time t

[LP] = concentration of living polystyryl lithium

k_p = propagation rate constant of the unassociated LP

K_{diss} = dissociation constant of dimeric polymers into monomeric species

i.e. the plot of

$$\ln \left[- \left(\frac{1}{[Sty]} \cdot \frac{d[Sty]}{dt} \right) \right] \quad \text{vs.} \quad \ln[LP]$$

is linear with a slope of 1/2. $k_p K_{diss}^{1/2}$ was found to be 0.93×10^{-2} $M^{1/2}$ s^{-1} when the reaction was carried out in benzene or toluene at ambient temperatures. The value is lower in cyclohexane, but only by a factor of 3. The comparable rates of propagation of the reaction proceeding in aromatic or aliphatic hydrocarbons are in contrast with the vast differences in the initiation rates when an aromatic hydrocarbon is replaced by an aliphatic.

The nature of the C-Li bond of polystyryl lithium in hydrocarbon solvents is still a matter of dispute[2]. Since the electronic spectrum of its solution in hydrocarbons or in THF is similar to that of polystyryl sodium in THF, the bond is thought to be most probably ionic rather than covalent.

When the polymerization is carried out in polar solvents of high dielectric constant, chain initiation is always so fast that the measured polymerization rates are those of propagation. The dimeric polystyryl lithium species dissociates in solvents such as THF. The kinetics of the anionic propagation of polystyryl sodium in THF were first investigated by Geacentov *et al* [31,32]. They adopted a capillary flow technique whereby styrene consumption was found to exhibit first order kinetics. Both Szwarc *et al* [33] and Schulz *et al* [34] reported a linear dependence of k_p on reciprocal of the square root of the concentration of living polymer; this was explained by the presence of free polystyryl anions in equilibrium with their ion pairs as the species responsible for propagation. In

dioxane, however, the rates of styrene polymerization are linearly proportional to both the active centre and monomer concentration and increase in the series $Li^+ < Na^+ < K^+ < Cs^+$[35-39]. These observations indicate that a simple contact ion-pair is the propagating species :

$$\sim PS_n^- \; Li^+ + \; Sty \xrightarrow{k_p} \sim PS_{n+1}^- \; Li^+$$

so that :

$$\frac{-d[Sty]}{dt} = k_p \, [Sty][\sim PS_n^- \; Li^+]$$

from which k_p can be determined experimentally.

The polymerization rate increases with an increase in dielectric constant of the solvent in the series dioxane < oxepane < tetrahydropyran < tetrahydrofuran. The activity of the propagating free anion (k_{p-}) has been shown to be greater than that of the ion pair ($k_{p+/-}$).

1.7 The Anionic Polymerization of Methyl Methacrylate

1.7.1 Termination and Transfer Reactions

The anionic polymerization of polar vinyl monomers by living systems poses a constant challenge to the polymer chemist[7,12]. Much of the work carried out in this field has been directed into the area of methyl methacrylate polymerization. Complications arise because of the carbonyl functionality which can impart physical interactions (e.g. association), as well as chemical side reactions (e.g. termination and transfer), especially in non-polar solvents. These reactions are commonly observed when working at temperatures higher than -75°C; or when using very low concentrations of living ends, as is necessary for the preparation of polymers with high molecular weight. The common features of these side reactions are :

(i) A downward curvature of the linear first-order plot of monomer concentration as a function of time i.e. $\ln([M]_o/[M])$ against time - indicating a decrease in the concentration of living ends ([LE]), caused by chain termination.

(ii) A broadening of molecular weight distribution. A low molecular weight tailing is found on the SEC chromatograms. The number average degree of polymerization, however, is still proportional to percentage conversion, since the total number of chains is determined by the concentration of initiator.

Polymerizations involving *tert*-butyl methacrylate were found to exhibit no termination reactions even at ambient temperatures[40]. Evidently the rate, and the mechanism of termination is influenced by the structure of the ion-pair. The positive inductive effect of the *tert*-butyl group decreases the carbonyl activity, and hence the termination rate constant.

Polymerizations of methyl methacrylate initiated by butyllithium in toluene, have shown some active centres to persist during polymerization at low temperature, since a new batch of monomer added after polymerization has been completed, will still polymerize. However, only a small fraction of the initiator produces growing chains; most being destroyed in side reactions. A large fraction of oligomeric products is obtained; even the higher molecular weight product has a broad molecular weight distribution. The chief source of these problems lies in the fact that both initiation and propagation can occur both at the C=C double bond and at the carbonyl group of the monomer, leading to termination or chain transfer. Three types of termination reactions were first discussed by Schreiber[41]:

(i) A reaction of the living end with the carbonyl group of the monomer resulting in the formation of a vinyl ketone, ("monomer termination") as shown in scheme 1.8.

(ii) Reaction of the living end with the ester group of another polymer chain resulting in chain coupling, ("intermolecular polymer termination") as shown in scheme 1.9.

(iii) Reaction of the living end with the antepenultimate ester group of its own polymer chain resulting in a cyclic β-keto ester structure, ("intramolecular polymer termination" or "backbiting") as shown in scheme 1.10.

All three reactions produce methoxide as a by-product. Wiles and Bywater[42] and Mita *et al* [43], showed that nearly all methoxide is produced in the initial stage of polymerization. As there is no polymer present at that time, the methoxide must be generated by the attack of the initiator on the carbonyl group of the monomer. This is shown in scheme 1.11.

Scheme 1.8 To Show "Monomer Termination" in the Anionic Polymerization of Methyl Methacrylate

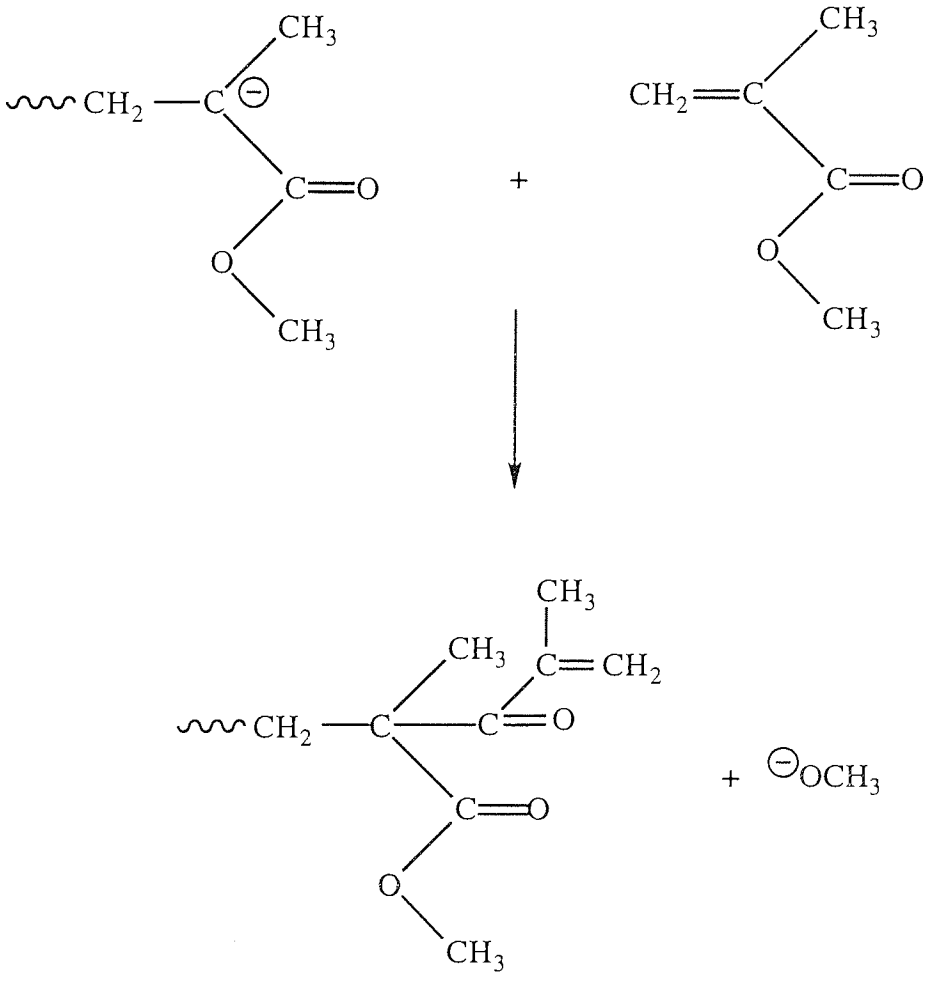

Scheme 1.9 To Show "Intermolecular Polymer Termination" in the Anionic Polymerization of Methyl Methacrylate

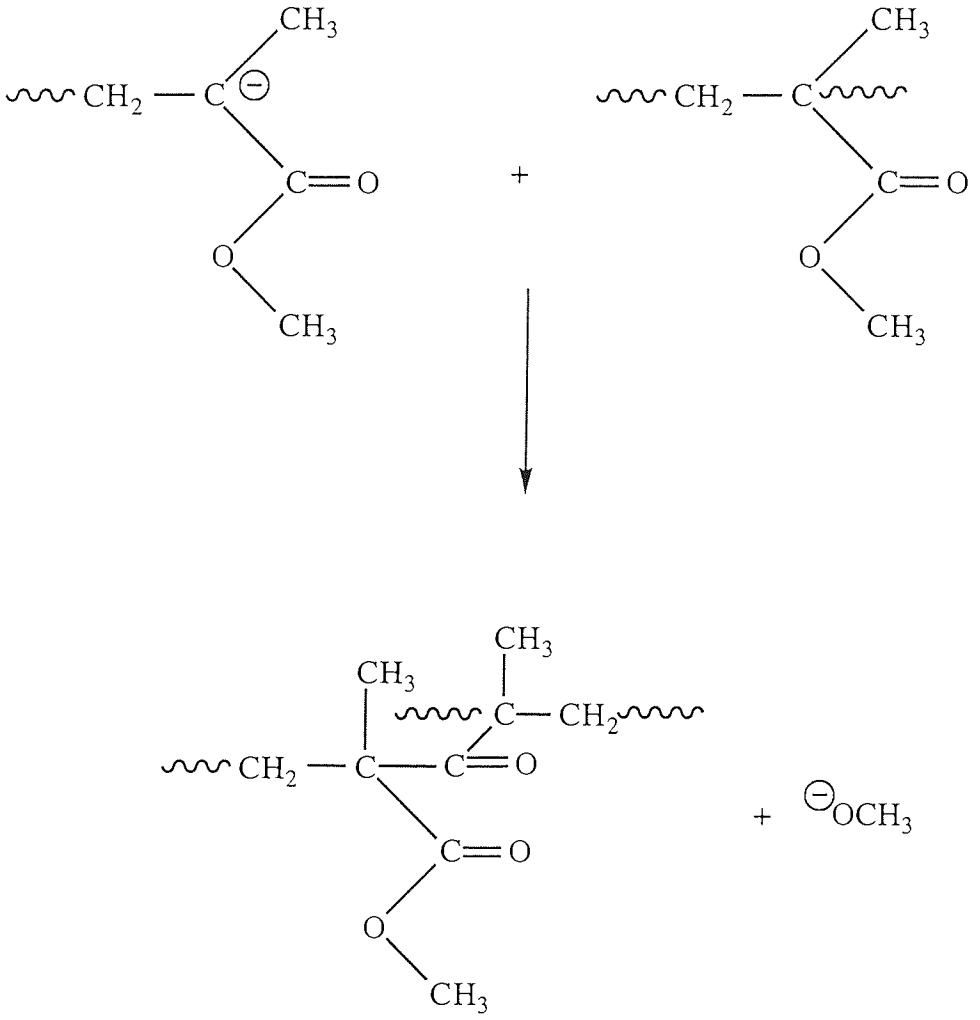

Scheme 1.10 To Show "Intramolecular Polymer Termination" in the Anionic Polymerization of Methyl Methacrylate

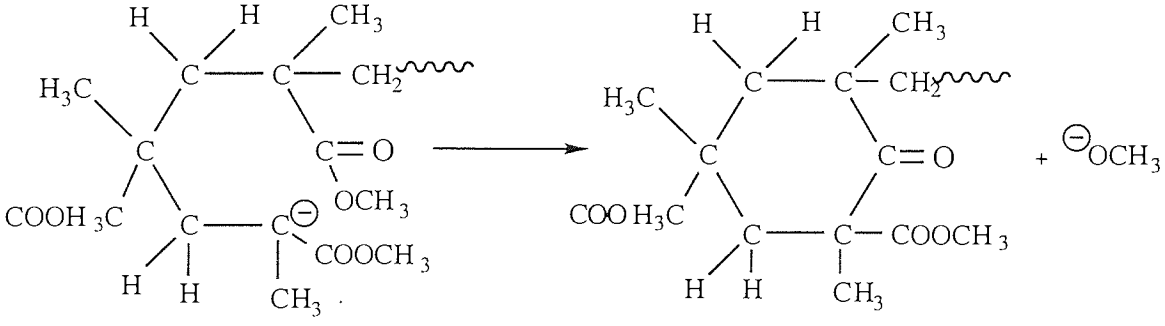

Scheme 1.11 Reactions of the Monomer with the Initiator Involved in the Polymerization of Methyl Methacrylate

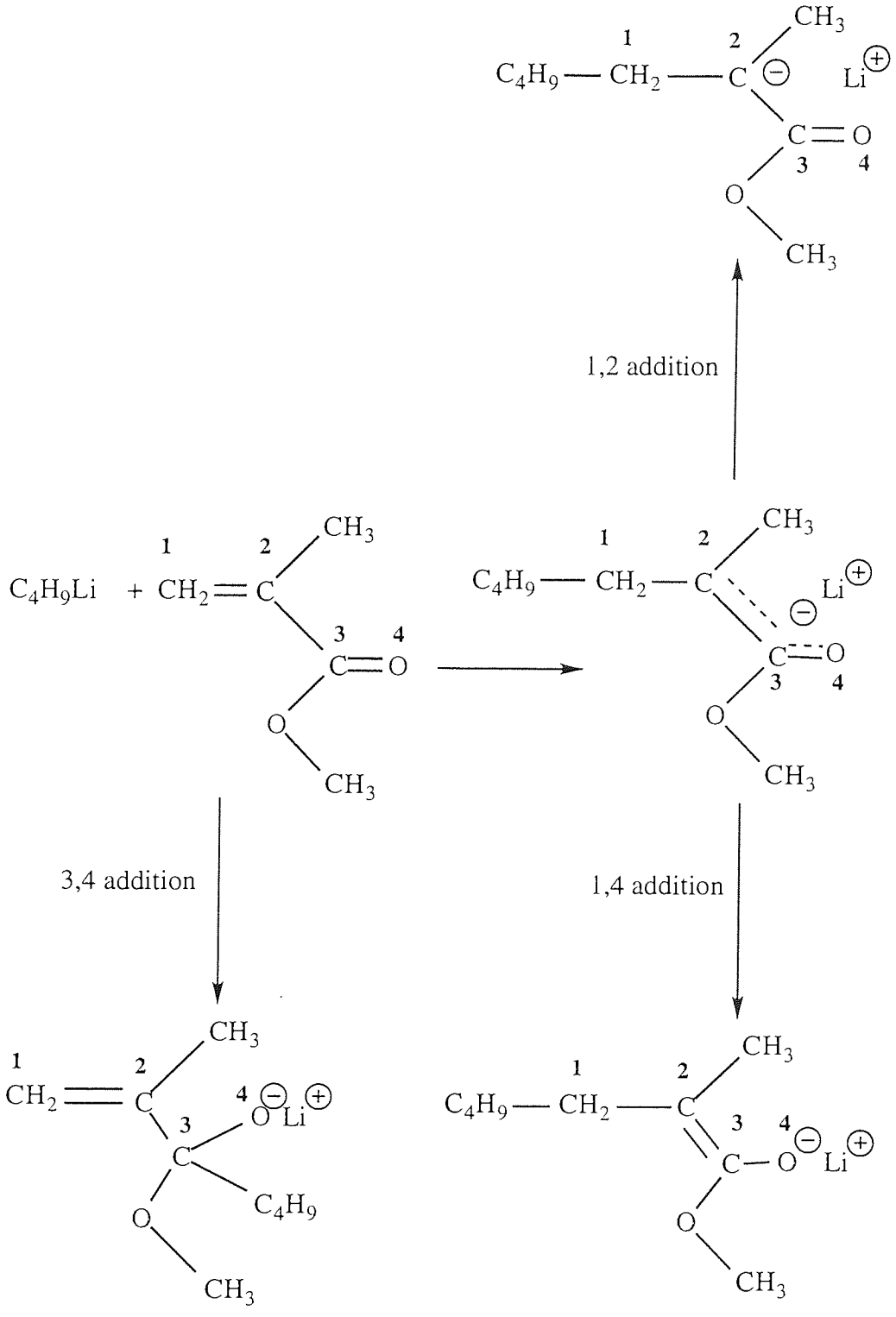

Only the reaction at the carbon-carbon double bond i.e. the 1, 2 addition reaction leads to chain growth. The product of reaction at the carbonyl function (1, 4 addition) can

eliminate lithium methoxide and form methyl pentyl ketene[7]. Appreciable fractions of methanol can be detected at the early stages of polymerization if the polymerization is terminated with acetic acid. Other complications arise from the addition of butyl isopropenyl ketone (produced by 3, 4 addition), to the growing chains obtained from 1, 2 addition at low temperatures. This is because the ketone is more reactive towards the propagating anions than MMA and hence most of the chains become capped with the unreactive vinyl ketone ion pair, producing oligomers such as :

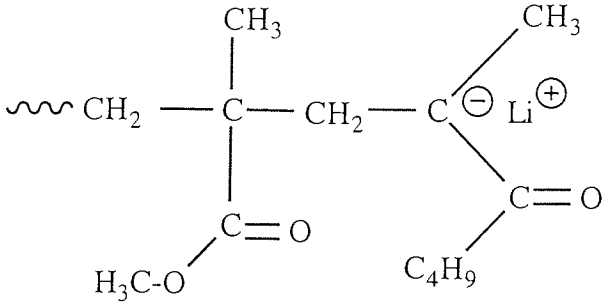

The vinyl ketone can also react with initiator molecules to form alcohols. The products of such additions were characterised using the initiators, phenyllithium in diethyl ether[41], butyllithium in hexane and THF[44] and butyllithium in toluene[45,46].

Although unreactive towards methyl methacrylate, these modified active centres add to methyl methacrylate more slowly than alkyl lithiums, but then propagate normally. Because addition to the vinyl ketone and monomer are competitive processes, some active centres may grow without reaction with the vinyl ketone. The polymer formed has a broad distribution of molecular weights under these conditions and butyllithium on its own, is not considered as a suitable initiator for the polymerization of methyl methacrylate.

Poly(methyl methacrylate) with a narrow molecular weight distibution has been synthesised under refined experimental conditions. Such products are achieved using low temperatures, polar solvents, less reactive or sterically hindered initiators which decrease reactivity towards the carbonyl function and ultrapure monomers that successfully prevent the occurrence of termination and chain transfer reactions. Some of these conditions were employed by Rembaum and Scwarz[47] who provided the early evidence for the feasiblity of methyl methacrylate polymerization. They investigated the anionic polymerization of

methyl methacrylate in THF at -78°C using sodium naphthalide or sodium polystyryl as initiator. The polymerization was found to be quantitative, completed within seconds but the resulting polymer was not living and appeared to be terminated within half an hour.

1.7.2 Early Studies in Kinetics of Methyl Methacrylate Polymerization

Until 1973, there were no reports of kinetic measurements carried out on the polymerization of methyl methacrylate in a polar solvent. This can be attributed to the experimental difficulties associated with kinetic measurements using U.V. absorption spectroscopy on a system that undergoes very high rates of polymerization[12]. When the concentration of living ends is 10^{-3} mol/L, the half-life for monomer addition to ion pairs is 5 seconds at -80°C and only 0.1 second at ambient temperatures. Lohr and Schulz[48,49], and also Mita *et al* [43] investigated the kinetics of polymerization of MMA in THF, with Na^+ and Cs^+ as counterions using flow tube techniques. Both groups showed that the reaction proceeds in an ideal way at low temperatures; initiation is fast compared to propagation and propagation follows first order kinetics with respect to monomer concentration (indicating the absence of termination reactions). The number average degree of polymerization was found to be proportional to percentage conversion (indicating the absence of transfer reactions). Lohr and Schulz obtained narrow molecular weight distribution polymers and demonstrated clearly that both free ions and ion-pairs participate in the propagation.

The kinetics measurements of both groups were inadequate to a certain degree in that, when using Na^+ as the counterion, only bifunctional initiators were used (i.e. sodium naphthalide and oligo-α–methylstyryl sodium). Warzelhan *et al* [50,51] showed that bifunctionally growing chains are able to form intramolecular associates, which differ in propagation rate constant, as well as tacticity of resulting polymer, from the monofunctionally growing species.

Schulz and coworkers[52,53], and later, Muller and coworkers[54], investigated the propagation kinetics over a temperature range of between -100°C and +20°C using cumylcaesium and benzyl-oligo-α-methylstyrylsodium. $Na(BPh)_4$ and $Cs(Ph_3BCN)$

were added as common ion salts to suppress the dissociation of propagating centres into free ions; the effect of this was to slow down the rate of polymerization, since free ions react much faster than ion pairs. The use of the flow tube reactor is unfavourable at low temperatures, and, therefore, reactions below -50°C were conducted in a stirred tank reactor, allowing kinetic measurements of reactions with half-lives of 2 seconds and longer to be taken by periodically extracting samples[55]. Polymerizations were rapid, even at -98°C, with monomer half lives of approximately 24 seconds, when sodium and caesium were used as the counterion, and 10 minutes for the lithium systems. Although some termination was observed at higher temperatures, the rate constants could be measured from the initial slope of the first-order logarithmic conversion-time curve. The initial concentration of the living ends was determined from the reciprocal of the gradient in the plot of the number average degree of polymerization as a function of percentage conversion, which remains linear when termination occurs. The Arrhenius plots for the propagating rate constants for ion pairs were found to be linear for both Na^+ and Cs^+ as the counterions, thus giving no evidence for the existence of more than one type of ion pair.

Only small differences in rate constant were observed among systems having Na^+ or Cs^+ as counterions, but the Li^+ system showed much slower rates. This behaviour is quite different from that observed in styrene polymerization, and appears to be characteristic of monomers in which intramolecular solvation of the counterion by polar groups, i.e. the penultimate ester group in the case of MMA, of the polymer chain can occur[54]. Another possibility can be attributed to the active species existing in a special form of a contact ion pair, in which the counterion is less close to the α-carbon atom and exhibits less influence on its reactivity[56].

Kraft *et al*[57], carried out kinetics studies on the anionic polymerization of methyl methacrylate using sodium and caesium as counterions in dimethylether (DME) and also confirmed that there was no dependence of the rate of polymerization on the counterion. As in THF, the Arrhenius plots of the propagating rate constants were found to be linear,

and, within experimental error, identical for the two counterions used; however, the rate constants were found to be higher when DME was used as solvent compared with THF.

Further investigation was carried out by Muller and Jeuck[18] using THF as the solvent in the presence of lithium and potassium counterions. They showed that the rate constant for Li^+ as the counterion was much lower, and the activation parameter higher than those for Na^+ and Cs^+. When K^+ was used as the counterion, the propagation rate constant was almost identical, within experimental error, to those of Na^+ and Cs^+. The activation energy using K^+ as the counterion, was estimated to lie between that of Na^+ and Cs^+. They concluded that there was a distinct dependence of the rate of polymerization of MMA on the counterion used, owing to the fact that a linear relationship existed between the logarithm of the propagation rate constant and the interionic distance.

The kinetics of the polymerization of *tert*-butyl methacrylate (TBMA) in THF were studied by Muller[40] with Na^+ and Cs^+ as the counterions. The rate constants for these systems were found to be considerably lower than for methyl methacrylate because of the higher activation energy required for TBMA polymerization. This was in contrast to the expectation of a higher steric factor caused by the bulkiness of the ester group. Moreover, rate constants for this system were found to be dependent on the counterion (Cs^+ producing values that were 4-10 times higher than the corresponding values for Na^+). It was believed that the counterion was closer to the carbanion for this system, accounted for by the positive inductive effect of the *tert*-butyl group increasing the negative charge density.

1.7.3 Tacticities of the Polymers

The tacticities of PMMA samples prepared in different solvents using a variety of counterions show a distinct trend, which is concerned with the polarity of the solvent and the solvatability of the counterion. Table 1.2[51,54,57] shows the tacticities of PMMA samples obtained in DME and THF, using mono- and bifunctional initiators and Na^+ and Cs^+ as the counterions.

Table 1.2 Tacticities of PMMA Samples Prepared in Counterion / Solvent Systems in the Presence of a Common Ion Salt

Counterion/Solvent	Temperature / °C	I	H	S	m	r
Na^+ / DME	-55	0.01	0.22	0.78	0.12	0.88
Cs^+ / DME	-65	0.02	0.37	0.60	0.21	0.79
Na^+ / THF	-61	0.04	0.36	0.58	0.23	0.77
Cs^+ / THF	-66	0.05	0.53	0.42	0.315	0.685
Na^+ / THF Bifunctional	-75	0.39	0.41	0.20	0.595	0.405

I, H, S, : isotactic (mm), heterotactic (mr/rm), syndiotactic (rr) triads; m, r : meso and racemic dyads.

The table shows that the degree of isotacticity decreases as the solvating power of the solvent does, exhibiting the following order :

Na / DME < Cs / DME ~Na / THF < Cs / THF.

This indicated that a close contact between carbanion and counterion favours isotactic propagation. Intramolecular chain end associates are thought to partly form in the polymerization when bifunctional initiators are used with Na^+ as the counterion in THF; this leads to different tacticities from the monofunctionally growing[50,51] species. These tacticities are intermediate between those produced in polar solvents by monofunctional initiators, and those produced in non-polar solvents, where association of the growing ends with methoxide or with the monomer is a possible reaction. It is difficult to compare the results of different research groups regarding the tacticities of methyl and alkyl methacrylates since, in many cases, anions are present to an unknown extent, and often bifunctional initiators are used leading to unknown amounts of intramolecular association. Intermolecular solvation may also occur in solvents of lower solvating power. Nevertheless Yuki and Hatada[58] have reviewed some of the different tacticities of polymethacrylates obtained under different conditions.

1.7.4 The Effect of Lithium Salts

Teyssie *et al*[59] synthesized block copolymers by sequential addition of methyl methacrylate or *tert*-butyl acrylate to living polystyryl anions. The polymerization was carried out in a 50/50 (v/v) benzene/THF mixture at -78° C, in the presence of lithium as a counterion. The block polymerization of MMA yielded disappointing results since half the initial poly(styrene) was recovered as homopolymer and the molecular weight distribution of the block copolymer was found to be bimodal. The situation was improved when a molar excess of lithium acetate was added to polystyryl lithium before starting the methyl methacrylate block polymerization. The percentage of the homopoly(styrene) fell to 13 % of the initial amount whereas the block copolymer exhibited the unimodal, but still broad distribution.

A final improvement was reported when lithium acetate was replaced by lithium chloride[60-64], resulting in more than 98% poly(styrene) being block copolymerized and a polydispersity index between 1.2 and 1.3. An even narrower polydispersity index of <1.1 was obtained when the polymerization was carried out in THF alone. Teyssie and co-workers concluded that LiCl had a dual favourable effect :-

(i) LiCl decreases the reactivity of polystyryl lithium towards methyl methacrylate resulting in a well-controlled initiation step free from side reactions on the monomer.

(ii) The propagation of the anionic polymerization of methyl methacrylate can now occur without transfer and termination reactions.

The effects of the LiCl on the molecular weight distributions of the copolymers of methyl methacrylate and *tert*-butyl acrylate obtained are shown in figures 1.9 and 1.10 respectively. It is quite clear that the ratio of the rate constants k_i / k_p is large enough to lead to a narrow molecular weight distribution.

Figure 1.9 Effect of LiCl on the Molecular Weight Distribution of PMMA - Size Exclusion Chromatograph of PMMA Synthesized in a 90/10 (v/v) Toluene/THF Mixture at -78°C with α-Methylstyryl Initiator

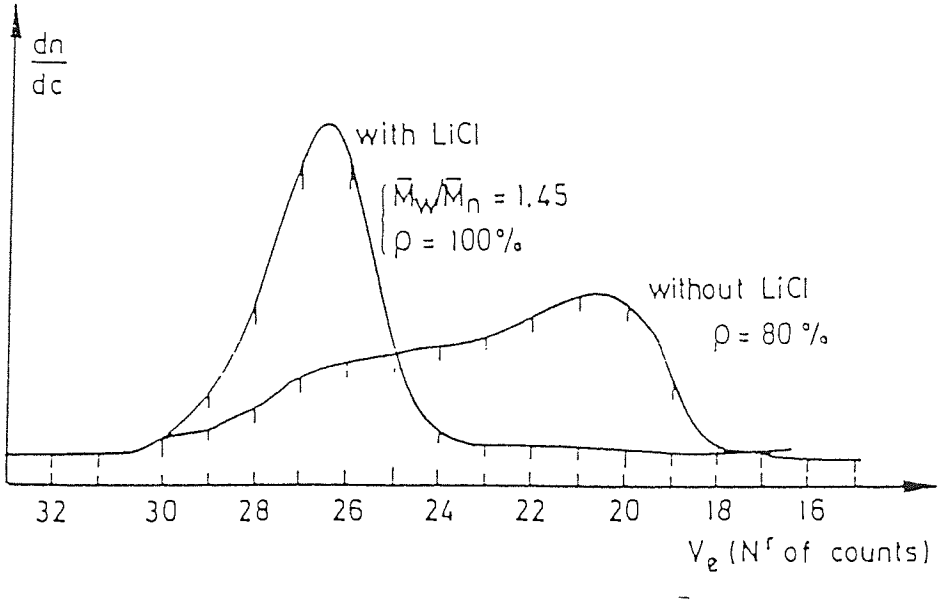

Figure 1.10. Effect of LiCl on the Molecular Weight Distribution of P*t*-BuMA - Size Exclusion Chromatograph of P*t*-BMA Synthesized at -78°C

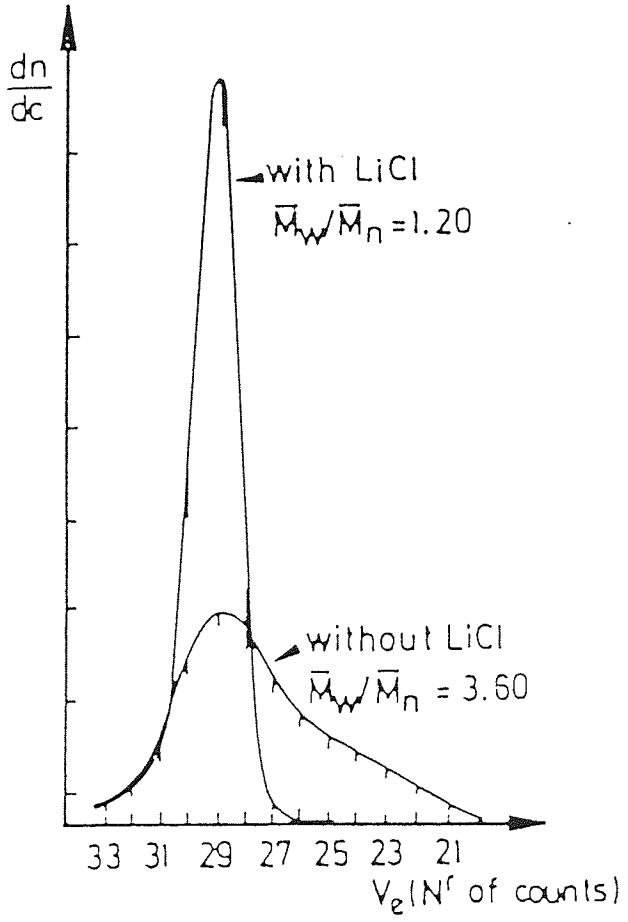

A systematic change of the LiCl / initiator (α-methyl styrene) ratio was found to result in a change in the molecular weight distribution of the poly(*t ert*-butyl acrylate) synthesized in THF at -78°C[59] . It was found that a 1/1 molar ratio or a slightly greater LiCl / ion pair adduct ratio had the most beneficial effect in successfully producing polymers of narrow molecular weight distributions.

In order to shed light on the possible interaction between the organolithium species and the LiCl, the ^{7}Li NMR spectra of $PS^{-}\ Li^{+}$ and $PMMA^{-}\ Li^{+}$ were recorded before and after the addition of various amounts of LiCl in THF at -60°C, as shown in table 1.3. When LiCl was added to $PS^{-}\ Li^{+}$, a single line was observed, the chemical shift of which was not the weighted average of that for LiCl and $PS^{-}\ Li^{+}$. This meant that the observed resonance could not be attributed to a fast exchange of Li^{+} between the salt and the organo compound but was most probably due to a complexed species in equilibrium with an excess of one or both of the starting lithium compounds.

Table 1.3 ^{7}Li Chemical Shift in $PS^{-}\ Li^{+}$ and $PMMA^{-}\ Li^{+}$ in THF at -60°C, With and Without Added LiCl

Li^{+} species	^{7}Li shift (ppm)	$[Li^{+}]$ (ml^{-1})
LiCl	0	0.02
$PS^{-}\ Li^{+}$	0.59	0.02
LiCl / $PS^{-}\ Li^{+}$ (1/2)	0.19	0.06
LiCl / $PS^{-}\ Li^{+}$ (1/1)	0.21	0.04
LiCl / $PS^{-}\ Li^{+}$ (2/1)	0.06	0.06
$PMMA^{-}\ Li^{+}$	0.42	0.02
LiCl / $PMMA^{-}\ Li^{+}$ (1/2)	0.42-0.11	0.06
LiCl / $PMMA^{-}\ Li^{+}$ (1/1)	0.15	0.04
LiCl / $PMMA^{-}\ Li^{+}$ (2/1)	0.06	0.06

It was concluded that LiCl interacts as well with the initiating species (styryl type anion) as it does with the propagating carbanion derived from methyl methacrylate. It was also

observed that, compared with the chemical shift reported for $PS^- Li^+$ and $PMMA^-Li^+$ alone, the value for the adduct was systematically smaller, in agreement with a loss of reactivity of the anionic species and making attack on the carbonyl function of the MMA less susceptible.

The initiation efficiency, f, (given by the concentration of growing chains divided by the concentration of the initiator) was clearly improved when the LiCl : initiator molar ratio was increased up to a value of 10[64].

Varshney *et al* [65] investigated the effect of lithium chloride on the polymer microstructure in the polymerization of *tert*-butyl acrylate in THF at -78°C. They found that the propagation rate constant was 20 times lower than when the polymerization was carried out in the absence of LiCl, and that the isotactic content of the polymers increased significantly when the [LiCl]/Initiator ratio was greater then 2. The effect of LiCl on the rate constant and microstructure of the polymers was attributed to complex formation between the LiCl and the living polymer chains.

In 1991, Muller *et al.*[66] demonstrated how the kinetics of propagation and termination, as well as the molecular weight distribution of methyl methacrylate polymers can be controlled by multiple equilibria between associated and non-associated ion pairs and ion pair ligand adducts. They showed that in the presence of LiCl, the formation of adducts of the active centres competes with association (as shown in figure 1.11).

Figure 1.11 To Show The Active Centres Involved in the Anionic Polymerization of Methyl Methacrylate in the Presence of Lithium Chloride

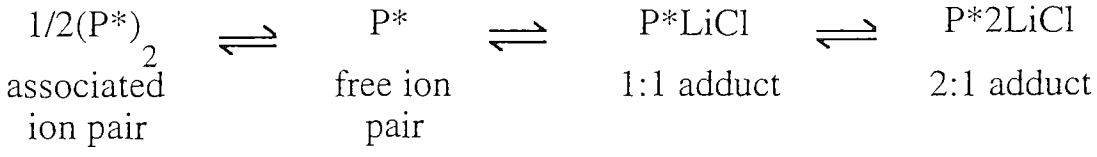

Hence the fraction of non-associated species increases on addition of LiCl. The effect of LiCl on the molecular weight distribution of poly(methyl methacrylate) was pronounced; with $\overline{M}_w/\overline{M}_n$ dropping from 1.3, to 1.04 in the presence of LiCl.

This phenomenon was explained in terms of the equilibrium between free and LiCl complexed ion pairs being much faster than that between free and associated ion pairs. In the case of the former, a macromolecule is reacting with a small molecule, whereas in the latter, two macromolecules are reacting together. Hence, the main function of LiCl was to deplete the system from slowly interconverting associates.

The existence of associated chain ends was demonstrated kinetically by decrease of the apparent propagation rate constant, k_p, with increasing concentration of active centres (P*), even in the presence of common ion salt[67]. The data clearly indicated that the reactivity of the associates was much lower than that of free ion pairs; the dynamics of the association equilibrium having a significant influence on molecular weight distribution of the polymers formed. A broadening of molecular weight distribution is therefore due to a rate of interconversion of associated and non-associated ion-pairs comparable to the rate of monomer addition. In *tert*-butyl acrylate, the effect of LiCl was found to be not so pronounced, since the molecular weight distributions are fairly narrow anyway. The fraction of associated forms in such systems is believed to be low.

Muller[66] concluded that the positions of the association/complexation equilibria strongly affect the kinetics of polymerization, whereas the dynamics are responsible for the molecular weight distributions of the polymers obtained.

Muller and Lochmann[68] also investigated the effect of lithium *tert*-butoxide (*t*-BuOLi) on the rate constants and equilibrium constants of reactions involved in the initial stage of anionic polymerization of methyl methacrylate. Reactions were carried out in THF, initiated by methyl 2-lithioisobutyrate at 23 +/- 3°C. They reported that addition of *t*-BuOLi decreases the rate constant of initiation and propagation by one order of magnitude; the rate constants of termination by cyclization decreases by two orders of magnitude. This leads to a tenfold higher preference of propagation with respect to termination and explains the favourable effect of the alkoxide.

1.7.5 The Effect of Aluminium Alkyls

The anionic polymerization of methacrylates in the presence of aluminium alkyls has been well documented over the last few years [69-76]. This is an area of growing interest since it enables polymerizations of methacrylates to be carried out, even at ambient temperatures, using apolar solvents whilst still retaining their 'living' character. Very little is as yet known about the effect of the aluminium alkyl on the mechanism of polymerization.

Hatada *et al.*[69-72] studied the polymerization of methyl methacrylate initiated by different butyllithium isomers in the presence of aluminium alkyls, at -78°C using toluene as solvent. They discovered that only with *tert*-butyllithium did they obtain highly syndiotactic polymers of narrow polydispersity index and in high yields . Both butyllithium and *sec*-butyllithium gave very low yields with broad, multimodal molecular weight distributions. As the temperature of polymerization was increased, the polydispersity index also increased and the yields decreased. They also reported that as the mole ratio of [Al]/[Li] increased, so did the initiator efficiency. From these results they concluded that the aluminium alkyl could cause the dissociation of the *tert*-butyllithium aggregates into monomeric species, thus increasing the efficiency of the initiator. Alternatively, it was considered that coordination of the aluminium alkyl to the carbonyl group of the monomer suppressed the addition of alkyllithiums to the carbonyl group and favoured the addition across the double bond to enable efficient propagation. The bulkier *tert*-butyl group of the alkyl lithium sterically hindered termination reactions involving attack on the carbonyl group, which was not the case with the butyllithium. NMR investigations suggested that the dimeric aluminium alkyl was coordinated to both the metallated enolate structure of the living chain end and to the penultimate ester group of the polymer, favouring syndiotactic propagation.

Ballard *et al.*[73] have carried out polymerizations of methyl methacrylate initiated by *tert*-butyllithium in the presence of (2,6-di-*tert*-butyl-4-methylphenoxy)diisobutylaluminium conducted at temperatures as high as 40°C. Triisobutylaluminium was modified by replacing one of the isobutyl groups by the bulkier phenoxy group. Even at such high

temperatures they obtained polymers with a polydispersity index as narrow as 1.05, which was believed to be possible because both the lithium and aluminium components contained groups with large cross-sectional areas. The propagating species in this case was suggested to be an enolate bound to a mixed lithium/aluminium counterion. Two different active centres (L_1 and L_2) were thought to be present which relate to the monomeric and dimeric species respectively, and are shown in scheme 1.12. The structures of the propagating species are based on the solid state oligomeric structure of $LiAl(C_2H_5)_4$. They proposed that these sorts of initiators are only effective in hydrocarbon solvents in which they are soluble; solvents which have been previously preferred for anionic polymerization such as THF cannot be used since they deactivate the initiator. In hydrocarbon solvents the separation between the anionic and cationic components is minimised, and the high cross-sectional area of the latter screens the propagating terminus of the polymer chain from side reactions. This was referred to as 'screened anionic polymerization'.

Haddleton *et al.*[74] have carried out work similar to Hatada *et al.* except that the polymerizations were carried out at higher temperatures (between 0-10°C). Their work supported that of Hatada *et al.*, in that they concluded that the nature of the living species was sensitive to the alkyl groups of both the aluminium and lithium components. They reported that when the alkyl group on each metal was bulkier, the polydispersity index was found to be narrower and percentage yield was higher. This was because much better control of the polymerization was obtained with triisobutylaluminium than with triethylaluminium. Contrary to Hatada's findings, however, they did have some success in producing narrow molecular weight distribution polymers of methyl methacrylate even when using butyllithium with triisobutylaluminium. Considerably narrower molecular weight distribution polymers were prepared when the aluminium alkyl was premixed with the monomer before addition of the alkyllithium, as opposed to addition of the aluminium alkyl to the alkyllithium first in order to form the initiating complex. From this they concluded that the order of reagent addition is important since it determines the structure of the initiating species.

Scheme 1.12 Structures of Propagating Centres L_1 and L_2 in the "Screened Anionic Polymerization" of Methyl Methacrylate in the Presence of Aluminium Alkyls (Ballard *et al*)

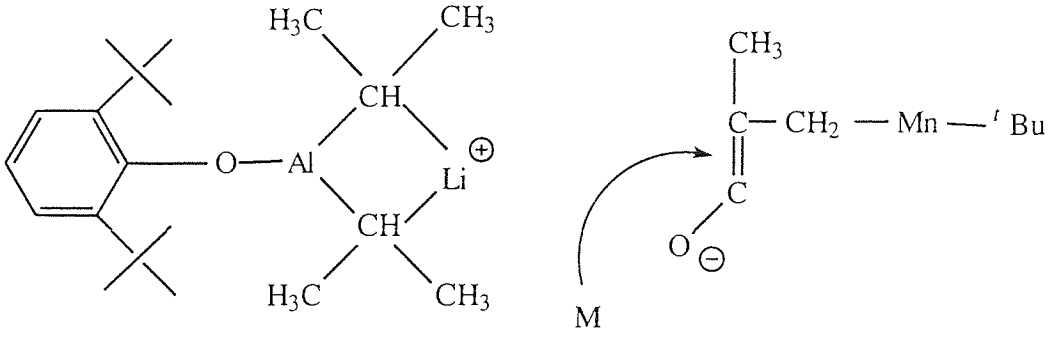

L_1

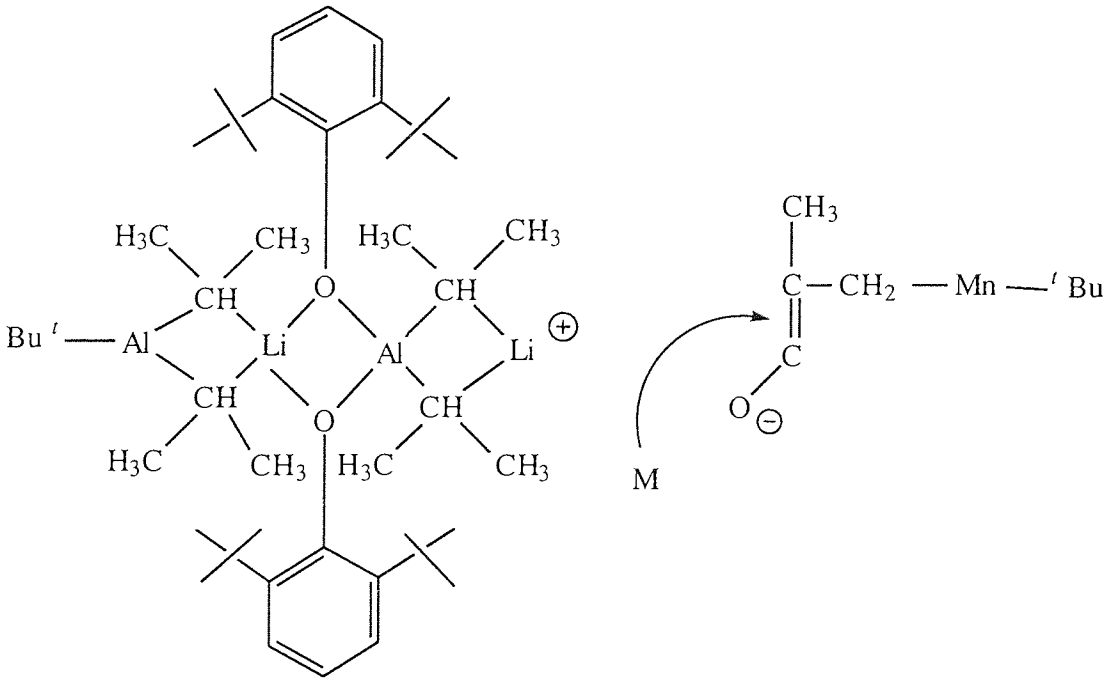

L_2

Muller *et al.*[75,76] carried out ^{13}C NMR studies using ethyl α-lithioisobutyrate (EiBLi) as a model compound for the chain end of living PMMA. They proposed that the active centre of polymerization in the presence of lithium and aluminium alkyls was a bimetallic 'ate' complex ([EiBLi-AlR_3]Li), with an increased covalent character of the metal-oxygen bond as shown in scheme 1.13.

Scheme 1.13 Formation of Bimetallic "Ate" Complex as Active Centre in the Presence of Aluminium Alkyls (Muller *et al*)

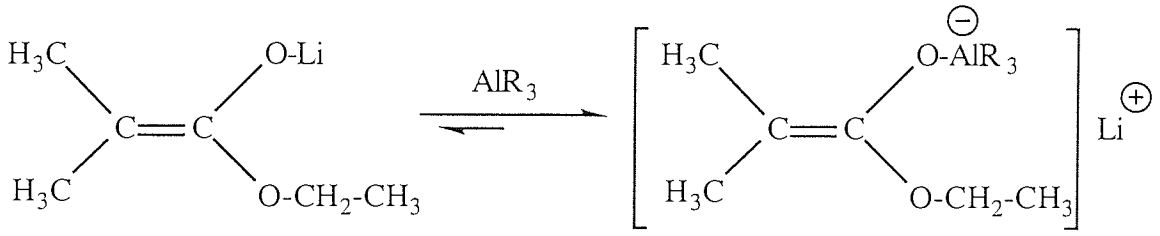

[EiB-AlR_3]Li

During the polymerization process, this can be formed from premixing the monomer with the aluminium alkyl followed by initiation using butyllithium, or, it can also be achieved by addition of the aluminium alkyl to the enolate formed, once butyllithium initiation has already taken place (see reaction scheme 1.14). They proposed that excess aluminium alkyl coordinates to the ester carbonyl groups of both the monomer and the polymer chains. The polymerizations were carried out at -78°C and the structure of the active species was ascertained from ^{13}C NMR studies of model compounds in toluene.

Scheme1.14 Mechanism to Show Initiation and Propgation of Methyl Methacrylate in the Presence of Lithium and Aluminium Alkyls (Muller *et al*)

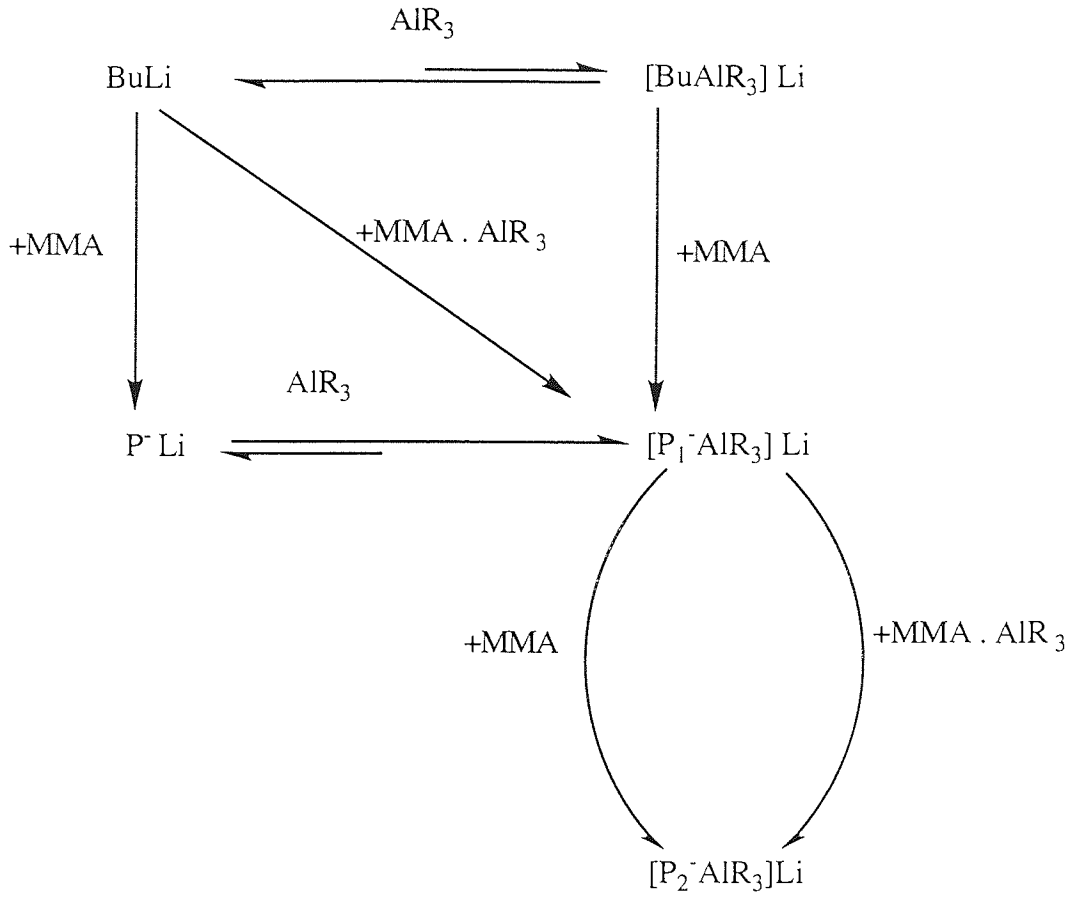

1.8 Block Copolymers

Block copolymers are defined as having a linear arrangement of blocks i.e. a block copolymer is a combination of two or more polymers joined end to end[7]. Star-block or radial block copolymers have branched structures, as do graft copolymers. The properties of graft copolymers may be similar to those of block copolymers if the number of grafts are small.

The increasing importance and interest in block copolymers arise mainly from their unique properties in solution and in the solid state, which are a consequence of their molecular structure. In particular, sequences of different chemical composition are usually incompatible and therefore have a tendency to segregate in space. Amphiphilic properties

in solution and microdomain formation in the solid state are directly related to specific molecular architectures, which can be designed using existing monomers and polymers. Some of these parameters will be discussed at greater depth in chapter six.

In recent years increasing effort has been devoted to the synthesis of novel copolymers and block copolymers in order to develop materials with predictable and controllable properties. Such materials include thermoplastic elastomers, polymers of predetermined functionality, and those which are used as ingredients for polymer alloys and blends[12]. As an indication of the commercial interest and activity in block copolymers, more than a thousand patents in the area were filed between 1976 and 1982, and the United States consumption of thermoplastic elastomers alone, which represents only part of the total block copolymer production, was found to be approximately 400,000 metric tonnes in 1985, with a growth rate of 9% per year[7].

Anionic polymerization is one of the preferred techniques for the preparation of well-defined block copolymers, owing to the lack of transfer and termination reactions under proper conditions. These living polymerization systems allow the preparation of nearly pure block copolymers of desired molecular weight, composition and structure. There are other advantages of using anionic polymerizations techniques for the preparation of block copolymers; these apply mainly to the polymerization of dienes, nonpolar vinylic monomers, cyclic ethers and cyclic sulphides :

(i) Block copolymers can be obtained either by successive polymerization of the monomers or by polymerizing the second monomer with functionalised prepolymers of the first monomer.

(ii) Multiblock copolymers of low polydispersity or of defined heterogeneity can be prepared by suitable coupling reactions or with bifunctional initiators.

(iii) Functionalised block copolymers can be obtained with suitable initiators or with specific terminating reagents.

The high reactivity of the living end of polymers in anionic polymerization, enables the possibility to obtain functionalised polymers and therefore block copolymers by deactivating with appropriate compounds. The deactivation of living poly(styrene), poly(isoprene), poly(butadiene) and poly(ethylene oxide) with a great variety of reagents leading to such end groups as hydroxyl, vinyl, ether and ester has been extensively reviewed[77]. Of special interest is the functionality of block copolymers with carboxyl or sulphonate groups which leads to ionomer-type block copolymers.

Methyl methacrylate can be used to prepare block copolymers. If methyl methacrylate is added to a polymerized styrene system the methyl methacrylate will grow on the styrene end as shown in scheme 1.15. The polystyryl living ends are red in colour which is due to excitation of pi electrons from the bonding to the antibonding orbital within the aromatic system of the propagating polystyryl anion. Styrene polymerization can be initiated using sodium naphthalenide or butyllithium in THF. On addition of methyl methacrylate the mass jellifies when the polymerization is carried out at -78°C[47].

A problem encountered within this polymerization system is the high reactivity of polystyryl anions towards the carbonyl group of methyl methacrylate, leading to termination and transfer reactions. This side reaction can be avoided by addition of 1,1 diphenylethylene or α-methyl styrene to cap the polystyryl ends prior to the methyl methacrylate polymerization[78]. This results in formation at the chain end, of diphenylmethyl anions or α-methyl styryl anions of lower nucleophilicity. These sites still initiate the polymerizations of methacrylic esters, but they are unable to attack the ester carbonyls. The use of alkali metal alkoxides and also borate derivatives has been proposed to prevent attack on the carbonyl group by polystyryl anions or other anionic initiators[52,53, 78-81].

Following the same concept Teyssie *et al* [60] investigated the behaviour of alkali and alkaline earth metal halides in the anionic block copolymerization of methyl methacrylate. The conclusions drawn from this investigation were that LiCl was more effective in controlling the molecular weight distribution of the polymers than $BaCl_2$ or $BaBr_2$.

Scheme 1.15 Mechanism of Block Copolymerization of Styrene and MMA

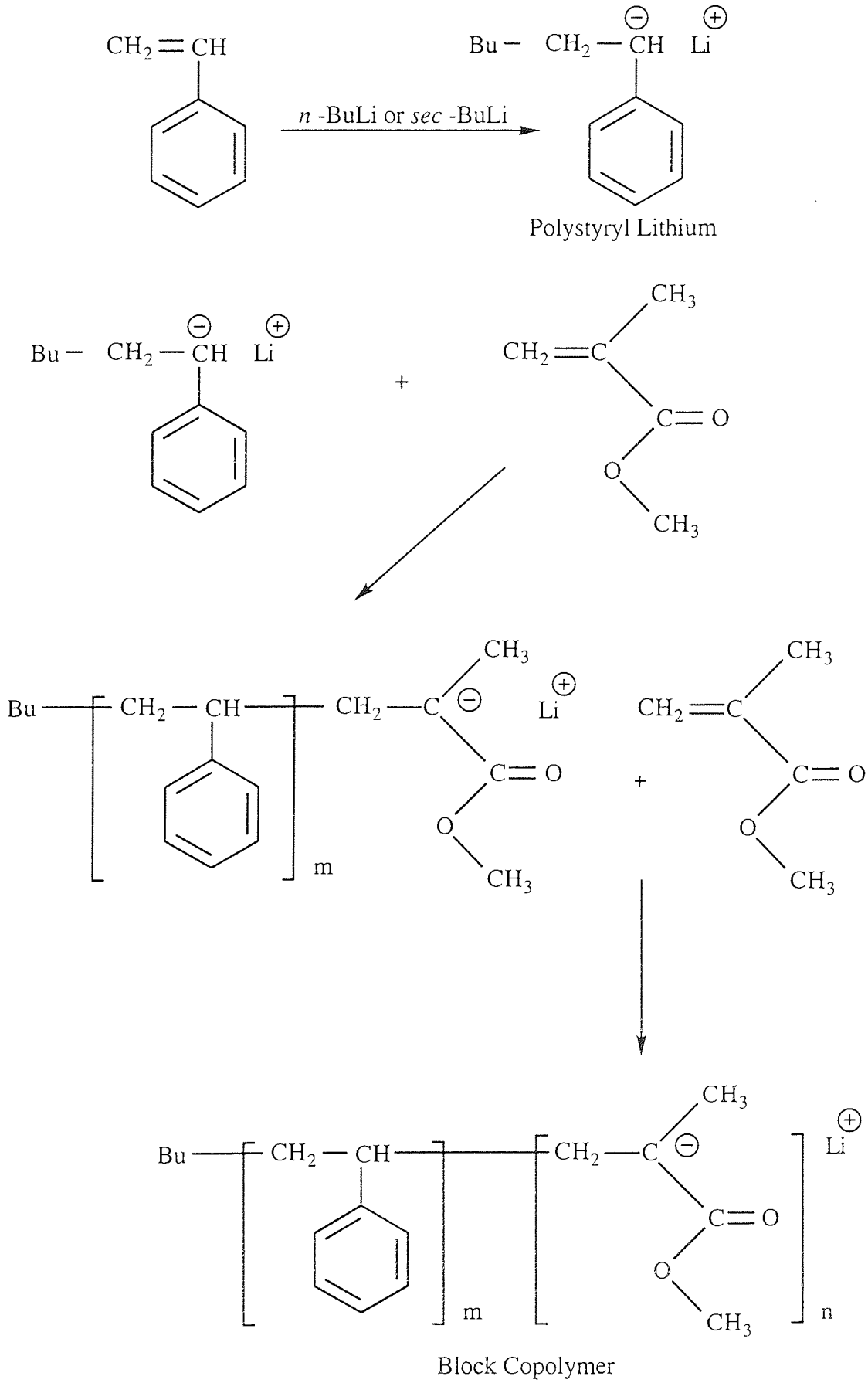

Copolymerization involving initiation of methyl methacrylate followed by addition of styrene to living poly(methyl methacrylate) is not a feasible reaction. The living ends of poly(methyl methacrylate) are not sufficiently active to initiate the polymerization of styrene, so that homo-polymerization of poly(methyl methacrylate) occurs and monomeric styrene is recovered.

1.9 Molecular Weight Distribution and Polydispersity

Polymers with very narrow molecular weight distributions are obtained if all the chain ends are initiated simultaneously and if during the reaction, no further initiation or termination occurs. Under these conditions, the molecular weight distribution resulting was described by Flory[82] :

$$\overline{M}_w/\overline{M}_n \approx 1.0$$

where $\overline{M}_w$ = weight average molecular weight

and $\overline{M}_n$ = number average molecular weight

In the above case the polymer is said to be monodisperse and the conditions employed are said to be almost perfect. If, however, the initiating centres do not start growing at exactly the same time, there will be some dispersity in the final polymer. Experimentally, non uniformity of conditions for instance, poor agitation, too rapid monomer addition and irregular temperature control also cause broadening of molecular weight distributions. Narrow molecular weight distributions are attributed to :-

(i) No termination or chain transfer.

(ii) A rate of initiation, k_i, faster than the rate of propagation, k_p.

(iii) Negligible extent of disproportionation during polymerization.

(iv) Uniform polymerization conditions with respect to temperature and concentration of reactants.

CHAPTER TWO

MATERIALS AND EXPERIMENTAL TECHNIQUES

2.1 Vacuum Techniques

One of the main problems associated with generating living polymer systems is the sensitivity of the anionic propagating centres to traces of moisture and oxygen. The same is true for the initiators and catalysts used. For this reason the preparation of monomers, solvents and catalyst systems, as well as the polymerizations themselves were carried out using high vacuum techniques, or under an atmosphere of argon using the Schlenk technique for transfer of materials. This technique enables the exclusion of impurities from the system.

2.1.1 The Vacuum Line

The vacuum line, shown in figure 2.1, was constructed of glass and consisted of a manifold and three PTFE taps, where degassing and distillation of solvents and monomers were carried out. The manifold could be sealed or connected to two vacuum pumps in series via a main PTFE tap. The Edwards rotary pump reduced pressures to 10^{-3} mm Hg, and a mercury diffusion pump enabled even lower pressures, approaching 10^{-5} mm Hg to be achieved. The pressure inside the system was indicated by a pirani gauge. Two liquid nitrogen traps were placed either side of the mercury diffusion pump, their purpose being to condense any vapour coming from the manifold so that the Edwards pump was protected during evacuation and to prevent mercury from contaminating the oil or the atmosphere.

Figure 2.1 The Vacuum Line

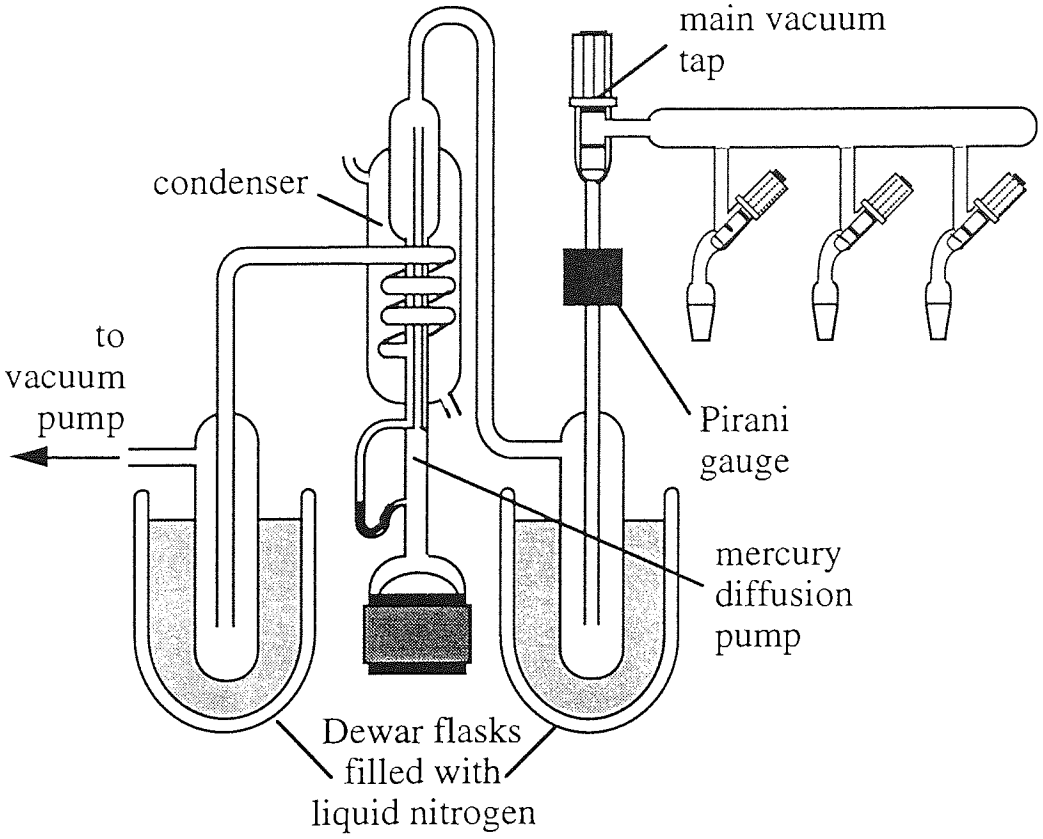

2.1.2 Treatment of Glassware

All the glass apparatus was cleaned thoroughly by soaking overnight with toluene or THF in order to remove any polymer residue. The apparatus was then cleaned by soaking overnight with a concentrated solution of sodium hydroxide which removed any residual high vacuum silicon grease. Finally the glassware was thoroughly washed with water and dried in an oven at 240°C for a period of at least 24 hours prior to use, after which it was transferred as quickly as possible to the vacuum line where it was immediately evacuated.

2.1.3 Freeze-Thaw Degassing of Liquids

In order to distil materials under vacuum, liquids had to be degassed using a freeze-thaw process prior to distillation. Gasses dissolved in the liquid at atmospheric pressure could

be removed in this way. A solvent flask was attached to the vacuum line with tap (a) closed (as shown in figure 2.2). The flask was then immersed in liquid nitrogen, which completely froze the contents of the flask within 10 minutes. Once frozen, tap (a) was opened and the system evacuated by opening the appropriate taps on the manifold. Once the pressures in the flask and the manifold were reduced to a minimum, tap (a) was shut and the manifold re-evacuated. The liquid nitrogen was removed and the contents of the flask were warmed, melting the frozen solvent and further releasing dissolved gasses. Re-freezing of the liquid left these gasses in the vacuum line. The process was repeated several times until no difference in vacuum was observed between freezing stages of the freeze-thaw process.

Figure 2.2 Solvent Flask for Use with Vacuum Line.

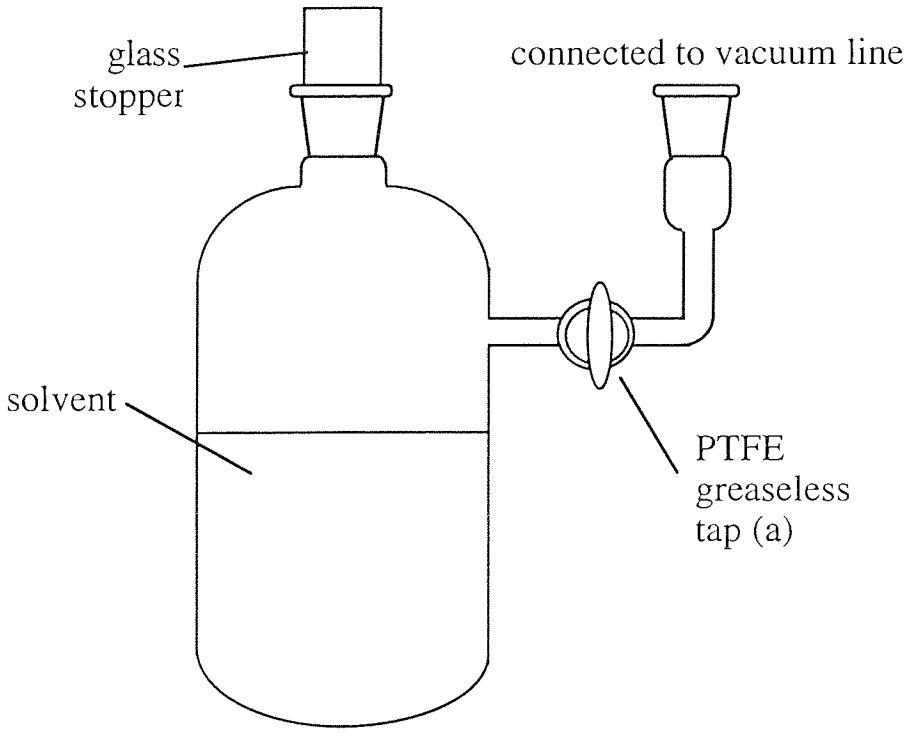

2.1.4 Trap to Trap Distillation

The degassed solvent, or monomer, could then be transferred to another flask on the high vacuum line by a trap-to-trap distillation. An empty receiver flask, which had been dried in an oven at 240 °C , was attached to the manifold and evacuated. The receiver flask was

immersed in liquid nitrogen and the main tap from the manifold to the pump was closed. The appropriate taps were then opened allowing the contents of the solvent flask to distil into the receiver flask.

2.2 Schlenk Techniques

The manifold of the vacuum line was connected permanently to an argon supply (see figure 2.3). A polymerization flask was attached to the line via one of the taps on the manifold and then evacuated. The main tap connected to the vacuum pumps was then closed, and argon was introduced into the manifold from the argon supply. A slight positive pressure of argon was maintained which was monitored via a bubbler. The tap to a flask was then removed, when argon was passed through, to inject initiators and catalysts under dry anaerobic conditions. The argon supply could also be used to withdraw aliquots of initiator solutions from the bottles with a syringe. For example, if butyllithium initiator was to be used, the bottle was connected to the argon supply with a wide bore syringe which penetrated the septum (Aldrich Sure Seal) of the bottle. Argon was then introduced into the bottle so that a slight positive pressure of inert gas was maintained whilst another syringe was used to withdraw a sample of the butyllithium via the septum.

Figure 2.3 The Argon Line.

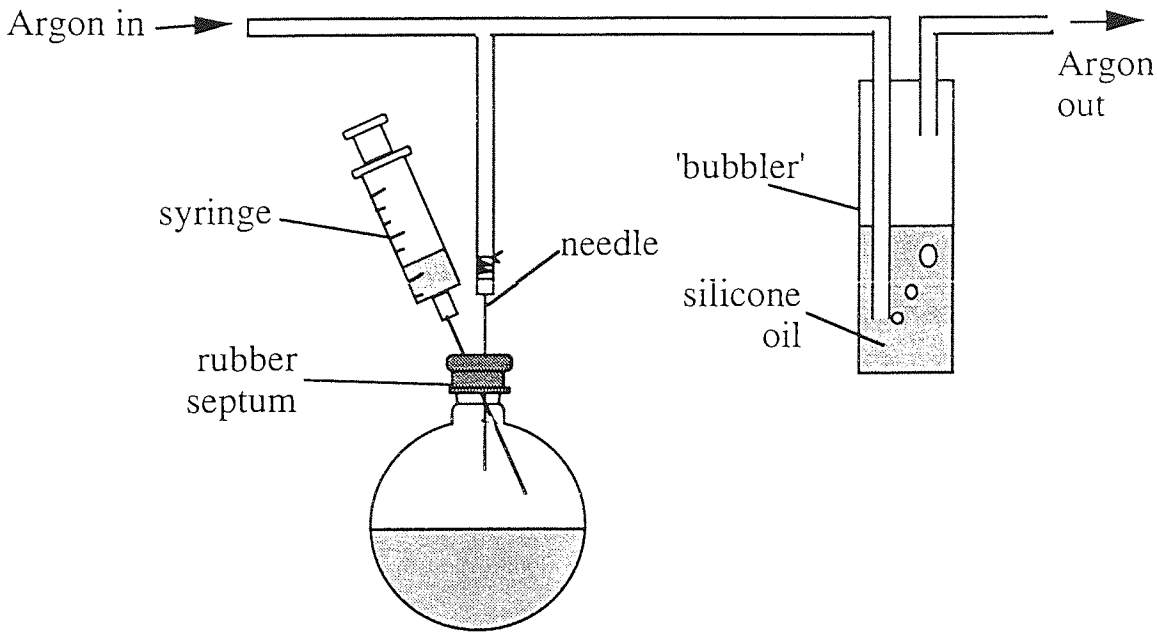

2.3 Apparatus

The use of a high vacuum storage system required specially designed glass vessels. Solvents and monomers were dried under vacuum or under argon in a solvent flask (see figure 2.2) and could be transferred to a polymerization flask by direct distillation. Alternatively, the solvent or monomer was distilled into a solvent storage flask (see figure 2.4) which possessed a joint enabling the vessel to be attached to the polymerization flask so that the dried solvent or monomer could be directly poured in.

Figure 2.4 Solvent Storage Flask

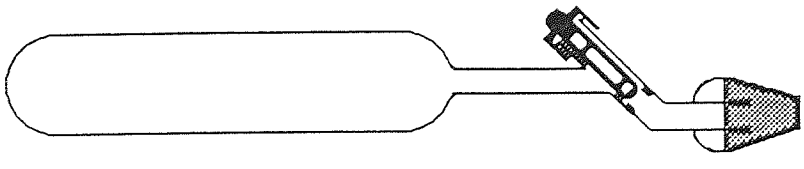

Catalyst solutions were prepared under argon using the Schlenk technique (see section 2.2) and stored in flasks of the type shown in figure 2.5. The solution was made up by injecting the initiator (or cocatalyst) into the large bulb of the catalyst flask into which excess solvent was distilled.

The solution was stored in the larger bulb of the flask, and when required, small amounts were transferred into the smaller bulb, already evacuated, by opening tap (a) while keeping tap (b) closed. Tap (a) was then closed and the flask was then transferred to the argon line and tap (b) opened, whilst argon was introduced into the small bulb. At this point tap (b) could be completely removed so that the solution could be withdrawn with a syringe and injected into the polymerization flask.

Figure 2.5 A Catalyst Flask

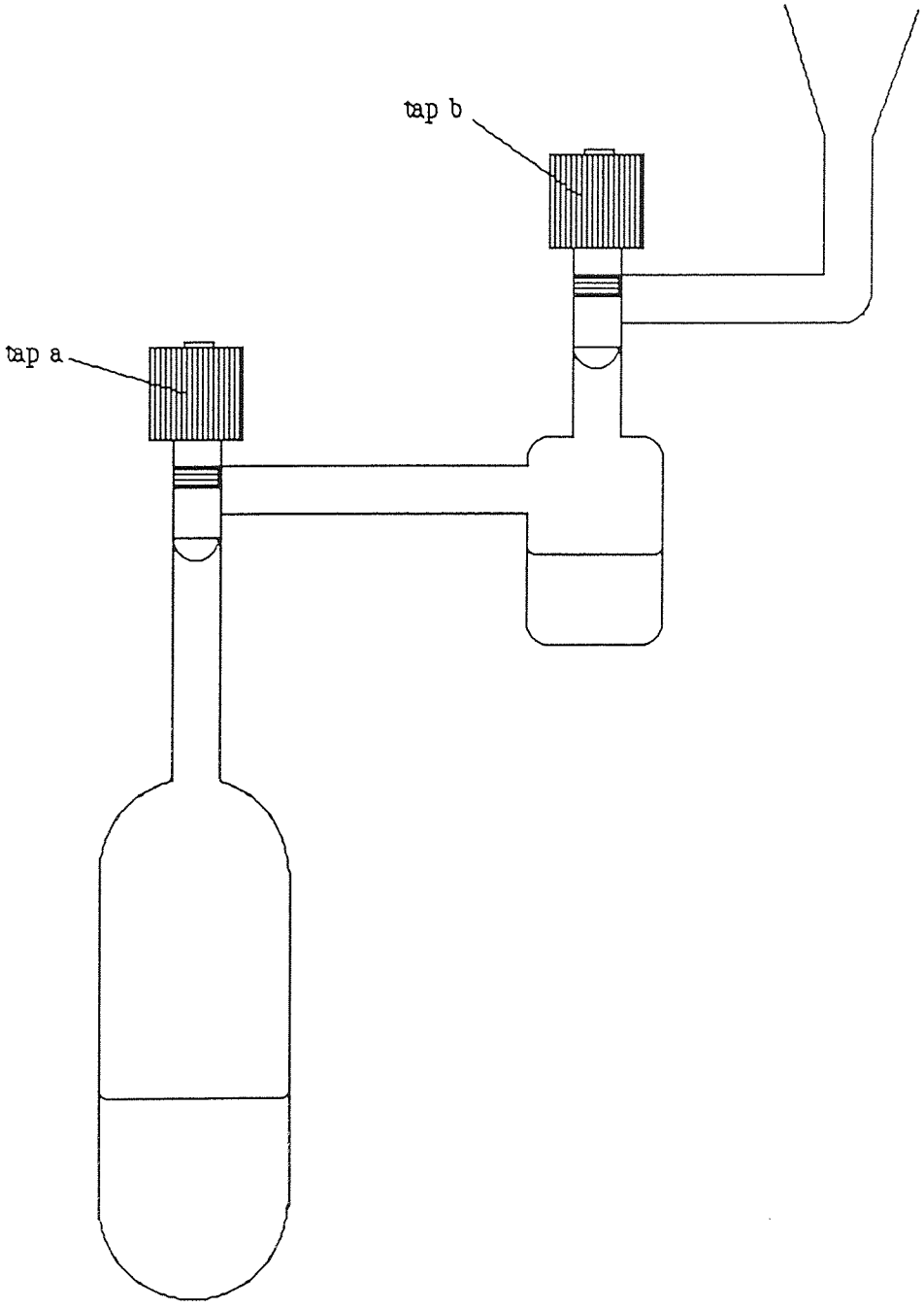

2.4 Preparation and Purification of Materials

2.4.1 Monomers

2.4.1.1 Methyl Methacrylate (MMA)

Methyl methacrylate of 99% purity was obtained commercially from the Aldrich Chemical Company, was inhibited with 65 ppm hydroquinone monomethyl ether which was removed by placing the monomer over sodium hydroxide pellets in a solvent flask for 24

hours. MMA was then distilled into another solvent flask containing calcium hydride where it was left to dry for 48 hours with the tap cracked open in order to enable hydrogen gas to escape.

During the earlier part of this project MMA was further dried by distilling it into a flask containing aluminium triethyl. This was a method devised by McGrath *et al* [83] whereby a yellow coloured solution formed when the methacrylate was placed in aluminium triethyl indicating the presence of a completely dry and ultrapure monomer. Care was taken when administering the aluminium triethyl since it is extremely pyrophoric in the presence of moisture and air. The aluminium triethyl was introduced into a clean dry flask under argon using the Schlenk technique (see section 2.2).

MMA was stored under refrigeration until required in order to prevent self-polymerization.

2.4.1.2 Styrene

Styrene of 99% purity was obtained from the Aldrich Chemical Company. It was inhibited with 10-15 ppm 4-tertbutylcatechol, which was removed by distillation from sodium hydroxide pellets as described in section 2.4.1.1.

The styrene was then distilled into a flask containing calcium hydride and left to dry for 48 hours with the tap of the flask cracked open. The styrene was further dried by distilling it into another flask containing freshly cut slices of sodium and a small amount of benzophenone. Following distillation, the styrene was degassed until the characteristic blue colour of the sodium/benzophenone radical anion complex was observed. This complex is very sensitive to oxygen and moisture and so could be used as an indicator of the efficiency of the drying process. Styrene was then stored under refrigeration until required.

Scheme 2.1 Formation of Sodium Benzophenone Complex

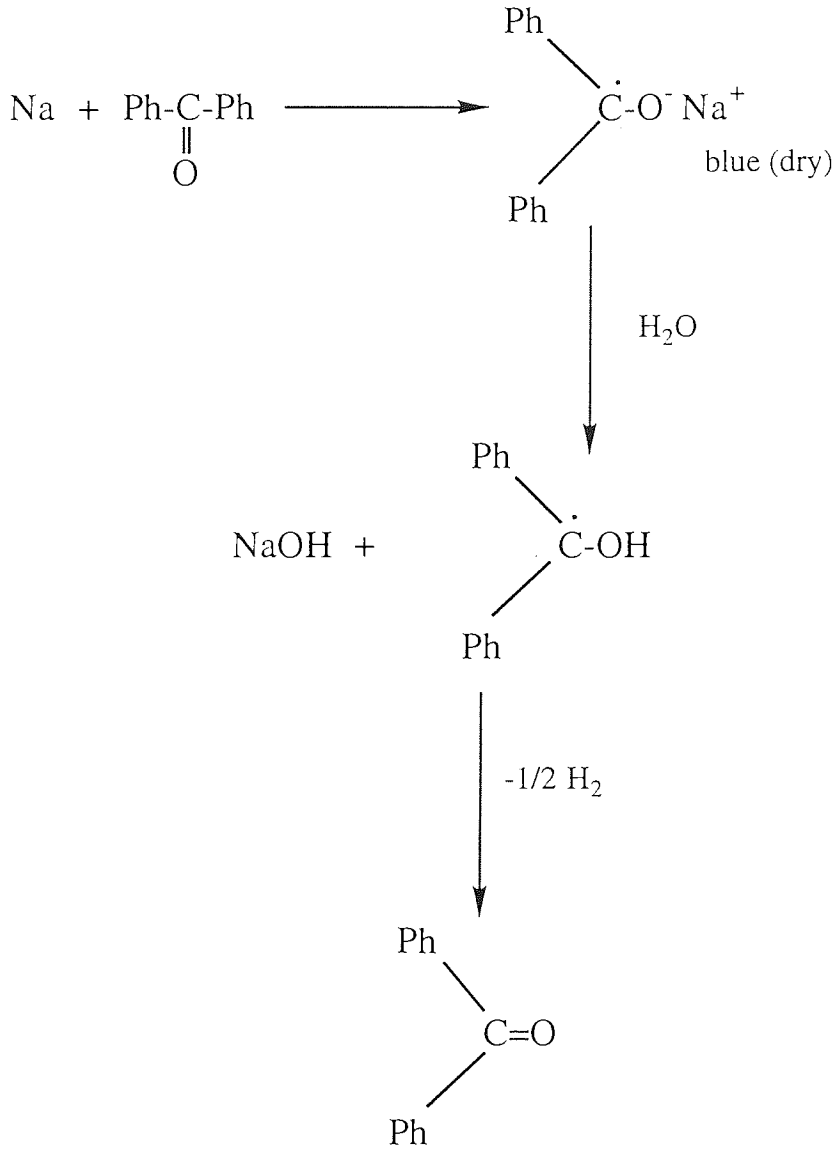

2.4.2 Solvents

2.4.2.1 Tetrahydrofuran (THF)

HPLC grade THF of 99.8% purity was obtained from Fisons, dried by standing over calcium hydride for 48 hours and then distilled into a flask containing the sodium/benzophenone complex. The indigo colour of the solution formed with the complex indicated its dryness and also the absence of peroxides. THF was stored in this way until required

2.4.2.2 Cyclohexane

A.C.S. spectrophotometric grade cyclohexane of 99+% purity was supplied by the Aldrich Chemical Company. It was dried in the same way as THF (see section 2.4.2.1).

2.4.2.3 Toluene

A.C.S. spectrophotometric grade toluene of 99.5% purity was supplied by BDH and dried over calcium hydride for 48 hours before use.

2.4.2.4 Methanol

Methanol of 99% purity was supplied by BDH and used for the purposes of precipitation of polymer samples out of solution.

2.4.3 Initiators and Catalysts

2.4.3.1 Butyllithium

Butyllithium was obtained from the Aldrich Chemical Company as a 1.6M solution in hexane. Ingress of moisture to the 'sure seal ' was prevented by transferring the initiator solution via the Schlenk technique (see section 2.2). Butyllithium was stored under refrigeration until required, in order to prevent decomposition.

2.4.3.2 *tert* -Butyllithium

tert -Butyllithium was obtained from the Aldrich Chemical Company as a 1.7M solution in pentane. It was stored and handled in the same way as butyllithium (see section 2.4.3.1).

2.4.3.3 Lithium Chloride (LiCl)

Anhydrous lithium chloride was obtained from Fisons. It was dried in a furnace at 350°C for 24 hours before use and transferred in a desiccator containing calcium chloride. A solution of the LiCl of known concentration was prepared by placing a weighed amount of LiCl into the large bulb of a catalyst flask and then distilling onto it a known volume of THF solvent.

2.4.3.4 Triethylaluminium

Triethylaluminium was obtained from Aldrich at 93% purity, packaged under nitrogen in a 'sure-pac' metal cylinder owing to its highly pyrophoric nature. It was stored in a cool, dry cupboard and transferred to the large bulb of the catalyst flask using the Schlenk technique (see section 2.2). A solution of known concentration was then prepared by distilling a known volume of dry toluene into the large bulb of the catalyst flask.

2.4.3.5 Triisobutylaluminium

Triisobutylaluminium was obtained from Aldrich at 99+% purity. It was packaged, stored and handled in the same way as triethylaluminium owing to its pyrophoric nature. A solution of the triisobutylaluminium was prepared in toluene using the method described for triethylaluminium (see section 2.4.3.4).

2.4.4 Drying and Purification Agents

2.4.4.1 Calcium Chloride

Anhydrous calcium chloride was obtained as a powder from B.D.H and was used as supplied.

2.4.4.2 Calcium Hydride

Anhydrous calcium hydride of 95% purity was obtained in powdered form from the Aldrich Chemical Company and used as supplied.

2.4.4.3 Sodium Metal

Sodium metal was supplied in paraffin oil by B.D.H. The paraffin oil was removed by washing with dry THF and any tarnished pieces of sodium were discarded before use.

2.4.4.4 Benzophenone

Benzophenone of 99% purity was obtained from Janssen Chimica and used as supplied.

2.4.4.5 Sodium Hydroxide

A.C.S. grade sodium hydroxide of 97+% purity was supplied in the form of pellets by the Aldrich Chemical Company and was used as supplied.

2.4.4.6 Silver Nitrate

Solid silver nitrate of 99+% purity was supplied by the Aldrich Chemical Company and prepared as a 0.1M solution.

2.5 Polymerization Techniques

2.5.1 Procedure

Polymerizations were carried out in a polymerization vessel of the type shown in figure 2.6.

Figure 2.6 The Polymerization Vessel

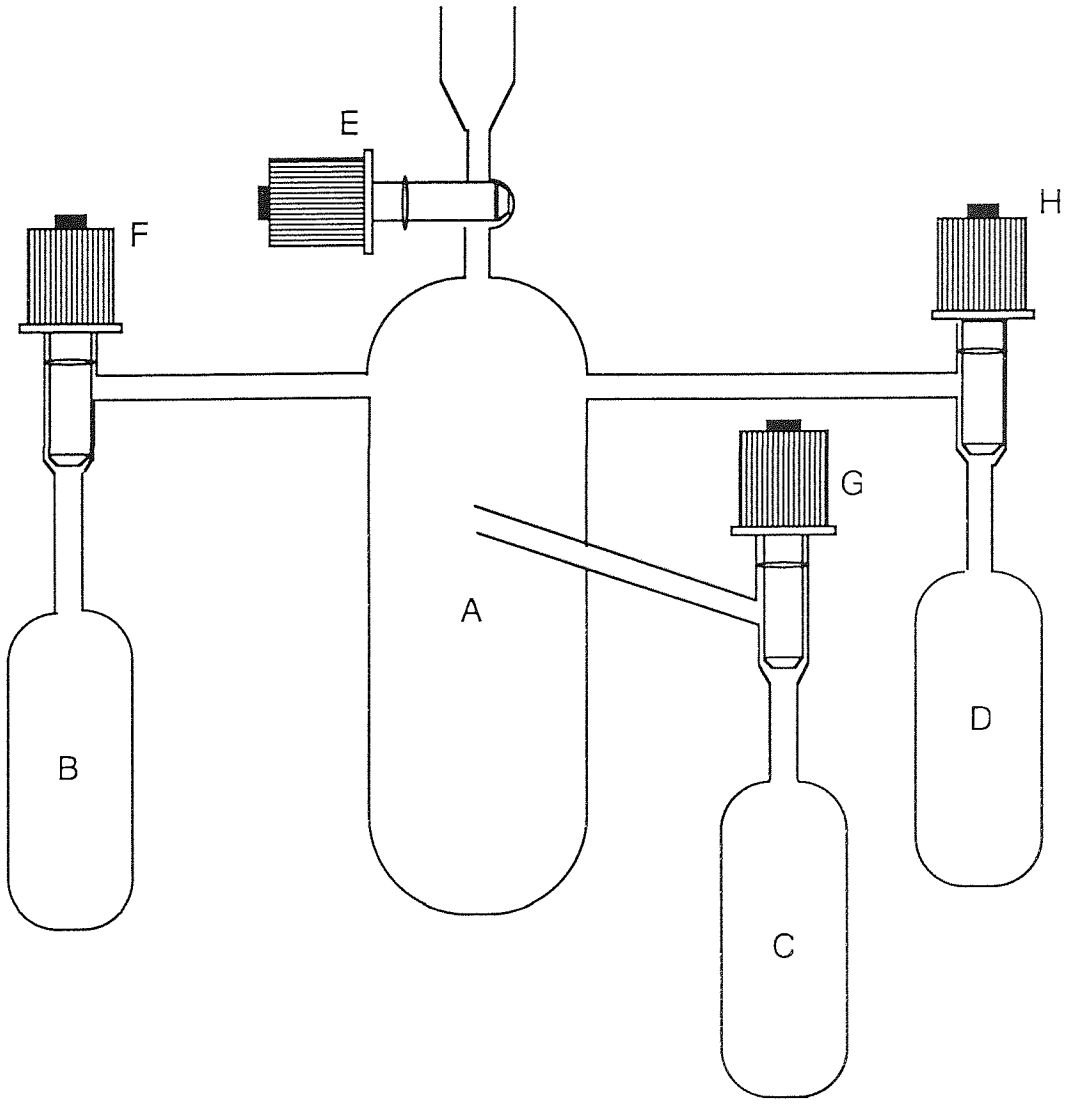

Typically, the monomer, e.g methyl methacrylate, was distilled into bulb B along with some solvent. The cocatalyst solution lithium chloride or aluminium alkyl, was then injected using the Schlenk technique into bulb C via tap G and a portion of the solvent required was also distilled into the bulb. The initiator, butyllithium, was injected via tap H

into bulb D by the Schlenk technique. The remaining quantity of solvent was distilled into the large bulb A. During copolymerization procedures the other monomer (styrene) was distilled into bulb A along with the solvent.

The apparatus was first immersed in a thermostatically controlled constant temperature bath for 30 minutes before polymerization was commenced. For lower temperature polymerizations an ice bath or methanol/cardice bath was used. Polymerization was then carried out by opening in turn the appropriate taps and sequentially pouring the cocatalyst, initiator and monomer solutions into bulb A, with vigorous shaking to ensure that all the reagents were thoroughly mixed.

Some polymerizations of methyl methacrylate were followed using SEC techniques. The extent of conversion of the polymerization could be followed by taking samples at appropriate time intervals, and injecting them through the SEC columns in order to monitor the increase in molecular weight, as a function of percentage conversion.

2.5.2 Dilatometry

2.5.2.1 Principles

Dilatometry is a technique used to measure changes in density of liquids[84]. During the course of a polymerization, the increase in density associated with the conversion of monomer to polymer can be used to monitor the extent of conversion in a polymerization.

The contracting reaction mixture is contained within a bulb of known volume attached to which is a capillary tube of uniform cross-sectional area. During reactions, the height of the meniscus in the capillary tube is measured, at noted times, using a cathetometer.

The accuracy of the technique depends upon a number of factors :

(i) The polymerization must be carried out at constant temperature in a thermostatted bath, in order to avoid thermal fluctuations of the meniscus.

(ii) When the polymerization is exothermic the heat evolved should be readily conducted to the walls of the vessel. Therefore, polymerizations should be conducted at rates that do not generate excessive heat.

(iii) The capillary of the dilatometer should be sufficiently narrow to detect small changes in volume and should be of uniform bore.

(iv) Polymerizations should be carried out at a rates that are readily followed.

(v) The extent of monomer to polymer conversion should be kept low otherwise the polymerization mixture may become too viscous for the meniscus to move.

In the analysis of the data generated, the density of the polymer is assumed to be the density of the polymer in the solid state. The error produced from this assumption is normally negligible.

2.5.2.2 Experimental

In this project dilatometry was used in an attempt to determine the kinetics of copolymerization of styrene and methyl methacrylate. The dilatometer used in this project is shown in figure 2.7.

Solutions of methyl methacrylate and styrene in THF were prepared separately and stored in solvent storage vessels (see figure 2.4). The dilatometer was then attached to the vacuum line via tap H and evacuated. The flask containing diluted MMA was attached to the dilatometer at tap I and the system was re-evacuated. Taps E and F were then opened to enable the MMA to be poured into bulb B of the dilatometer and tap F was then closed. The flask containing MMA was removed and that containing diluted styrene was attached. The system was evacuated and the styrene solution was poured into bulb A via tap E using the same method as for MMA. Tap E was then closed and the dilatometer was then removed from the vacuum line. The amounts of each solution admitted to the dilatometer were determined by weighed difference. The cocatalyst and initiator solutions were sequentially injected into bulb A via the subaseal D. Tap F was then opened and the dilatometer vigorously shaken to enable the reagents to mix in bulb B, at which point the

timer was started. Tap G was then opened and the solution poured into bulb C, which enabled the capillary K to fill with the homogeneous solution so that the meniscus was almost to the top of the capillary. Space was left at the top at point J to account for expansion of the solution when placed in a warm water bath. The dilatometer was then completely immersed into a water bath set at constant temperature and the change in meniscus height at appropriate time intervals was determined using a cathetometer.

Figure 2.7 The Dilatometer

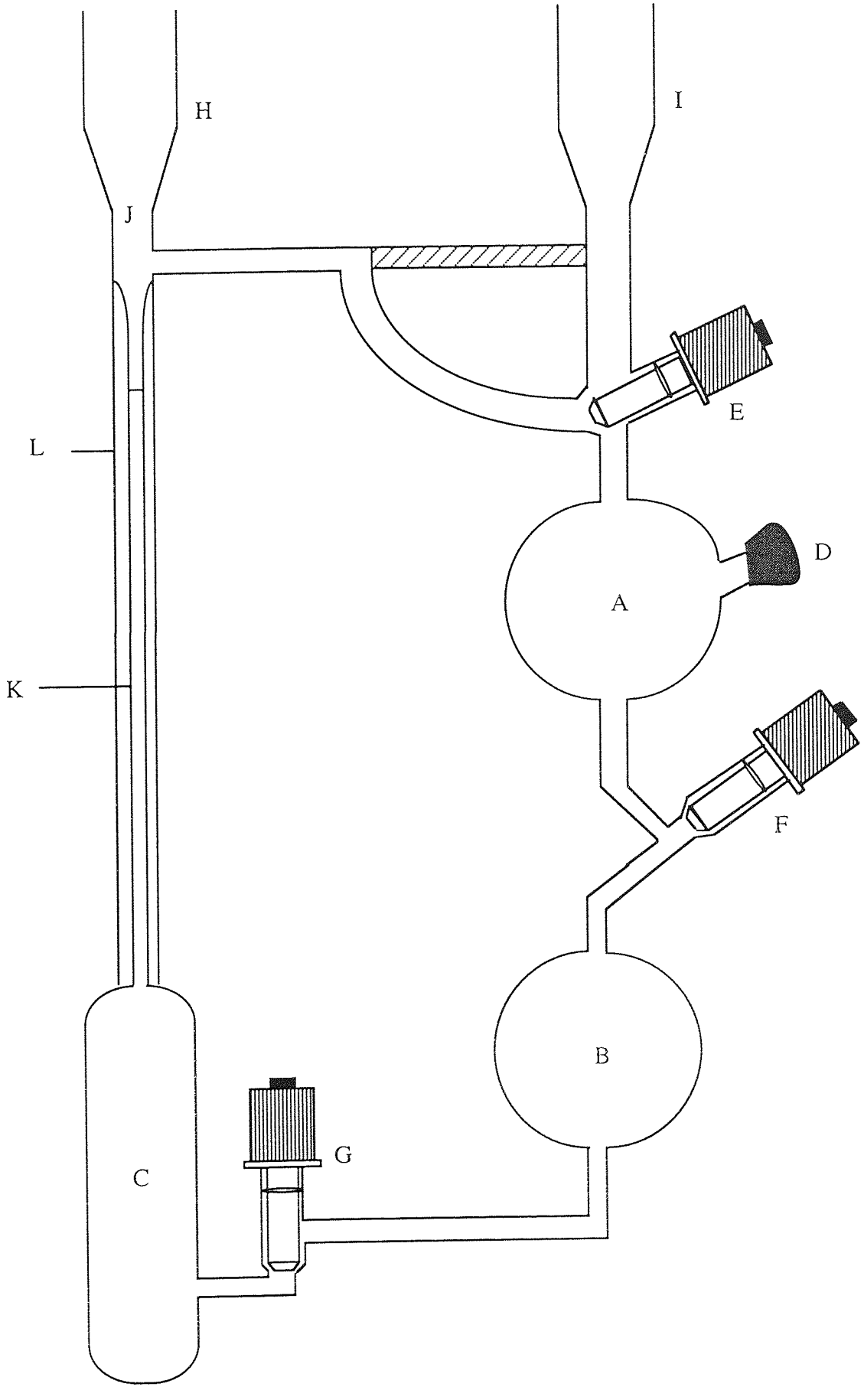

2.5.2.3 Discussion

The distance moved by the meniscus (Δh / cm) between two points in the capillary gives a decrease in volume (ΔV / cm^3) of

$$\Delta V = \pi r^2 \Delta h \qquad (2.1)$$

where r = radius of the capillary / cm

When m grams of monomer is completely converted to m grams of polymer, the volume of contraction would be :

$$\Delta V = V_p - V_m = \frac{m}{\rho_p} - \frac{m}{\rho_m} = m\frac{(\rho_m - \rho_p)}{\rho_p \cdot \rho_m} \qquad (2.2)$$

Then :

$$\frac{1}{\Delta V} = \frac{1}{m}\frac{\rho_p \cdot \rho_m}{(\rho_m - \rho_p)} \qquad (2.3)$$

where V_p = volume of polymer

V_m = volume of monomer

ρ_p = density of polymer

ρ_m = density of monomer

If ΔM is the number of moles of monomer polymerized then

$$\Delta M = \frac{m}{M} = \frac{\Delta V}{M}\frac{\rho_p \cdot \rho_m}{(\rho_m - \rho_p)} \qquad (2.4)$$

where M = molecular weight of polymer.

Assuming that the volume of the dilatometer (V) is much greater than the total volume change (ΔV), then any variation in the monomer concentration $\Delta[M]$ can be approximated to:

$$\Delta[M] = \frac{\Delta M}{V} = \frac{1}{V}\frac{\Delta V}{M}\frac{\rho_p \cdot \rho_m}{(\rho_m - \rho_p)} = \frac{\pi r^2 \Delta h}{VM}\frac{\rho_p \cdot \rho_m}{(\rho_m - \rho_p)} \qquad (2.5)$$

where $\frac{\pi r^2}{VM}\frac{\rho_p \cdot \rho_m}{(\rho_m - \rho_p)}$ is a constant (K) for the system under study

So that $$\Delta[M] = K\Delta h \qquad (2.6)$$

For the system studied in this investigation, the value of K was calculated from the following :

r = radius of capillary (0.05 cm)

V = volume of bulb (20.5 cm^3)

ρ_m = density of MMA (0.935 g cm^{-3})

ρ_p = density of PMMA (1.19 g cm^{-3})

2.5.3 Recovery of Polymers

Polymers were recovered by releasing the vacuum in the polymerization vessel to nitrogen and pouring the contents into approximately 300 cm^3 of stirred cold methanol. The polymer was filtered and reprecipitated from THF by pouring into more methanol. Final recovery of the polymer was obtained by filtering the solid at the pump or distilling off the methanol on the rotary evaporator and leaving it to dry under vacuum at 40°C for 24 hours.

2.6 Analytical Techniques

2.6.1 Size Exclusion Chromatography (SEC)

2.6.1.1 Principles

Size Exclusion Chromatography (SEC), otherwise known as Gel Permeation Chromatography (GPC), is a technique used to determine the molecular weight distributions of polymer samples. In this technique polymer samples are separated into fractions according to the hydrodynamic volume of the polymer molecules by means of a sieving action. Samples in solution are passed through a series of columns containing a stationary phase of cross-linked polystyrene beads, which swell when solvent is introduced into the column. This stationary phase is constructed so that when swelling occurs, surface pores with a distribution of pore sizes are generated. Each pore allows only polymer chains of hydrodynamic volume smaller or equal to the volume of the pore to enter it. The larger polymer chains therefore have a smaller pore volume available to them than the smaller polymer molecules and consequently move more rapidly through the column.

Figure 2.8 The Size Exclusion Chromatograph

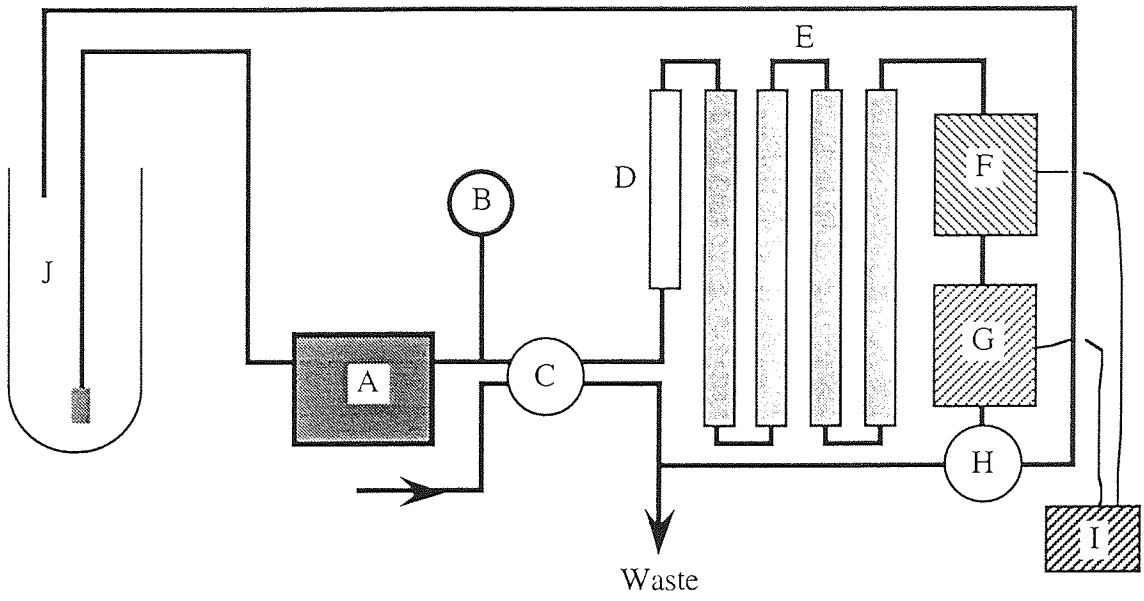

A	HPLC pump	B	Pressure gauge	C	Valve and loop injector
D	Pre-column	E	PL-Gel columns	F	RI detector
G	UV detector	H	Solvent Recycler	I	Chart recorder
J	Solvent reservoir				

2.6.1.2 Experimental

The eluent used for SEC was HPLC grade THF which was pumped at 1 cm^3 per minute by a Knauer HPLC pump (A). Samples of the polymer were prepared in THF (1-2% w/v) and injected into the columns by a 100µl valve and loop injector system. The solution was pumped through a series of four µ-PL gel columns supplied by Polymer Laboratories and a short pre-column which removed any suspended material. The SEC columns had exclusion limits of 10^2, 10^3, 10^4, and 10^5 Å respectively. After separation in these columns, the polymer was detected by passing the outflow from the last column through a differential refractometer (F) and UV / visible spectrophotometer detector (G). These detectors were connected in series and both were supplied by Polymer Laboratories; the outputs from these were recorded on a dual-pen chart recorder (I). The differential refractometer continuously monitored the refractive index (R.I.) of the eluting solution and compared it with the R.I. of pure eluent. Any difference between the two

generated a deflection on the chart recorder which was proportional to the concentration of the eluting polymer at that time. The UV detector responded to chromophoric groups either attached to, or part of the polymer backbone e.g. polystyrene. The response this detector gave was proportional to the concentration of the solute presesnt in the solution and the molar extinction coefficient of the solute at the set wavelength. While samples were passing through the column, any solvent containing polymer particles was run to waste, but pure uncontaminated solvent was re-routed back to the solvent reservoir (J) via the solvent recycler (H).

For copolymerizations of styrene and methyl methacrylate, a direct comparison of the heights of the two different traces obtained from the R.I. and UV detectors respectively, enabled the estimation of the quantity of polystyrene found in the copolymer.

2.6.1.3 Calibration of the SEC

To estimate the number and weight average molecular weights it was necessary first to determine how the molecular weight of eluted polymer varied over the range of elution volumes. Thus the columns were calibrated with polystyrene standards (obtained from Polymer Laboratories) and any values quoted for $\overline{\overline{M}}_n$ or $\overline{\overline{M}}_w$ are with respect to polystyrene. Polystyrene samples of narrow molecular weight distribution and of known molecular weights were injected into the column. The elution volume of the polymer sample of specific molecular weight was measured and a calibration curve was plotted as shown in figure 2.9. Comparison of the elution volumes of different polymer samples enables a polystyrene equivalent molecular weight for most polymers to be obtained.

Figure 2.9 Calibration Curve for SEC (Polystyrene)

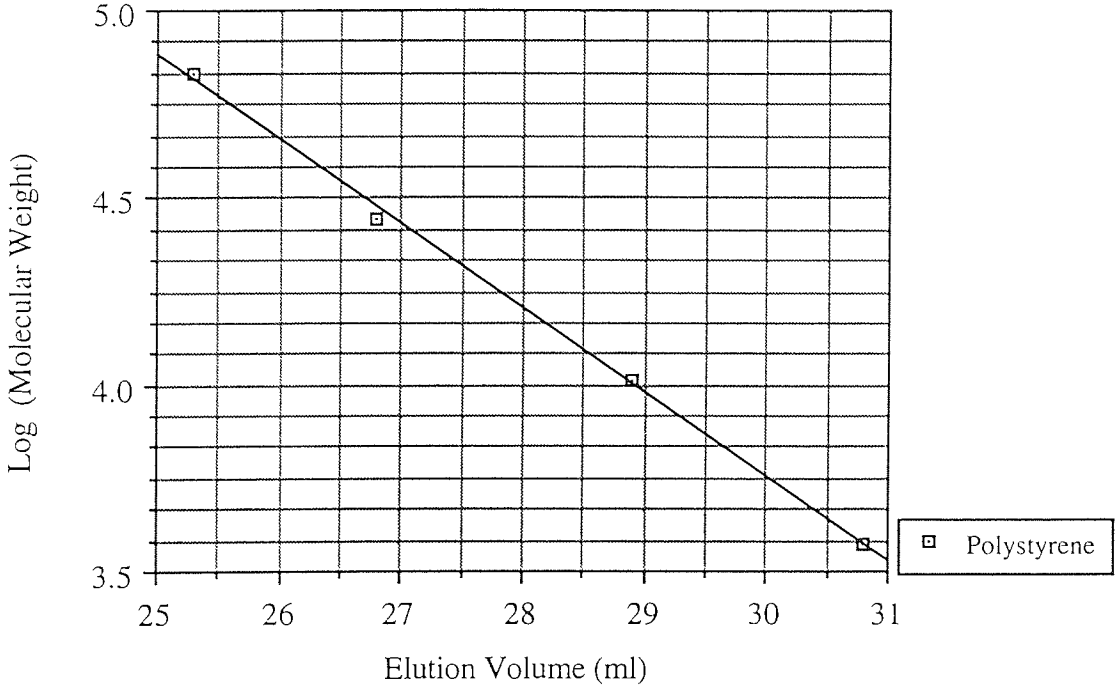

Figure 2.10 A Typical SEC Trace.

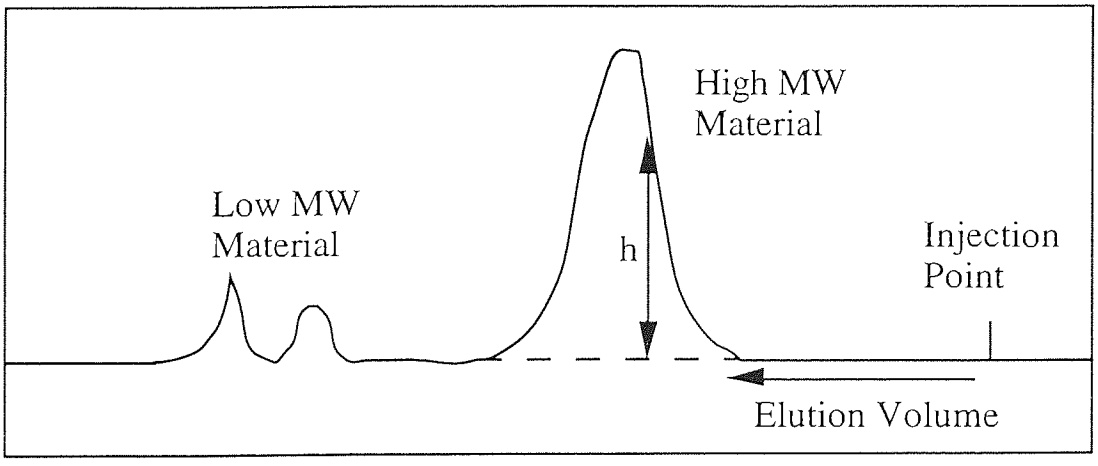

To determine the number average molecular weight $\overline{M}_n$, and the weight average molecular weight $\overline{M}_w$, of a polymeric material analysis of the chromatogram, which shows the dependence of refractive index (Δn) or absorbance (A) of the eluent on elution volume, has to be carried out. If a differential refractometer is used, Δn at any particular elution

volume is proportional to the perpendicular height (h_i). Δn is proportional to the concentration c_i, of the polymer in the eluent; and hence the weight fraction W_i, of the polymer in a sample of that particular molecular weight (M_i).

From these relationships $\overline{M}_n$ and $\overline{M}_w$ can be calculated since :

$$\overline{M}_n = \frac{\sum N_i M_i}{\sum N_i} \quad \text{and} \quad \overline{M}_w = \frac{\sum N_i M_i^2}{N_i M_i} \qquad (2.7)$$

where N_i = number of molecules of molecular weight M_i in a given sample

If W_i is the weight fraction of polymer of molecular weight M_i in a given fraction then NiMi α Wi and,

$$N_i \alpha \frac{W_i}{M_i} \qquad (2.8)$$

$$\therefore \overline{M}_n = \frac{\sum W_i}{\sum W_i/M_i} \quad \text{and} \quad \overline{M}_w = \frac{\sum W_i M_i}{\sum W_i} \qquad (2.9)$$

Given the above relationships :

$$\overline{M}_n = \frac{\sum h_i}{\sum h_i/M_i} \quad \text{and} \quad M_w = \frac{\sum h_i M_i}{\sum h_i} \qquad (2.10)$$

The calibration curve provides the dependence of M_i on elution volume and hence values of the above averages can be obtained by carrying out the summations shown in equation (2.10). In practice, this data was processed using Excel 3, a spreadsheet package run on a Macintosh 'Classic' 40Mb computer.

2.6.2 Gas Chromatography (GC)

2.6.2.1 Principles

Gas Chromatography (GC), is used for the separation of mixtures of volatile compounds which may differ in boiling point by only a fraction of a degree[85]. The sample to be analysed is volatilised and swept by a stream of carrier gas through a heated column containing an absorbent support with a specific large surface area impregnated with an involatile liquid which acts as the stationary phase (see figure 2.11). The carrier gas must

be inert to both the column material and the components of the sample. Nitrogen, helium or argon may be used depending on the detector used.

The partition component of a mixture between the stationary phase and the carrier gas depends on a combination of its volatility and interaction with the stationary phase. The components of the mixture separate on the column according to a difference in partition factors then pass in turn over a detector, in this case a flame ionization detector. The lapsed time between injection onto the column and elution of a particular component is referred to as the retention time. Increasing the rate of flow of carrier gas, as well as raising the oven temperature surrounding the coil, increases the rate of elution.

Figure 2.11 The Gas Chromatograph

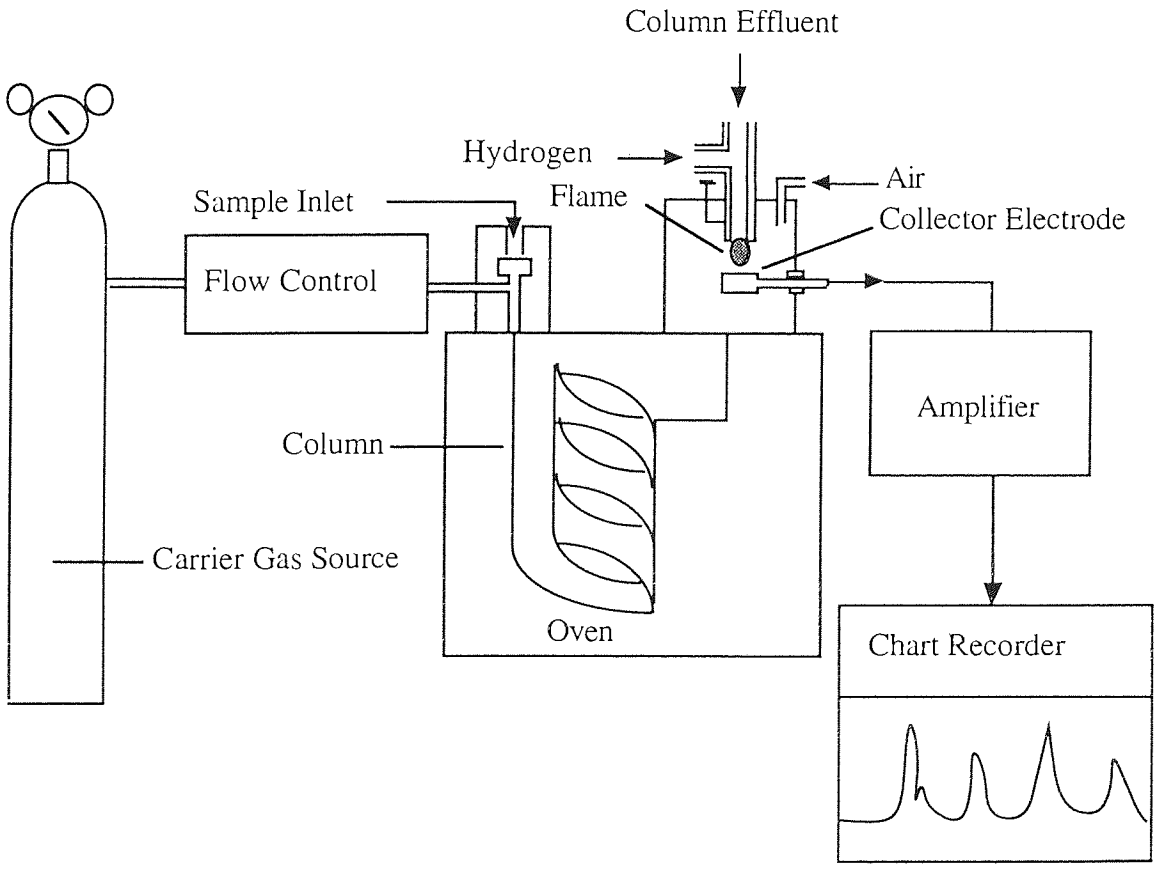

2.6.2.2 Experimental

The instrument used during the course of this project was a Pye Unicam GCD Chromatograph. 1µl samples were introduced onto the column by syringe via the

injection port. The samples were volatilised and carried over by nitrogen gas. The combination of a silicon grease stationary phase for the column, and an oven temperature set at 90°C gave the best separation of components for the samples analysed in this project. The separated components were passed over a flame ionization detector; the response from which was sent to a Hewlett Packard data collector and printer complete with integrator. The integrator calculated the areas under the peaks corresponding to the separated components in order to give a measure of the relative quantities of materials present in the original sample mixture.

In this project GLC was used to analyse the extent of conversion in the polymerization system. Samples were removed from the polymerization mixture at appropriate time intervals and injected into the GLC in order to monitor the decay in monomer concentration as it was converted into polymer. The areas under the MMA peaks were converted into concentrations by means of plotting a calibration curve (see figure 2.12). This was achieved by injecting samples of MMA of known concentration made up as solutions in toluene which acted as standards. The peak areas of the MMA and toluene samples at specific concentrations was measured and a calibration curve was plotted. Comparison of the peak areas for different MMA concentrations in a polymerization mixture enabled the exact concentration of MMA at a particular time during the polymerization to be obtained.

Figure 2.12 Calibration Curve for GC (MMA)

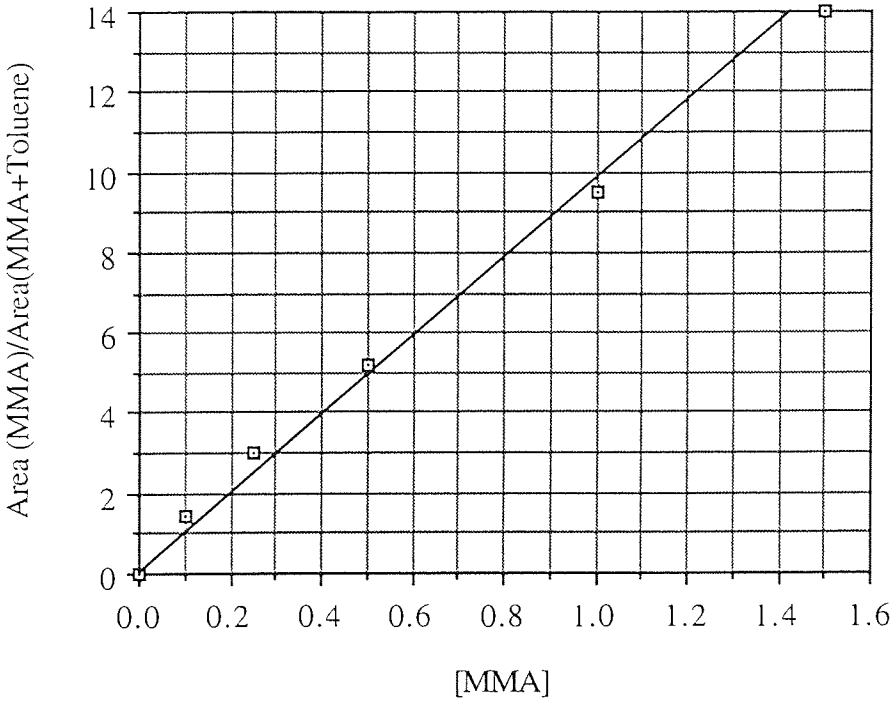

2.6.3 Nuclear Magnetic Resonance Spectroscopy (NMR)

2.6.3.1 Experimental

During the course of this project high resolution NMR spectroscopy was carried out on a AC300 Bruker Fourier Transform spectrometer operating at 300 MHz. A solution of the solid polymer sample was made up by dissolving in deuterated chloroform ($CDCl_3$) and the sample tube was placed precisely between the poles of a powerful magnet to create an energy difference between the two states. Both ^{1}H NMR and ^{13}C NMR spectra were obtained.

2.6.3.2 Determination of Stereochemistry of Methyl Methacrylate Polymers

During the course of this project NMR was used to determine the stereochemistry of the methyl methacrylate polymers obtained. In PMMA three different steric configurations of the polymer exist which are shown in figure 2.13.

Figure 2.13 Three Steric Configurations of PMMA

ISOTACTIC TRIAD

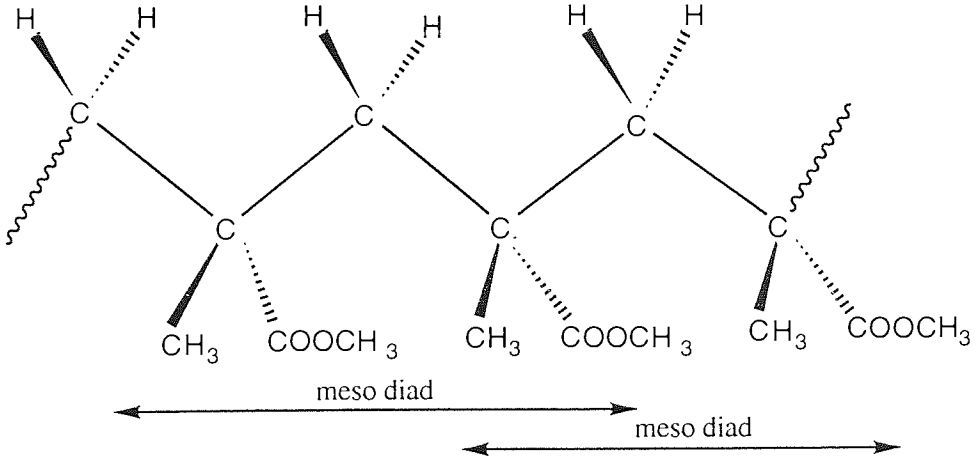

SYNDIOTACTICTRIAD

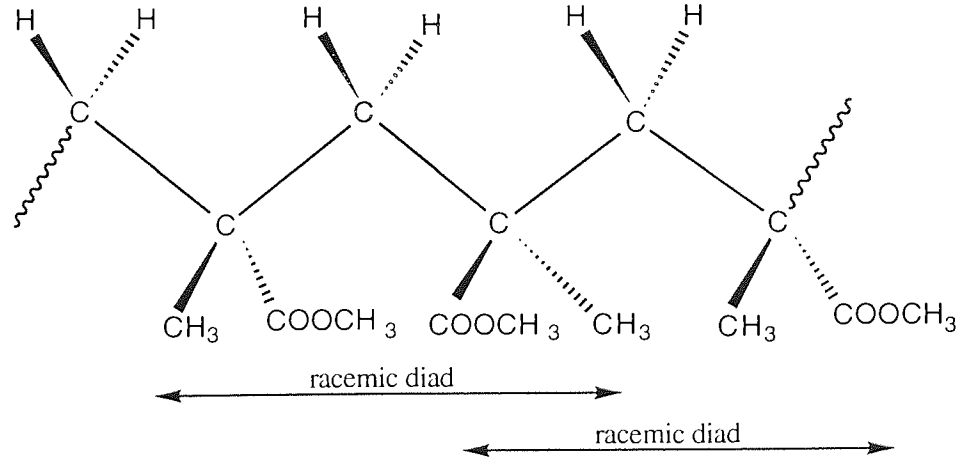

HETEROTACTIC TRIAD

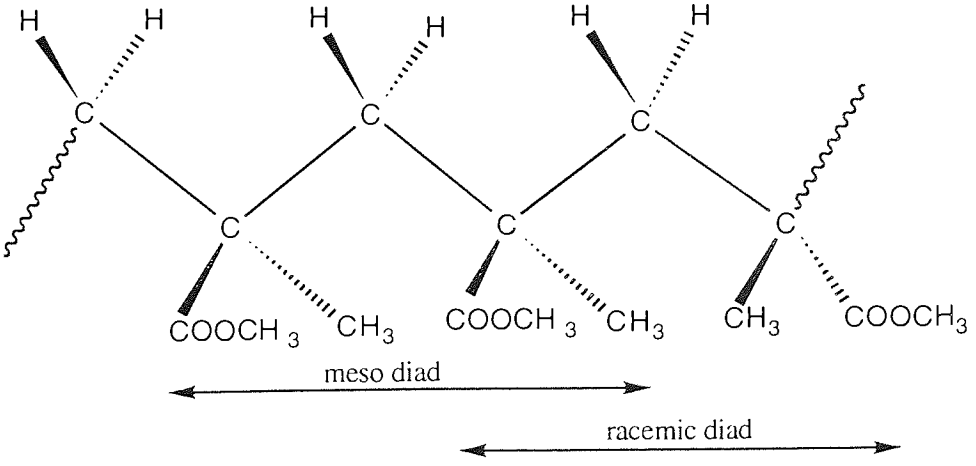

The polymer chain can be arranged in a planar zig-zag conformation, whereby the substituents on alternate carbon atoms may project either in front of or behind the plane of the chain. The stereochemical nomenclature of the chain can be simplified by considering it to be composed of a number of consecutive diad units. A diad is defined as comprising of two methine carbons and each diad can be described as either a meso (m), or racemic (r), diad. When all the diads in the polymer chain are all of the meso type, the substituents on all the carbon atoms project in the same direction with respect to the planar zig-zag polymer chain and such structures are referred to as ISOTACTIC. A polymer chain comprising exclusively of racemic diads is known as a SYNDIOTACTIC polymer, and the substituent groups alternate regularly in direction of projection. When there is a statistical distribution of meso and racemic diads along the backbone of the chain the structure is known as HETEROTACTIC or ATACTIC.

In pure PMMA three types of protons are present :

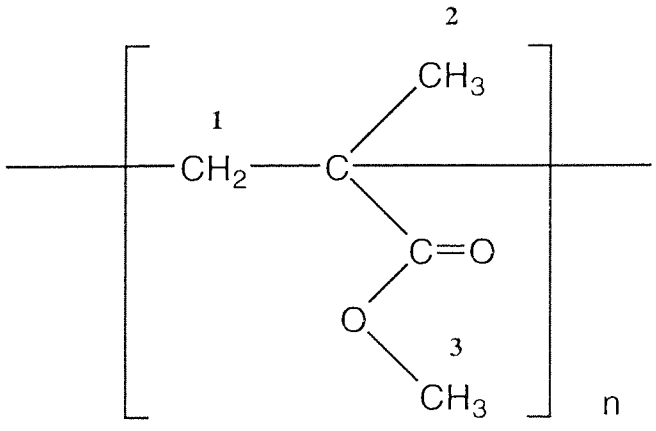

The ^1H NMR spectrum of PMMA is composed only of single peaks and there are no coupling effects since there is no α hydrogen on the quartenary carbon atom. There are, however, three peaks associated with the α-CH_3 group due to the three different steric configurations of PMMA. For the purposes of ^1H NMR measurements, three consecutive monomer units in a chain are considered to define a triad. The three equivalent protons of the α-CH_3 group absorb radiation at a single frequency, but this frequency is different for each of the three kinds of triad because the environment of the α-CH_3 in each of the triads is different. Thus in a sample with a mixture of

configurations, a triple peak will be observed and the area under each of these peaks will correspond to the amount of each triad present in the polymer chain.

The fraction of each configuration, P_i (isotactic), P_s (syndiotactic), and P_h (heterotactic), measured from the respective peak areas, can be related to σ; that a monomer adding on to the end of a growing chain, will do so in order to generate a meso diad in the chain i.e. σ, is the probability of a diad in the polymer being an isotactic diad.

By definition :-

$$P_i = \sigma^2 \qquad \text{(mm)}$$

$$P_s = (1-\sigma)^2 \qquad \text{(rr)}$$

$$P_h = 1 - Pi - Ps = 2(\sigma - \sigma^2) = 2\sigma\,(1-\sigma) \qquad \text{(rm)(mr)}$$

The proportion of heterotactic units rises to a maximum at $\sigma = 0.5$ (random propagation). For a random polymer, the ratios i : h : s = 1 : 2 : 1.

2.6.4 Infrared Spectroscopy (IR)

Samples of the polymers were prepared as KBr discs and their structures characterised using a 1710 Perkin-Elmer Fourier Transform spectrometer. Small amounts of the polymer samples were ground with oven-dried (120°C) potassium bromide (KBr) powder until a homogeneous mixture was produced. Discs were prepared by compressing this mixture in a hydraulic press and die. The spectra were produced from the data, obtained as a set of ten scans at a resolution of 4 cm^{-1}, and manipulated using a Perkin-Elmer infra-red data manager.

2.6.5 U.V/Visible Spectrophotometry

UV/Visible spectroscopy has often been used to detect the presence of conjugation in multiple bonded systems. The π - π * transition is often intense and occurs around 180 nm for an isolated double bond. As the degree of conjugation increases, the absorption shifts to progressively longer wavelengths (e.g butadiene, λ_{max} = 217 nm; hexatriene, λ_{max} = 258 nm)

UV/Visible spectra of the soluble polymer samples were recorded on a SP8-100 Pye Unicam spectrophotometer using a solution of the polymer in a quartz cuvette cell with an optical path length of 10mm. HPLC grade THF was used as solvent and reference. In this project uv/visible spectrophotometry was used to determine the composition of copolymers of styrene and methyl methacrylate by comparing the extinction coefficient of the copolymer with that for polystyrene. Samples of polystyrene or copolymer were dissolved in THF to prepare solutions of several different concentrations. The absorbance at 254 nm was obtained for each solution, since polystyrene shows a λ_{max} at 254 nm. A graph was plotted of absorbance against concentration and the gradient of the line obtained gave the extinction coefficient for that sample.

In a typical analysis of a copolymer the percentage composition of polystyrene and hence, that of PMMA could be obtained.

2.6.6 Determination of the Concentration of LiCl/THF Solution.

Lithium chloride was prepared as a solution in THF in a catalyst flask as described in section 2.3. The concentration of this solution was determined accurately by potentiometric titration; a technique developed by Ingram[86].

2.6.6.1 Experimental

Exactly 1ml of the LiCl/THF solution to be determined was syringed accurately into a 100 ml beaker to which approximately 20 mls of water was added. This was titrated against 0.1M silver (I) nitrate solution. The titration results in the formation of silver chloride :

$$K_s = [Ag^+] [Cl^-]$$

The apparatus used to carry out titration is shown in figure 2.14).

Figure 2.14 Potentiometric Titration Apparatus

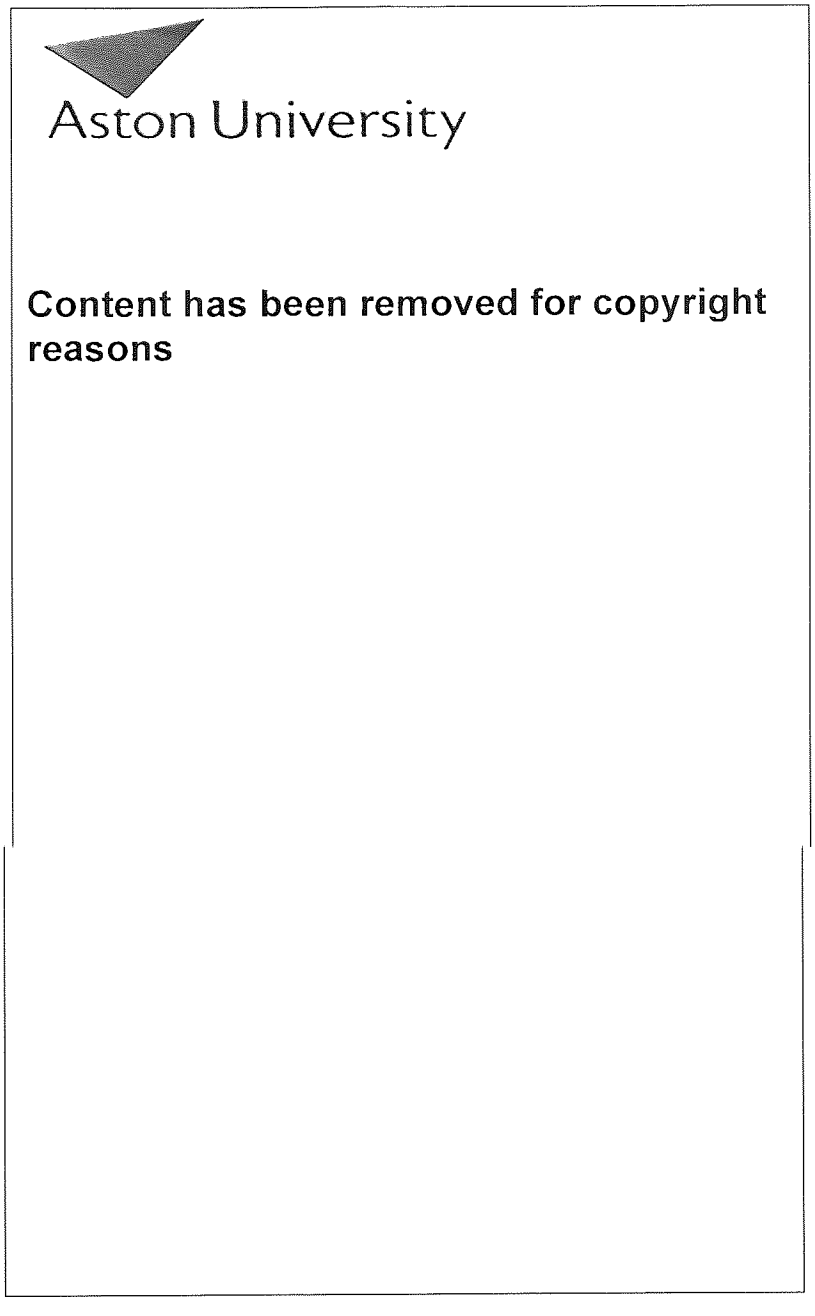

It

A Corning 220 millivolt meter was used to follow the potential difference of the half-cell Ag/Ag^+, using a combination electrode constructed from silver wire (supplied by Fisons) and a Ag/AgCl reference electrode (supplied by Gallenkamp).

$$Ag \longrightarrow Ag^+ + e^-$$

$$E = E^{\circ} + \frac{RT}{F} \ln \frac{[Ag^{+}]}{[Ag]}$$

The voltage was plotted against the volume of silver (I) nitrate solution added, to produce a curve with a sharp increase in voltage at the equivalence point, owing to an excess of Ag^{+} when the Cl^{-} are depleted (see figure 2.15).

The system was tested using standard solutions of sodium chloride and titrations were performed in duplicate to an accuracy of ±0.5 % .

Figure 2.15 Plot of Voltage against Volume of Silver Nitrate in the Potentiometric Titration of Lithium Chloride Solution

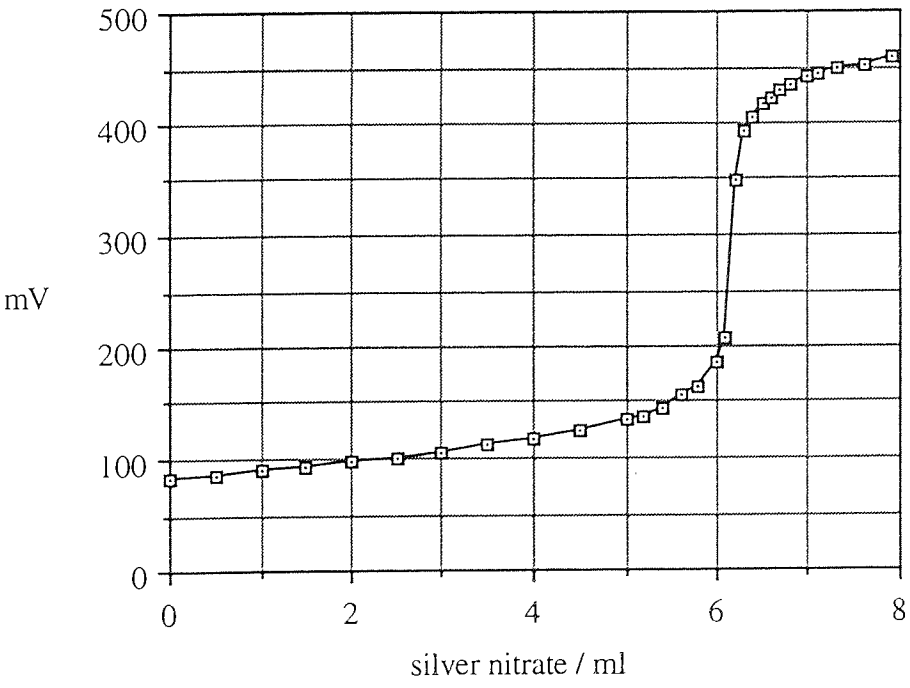

From the volume of silver nitrate at the equivalence point, the concentration of chloride ions in the 1 ml sample of LiCl in a solution of THF can be accurately determined.

CHAPTER THREE

ANIONIC BLOCK COPOLYMERIZATION OF STYRENE AND METHYL METHACRYLATE IN THE PRESENCE OF LITHIUM CHLORIDE

3.1 Introduction

The synthesis of methyl methacrylate polymers and block copolymers in the presence of lithium chloride was first pioneered by Teyssie *et al.*[59,60], who demonstrated that living poly(methyl methacrylate) could be prepared using anionic polymerization techniques. The molecular weight distributions of the polymers obtained were found to be considerably lower when LiCl was added to the initiator, which was butyllithium. Teyssie and co-workers concluded that the LiCl formed adducts with the propagating centres, which prevented the occurrence of transfer and termination reactions.

Contrary to the findings of Teyssie *et al*, Muller *et al* [66] showed that LiCl had no effect on the termination of MMA polymerization. Muller and co-workers demonstrated by kinetic studies that the main function of the LiCl was to deplete the system of slowly interconverting associated/non-associated ion pair equilibria and hence produce polymers of narrow molecular weight distribution. This was believed to be achieved by the formation of LiCl adducts, which compete with association of ion pairs and since the equilibrium between free and LiCl complexed ion pairs is faster than that between free and associated ion pairs, the equilibrium lies towards the former. Hence the fraction of non-associated species increases on addition of LiCl. The reactivity of the associates was found to be much lower than that of free ion pairs; the dynamics of the association equilibrium having a significant influence on molecular weight distribution of the polymers formed. A broadening of molecular weight distribution is therefore due to a rate of interconversion of associated and non-associated ion-pairs comparable to the rate of monomer addition. Muller concluded that the positions of the association/complexation

equilibria strongly affect the kinetics of polymerization, whereas the dynamics are responsible for the molecular weight distributions of the polymers obtained.

This chapter describes work carried out on the anionic block copolymerization of styrene and methyl methacrylate in the presence of lithium chloride. The effect of LiCl on the molecular weight distributions of the polymers was investigated. An attempt to study the kinetics of polymerization using dilatometry was undertaken, in order to grasp a better understanding of the role of LiCl on the mechanism of polymerization.

3.2 Experimental

A series of experiments was designed to carry out block copolymerizations of styrene and methyl methacrylate using butyllithium initiator in the presence of lithium chloride. The ratio [LiCl]/[BuLi] was altered to ascertain its effect on the molecular weight distribution on the polymers produced. The extent of conversion for some of the polymerizations was investigated using dilatometry.

3.2.1 Polymerization

The polymerizations were carried out in the polymerization vessel shown in figure 2.6, section 2.5.1. Transfer of all reagents into the vessel was carried out as described in section 2.5.1. The solvent, THF, was distilled into bulb A of the vessel along with the styrene. The BuLi in bulb D, was added to the solution of styrene in bulb A, by opening tap H. The resulting polystyryl lithium formed was deep red, which indicated the presence of living polystyryl ends. The LiCl, as a solution in THF, was added immediately to the polystyryl lithium from bulb C. Upon addition of the LiCl, the polystyryl lithium exhibited no change in the intensity of colour, indicating that the active centres were left intact by addition of the dry lithium chloride. The polymerization vessel was placed in a methanol/cardice bath at a temperature of -78°C . Finally, MMA, as a solution in THF, was poured into bulb A from bulb B. Upon addition of MMA the polymerization mixture turned clear, indicating that the nature of the propagating end had changed. The ensuing copolymerization appeared to be rapid and highly exothermic, but

was allowed to proceed for 24 hours. The polymeric samples were recovered and dried by the method described in section 2.5.3.

For some of the copolymerizations a stock solution of polystyryl lithium in THF, was previously prepared in a catalyst flask (see figure 2.5, section 2.3) for the initiation of MMA. The polymerization of styrene was allowed to proceed at 60°C for a period of 24 hours after which time the red colour had disappeared indicating that the living ends had been killed. This solution was therefore no longer useful for the initiation of MMA polymerization. The degradation of the polystyryl lithium is thought to be caused by the reaction of the living polystyryl ends with THF, which induces a ring opening attack.

When the polystyryl lithium was prepared by replacing THF with cyclohexane, it was found that the living ends remained active for a period of weeks. A bright orange colour was observed initially, which appeared to deepen to a dark red with the passage of time. This can be attributed to the formation of polystyryl lithium aggregates in the hydrocarbon solvent. The polystyryl lithium formed was used to initiate the polymerization of MMA. Experiments CP7-CP9 were carried out using a stock solution of polystyryl lithium in cyclohexane.

Table 3.1 shows the conditions used for the various copolymerizations and the percentage conversions of the polymers obtained. The extent of conversion in these reactions was determined by weighing the amount of polymer obtained when the polymerizate was precipitated in methanol. This method introduced the possibility of error which was estimated to be as high as 30%, because of the loss of polymer on recovery of the samples. The percentage conversions for these copolymerizations were calculated based on the assumption that 100% conversion of styrene had occurred, i.e. the figures quoted are for the extent of conversion of methyl methacrylate.

Table 3.1 Conditions of Polymerization and Percentage Conversions for CP1-CP9, in the Anionic Block Copolymerization of Styrene and Methyl Methacrylate in the Presence of LiCl

Block Copolymer	10^3 x MMA moles	10^3 x styrene moles	10^3 x BuLi moles	10^3 x LiCl moles	[LiCl] / [BuLi]	% Conv.
CP1	285	54	1.6	2.35	1.5	80
CP2	106	38	4.96	0.54	0.1	44
CP3	53	40	3	1.24	0.4	60
CP4	52	14	3	2.5	0.8	86
CP5	40	6.4	1.5	2.5	1.66	85
CP6	60	40	1.5	5	3.33	47
CP7 a	110	4.4	0.54	0.83	1.5	18
CP8 a	130	5.4	0.67	1.04	1.6	8
CP9 b	120	5.4	0.53	1.05	2	63

Solvent : THF (~50 cm^3) Temperature : -78°C

a = polystyryl lithium in cyclohexane : [styrene] = 1.68 mol dm^{-3}, [BuLi]= 0.21 mol dm^{-3}
b = polystyryl lithium in cyclohexane : [styrene] = 1.64 mol dm^{-3}, [BuLi]= 0.16 mol dm^{-3}

The advantage of carrying out polymerizations using a stock solution of polystyryl lithium, is that small aliquots of the polystyryl lithium could be withdrawn from the catalyst flask and injected into bulb A of the polymerization vessel as required. The method introduces further accuracy and enables better control of the molar ratios of reagents used. This control was required to enable the concentrations of reagents to be reduced, so that the rate of reaction could be decreased to a level whereby the polymerization could be followed. The procedure was also found to be time saving, as a fresh solution of polystyryl lithium need not be prepared for each polymerization.

The data shown in table 3.1 indicate that 100% conversion of MMA does not occur for CP1-CP9; this suggests the possibility of termination reactions occurring within the system, which could take place by :

(i) the attack of the highly reactive polystyryl anions on the carbonyl group of MMA

or (ii) the presence of impurities in the system such as oxygen and moisture.

Although precautions were taken to ensure that the polymerization system was completely free from moisture and oxygen it is likely that some termination was caused by the presence of impurities. This is supported by the fact that such termination reactions occur immediately upon addition of polystyryl lithium to MMA, causing a decrease in concentration of polystyryl lithium and resulting in an increase in molecular weight of the PMMA fragments obtained. Since the molecular weights of polymers obtained are higher than the theoretically expected values (see section 3.3) it is assumed that termination was caused by the presence of impurities within the system.

It is believed that the reactivity of the polystyryl anions can be decreased by capping the living ends with 1,1 diphenylethylene or α-methyl styrene; this would reduce the attack of the anions on the carbonyl group of MMA and enable propagation to take place at the C=C bond.

The percentage yields obtained for CP1-CP6 are considerably higher than for those obtained for CP7-CP9. The low extent of conversion obtained from the latter polymerizations can be attributed to inefficient initiation. These polymerizations were initiated by withdrawing aliquots of polystyryl lithium in cyclohexane from a stock solution . The polystyryl lithium is thought to associate in cyclohexane; the associated species are unable to initiate MMA polymerization and hence a large proportion of unreacted initiator remains. The initiation process is also thought to be slower, owing to the slow interconversion between associated and non-associated species.

3.2.2 Dilatometry

3.2.2.1 Experimental

An attempt was made to investigate the kinetics of the block copolymerizations using dilatometry. The polymerizations were carried out in a dilatometer (see figure 2.7) as described in section 2.5.2.2. Initially the polymerization was carried out at -78°C by immersing the dilatometer in a thermostatically controlled low temperature bath which had previously been filled with a methanol/cardice mixture. However, the low temperature employed caused a contraction of the taps attached to the dilatometer, enabling methanol to seep in and terminate the polymerization. This was clearly observed since the polymer had precipitated out in methanol. Subsequently, all the following dilatometry experiments were carried out in a thermostatically controlled water bath at ambient temperature. Table 3.2 shows the conditions of polymerization used and the percentage conversions of the polymers obtained from the dilatometry experiments.

Table 3.2 Conditions of Polymerization and Percentage Conversions for CP10-CP12, in the Anionic Block Copolymerization of Styrene and Methyl Methacrylate in the Presence of LiCl, Using Dilatometry

Block Copolymer	CP10	CP11	CP12
10^3 x MMA moles	90	70	107
10^3 x styrene moles	20	24	16
10^3 x BuLi moles	1.5	1.5	3
10^3 x LiCl moles	3	3	3
[LiCl] / [BuLi]	2	2	1
10^3 x 1,1DPE moles	-	–	2
Polymerization Temperature / °C	20	35	38
Percentage Conversion	16	24	16

A slight alteration was made to the polymerization procedure for CP12, in that 2 x 10^{-3} moles of 1,1 diphenylethylene was injected through the subaseal into the bulb containing the polystyryl lithium, after the addition of LiCl. The purpose of this addition was to cap the living polystyryl ends with the less reactive diphenylethylene ends and hence promote more efficient initiation of MMA.

Following the polymerization procedure for CP10, a control experiment was set up. The polymerization (CP10) was terminated after 24 hours and the dilatometer was re-immersed in the water bath, at the temperature of polymerization, containing the terminated polymerization mixture . The timer was started at the point of immersion, and any changes in the of meniscus level were monitored. The observations indicated that there was a contraction in volume of the mixture even though the polymerization had been terminated. This contraction in volume was thought to be attributed to a change in temperature when placing the dilatometer in the water bath. A plot of the readings obtained from the control experiment are almost identical to those taken for CP10 (see figure 3.1). This result strongly suggests that the contraction in volume obtained for CP10, was not due to the polymerization process but may have been associated with temperature fluctuations.

Figure 3.1 Plot of Height as a Function of Time for CP10 and Control Experiment in the Anionic Block Polymerization of Methyl Methacrylate, Initiated by Polystyryl Lithium in the Presence of LiCl

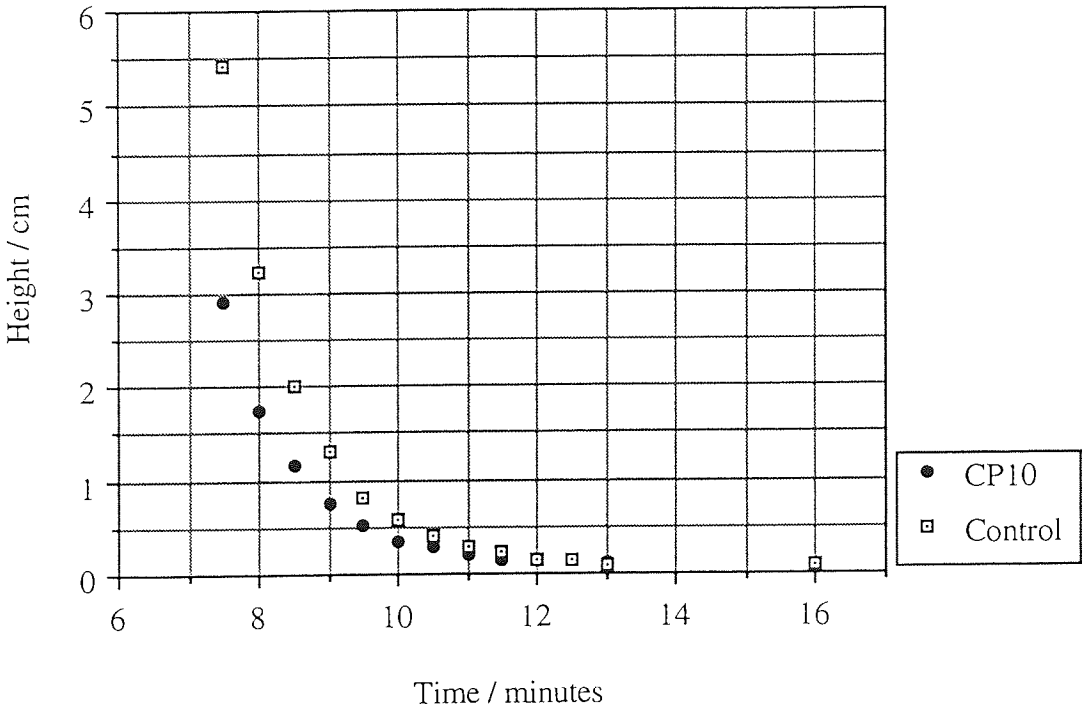

3.2.2.2 Discussion

Contractions in volume were recorded as changes in height, which were then converted to decreases in concentration of methyl methacrylate using the relationship :

$$\Delta[MMA] = K\Delta h$$

where $\frac{\pi r^2}{VMm} \frac{\rho p.\rho m}{\rho m - \rho p}$ is a constant (K) for the system under study. The following graphs show the decay in concentration of MMA as a function of time for CP10-CP12. These were then used to obtain logarithmic conversion-time plots for the polymerizations.

Figure 3.2 Plot of Decay in [MMA] as a Function of Time for CP10, Initiated by Polystyryl Lithium in the Presence of LiCl

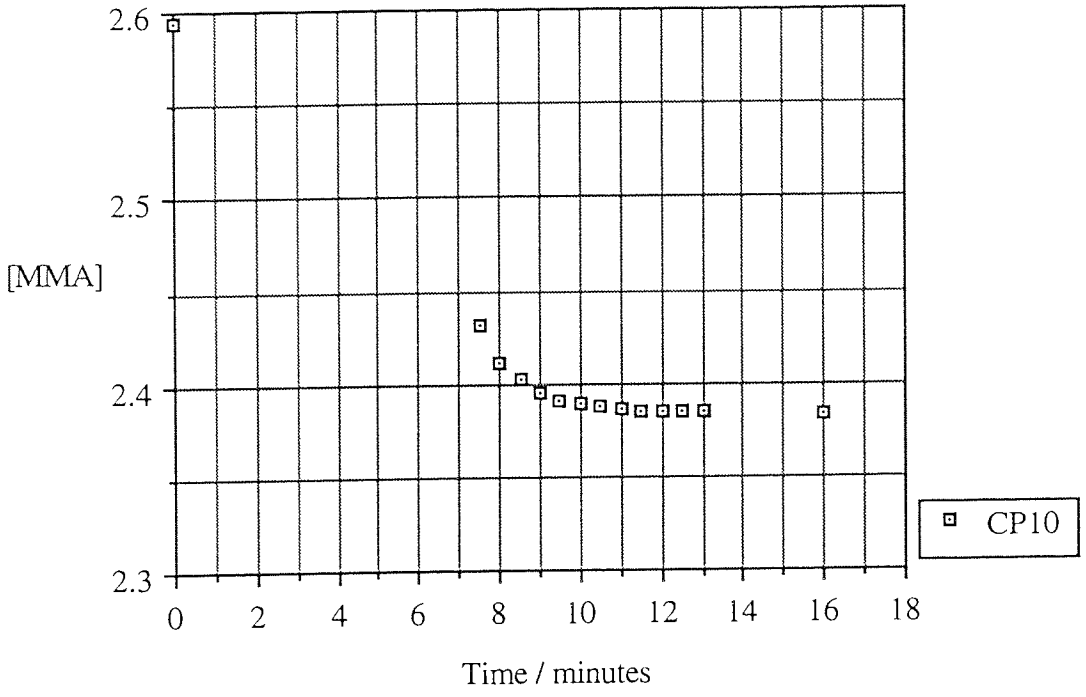

Figure 3.3 Logarithmic Conversion-Time Plot for CP10

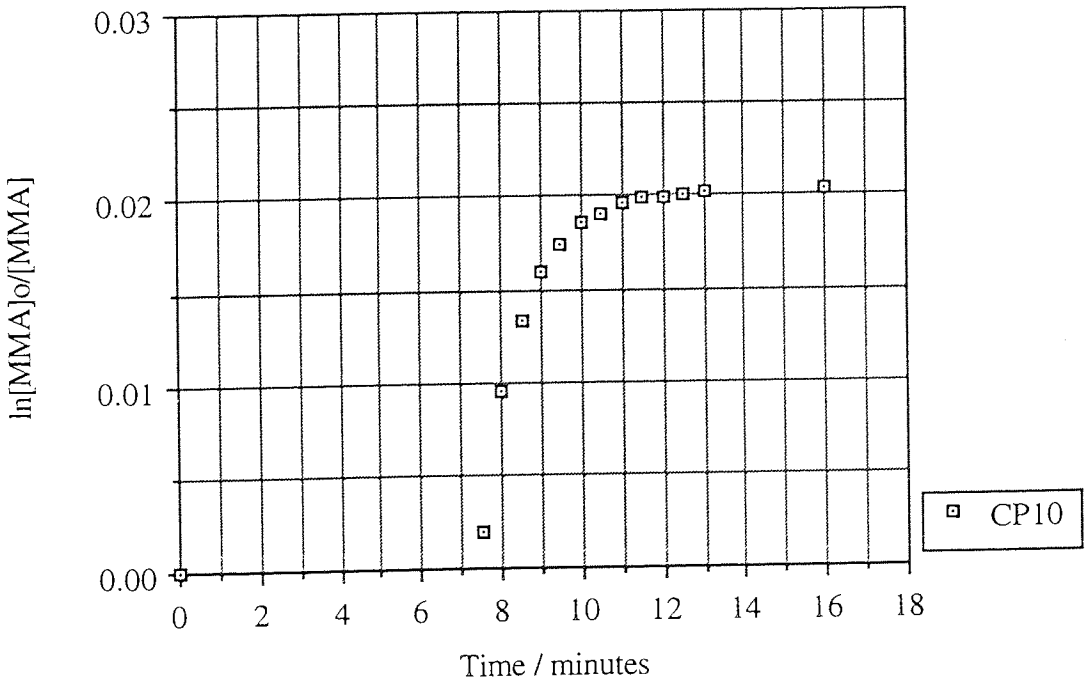

Figure 3.4 Plot of Decay in [MMA] as a Function of Time for CP11, Initiated by Polystyryl Lithium in the Presence of LiCl

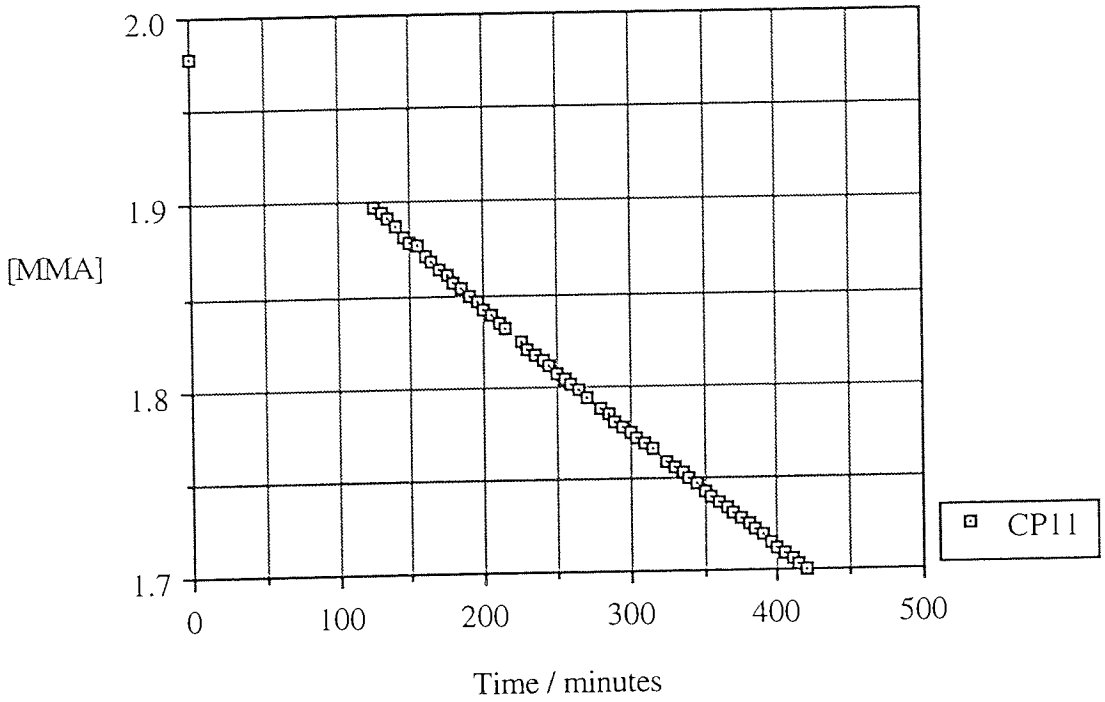

Figure 3.5 First Order Logarithmic Conversion-Time Plot for CP11

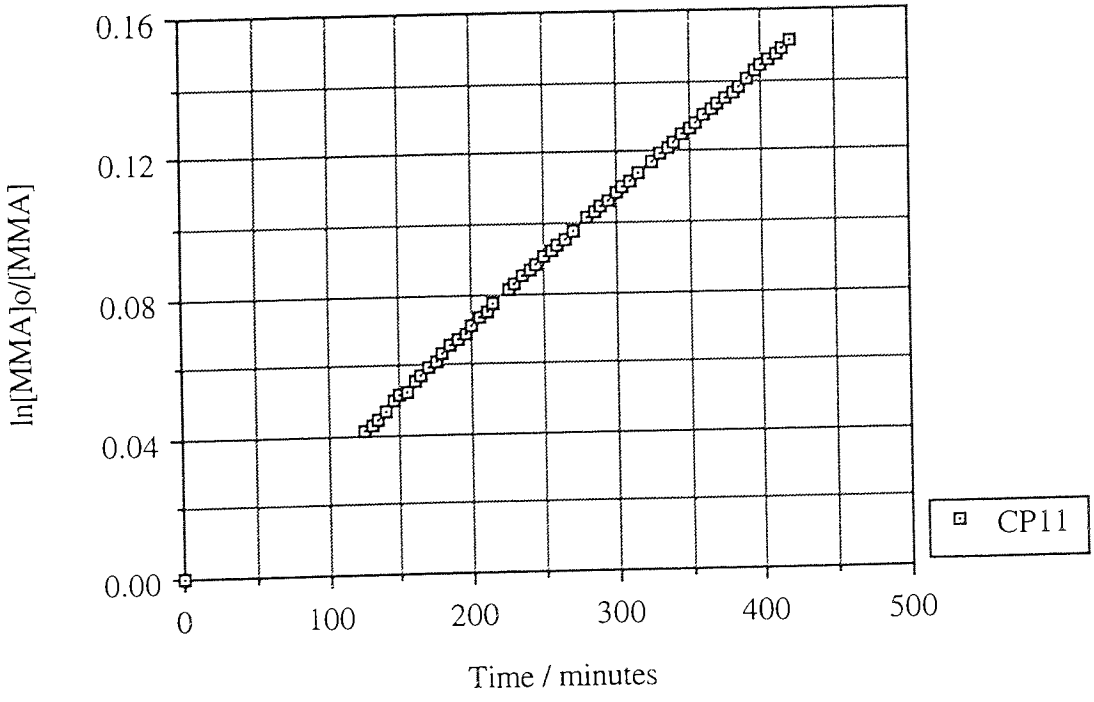

Figure 3.6 Plot of Decay in [MMA] as a Function of Time for CP12, Initiated by Polystyryl Lithium in the Presence of LiCl

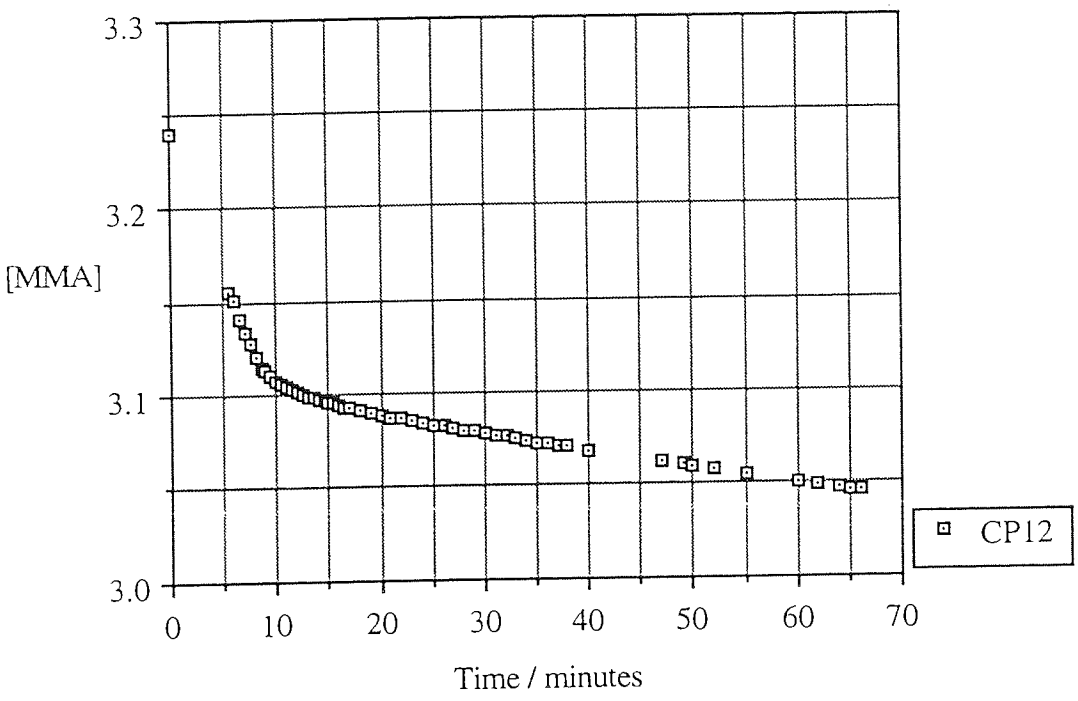

Figure 3.7 Logarithmic Conversion-Time Plot for CP12

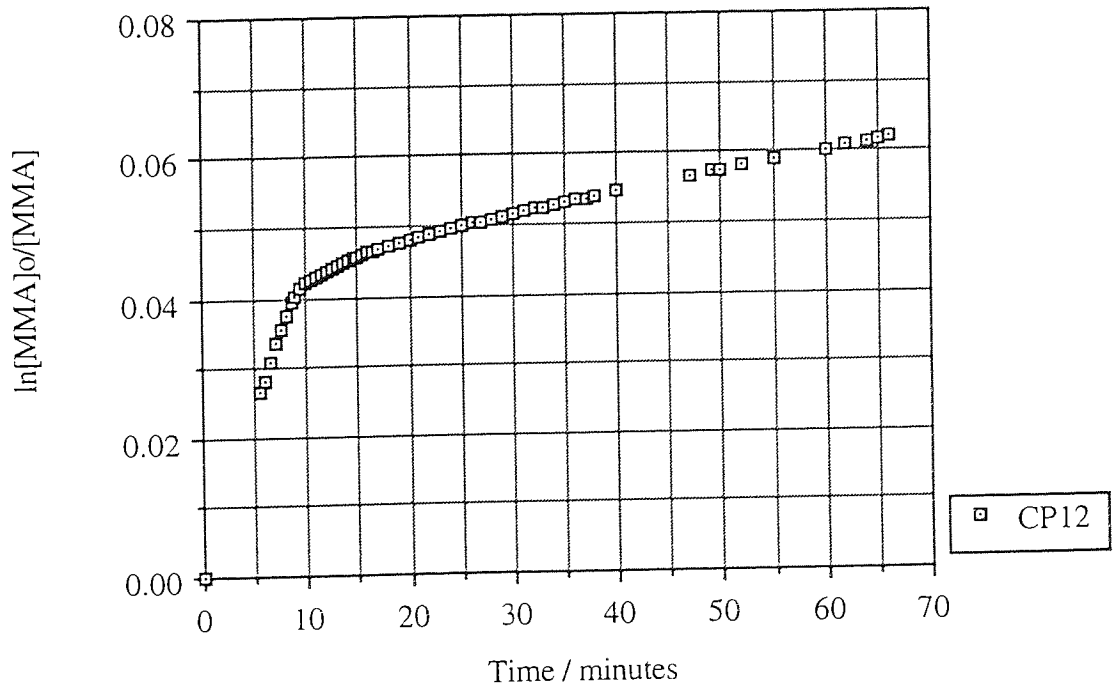

From the plots shown, it appears that CP11 follows first order kinetics with respect to decay in MMA concentration. CP10, however, does not exhibit first order kinetics and it is highly probable that the changes in height monitored are not due to polymerization but are attributable to fluctuations in temperature. CP12 does not appear to follow simple first order kinetics either. It should be noted that for all the polymerizations carried out using dilatometry, the percentage conversions obtained are low. This can be seen from the small decrease in concentration of MMA and is thought to be due to the occurrence of side reactions at such high temperatures of polymerization. There is no certainty as to whether the changes in height monitored for all the dilatometry experiments are attributable to polymerization or whether they are because of fluctuations in temperature. This technique is therefore considered to be unsuitable for following the kinetics of reaction under the conditions employed for this type of polymerization.

3.3 SEC Analysis

The copolymer samples obtained were analysed using SEC as described in section 2.6.1. A typical trace, taken from CP1, is shown in appendix 1. Table 3.3 shows the molecular weights, molecular weight distributions and the percentage initiation efficiency of the polymers obtained.

Table 3.3 Molecular Weight Distributions and Initiator Efficiencies in the Anionic Block Copolymerization of Styrene and Methyl Methacrylate in the Presence of LiCl

Block Copolymer	Type of Distribution	$\overline{M}_n$	$\overline{M}_w$	Polydispersity	Initiator Efficiency (%)
CP1	broad, bimodal	40300	104200	2.6	35
CP2	broad, multimodal	14700	42000	2.9	7
CP3	narrow, high mw shoulder	37300	109000	2.9	3
CP4	broad, bimodal	179600	280300	1.6	1
CP5	broad, bimodal	110400	187000	1.7	2
CP6	broad, multimodal, high mw shoulder	12300	61800	5	15
CP7	narrow, bimodal	229400	303800	1.3	2
CP8	narrow, bimodal	194000	242200	1.2	1
CP9	narrow, bimodal	141200	232100	1.6	10
CP10	very broad, unimodal	4200	12700	3	23
CP11	broad, bimodal	23300	57200	2.45	5
CP12	very broad, unimodal	5600	22300	4	10

The data shows a wide range of molecular weights and molecular weight distributions for the copolymers obtained. The differences can be attributed to the different types of procedures used for the polymerizations. Some of the polymerizations appear to exhibit broad, multimodal molecular weight distributions whereby the overlapping of peaks makes their deconvolution difficult. The polydispersity indices quoted for such copolymers are overall molecular weight distributions.

The molecular weight distributions obtained for CP7-CP9 are bimodal and two distinct peaks are observed. The higher molecular weight curve is thought to correspond to copolymer and the lower molecular weight curve is believed to be a large quantity of

unreacted polystyryl lithium, since when polystyryl lithium alone was passed through the SEC columns, it was eluted at the same point as the lower molecular curve obtained from the copolymer. This supports the notion that when the polymerizations were carried out using a stock solution of polystyryl lithium, the initiation is inefficient owing to the association of polystyryl lithium in cyclohexane, or because some of the polystyryl lithium is killed off in the early stages of polymerization.

The existence of copolymer was verified from the response given by the UV detector. The UV detector responds to chromophoric groups which are either attached to, or are a part of the polymer backbone e.g. polystyrene. The response this detector gives is proportional to the concentration of solute present in the solution and the molar extinction coefficient of the solute at the set wavelength. The wavelength, set at 254 nm, is the maximum absorbance for polystyrene. A deflection on the chart recorder which corresponds to the UV detector, appears at the same point as the deflection corresponding to the RI detector, for both the unreacted polystyryl lithium and the copolymer. The presence of the UV signal at the point where the higher molecular weight material is eluted, indicates that this material contains polystyrene and is most likely to be copolymer. However, the height of the peak obtained from the UV signal is small compared with the height obtained from the RI signal, indicating that only a small amount of polystyrene is present. Appendices 2 and 3 show the UV absorbances at 254 nm of pure poly(styrene) and pure poly(methyl methacrylate) respectively. Although there is a UV signal from PMMA, the deflection is small and PMMA can be assumed to absorb negligibly since the factor is 1/200 th of that of polystyrene. It is therefore assumed that any UV deflection that is observed in the copolymer corresponds to that of polystyrene. The molecular weights quoted for these polymerizations correspond to those of the higher molecular weight material i.e. the copolymer.

The majority of the copolymers obtained appeared to exhibit high polydipersity indices and low initiatior efficiency. These findings are contrary to the work carried out by Teyssie *et al*, whereby copolymers of narrow molecular weight distribution were obtained when they carried out polymerizations in THF at -78°C. It is believed that the polystyryl

lithium may be participating in side reactions by attacking the carbonyl ester group of MMA. There was no improvement in the initiation efficiency for CP12, whereby the reactivity of the polystyryl lithium was decreased upon capping the living ends with 1,1, diphenylethylene before the addition of MMA. However, it is generally believed that the combination of a capping agent such as 1,1, diphenylethylene or α-methyl styrene, together with LiCl is essential for the synthesis of block copolymers with narrow molecular weight distribution. The plot of polydispersity as a function of [LiCl]/[BuLi], is shown in figure 3.8.

Figure 3.8 Plot of Polydispersity as a Function of [LiCl/BuLi] for CP1-CP12, in the Anionic Block Copolymerization of Styrene and Methyl Methacrylate in the Presence of LiCl

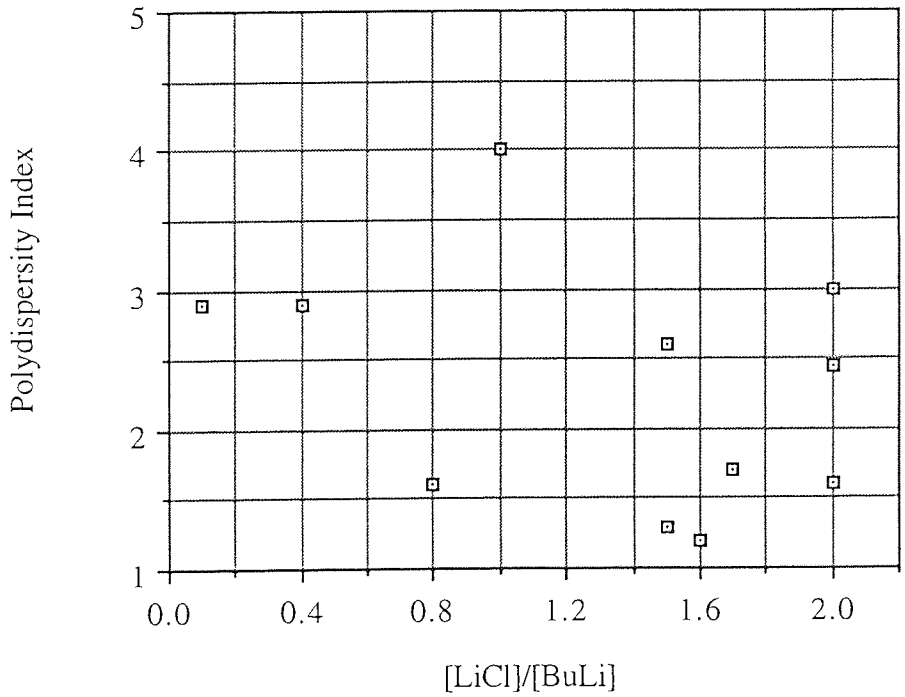

There appears to be a slight trend towards a decrease in polydispersity as the [LiCl]/[BuLi] is increased but the data is highly scattered. Teyssie *et al* [64], showed that the molecular weight distribution significantly narrowed as the [LiCl]/[BuLi] was increased to a value of 2 and polydispersity values as low as 1.09 could be reproducibly

obtained when they polymerised MMA initiated by α-methylstyryl lithium in THF at -78°C.

3.4 Infrared Spectroscopy Analysis

The polymer samples were analysed by FTIR as described in 2.6.4. The spectra obtained for CP5 and CP6 are shown in appendices 4 and 5 respectively. They are typical of the spectra obtained for CP1-CP12. Table 3.4 shows the data obtained from the absorption frequencies for CP5 and CP6.

Table 3.4 FTIR Analysis for CP5 and CP6 in the Anionic Block Copolymerization of Styrene and Methyl Methacrylate in the Presence of LiCl.

Band Frequency ν / cm^{-1}		Assignment
CP5	CP6	
3438 (w)	3437 (w)	Hydrogen Bonded -OH
	3083 (s), 3060 (s)	Aryl deformation or C-H stretching of $C=CH_2$ from MMA monomer
2999 (s)	3026 (s), 2999 (s)	Aryl Hydrogens
2952 (m)	2950 (m), 2927 (w)	$=CH_2$, =CH, $-CH_3$, saturated C-H deformation
1732 (s)	1732 (s)	Deformation of -C=O from saturated ester group
1603 (w), 1488 (s)	1602 (w), 1493 (s)	Aryl deformations
1452 (s), 1387 (m)	1452 (s), 1387 (m) 1364 (m)	$=CH_2$, =CH, $-CH_3$ deformations
1274 (s), 1244 (s) 1195 (s), 1149 (s)	1272 (s), 1243 (s) 1194 (s), 1150 (s)	Deformation of C-O of ester group

The data from the spectra indicate that the samples contain some impurities since, the broad absorption peak in the region of 3440 cm^{-1} shows the presence of water or methanol from inefficient drying. The copolymers exhibit strong absorbance frequencies at 1732 cm^{-1}, to which the carbonyl group of PMMA can be assigned. Strong absorbance

in the aryl region can be attributable to polystyrene. It is difficult to ascertain from the spectra whether the samples are copolymers, or a mixture of homopolymers.

3.5 NMR Analysis

3.5.1 ^{1}H NMR

The polymer samples were analysed by NMR as described in section 2.6.3. Appendix 6 shows the ^{1}H NMR spectrum of the block copolymer of styrene and methyl methacrylate obtained for CP6. Table 3.5 assigns the chemical shifts δ, of the peaks corresponding to the spectrum of the copolymer.

Table 3.5 ^{1}H NMR Analysis of Polystyrene-*b*-PMMA for CP6, in the Anionic Block Copolymerization of Styrene and Methyl Methacrylate in the Presence of LiCl.

Chemical Shift (ppm)	Assignment	Area
0.855	-CH_3 syndiotactic (rr)	134.8
1.017	heterotactic (mr)	64.9
1.25	isotactic (mm)	6.6
	from PMMA	
1.429	-CH_2 from PMMA backbone	104.8
1.807	-CH_2 from polystyrene backbone	106
1.875		81.5
3.582	-CH_3O from PMMA	219.3
6.552	aromatic protons from polystyrene	93.3
7.023		142.6

The ^{1}H NMR spectrum indicates the presence of both polystyrene and PMMA resonances. The spectrum is typical of those obtained for CP1-CP9. The tacticitiy of the copolymer obtained from CP6 was determined. Analysis of the relevant areas

corresponding to the -CH_3 peaks on the spectrum for CP6 showed that $\sigma = 0.19$. This corresponds to an isotactic content of 3%, syndiotactic 65% and heterotactic 31%.

The spectra obtained for CP10 and CP11 resemble those of homopolystyrene, with an additional peak of low intensity at ~3.5 ppm, which represents the methyl ester group from MMA monomer. A slightly higher intensity peak for the carbonyl group was seen in the spectrum for CP12. It would appear that for those polymerizations carried out using dilatometry, very little or no copolymerization had occurred and homopolystyrene was obtained. This can be attributed to the high temperatures at which these experiments were conducted, which resulted in the occurrence of side reactions of the polystyryl lithium with the carbonyl group of MMA. The results confirm the belief that dilatometry is not a suitable technique for carrying out this type of polymerization.

3.5.2 ^{13}C NMR

Appendix 7 shows the ^{13}C NMR spectrum of the block copolymer of styrene and methyl methacrylate obtained for CP6. Table 3.6 assigns the chemical shifts δ, of the peaks corresponding to the spectrum of the copolymer.

Table 3.6 ^{13}C NMR Analysis of Polystyrene-*b*-PMMA for CP6, in the Anionic Block Copolymerization of Styrene and Methyl Methacrylate in the Presence of LiCl.

Chemical Shift (ppm)	Assignment
16.772 18.822	$-CH_3$ syndiotactic (rr) heterotactic (mr) from PMMA
44.662 44.987	$-CH_2$ syndiotactic (rr) heterotactic (mr) from PMMA
51.613	$-CH_3O$ from PMMA
54.176	quaternary carbon from PMMA
125.568 127.938	aromatic carbons from polystyrene
176.807 177.624 177.911	-C=O syndiotactic (rrrr) heterotactic (rrrm) heterotactic (rrmm) from PMMA

The peaks indicate the presence of both polystyrene and PMMA. The -C=O group is shown to be pentad sensitive in this case but there is no indication of the presence of the isotactic configuration (mmmm). This is confirmed by the ^{1}H NMR where there appears to be only a weak signal (~3%) relating to the isotactic content of the PMMA structure.

3.6 U.V/Visible Spectrophotometry

Figure 3.9 shows plots of absorbance as a function of concentration for polystyrene and CP8 :

Figure 3.9 Plots to Show Absorbance as a Function of Concentration in UV Spectrophotometry Analysis of Polystyrene and CP8.

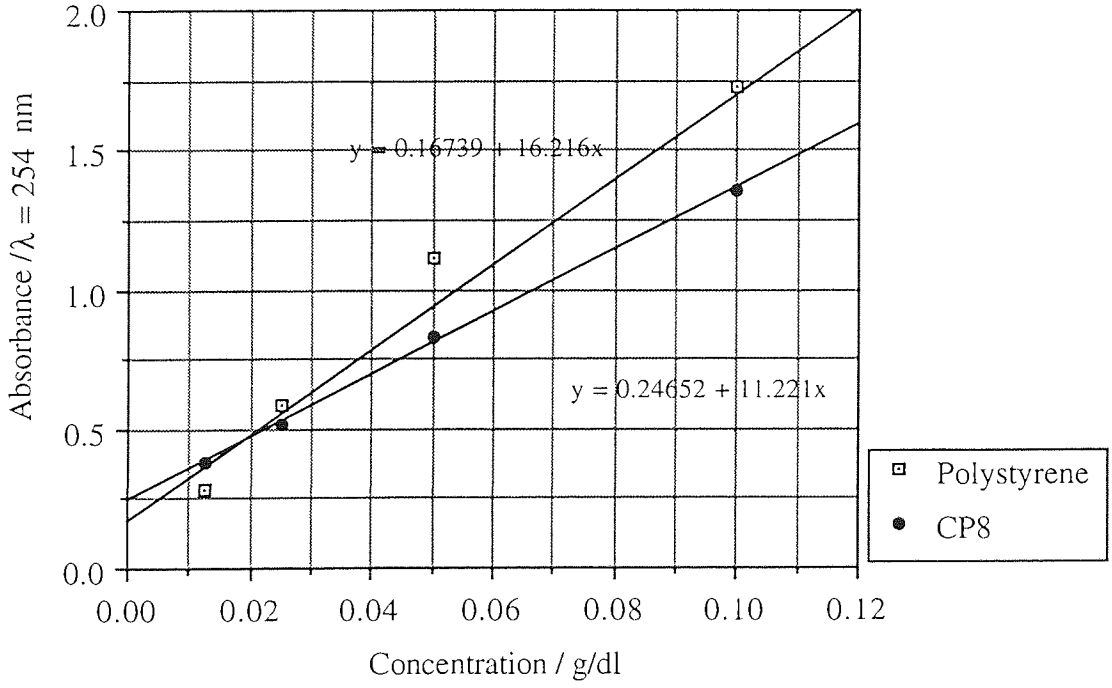

The gradients of the lines correspond to the extinction coefficients of each of the polymers. The percentage composition of polystyrene in the copolymer was determined by comparison of the extinction coefficients of polystyrene and CP8. CP8 was found to have a composition of 62% polystyrene and 38% PMMA.

3.7 Discussion

The results obtained from the experiments conducted show no conclusive relationship between the concentration of lithium chloride and the molecular weight distributions of the copolymers obtained, although there appears to be a slight trend towards decrease in polydispersity as the concentration of lithium chloride is increased. The molecular weight distributions obtained from the copolymerizations were found to exhibit broad, multimodal behaviour under the conditions employed. It is evident that living polymers of narrow polydispersity index can only be obtained when the system is completely free from side reactions on the carbonyl moiety of MMA. The system under investigation appeared to exhibit termination reactions, supported by the fact that the initiator efficiencies were low and large quantities of unreacted polystyryl lithium remained. It is thought that elimination of side reactions can only be achieved if the polymerizations are carried out at low temperatures and when the reactivity of the initiator is decreased by addition of a capping agent, such as α–methyl styrene, or 1,1 diphenylethylene. It was found that addition of 1,1 diphenyl ethylene to polystyryl lithium afforded no improvement in efficiency of initiation of MMA when included in one of the dilatometry experiments.

Dilatometry was found to be an inefficient technique for determination of the kinetics of polymerization. The results obtained from the dilatometry experiments are inconclusive, owing to the high temperatures at which polymerizations were conducted. In order to successfully follow the kinetics of polymerization, it is believed that the temperature and the concentrations of reagents need to be at a level whereby the polymerization is sufficiently slow. The temperatures employed for the dilatometry experiments were too high, since the rate of polymerization was increased to a level at which reactions were too fast to follow.

CHAPTER FOUR

THE ANIONIC POLYMERIZATION OF METHYL METHACRYLATE IN THE PRESENCE OF LITHIUM AND ALUMINIUM ALKYLS

4.1 Introduction

This chapter describes work carried out on the anionic polymerization of methyl methacrylate in the presence of lithium and aluminium alkyls at ambient temperatures. In particular, this work was concerned with an investigation of the effects of the structures of the lithium and aluminium alkyls on the efficiency of initiation. The efficiency of the initiator systems used could be assessed from the measurement of molecular weight and molecular weight distribution, as discussed earlier in section 2.5.1. A study of the kinetics of polymerization was carried out in order to grasp a better understanding of the mechanism of polymerization.

4.2 Experimental

A series of experiments was designed to follow the kinetics of the polymerization of methyl methacrylate in the presence of lithium alkyls and aluminium alkyls. The polymerizations were carried out using different combinations of the initiator and cocatalyst :-

i). butyllithium/triethylaluminium

ii). *tert*-butyllithium/triethylaluminium

iii). *tert*-butyllithium/triisobutylaluminium

4.2.1 Polymerization

The polymerizations were carried out in the polymerization vessel shown in figure 2.6 section 2.5.1. The solvent used for polymerization was generally toluene, although an attempt at polymerization using cyclohexane was also made. Transfer of all the reagents into the vessel was carried out as described in section 2.5.1. The vessel was shaken vigorously after the addition of each reagent. Following the addition of the alkyllithium to the alkylaluminium in excess toluene, the vessel was left at the polymerization temperature for 30 minutes to enable the formation of an initiating complex. Most reactions were carried out at 25°C in a thermostatically controlled bath. Upon addition of the methyl methacrylate to the initiating solution in bulb A, the timer was started. Initially the solution turned yellow after the addition of the monomer, and the colour disappeared as the polymerization proceeded. The polymerization mixture was transferred from bulb A into bulbs B and D by opening taps F and H respectively. The vessel was then attached to the argon line and known volumes of the polymerization mixture were removed by syringe at appropriate time intervals using the Schlenk technique (described in section 2.2). These samples were then analysed in order to monitor the molecular weight changes using SEC and to follow the kinetics of polymerization using GC as described in sections 2.6.1 and 2.6.2 respectively. The polymeric samples were recovered and dried by the method described in section 2.5.3.

4.3 Polymerization of Methyl Methacrylate Initiated by Butyllithium/Triethylaluminium

4.3.1 Butyllithium/Triethylaluminium Initiated MMA in Cyclohexane.

4.3.1.1 Experimental

Methyl methacrylate was polymerized as described in section 4.2.1 using BuLi/$AlEt_3$ as the initiating system and cyclohexane as the solvent. 0.26 moles of MMA were added to 1.3×10^{-3} moles of BuLi and 3.9×10^{-3} moles of $AlEt_3$ in 50 cm^3 of cyclohexane. The ratio of the reagents used was as follows :

MMA	:	BuLi	:	$AlEt_3$
200	:	1	:	3

The polymerizaton was carried out at 0°C without following the reaction kinetics and therefore the system was not disturbed by removal of samples.

Upon addition of the $AlEt_3$ to the solution of BuLi in cyclohexane at 0°C a white "flaky" precipitate was obtained which was attributed to the formation of a complex between BuLi and $AlEt_3$. Some of the initiating species was kept aside from the polymerization mixture and the 'flaky' precipitate disappeared and dissolved when excess toluene was added to it. Upon addition of the MMA to the initiating complex a yellow solution appeared initially, which was rapidly replaced by a solid white precipitate, attributable to the formation of insoluble PMMA. The polymerization appeared to be very rapid and highly exothermic, but was allowed to proceed for 24 hours. The polymer was recovered from the vessel by addition of toluene, in which it was found to be soluble. The solution was then poured into methanol, and the polymer precipitate obtained was filtered, dried and analysed (yield 62%).

4.3.1.2 NMR Analysis

4.3.1.2.1 ^{1}H NMR.

Appendix 8 shows the ^{1}H NMR spectrum of the PMMA obtained. Table 4.1 shows the chemical shifts (δ, ppm) of the various peaks obtained corresponding to the spectrum of PMMA.

Table 4.1 ^{1}H NMR Analysis of PMMA Initiated by BuLi/$AlEt_3$ in Cyclohexane

Chemical Shift (ppm)	Assignment	Area
0.78	syndiotactic -CH_3 (rr)	115.7
0.96	heterotactic -CH_3 (mr)	67.1
1.15	isotactic -CH_3 (mm)	11.9
1.34	-CH_2	10.8
1.38		18.7
1.84		108.2
3.54	-CH_3-O	190.7

The value of σ can be determined from analysis of the ^{1}H NMR spectrum as follows :

$$P_s = (1-\sigma)^2 = \frac{\text{Area under syndiotactic -}CH_3\text{ peak}}{\text{Total area under -}CH_3\text{ peaks}}$$

Analysis of the relevent areas corresponding to the -CH_3 peaks on the spectrum showed that σ = 0.23. This corresponds to an isotactic content of 5.3%, syndiotactic 59% and heterotactic 35.4%.

4.3.1.2.2 ^{13}C NMR

Appendix 9 shows the ^{13}C NMR spectrum of the PMMA obtained. Table 4.2 shows the chemical shifts (δ, ppm) of the various peaks obtained corresponding to the spectrum of PMMA.

Table 4.2 ^{13}C NMR Analysis of PMMA Initiated by BuLi/$AlEt_3$ in Cyclohexane

Chemical Shift (ppm)	Assignment
16.38	syndiotactic -CH_3 (rr)
18.63	heterotactic -CH_3 (mr)
44.45	syndiotactic -CH_2 (rr)
44.80	heterotactic -CH_2 (mr)
51.74	-CH_3O
52.65	quaternary carbon.
177.00	-C=O syndiotactic (rrrr)
177.75	heterotactic (rrrm)
178.04	heterotactic (rrmm)
178.33	heterotactic (rmmm)

The ^{13}C NMR spectra shows the presence of only syndiotactic and heterotactic diads relating to the -CH_2 and -CH_3 groups. The -C=O group is shown to be pentad sensitive in this case but there is no indication of the presence of the isotactic configuration (mmmm). This is confirmed by the ^{1}H NMR where there appears to be only a weak signal (~ 5%) relating to the isotactic content of the PMMA structure.

4.3.1.3 SEC Analysis

The SEC trace of the PMMA obtained shows a very broad trimodal molecular weight distribution (see appendix 10). Analysis of the trace using the procedure described in section 2.6.1.3 showed :

$\overline{M}_n = 2300$

$\overline{M}_w = 26500$

polydispersity index (PDI) =11.64

4.3.1.4 Discussion

The polymerization of methyl methacrylate initiated by BuLi/$AlEt_3$ using cyclohexane as the solvent produced a predominantly syndiotactic polymer in ~60% conversion but with a very broad molecular weight distribution. The breadth of the molecular weight distribution suggests that the polymerization may not be a living system or that more than one propagating species was present. The polymerization may have been complicated by the fact that both the initiating species and the polymer produced were found to be insoluble in cyclohexane. Both the initiator and the polymer, however, were found to be more soluble in toluene which was the solvent used for subsequent polymerizations.

4.3.2 Butyllithium/Triethylaluminium Initiated MMA in Toluene.

Polymerizations of MMA, initiated by BuLi/$AlEt_3$, using toluene as solvent were carried out as described in section 4.2.1. The kinetics of the polymerizations were followed using GC and the changes in molecular weight were determined using SEC.

4.3.2.1 Experimental

The following polymerizations were carried out using the quantities of reagents shown in table 4.3 :

Table 4.3 Conditions for the Polymerization of MMA, Initiated by BuLi/$AlEt_3$

Polymerization No.	10^3 x $\frac{MMA}{moles}$	10^3 x $\frac{n\text{-}BuLi}{moles}$	10^3 x $\frac{AlEt_3}{moles}$	$\frac{[AlEt_3]}{[BuLi]}$
P1	146	0.75	2.35	3
P2	117	0.59	1.80	3
P3	114	0.57	1.70	3
P4	121	0.60	1.80	3
P5	105	0.53	2.70	5
P6	123	0.60	3.00	5
P7	106	0.5	2.5	5

Solvent : toluene
[MMA] : 1.7 +/- 0.2 mol dm^{-3}
Temperature : 25 +/- 1°C
[MMA]/[BuLi] = 200

Experiment P1 was used as a trial to indicate the concentrations of components required for successful polymerization. The analysis of the results showed that P1 gave an overall conversion of 89% after polymerization had been completed. The kinetics of polymerization were then followed for all subsequent polymerizations.

Figure 4.1 shows the percentage conversion of monomer to polymer as a function of time for P2, P3 and P4; reactions carried out under very similar conditions. The extent of conversion in these reactions was determined by weighing the amount of polymer

obtained, when a known volume of polymerizate was precipitated in methanol. This method introduced the possibility of error because of the inaccuracy in the measurement of the volume of samples of polymerizate withdrawn, and loss of polymer on recovery of the samples. These errors are shown implicitly in figure 4.1 and were estimated to be as high as 30%.

Figure 4.1 To Show Extent of Conversion as a Function of Time for Three Polymerizations of MMA Initiated by $BuLi/AlEt_3$

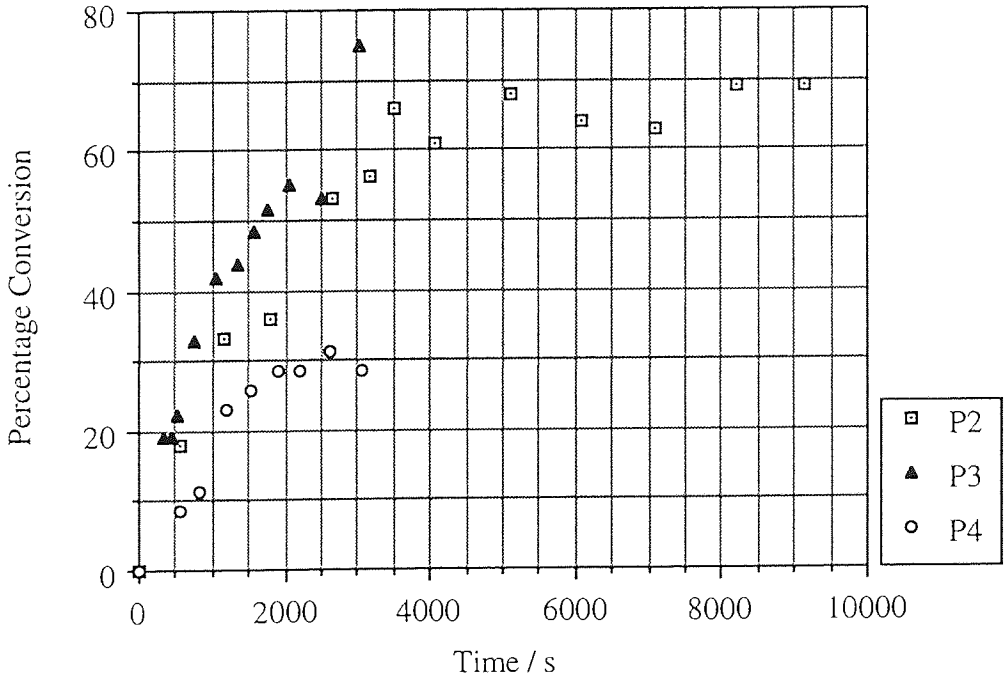

The plots show a steady increase in percentage conversion with respect to time. The trends shown in P2 and P4 suggest that the plots level off before 100% conversion is achieved. The polymerization has probably terminated because of side reactions or the presence of terminating agents which have been introduced into the system during sample removal. The latter explanation is the most likely since in P4, the overall percentage conversion is low. From these results, it is evident that it is difficult to take samples without disturbing the polymerization and allowing traces of oxygen and/or moisture to enter, even though every precaution was taken to use clean, dry syringe needles when samples were withdrawn. This problem is evident from the fact that the overall

percentage conversions obtained in P2-P4, were considerably less than that from P1, which was left undisturbed throughout the reaction.

4.3.2.2 GC Analysis

Determination of the extent of conversion by analysis of the weights of polymeric samples, was further exacerbated by the fact that during the polymerization the polymer produced was precipitating and accumulating at the bottom of the polymerization vessel. Consequently, an accurate determination could not be made of the percentage conversions of the samples analysed by weights, because the polymer was not evenly dispersed within the polymerization mixture. A more accurate way of determining percentage conversion was thought to involve the use of GC. Such analysis would then follow the decay of the concentration of MMA as a function of time, as opposed to the quantity of polymer produced (see section 2.6.2.2). An advantage of this method was the fact that precipitation of the polymer would not affect the concentration of MMA.

The following graph shows the consumption of MMA as a function of time for experiments P5, P6 and P7; reactions carried out under similar conditions. These were then used to obtain logarithmic conversion-time plots.

Figure 4.2 To Show the Decay in Concentration of Monomer as a Function of Time for Three Polymerizations of MMA Initiated by $BuLi/AlEt_3$

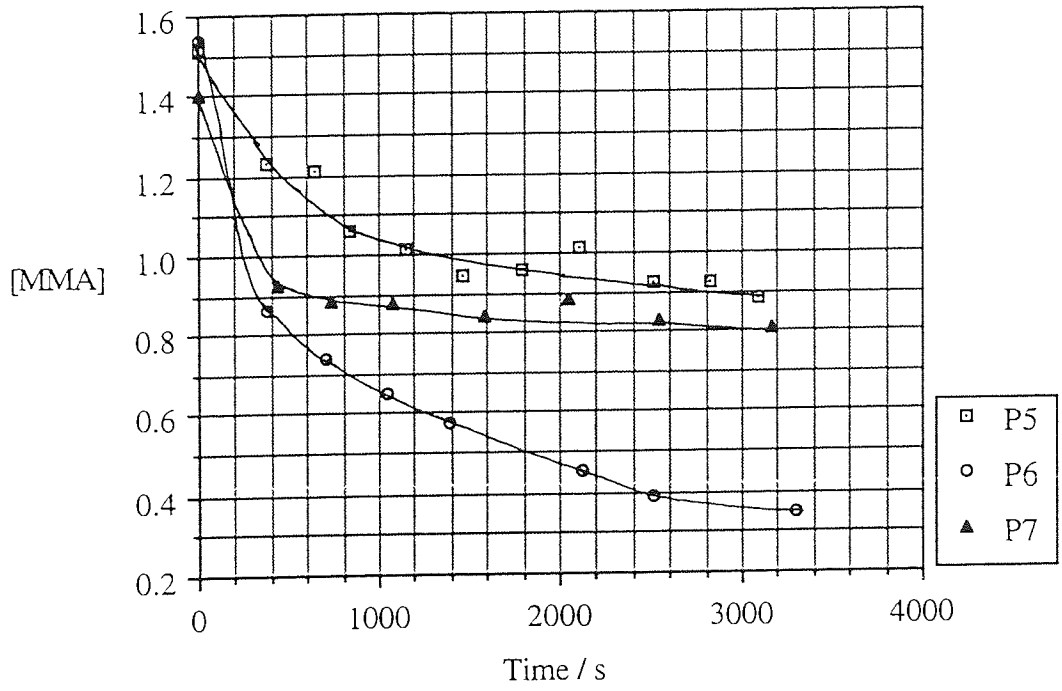

From the plots showing the decay in monomer concentration with respect to time (figure 4.2), the overall percentage conversions were calculated as 42%, 78% and 42% for P5, P6 and P7 respectively. The yields were found to be slightly lower when the [Al]/[Li] ratio was increased from 3 to 5; the difference, however, was not significant and could therefore be attributed to experimental error. The overall yields obtained for the different polymerizations (P1-P7), were found to lie between 30-90%. Hatada *et al* [69] achieved a yield of only 8.9 % when they carried out the polymerization using the same initiating system at -78°C.

Figure 4.3 Logarithmic Conversion Plots as a Function of Time For P5 and P7

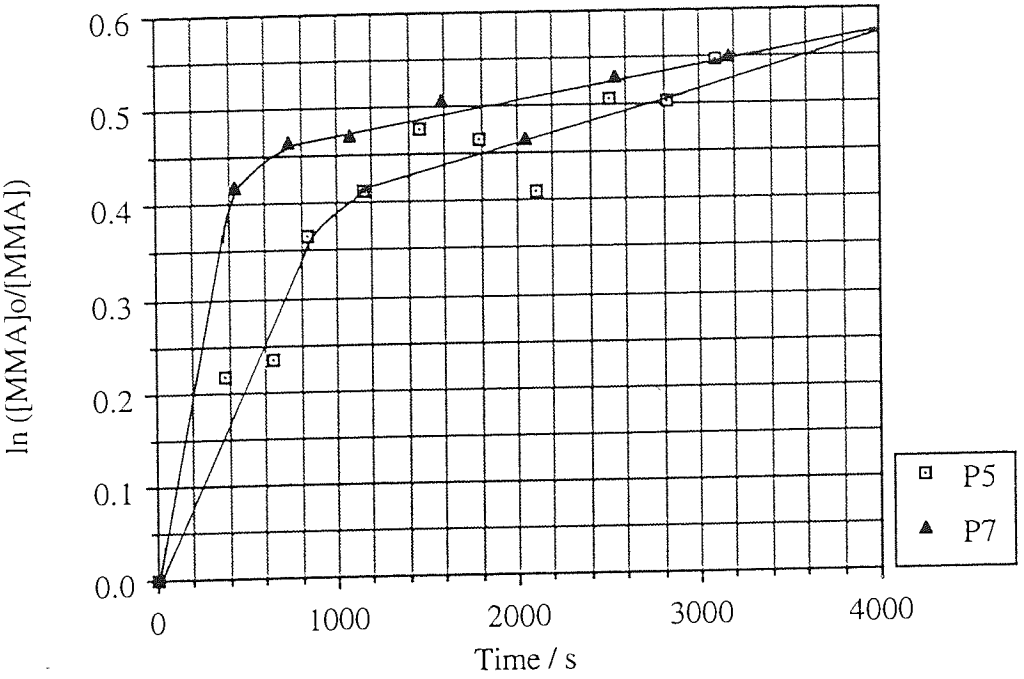

Figure 4.4 Logarithmic Conversion Plot as a Function of Time for P6

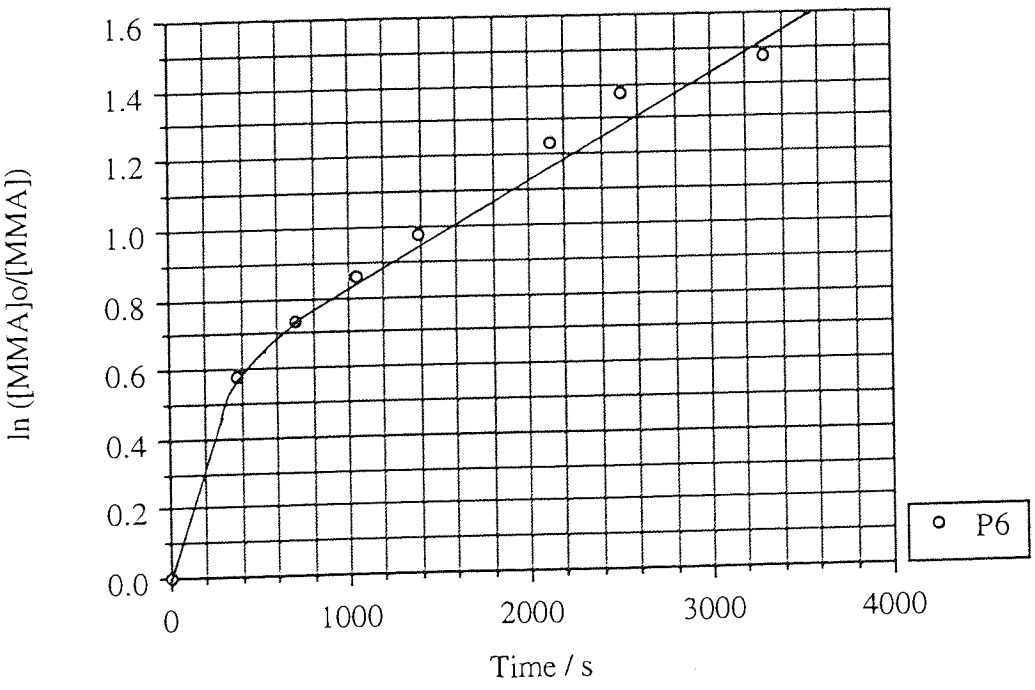

The plots showing logarithmic conversion of monomer as a function of time (figures 4.3 and 4.4), indicate a significant change in the slope near the beginning of the polymerization; the reactions following first order decay with respect to the concentration of monomer after an initial large decrease in [MMA]. These results are in agreement with those of Muller *et al* [75] who recently reported the change in gradient when carrying out the polymerization initiated by *t*-butyllithium/triethylaluminium or triisobutylaluminium at -78°C.

There is no obvious explanation for the decrease in rate of the polymerization, except a change in mechanistic dependences, and since the second part of the logarithmic conversion-time plot is linear it cannot be attributed to termination. This phenomenom could be explained by the existence of a critical degree of polymerization ($\overline{DP}_n$), at which point the polymerization rate decreases, relating to a change in structure of the active chain end causing a decrease in activity.

Muller *et al* [76] reported that the propagating centre in the polymerization was a bimetallic 'ate' complex ([PMMA-AlR_3]Li). They deduced this from ^{13}C NMR studies of the unimeric model of the living polymer chain end, ethyl α-lithioisobutyrate. They proposed that excess aluminium alkyl coordinates to the carbonyl groups of both the monomer and the polymer chains, and that coordination to the polymer could possibly cause a decrease in activity of the chain ends. Consequently, the amount of aluminium alkyl available to coordinate with the monomer would be reduced as the concentration of polymer increases. MMA and Methyl Pivilate (MPiv) were mixed with the aluminium alkyl at room temperature. The MPiv was used as a model of the polymer chain. They found that shift of electron density towards the oxygen atom of the carbonyl group in the monomer increases the polarization of the vinyl double bond which would probably lead to the activation of monomer (MMA•AlR_3) and hence acceleration of polymerization. The polarization of the carbonyl group of the polymer chain , however, enables a nucleophilic attack on the propagating centre to occur, thus accelerating back-biting termination (see scheme 4.1). These findings were in agreement with Inoue *et al* [87] who attributed a

dramatic acceleration of polymerization by aluminium thiolate complexes of porphyrin to the formation of activated monomer in the living polymerization of MMA .

Scheme 4.1. Coordination of Aluminium Alkyl to the Ester Groups of the Monomer (MMA) and the Model of the Polymer Chains (MPiv) (Muller *et al*)

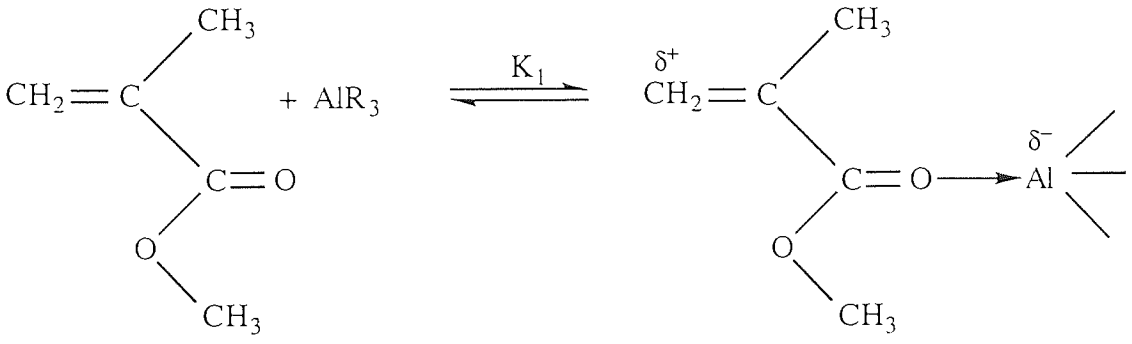

MMA • AlR_3

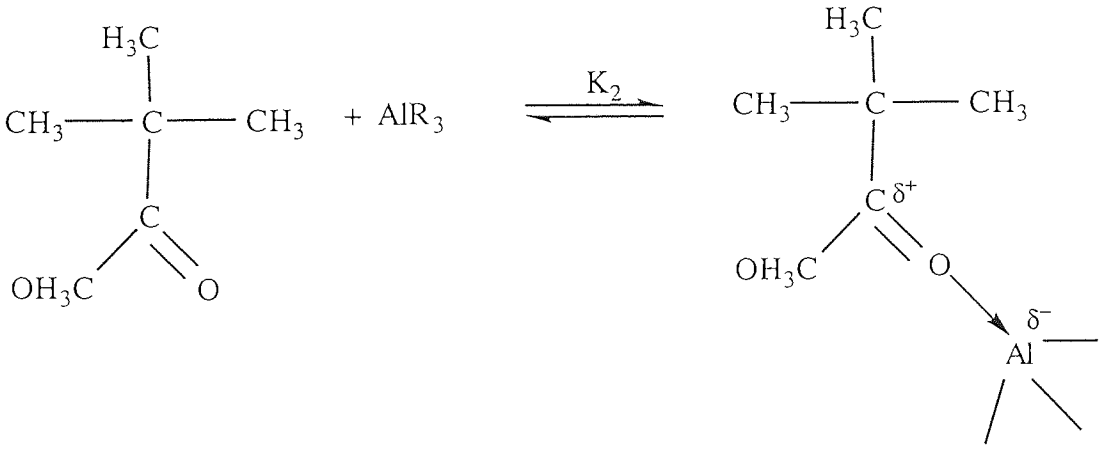

MPiv • AlR_3

The observations from the polymerizations carried out in these studies confirm Muller's theory, in that on addition of MMA to the initiating system, the solution turns yellow, which suggests the formation of a complex between the carbonyl group of the MMA and the aluminium alkyl[83]. This colour disappears as monomer is converted to polymer, since the π electrons are not so highly delocalised when addition across the double bond takes place in monomer molecules. Assuming that the aluminium alkyl coordinates to the ester carbonyls of both the monomer and the polymer, the fraction of aluminium alkyl

available for coordination to the monomer is decreased as the concentration of polymer increases. This will reduce the proportion of activated monomer present and could explain the decrease in activity of the chain ends and, hence, the decrease in the rate of polymerization. The kinetics of polymerization can be determined as follows:

$$Al_f + M \underset{}{\overset{K_1}{\rightleftharpoons}} AlM$$

$$Al_f + P \underset{}{\overset{K_2}{\rightleftharpoons}} AlP$$

Therefore, $$K_1 = \frac{[AlM]}{[Al]_f [M]}$$

$$K_2 = \frac{[AlP]}{[Al]_f [P]}$$

where $[P] = [M]_o - [M]$ = concentration of PMMA at time t

$[M]$ = concentration of MMA at time (t). $[M]_o$ = initial concentration of MMA

and $[Al]_f$ = concentration of unreacted aluminium alkyl

$[AlM]$ = concentration of aluminium alkyl coordinated monomer

$[AlP]$ = concentration of aluminium alkyl coordinated polymer.

$$[AlM] = K_1 [Al]_f [M]$$

$$[AlP] = K_2 [Al]_f [P]$$

$$\frac{[AlM]}{[AlP]} = \frac{K_1 [M]}{K_2 [P]}$$

$$[AlP] = \frac{K_2 [P]}{K_1 [M]} \cdot [AlM]$$

$$[Al]_o = [Al]_f + [AlM] + [AlP]$$

where $[Al]_o$ = initial concentration of aluminium alkyl

If alkyl aluminium complexes strongly with the ester group, then :

$$[Al]_f << [AlM]$$

and $$[Al]_f << [AlP]$$

therefore, since $[Al]_f$ is negligible :

$$[Al]_o = [AlM]\left(1 + \frac{K_2\,[P]}{K_1\,[M]}\right)$$

$$[AlM] = \frac{K_1[M]}{K_1[M] + K_2[P]} \cdot [Al]_o$$

If the AlM complex is the "active" monomer in the propagation, the rate of polymerization can be determined as follows :

$$P_n^- Li^+ + AlM \xrightarrow{k_p} P_{n+1}^- Li^+$$

Therefore, $$\frac{-d[M]}{dt} = k_p\,[P_n^- Li^+]\,[AlM]$$

$$\frac{-d[M]}{dt} = k_p\,[P_n^- Li^+]\,[Al]_o \cdot \frac{K_1[M]}{K_1[M] + K_2[P]}$$

where $P_n^- Li^+$ = living ends

$$\int_{[M]_o}^{[M]} \frac{K_1\,[M] + K_2([M]_o - [M])}{K_1[M]} \cdot d[M] = -k_p[P_n^- Li^+]\,[Al]_o \int_0^t dt$$

$$\int_{[M]_o}^{[M]} \left(1 + \frac{K_2[M]_o}{K_1[M]} - \frac{K_2}{K_1}\right) d[M] = -k_p[P_n^- Li^+]\,[Al]_o\,t$$

$$\int_{[M]_o}^{[M]} \left(\left\{\frac{K_1 - K_2}{K_1}\right\} + \frac{K_2[M]_o}{K_1} \cdot \frac{1}{[M]}\right) d[M] = -k_p[P_n^- Li^+]\,[Al]_o\,t$$

$$\frac{K_1-K_2}{K_1}\left([M] - [M]_o\right) + \frac{K_2[M]_o}{K_1} \ln\frac{[M]}{[M]_o} = -k_p[P_n^- Li^+]\,[Al]_o\,t$$

$$-\left(\frac{K_1-K_2}{K_1}\right)[P] + \frac{K_2[M]_o}{K_1} \ln\frac{[M]}{[M]_o} = -k_p[P_n^- Li^+]\,[Al]_o\,t$$

$$\left(\frac{K_2-K_1}{K_1}\right)[P] + \frac{K_2[M]_o}{K_1} \ln\frac{[M]}{[M]_o} = -k_p[P_n^- Li^+]\,[Al]_o\,t$$

$$(K_2-K_1)\,[P] + K_2[M]_o \ln\frac{[M]}{[M]_o} = -k_pK_1[P_n^- Li^+]\,[Al]_o\,t$$

If $K_2 = 0$, and K_1 is large, then :

$$-K_1[P] = -k_pK_1[P_n^- Li^+][Al]_ot$$

$$[P] = k_p[P_n^- Li^+][Al]_ot$$

and $[Al]_o = [AlM]$ since all the aluminium complexes with free monomer when AlP does not exist. In this case the rate is found to be independent of the concentration of free monomer but is found to be dependent on the concentration of "activated" monomer.

If $K_2 \neq 0$, a logarithmic conversion-time plot shows that the polymerization does not follow simple first order kinetics because it is believed that [AlP] is an important factor in determination of the rate of polymerization. The concentration of polymer is a function of time and this causes a change in gradient as the polymerization proceeds, according to the equation :

$$\ln\frac{[M]}{[M]_o} = \frac{(K_1-K_2)\,[P]}{K_2[M]_o} - \frac{k_pK_1[P_n^- Li^+]\,[Al]_o\,t}{K_2[M]_o}$$

^{13}C NMR studies carried out by Muller *et al*[76] showed that the aluminium alkyl is bound somewhat stronger to the polymer than the monomer ester groups; this would explain the non-first order kinetics observed in these polymerizations.

4.3.2.3 SEC Analysis

The polymer samples taken from the polymerizations were analysed by SEC. Table 4.4 shows the molecular weight distributions obtained for experiments P1-P7.

Table 4.4 The Molecular Weight Distributions for Experiments P1-P7 in the Anionic Polymerization of MMA, Initiated by $BuLi/AlEt_3$

Polymerization No	$\overline{M}_n$ / g mol^{-1}	$\overline{M}_w$ / g mol^{-1}	Polydispersity
P1	24600	70300	2.9
P2	38200	70600	1.9
P3	36000	76400	2.1
P4	23000	45700	2.0
P5	25000	57800	2.3
P6	24200	88000	3.6
P7	28900	65500	2.3

All the polymers obtained showed bimodal molecular weight distributions, the reasons for which are discussed later in this section. The figures quoted in table 4.4 are for the overall molecular weights obtained at the end of all the polymerizations. The polydispersity indices were found to lie between 1.9-3.6. There was a small increase in polydispersity index when the [Al]/[Li] ratio was increased from 3 to 5. Hatada *et al* [69] obtained a polydispersity index of 9.6 when carrying out the polymerization using the same initiating system, at -78°C.

Dependence of molecular weight on conversion for P2, P3 and P4 is plotted in the following series of graphs :-

Figure 4.5 Increase in $\overline{M}_n$ as a Function of Percentage Conversion for P2

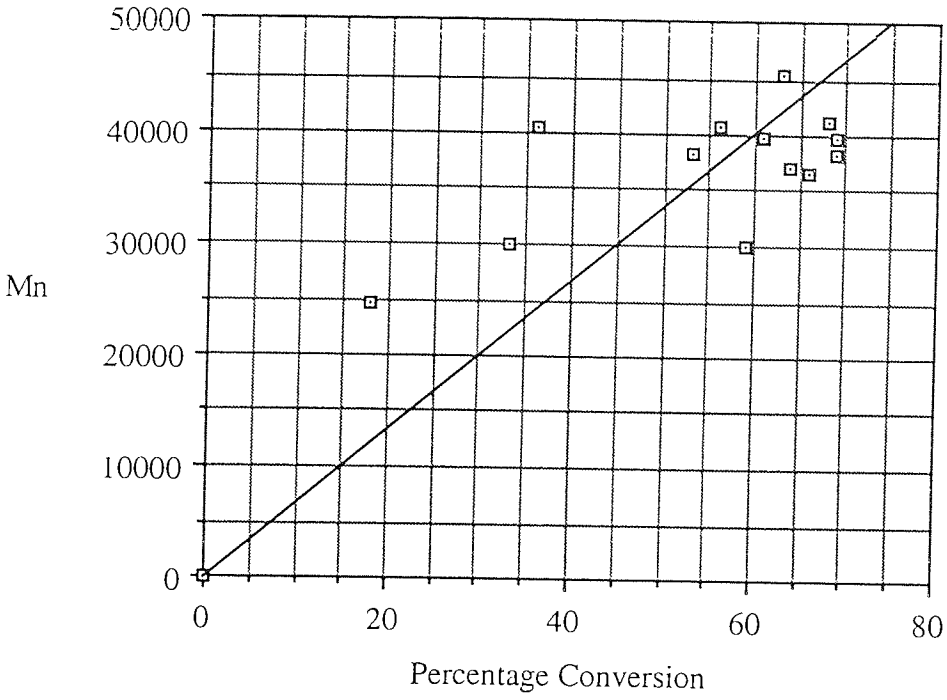

Figure 4.6 Increase in $\overline{M}_n$ as a Function of Percentage Conversion for P3

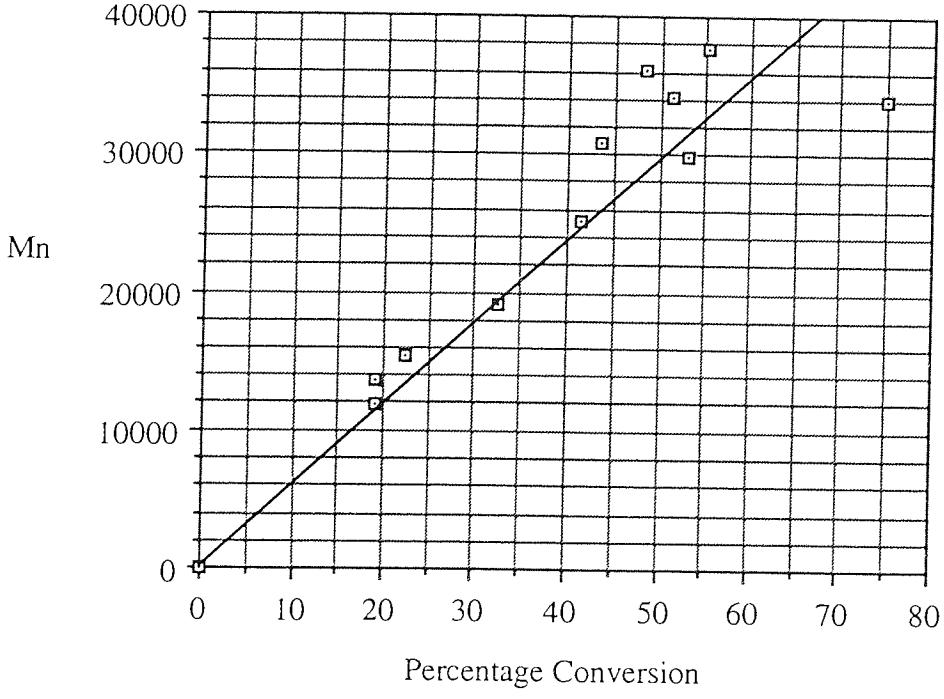

Figure 4.7 Increase in $\overline{M}_n$ as a Function of Percentage Conversion for P4

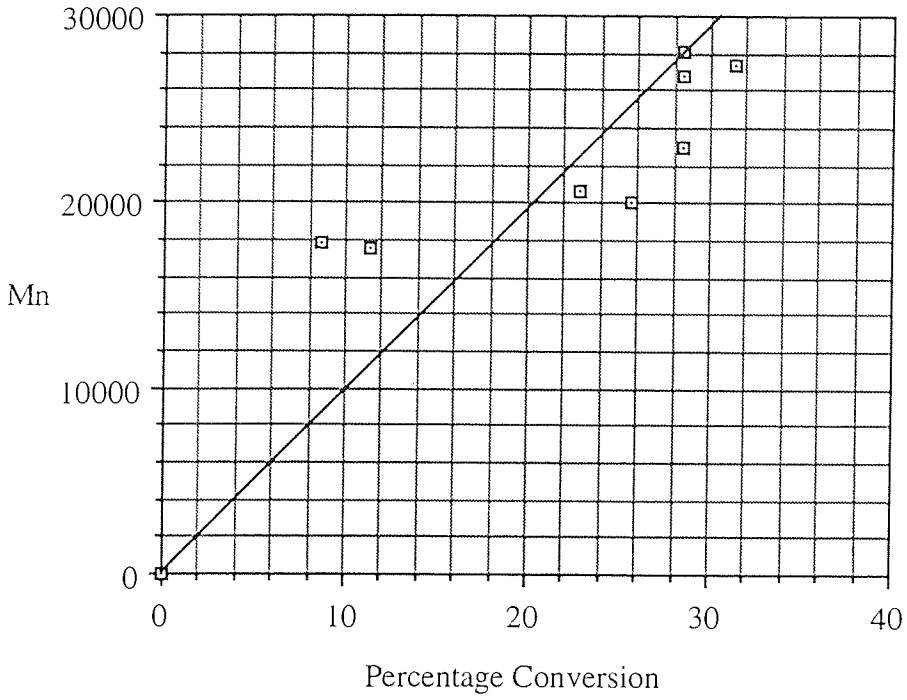

These graphs show some evidence that the polymerization system is 'living' since there appears to be a linear relationship between the increase in molecular weight with respect to percentage conversion. There was no correlation between molecular weight and percentage conversion for P5, P6 and P7. The irreproducibility associated with these polymerizations could be attributed to the fact that they showed bimodal molecular weight distributions making it difficult to obtain accurate molecular weights. Appendices 11 and 12 show SEC traces for P3, taken from samples at 19% and 75% conversion respectively. These traces are typical for these polymerizations. For the purposes of plotting the data the lower molecular weight curve was used for the calculation of $\overline{M}_n$ and $\overline{M}_w$ values for the first few samples but as the polymerizations proceeded the two curves overlapped making them indistinguishable. The molecular weights obtained for the final few samples were overall, combined molecular weight distributions from both the curves, with fairly broad polydispersity indices.

The bimodal distribution is explained most simply by the presence of two active centres in the propagating stages of polymerization. The two active centres can be attributed to the

presence of two different types of initiating species. Two possibilities are considered below :

(i) The initiating species could be either the initiating complex formed between BuLi and $AlEt_3$ (**2**), or any unreacted BuLi on its own (**1**). This is shown in reaction scheme 4.2 :

Scheme 4.2 To Show BuLi/$AlEt_3$ Complex Formation as the Initiating Species in the Anionic Polymerization of MMA in the Presence of Aluminuim Alkyls

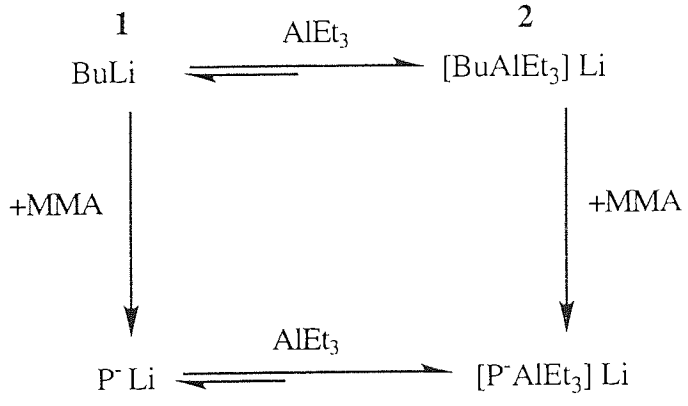

P^- = active chain end

(ii) Initiation could be caused by either complex formation between the BuLi and $AlEt_3$ before addition of MMA (2), or by addition of BuLi to a complex formed between $AlEt_3$ and MMA (3). The presence of the latter complex was suggested by Muller *et al* [75] and its formation is shown in reaction scheme 4.3 :

Scheme 4.3 To Show MMA/$AlEt_3$ Complex Formation in the Anionic Polymerization of MMA in the Presence of Aluminuim Alkyls

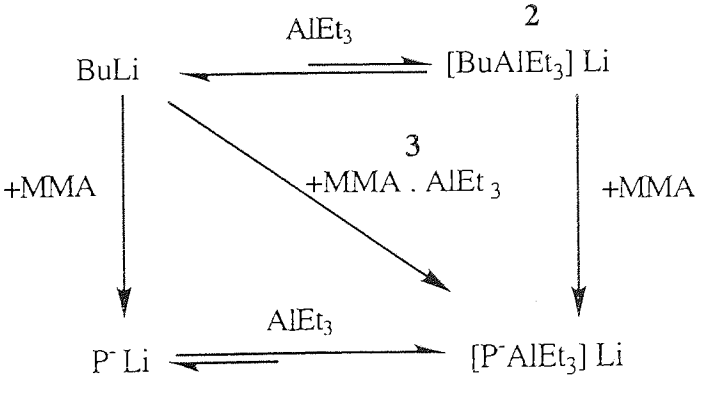

P^- = active chain end

Further evidence to support Muller's theory is the observation that on addition of MMA to the initating system, the solution turns yellow, which suggests the formation of a complex between the carbonyl group of the MMA and the aluminium alkyl has occurred[83].

The following graphs show plots of the number average degree of polymerization ($\overline{DP}_n$), against percentage conversion for P2, P3 and P4.

Figure 4.8 Increase in $\overline{DP}_n$ as a Function of Percentage Conversion for P2

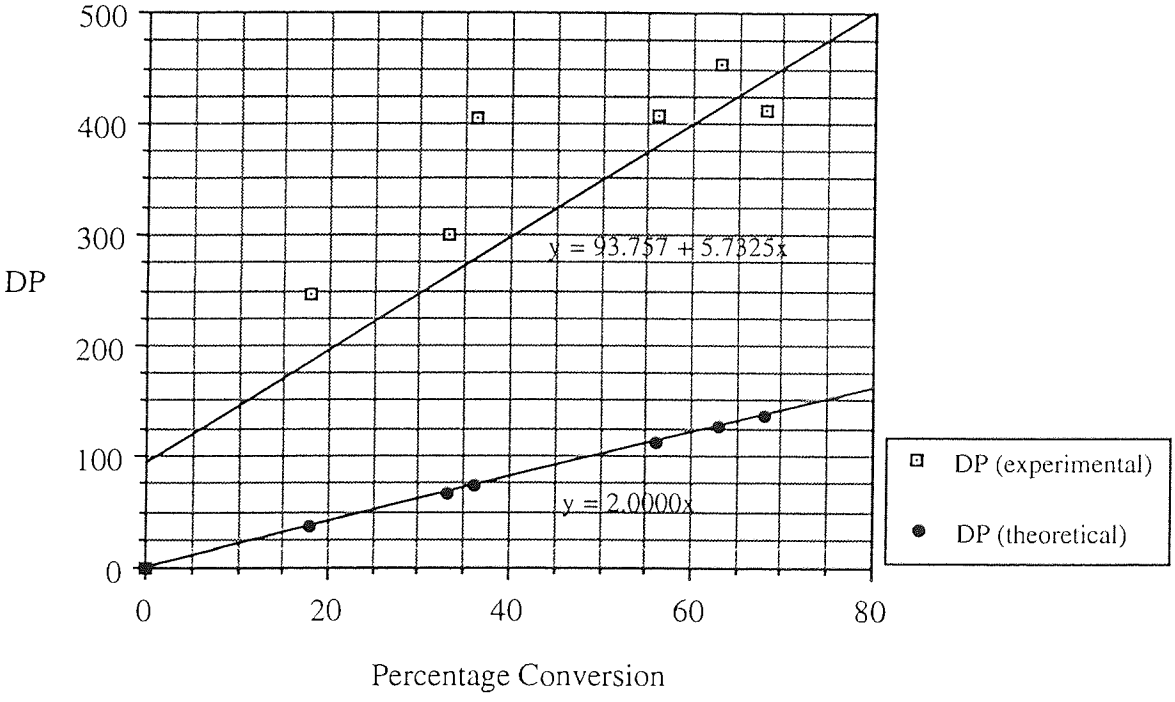

Figure 4.9 Increase in $\overline{DP}_n$ with respect to Percentage Conversion for P3

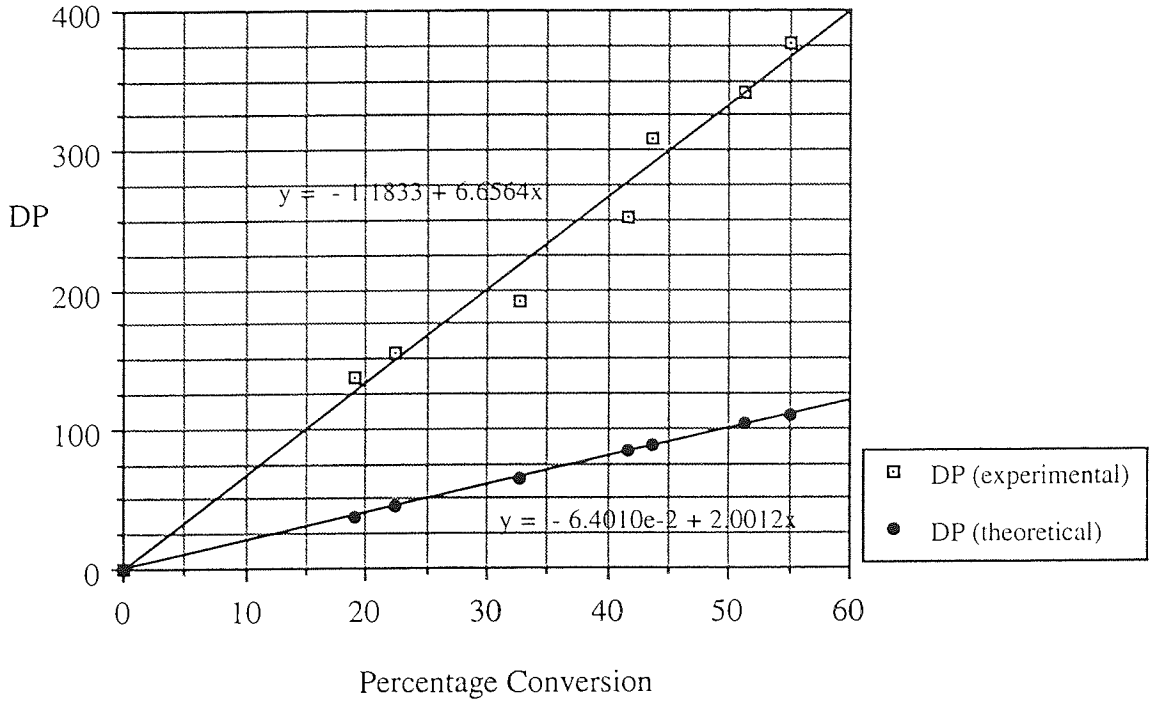

Figure 4.10 Increase in $\overline{DP}_n$ with respect to Percentage Conversion for P4

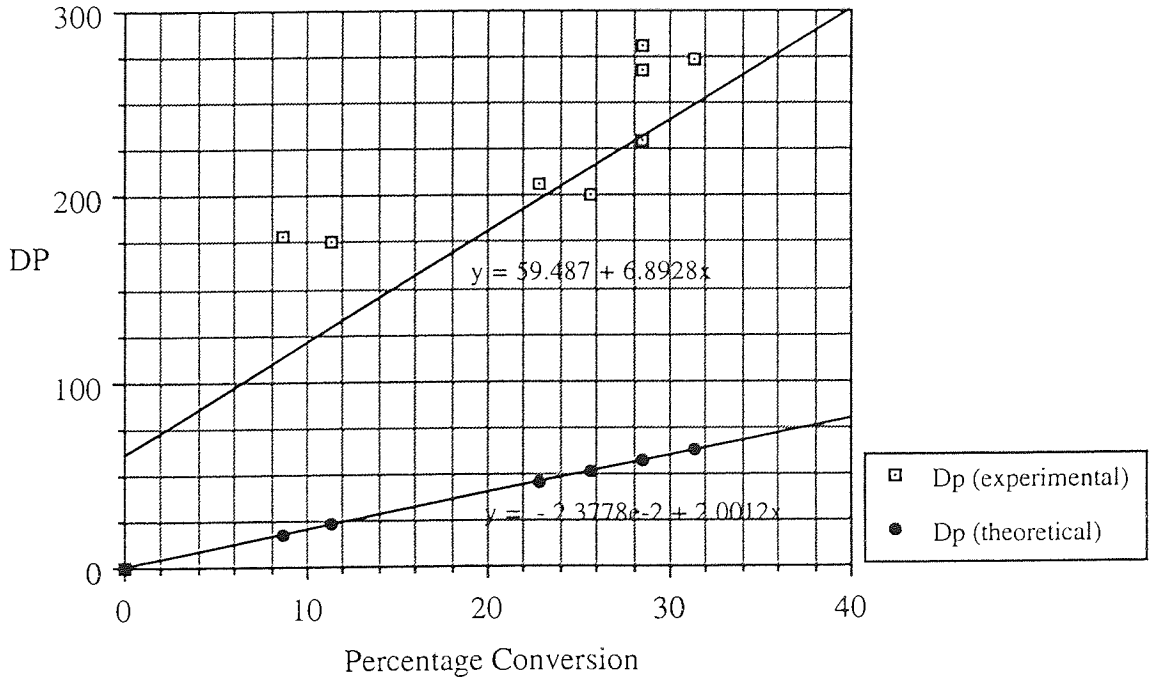

The experimental $\overline{DP}_n$ values were obtained directly from the molecular weights of the polymerizations. The theoretical value, at any time, was determined asuming 100% initiation. The number average degree of polymerization was calculated as follows :

$$\overline{DP}_n \text{ (experimental)} = \frac{\overline{M}_n}{rmm}$$

$$\overline{DP}_n \text{ (theoretical)} = \text{percentage conversion} \times \frac{[MMA]_0}{[BuLi]_0}$$

where $[MMA]_0$ = initial concentration of MMA

$[BuLi]_0$ = initial concentration of BuLi

rmm = molecular weight of MMA

$\overline{M}_n$ = number average molecular weight of PMMA

The initiator efficiency (f) for P3 was calculated from the equations of the respective lines relating to the experimental and the theoretical $\overline{DP}_n$ values (see figure 4.9). P3 was chosen to calculate the value f, since it showed the best fit line for $\overline{DP}_n$ (experimental).

$$\overline{DP}_n \text{ (theoretical)} = \text{percentage conversion} \times \frac{[MMA]_0}{[BuLi]_0}$$

$$\overline{DP}_n \text{ (experimental)} = \frac{[MMA]_0 - [MMA]_t}{f\,[BuLi]_0} = \frac{\text{percentage conversion } [MMA]_0}{f\,[BuLi]_0}$$

$$\overline{DP}_n \text{ (experimental)} = \frac{\overline{DP}_n \text{ (theoretical)}}{f}$$

where $[MMA]_t$ = concentration of MMA at time t

The efficiency of initiation could then be determined from a comparison of the slopes of the experimental and theoretical dependences. For P3 the efficiency of initiation was

determined as 0.3 or ~ 30%. The result shows that the efficiency of the initiator is not very high. The effect of changing the alkyl groups on both the aluminium and the lithium components on the initiator efficiency is discussed later in this chapter.

4.3.2.4 NMR Analysis

4.3.2.4.1 ^{1}H NMR.

Appendix 13 shows the ^{1}H NMR spectrum of the PMMA obtained for P3 which is typical of the spectra obtained for P1-P7. Table 4.5 assigns the chemical shifts δ, of the peaks corresponding to ^{1}H NMR spectrum of PMMA for P3.

Table 4.5 ^{1}H NMR Analysis of PMMA from P3, Initiated by BuLi $AlEt_3$ (Toluene)

Chemical Shift (ppm)	Assignment	Area
0.77	-CH_3 syndiotactic (rr)	75.6
0.95	heterotactic (mr)	43.3
1.14	isotactic (mm)	8.6
1.34		10.6
1.74	-CH_2	81.0
1.82		
3.53	-CH_3CO	129.7

Analysis of the relevent areas corresponding to the -CH_3 peaks on the spectrum showed that σ = 0.23. This corresponds to an isotactic content of 6.7%, syndiotactic 58.8% and heterotactic 33.7%. The results show that the polymers produced from experiments P1-P7 exhibit a greater proportion of the syndiotactic configuration.

4.3.2.4.2 ^{13}C NMR

Appendix 14 shows the ^{13}C NMR spectrum of the PMMA obtained for P3, which is typical of the spectra obtained for P1-P7. Table 4.6 assigns the chemical shifts δ, of the peaks obtained from the ^{13}C NMR spectrum of PMMA for P3.

Table 4.6 ^{13}C NMR Analysis of PMMA from P3, Initiated by BuLi/$AlEt_3$ (Toluene)

Chemical Shift (ppm)	Assignment
16.30	$-CH_3$ syndiotactic (rr)
18.57	heterotactic (mr)
20.90	isotactic (mm)
44.39	$-CH_2$ syndiotactic (rr)
44.73	heterotactic (mr)
45.38	isotactic (mm)
51.71	$-CH_3CO$
54.28	quaternary carbon
176.86	-C=O syndiotactic (rrrr)
177.70	heterotactic (rrrm)
177.95	heterotactic (rrmm)

The ^{13}C NMR spectra shows the presence of all three triad configurations relating to the $-CH_2$, $-CH_3$ groups and only the syndiotactic and heterotactic configurations relating to the -C=O group.

4.3.2.5. Discussion

From the results obtained from this set of experiments it can be seen that this initiating system is capable of producing PMMA of up to 90 % yield and polydispersity index of 2. The bimodal molecular weight distributions may be attributable to the presence of two initiating species. The curvature obtained from the logarithmic conversion-time plots, shows a decrease in the rate of propagation which could be attributable to a decrease in concentration of activated monomer, resulting from an increase in concentration of aluminium alkyl coordinated polymer. These two competing processes are thought to be the cause of a decrease in the rate of polymerization which occurs as the proportion of polymer coordinated to aluminium alkyl increases. The system has shown some evidence of living character; the initiator efficiency, however, is low and the results are not consistently reproducible. There is no apparent improvement in either the yield or the molecular weight distribution when the [Al]/[Li] ratio is increased from 3 to 5. In fact, contrary to findings in the literature [69-74], the yields are actually lower and the polydispersities higher when the ratio is increased. It was thought that the results obtained from these experiments may be dependent on the temperature of polymerization and the nature of the lithium and aluminium alkyl components.

4.4 Polymerization of Methyl Methacrylate Initiated by *tert*-Butyllithium/Triethylaluminium

This section describes the results obtained from a series of polymerizations of MMA initiated by *t*-BuLi/$AlEt_3$ using toluene as the solvent. The polymerizations were carried out as described in section 4.2.1. The kinetics of the polymerizations were followed using GC and molecular weight changes were monitored using SEC.

4.4.1 Experimental

The following polymerizations were carried out using the quantities of reagents shown in table 4.7 :

Table 4.7 Conditions for the Polymerization of MMA Initiated by *t*-BuLi/$AlEt_3$

Polymerization No	10^3 x $\frac{\text{MMA}}{\text{moles}}$	10^3 x $\frac{t\text{-BuLi}}{\text{moles}}$	10^3 x $\frac{AlEt_3}{\text{moles}}$	$\frac{[\text{MMA}]}{[\text{BuLi}]}$	$\frac{[AlEt_3]}{[t\text{-BuLi}]}$
P8	124	0.62	1.860	200	3
P9	90	0.12	0.363	750	3
P10	100	0.25	1.240	400	5

Solvent : toluene Temperature : 30 +/- 1°C [MMA] : 1.4 +/- 0.2 mol dm^{-3}

4.4.2 GC Analysis

The following graphs show the decay of the concentration of MMA as a function of time, which were then used to obtain logarithmic conversion-time plots for P8, P9 and P10.

Figure 4.11 To Show the Decay in Concentration of Monomer as a Function of Time for Three Polymerizations of MMA Initiated by *t*-BuLi/$AlEt_3$

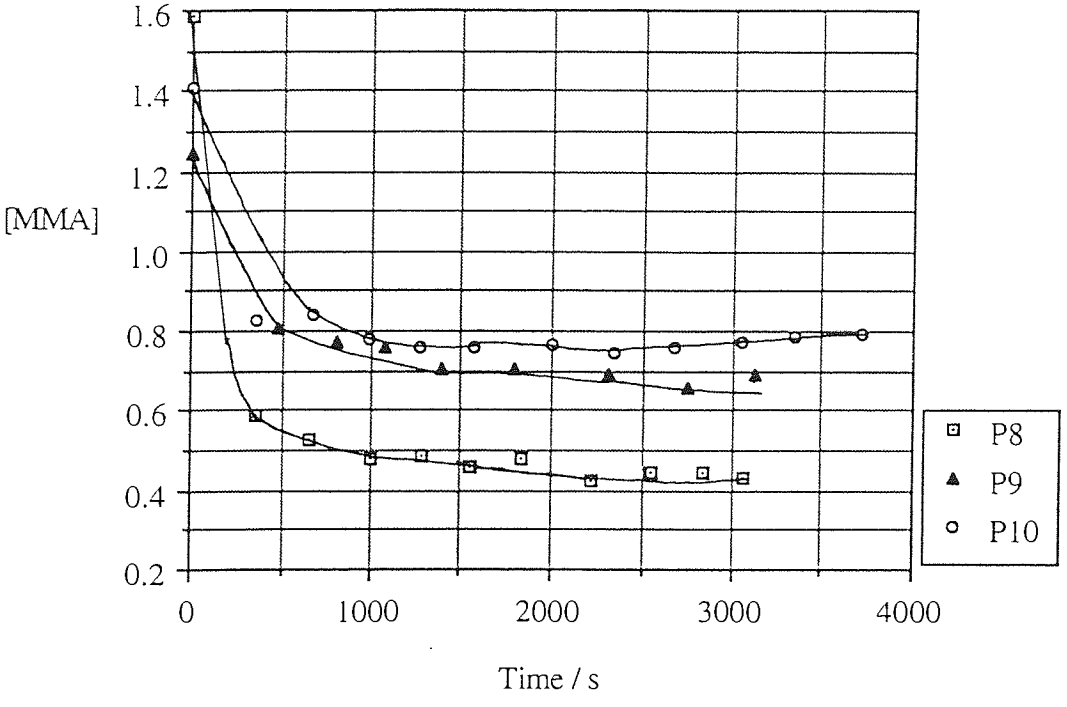

The plots of the decay in monomer concentration as a function of time show that the polymerizations were all fairly rapid even when the initiator concentration was greatly reduced, as it was for P9. The samples which were withdrawn, are thought to be taken towards the end of the polymerizations, since there was not much further decrease in monomer concentration.

The percentage yields obtained at the end of the polymerizations were calculated from the decay in monomer concentration and were found to be 73%, 51% and 44% for P8, P9 and P10 respectively. The yields strongly suggest that the technique of withdrawal of samples can cause termination of some of the living chains, since it may enable terminating agents to enter the system. All the logarithmic conversion-time plots exhibit a curvature (see figures 4.12 and 4.13) similar to those obtained from the BuLi/$AlEt_3$ system.

Figure 4.12 Logarithmic Conversion Plots as a Function of Time For P8 and P9

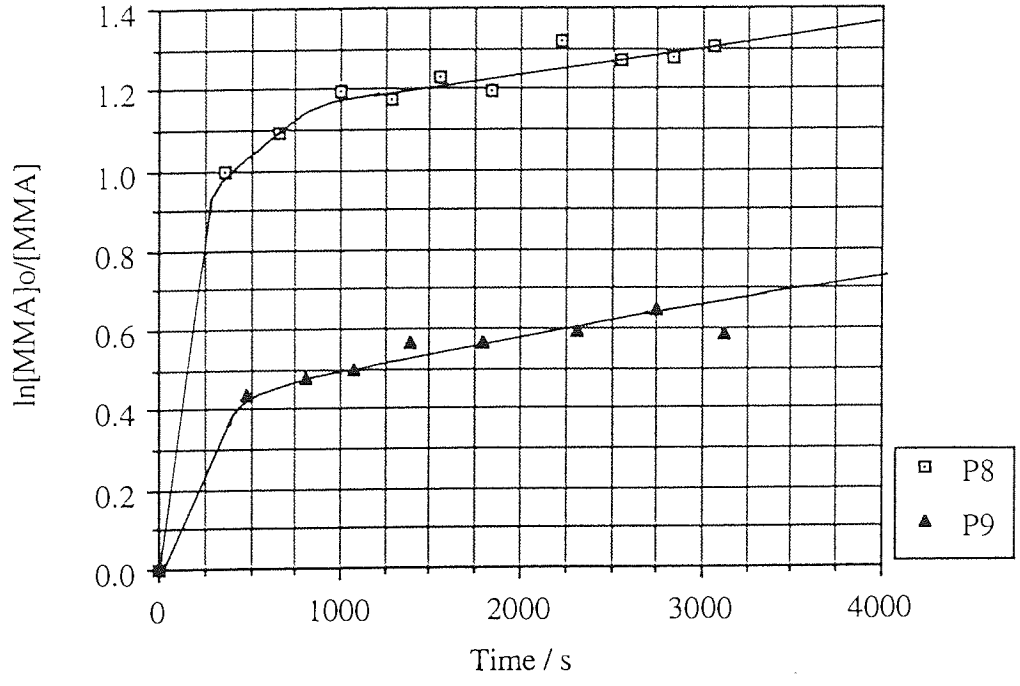

Figure 4.13 Logarithmic Conversion Plot as a Function of Time For P10

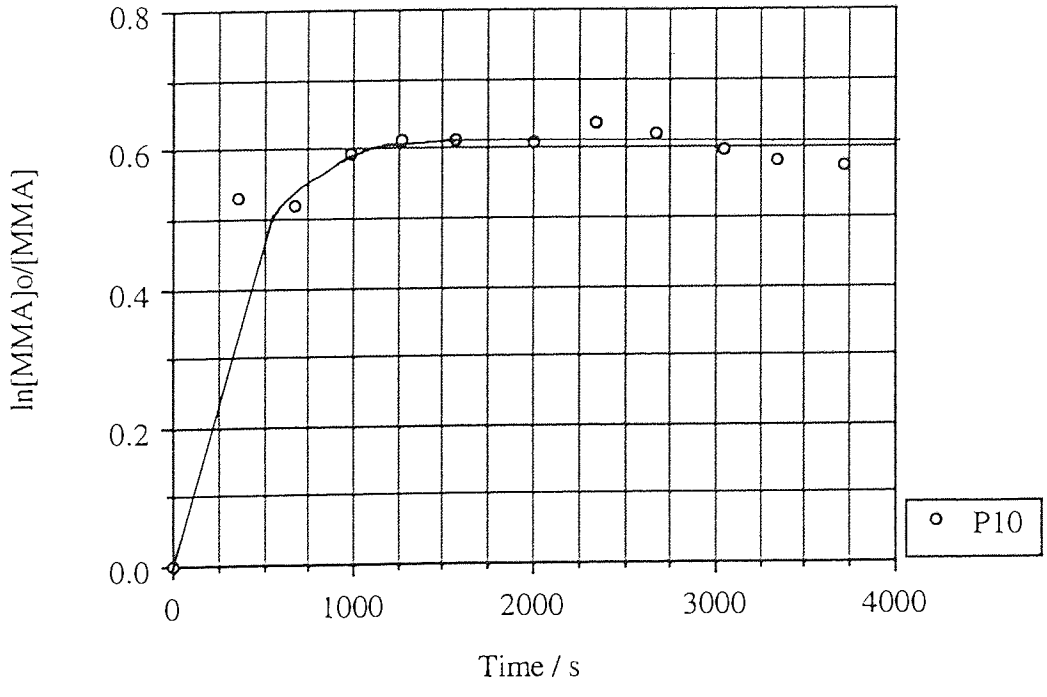

4.4.3 SEC Analysis

Samples taken from the polymerizations were analysed using SEC. Table 4.8 shows the molecular weight distributions obtained for P8-P10.

Table 4.8 The Molecular Weight Distributions for Experiments P8-P10 in the Anionic Polymerization of MMA Initiated by *t*-BuLi/$AlEt_3$

Polymerization No.	$\overline{M}_n$ / g mol^{-1}	$\overline{M}_w$ / g mol^{-1}	Polydispersity
P8	19700	32200	1.6
P9	16900	28900	1.7
P10	40300	74600	1.9

The results show that the molecular weight distributions obtained were narrower than those obtained for the BuLi/$AlEt_3$ system. All the SEC traces were unimodal apart from P10, where a bimodal distribution was obtained. The SEC traces obtained from a sample taken from P9 and P10 are shown in appendices 15 and 16 respectively. There was a slight broadening of molecular weight distribution as the [Al]/[Li] ratio was increased from 3 to 5; this confirms the results obtained on the work which was carried out on the BuLi/$AlEt_3$ system.

The unimodal distributions obtained confirm the work conducted by Hatada *et al* [69]. This suggests that the bulkier *t*-butyl group must sterically hinder the attack of the initiator on the carbonyl group of MMA and therefore minimise the occurrence of side reactions during initiation. It is also believed that since *t*-BuLi gives rise to faster initiation compared with BuLi, the initiation of chains occurs simultaneously resulting in polymers of unimodal molecular weight distribution. There are strong indications that one type of propagating species and hence, one type of initiating species is predominant in this polymerization system.

It is believed that the reason for the broader molecular weight distribution for P10 was due to a change in structure of the initiating species. The *t*-BuLi used for P10 was

prepared in a catayst flask by diluting with toluene, and the required amount was syringed out for the polymerization. The catalyst solution had been made up previously and had also been used for P9. Before injecting the *t*-BuLi for P10 it was noticed that the colour of the solution had changed to a bright red colour, since it had last been used in P9. The change in colour had been due to the reaction of *t*-BuLi with the toluene, by causing a proton to be abstracted and form 2-methyl propane. This is shown in scheme 4.4.

Scheme 4.4 The Reaction of *t*-BuLi with Toluene to Form a New Initiating Species

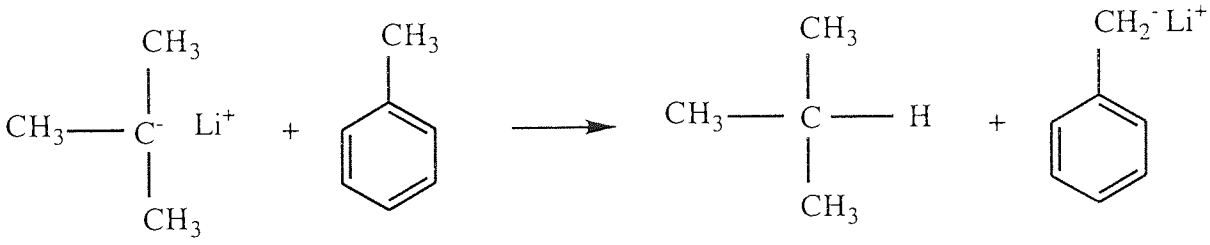

The initiator then reacts in the polymerization in the same way as BuLi and hence a bimodal molecular weight distribution is obtained for P10.

Plots of increase in molecular weight as a function of percentage conversion for P8 and P9 are shown in figure 4.14 :

Figure 4.14 Increase in $\overline{M}_n$ as a Function of Percentage Conversion for P8 and P9

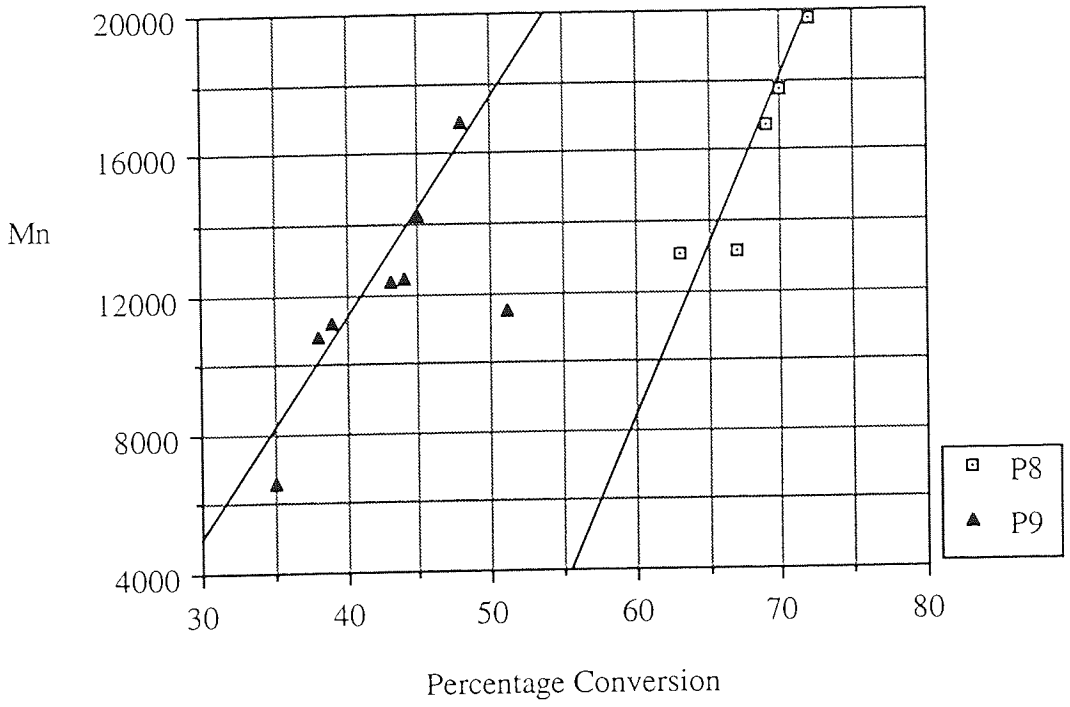

The plots show some evidence of a 'living' polymerization system since there appears to be a linear relationship between the increase in molecular weight with respect to percentage conversion. However, if the plots were to be extrapolated back to zero, it would appear that the relationship between molecular weight as a function of conversion may deviate from linearity. There was no correlation between molecular weight and percentage conversion for P10 and the points were randomly scattered.

The following graphs show plots of experimental and theoretical $\overline{DP}_n$ values with respect to percentage conversion for P8 and P9.

Figure 4.15 Increase in $\overline{DP}_n$ as a Function of Percentage Conversion for P8

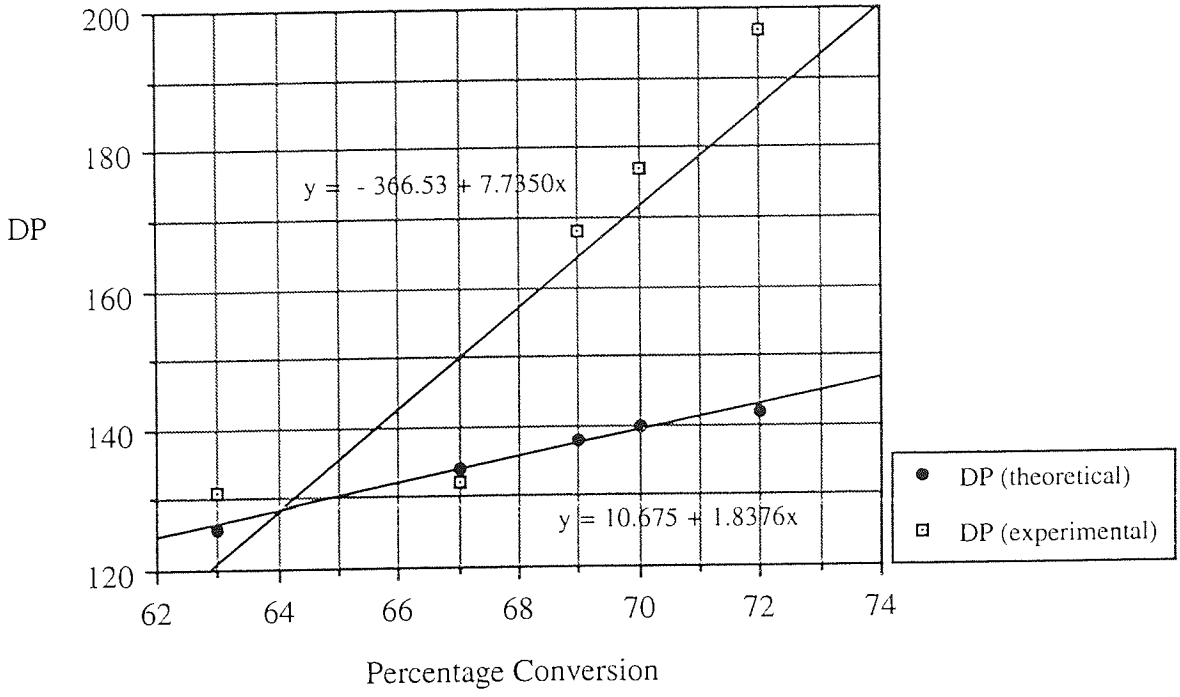

Figure 4.16 Increase in $\overline{DP}_n$ as a Function of Percentage Conversion for P9

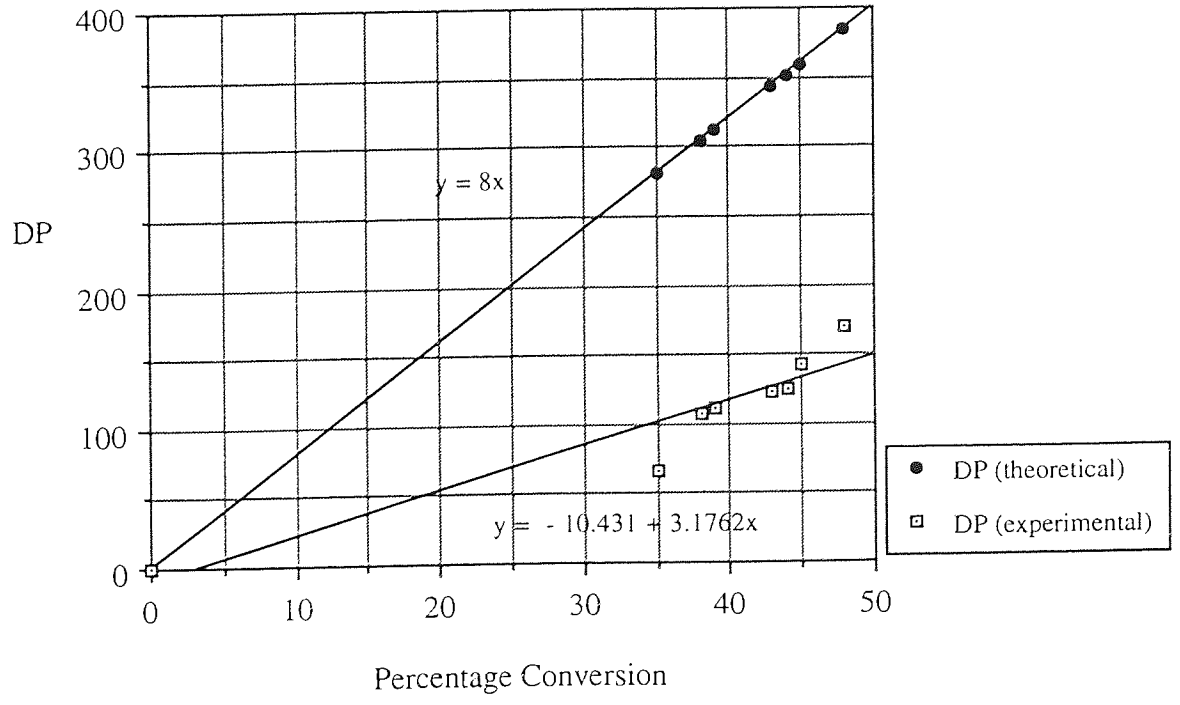

The initiator efficiencies (f) for P8 and P9 were calculated as described in section 4.3.2.3, from the equations of the respective lines relating to the experimental and the theoretical $\overline{DP}_n$ values (see figures 4.15 and 4.16). The values obtained for P8 and P9 were 24% and 251% respectively. P8 shows an initiator efficiency which is comparable to that obtained for the BuLi/$AlEt_3$ system. P9, however, shows an extremely high initiator efficiency, the value exceeding that of the theoretical value of 100%. In this polymerization it is evident that initiation of a greater number of monomer molecules has occurred to create more polymer chains, but the chains were terminated since the molecular weights obtained were lower than the expected values. This can be explained by the fact that a low initiator concentration was used for P9, hence the proportion of terminating agents, such as oxygen and moisture, within the system were larger in comparison to previous polymerizations.

4.4.4 NMR Analysis

4.4.4.1 ^{1}H NMR.

Appendix 17 shows the ^{1}H NMR spectrum of the PMMA obtained for P9 which is typical of the spectra obtained for P8-P10. Table 4.9 assigns the chemical shifts δ, of the peaks corresponding to the ^{1}H NMR spectrum of PMMA.

Table 4.9 ^{1}H NMR Analysis of PMMA from P9, Initiated by *t*-BuLi/$AlEt_3$

Chemical Shift (ppm)	Assignment	Area
0.79	-CH_3 syndiotactic (rr)	282.0
0.98	heterotactic (mr)	222.6
1.11	isotactic (mm)	56.7
1.77		154.6
1.85	-CH_2	185.9
1.98		
3.55	-CH_3CO	551.5

Analysis of the relevent areas corresponding to the -CH_3 peaks on the spectrum showed that $\sigma = 0.29$. This corresponds to an isotactic content of 10%, syndiotactic 50% and heterotactic 40%. The results show that the proportion of isotactic and heterotactic polymer produced is slightly greater than for the BuLi/$AlEt_3$ system.

4.4.4.2 ^{13}C NMR

Appendix 18 shows the ^{13}C NMR spectrum of the PMMA obtained for P9, which is typical of the spectra obtained for P8-P10. Table 4.10 assigns the chemical shifts δ, of the peaks obtained from the ^{13}C NMR spectrum of PMMA.

Table 4.10 ^{13}C NMR Analysis of PMMA from P9, Initiated by *t*-BuLi/$AlEt_3$

Chemical Shift (ppm)	Assignment
16.33	-CH_3 syndiotactic (rr)
18.59	heterotactic (mr)
20.92	isotactic (mm)
44.40	-CH_2 syndiotactic (rr)
44.75	heterotactic (mr)
45.40	isotactic (mm)
51.72	-CH_3CO
54.33	quaternary carbon
176.87	-C=O syndiotactic (rrrr)
177.03	heterotactic (rrrm)
177.71	heterotactic (rrmm)
178.01	heterotactic (rmmm)

The ^{13}C NMR spectra shows the presence of all three triads relating to the -CH_2 and -CH_3 groups. The -C=O group is shown to be pentad sensitive, similar to the PMMA produced from the BuLi/$AlEt_3$ system in cyclohexane. Again, there is no indication of the presence of the isotactic configuration (mmmm).

4.4.5 Discussion

From the results obtained from this set of experiments it is evident that when the BuLi is replaced by *t* - BuLi as the initiator, the polymers produced are of a unimodal, narrower molecular weight distribution. This can be attributed to the fact that the bulkier *t* -butyl group sterically hinders the carbonyl group of the MMA from side reactions during initiation and that initiation is rapid. The presence of one predominant initiating species is strongly indicated in this system. However, there appears to be no improvement on the initiator efficiency when *t*- BuLi is used instead of BuLi. The system has shown some evidence of living character, but the extent of conversion exhibited in these polymerizations is still fairly low. The findings confirm the work carried out on the BuLi/$AlEt_3$ system, whereby there is a distinct decrease in rate of polymerization at a critical $\overline{DP}_n$ value and a slight increase in polydispersity index is observed when the [Al]/[Li] ratio is increased from 3 to 5.

4.5 Polymerization of Methyl Methacrylate Initiated by *tert*-Butyllithium/Triisobutylaluminium

This section describes the results obtained from a series of polymerizations of MMA initiated by *t*-BuLi/$Al(^iBu)_3$ using toluene as the solvent. The polymerizations were carried out as described in section 4.2.1. The kinetics of the polymerizations were followed using GC and molecular weight changes monitored using SEC.

4.5.1 Experimental

The following polymerizations were carried out using the quantities of reagents shown in table 4.11 :

Table 4.11 Conditions for the Polymerization of MMA Initiated by *t*-BuLi/Al(^{i}Bu)$_3$

Polymerization No	10^3 x $\frac{\text{MMA}}{\text{moles}}$	10^3 x $\frac{t\text{-BuLi}}{\text{moles}}$	10^3 x $\frac{\text{Al}(^i\text{Bu})_3}{\text{moles}}$	$\frac{[\text{MMA}]}{[t\text{-BuLi}]}$	$\frac{[\text{Al}(^i\text{Bu})_3]}{[t\text{-BuLi}]}$
P11	116	0.146	0.728	800	5
P12	119	0.297	1.49	400	5

Solvent : toluene Temperature : 28 +/- 1°C [MMA] : 1.6 +/- 0.2 mol dm^{-3}

4.5.2 GC Analysis

The following graphs show the decay of the concentration of MMA as a function of time, which were then used to obtain logarithmic conversion-time plots for P11and P12 :

Figure 4.17 To Show the Decay in Concentration of Monomer as a Function of Time for Two Polymerizations of MMA Initiated by *t*-BuLi/Al(^{i}Bu)$_3$

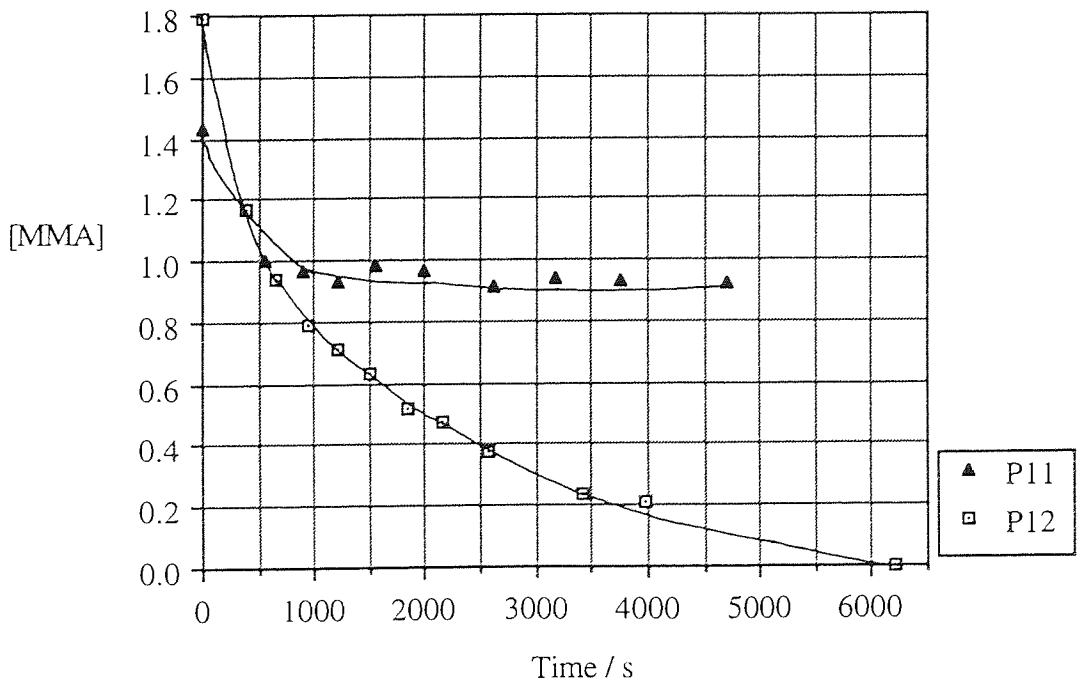

Figure 4.18 Logarithmic Conversion Plots as a Function of Time For P11 and P12

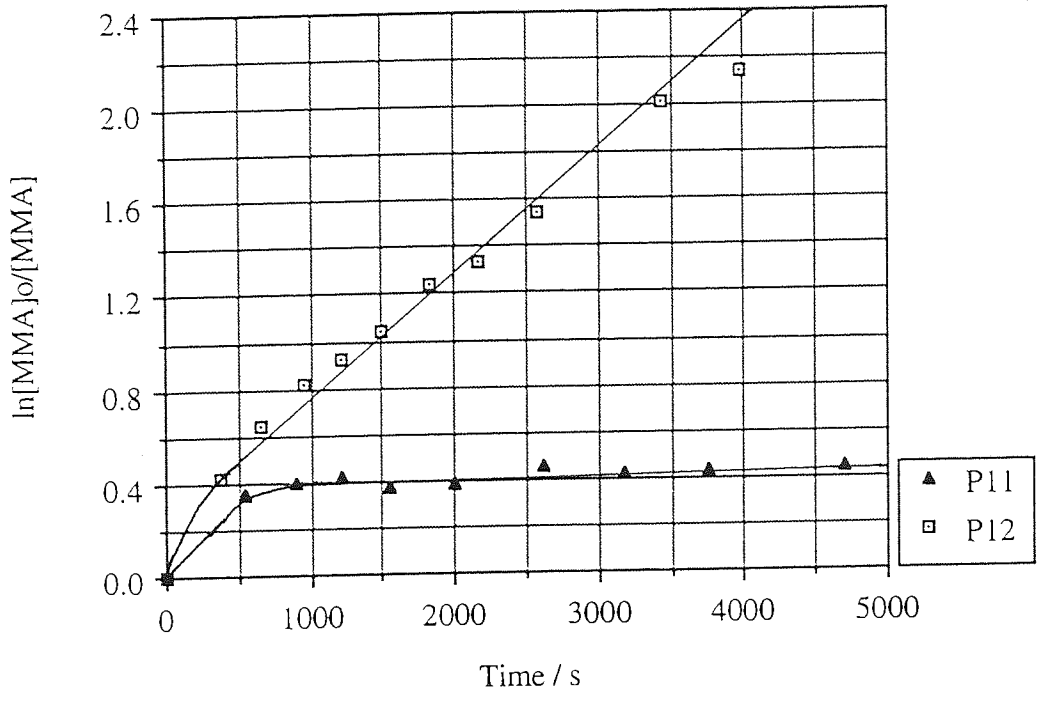

The percentage yields obtained at the end of the polymerizations were calculated from the decay in monomer concentration and were calculated as 36% and 100% for P11 and P12 respectively. The termination observed in P11 can be attributed to the very low initiator concentration used, since the concentration of terminating agents within this system was proportionately higher compared with that of P12.

4.5.3 SEC Analysis

The polymer samples taken from the polymerizations were analysed using SEC. Table 4.12 shows the molecular weight distributions obtained for P11 and P12.

Table 4.12 The Molecular Weight Distributions for Experiments P11 and P12 in the Anionic Polymerization of MMA Initiated by *t*-BuLi/Al(^{i}Bu)$_3$

Polymerization No.	$\overline{M}_n$ / g mol^{-1}	$\overline{M}_w$ / g mol^{-1}	Polydispersity
P11	28900	48800	1.7
P12	47900	89600	1.9

Appendix 19 shows an SEC chromatogram for a sample taken from P12. The traces from the samples show that polymer of fairly narrow, unimodal molecular weight distribution was obtained. The polydispersities for P11 and P12 are comparable to those obtained with the *t*-BuLi/AlEt$_3$ system. The following graph shows the increase in molecular weight as a function of percentage conversion for P12 :

Figure 4.19 Increase in $\overline{M}_n$ as a Function of Percentage Conversion for P12

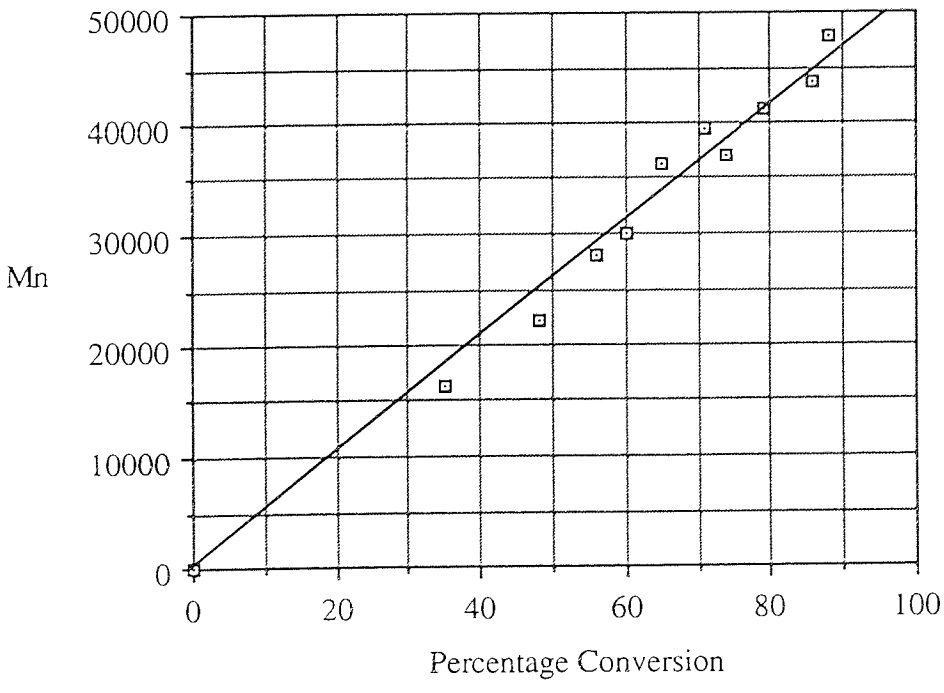

Figure 4.19 clearly shows that the increase in molecular weight as a function of percentage conversion is linear, which is typical of a 'living' polymerization system. Figure 4.20 shows plots of theoretical and experimental $\overline{DP}_n$ values with respect to percentage conversion for P12 :

Figure 4.20 Increase in $\overline{DP}_n$ as a Function of Percentage Conversion for P12

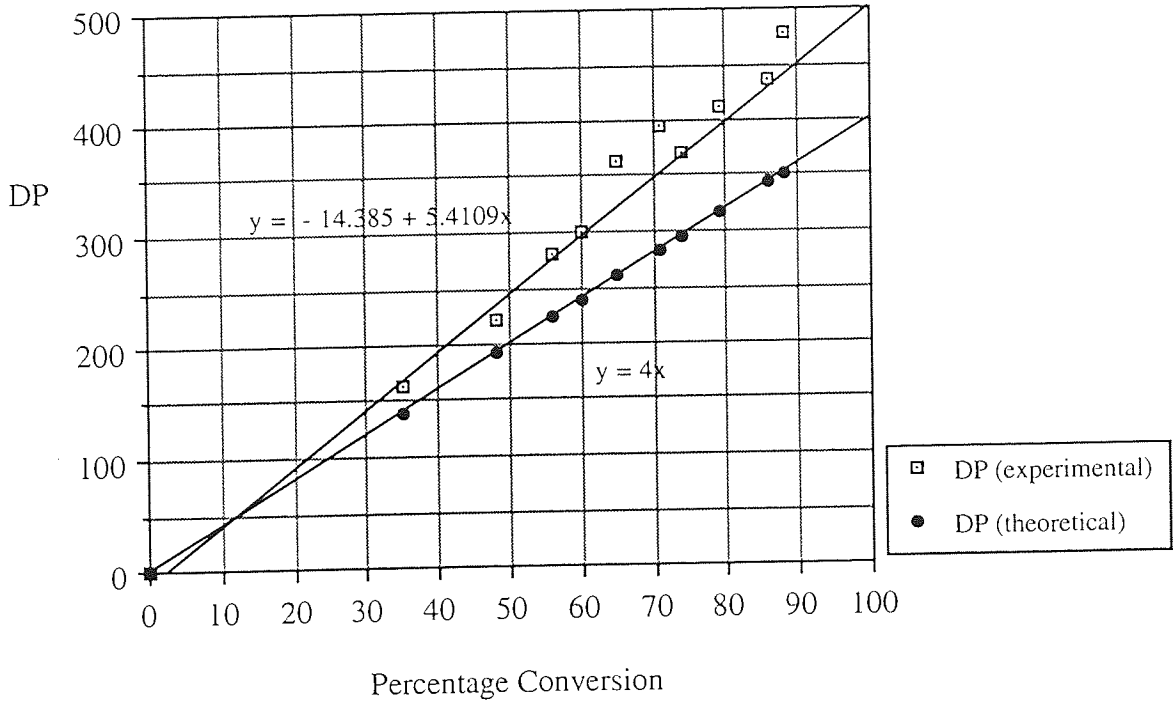

The initiator efficiency for the system was calculated as 78% using the method described in section 4.3.2.3. Hence the efficiency of the initiator was found to be substantially higher when the $AlEt_3$ was replaced by $Al(^iBu)_3$, since the values for the $BuLi/AlEt_3$ and the *t*-$BuLi/AlEt_3$ systems were found to be 30% and 24% respectively. These results suggest that the efficiency of the initiator depends solely on the size of the alkyl group on the aluminium component of the initiating system, and is not significantly affected by the size of the alkyl group on the lithium component.

4.5.4 Premixing of Methyl Methacrylate with $Al(^iBu)_3$

4.5.4.1 Experimental

MMA was polymerized using the *t*-BuLi/$Al(^iBu)_3$ initiating system (P13), but on this occasion the mode of addition of reagents was altered slightly. The $Al(^iBu)_3$ was premixed with the MMA before addition of the *t*-BuLi, instead of premixing the $Al(^iBu)_3$ with the *t*-BuLi before addition of the MMA; which had been the case for the previous polymerizations. 5.57×10^{-4} moles of *t*-BuLi were added to 0.11 moles of MMA and 2.78×10^{-3} moles of $Al(^iBu)_3$ in 44 cm^3 of toluene. The MMA formed a yellow solution with the $Al(^iBu)_3$ in toluene, and the mixture was left to stand at the polymerization temperature for 1 hour before addition of the *t*-BuLi. The ratios of the reagents used were as follows :

MMA	:	*t*-BuLi	:	$Al(^iBu)_3$
200	:	1	:	5

The polymerization was carried out at 25° C without following the reaction kinetics and therefore the system was not disturbed by removal of samples. The polymerization appeared to be very rapid and highly exothermic, but was allowed to proceed for 24 hours.

4.5.4.2 Results and Discussion

On recovery of the polymer a percentage yield of 99% was obtained. The SEC trace of the PMMA showed a unimodal molecular weight distribution. Analysis of the trace showed :

$\overline{M}_n = 14902$

$\overline{M}_w = 30917$

polydispersity index (PDI) =2.07

From the results it is clear that although the percentage yield obtained is just as high as for P12, the molecular weight distribution is slightly broader. The initiator efficiency was calculated as 132%, which is higher than the theoretical value. This result is contrary to the findings of Haddleton and Hunt[74], since they obtained much lower initiator efficiencies at 0°C when they premixed the MMA with $Al(^iBu)_3$, compared to when they premixed the *t*-BuLi with $Al(^iBu)_3$.

4.5.5 NMR Analysis

4.5.5.1 ^{1}H NMR

Appendix 20 shows the ^{1}H NMR spectrum of the PMMA obtained for P12. Table 4.13 assigns the chemical shifts δ, of the peaks corresponding to the ^{1}H NMR spectrum of PMMA.

Table 4.13 ^{1}H NMR Analysis of PMMA from P12, Initiated by *t*-BuLi/$Al(^iBu)_3$

Chemical Shift (ppm)	Assignment	Area
0.81	$-CH_3$ syndiotactic (rr)	76.6
0.99	heterotactic (mr)	40.4
1.18	isotactic (mm)	6.1
1.78	$-CH_2$	44.8
1.86		
1.99		32.1
3.57	$-CH_3CO$	117.6

Analysis of the relevent areas corresponding to the $-CH_3$ peaks on the spectrum showed that $\sigma = 0.21$. This corresponds to an isotactic content of 5%, syndiotactic 62% and heterotactic 33%. The results show that the polymer produced has a very large proportion of syndiotactic configuration and a very small proportion of isotactic.

4.5.5.2 ^{13}C NMR

Appendix 21 shows the ^{13}C NMR spectrum of the PMMA obtained for P12. Table 4.14 assigns the chemical shifts δ, of the peaks corresponding to the ^{13}C NMR spectrum of PMMA.

Table 4.14 ^{13}C NMR Analysis of PMMA from P12, Initiated by *t*-BuLi/Al(^{i}Bu)$_3$

Chemical Shift (ppm)	Assignment
16.40	$-CH_3$ syndiotactic (rr)
18.67	heterotactic (mr)
44.50	$-CH_2$ syndiotactic (rr)
44.80	heterotactic (mr)
51.81	$-CH_3CO$
54.19	quaternary carbon
176.98	-C=O syndiotactic (rrrr)
177.81	heterotactic (rrrm)
178.11	heterotactic (rrmm)

The ^{13}C NMR spectra shows the presence of only syndiotactic and heterotcatic diads relating to the $-CH_2$, $-CH_3$ and C=O groups.

4.5.6 Discussion

The results obtained from the *t*-BuLi/Al(^{i}Bu)$_3$ system showed that this system exhibited the highest initiator efficiency of the three lithium and aluminium alkyl systems investigated for the polymerization of MMA. This was the only system of the three where 100% conversion was achieved, even though the polymerizations were carried out at higher temperatures than are normally employed for anionic polymerizations of MMA. It is believed that the bulkier triisobutyl group on the aluminium component was better at protecting the carbonyl group of the MMA from side reactions, and thus preventing the

occurrence of termination reactions . The aluminium alkyl is thought to be coordinated to the carbonyl group of the MMA in order to achieve this. This can be seen from the characteristic yellow colour obtained when the MMA is first added to the aluminium alkyl; the colour gradually disappears when the monomer molecules are converted into polymer chains.

The efficiency of the initiator did not change when the BuLi was replaced by *t*-BuLi, however, the efficiency was vastly improved when the $AlEt_3$ was replaced by the $Al(^iBu)_3$. These results suggest that the efficiency of the initiator depends solely on the size of the alkyl group on the aluminium component of the initiating system, and is not significantly affected by the size of the alkyl group on the lithium component. The polydispersity indices of the polymer products were found to be approximately the same for both the *t*-BuLi/$AlEt_3$ and the *t* -BuLi/$Al(^iBu)_3$ systems.

When the polymerization was conducted by premixing the triisobutylaluminium with the monomer before the addition of initiator, both the extent of conversion of monomer and the initiator efficiency were high, but the molecular weights were lower than the theoretically expected values.

The aluminum alkyl is thought to be coordinated to the carbonyl groups of both the monomer molecules and the polymer chains, and the increasing proportion of aluminium alkyl coordinated polymer causes a decrease in the rate of propagation at a critical degree of polymerization, owing to a decrease in concentration of activated monomer.

CHAPTER FIVE

THE ANIONIC BLOCK COPOLYMERIZATION OF STYRENE AND METHYL METHACRYLATE IN THE PRESENCE OF ALUMINIUM ALKYLS

5.1 Introduction

Although the anionic polymerization of MMA in the presence of aluminium alkyls has been well documented over the last few years[69-76], there are no reports in the literature about the effect of aluminium alkyls on block copolymer formation. This chapter describes a series of experiments designed to synthesize block copolymers of styrene and MMA using a *tert*-BuLi/Al(^{i}Bu)$_3$ initiating system.

Styrene was initiated by *t*-BuLi to form polystyryl lithium, followed by addition of the Al(^{i}Bu)$_3$. The 'living' polystyryl propagating chain end was then used to initiate MMA polymerization to form a block copolymer. Alternatively the polystyryl lithium was added to MMA which had been premixed with Al(^{i}Bu)$_3$. The effect of the mode of addition of reagents in the copolymerization is a further step towards deducing the mechanistic role of the aluminuim alkyl.

5.2 Experimental

The block copolymerization of styrene and MMA was carried out in a series of experiments, using the polymerization vessel shown in figure 2.6 section 2.5.1. Transfer of reagents into the vessel was carried out as described in section 2.5.1. Styrene polymerization was initiated by *t*-BuLi in a solution of cyclohexane in bulb A of the polymerization vessel. The polymerization was allowed to proceed at 60°C. The polystyryl lithium was then diluted using toluene which had been previously distilled into

bulb D of the vessel. The dilution caused the colour of the polystyryl lithium to pale slighty. A sample of the polystyryl lithium was kept aside for analysis.

A solution of $Al(^iBu)_3$ in toluene was added from bulb C to the polystyryl lithium; this caused the characteristic red colour to disappear. This suggests that the aluminium alkyl reacts with the polystyryl lithium and changes the structure of the propagating chain end. Finally, a solution of MMA in toluene was poured into bulb A, from bulb B. Initially the polymerization mixture turned yellow upon addition of MMA, but the colour gradually disappeared as the copolymerization proceeded. The formation of the yellow solution is indicative of complex formation between the carbonyl ester group of MMA and the $Al(^iBu)_3$. Copolymerization was allowed to proceed for 24 hours without disturbing the polymerization mixture. The polymeric samples were recovered and dried by the method described in section 2.5.3.

Table 5.1 shows the conditions of polymerization including the extent of conversion for CP1-CP5 :-

Table 5.1 The Conditions of Polymerization and Percentage Conversions Obtained for CP1-CP5, in the Anionic Block Copolymerization of Styrene and Methyl Methacrylate in the Presence of $Al(^iBu)_3$.

Block Copolymer	CP1	CP2	CP3	CP4	CP5
10^3 x $\frac{MMA}{moles}$	126	170	101	114	128
10^3 x $\frac{styrene}{moles}$	23	18	19	19	14
10^3 x $\frac{t\text{-BuLi}}{moles}$	0.63	0.85	1.01	0.57	0.64
10^3 x $\frac{Al(^iBu)_3}{moles}$	1.89	2.55	1.52	2.84	3.19
$\frac{[Al(^iBu)_3]}{[t\text{-BuLi}]}$	3	3	3	5	5
Temperature / °C	29	28	-78	25	60
Time / minutes (Polystyrene Polymerization)	25	1440	20	60	40
Percentage Conversion	54	12	30	99	100

Solvent : Toluene [MMA] : 1.4 +/- 0.4 mol dm^{-3}

The polymerization of styrene took place at 60°C in cyclohexane (10-15 cm^3). The time allowed for the polymerization of styrene, before the addition of MMA, is also indicated in table 5.1.

CP4 was carried out by premixing the monomer with the $Al(^iBu)_3$ prior to the addition of polystyryl lithium, similar to that described in section 4.5.4.1. All other copolymerizations were carried out by premixing the $Al(^iBu)_3$ with polystyryl lithium prior to the addition of MMA.

5.3 Analysis of Results

The extent of conversion in these reactions was determined by weighing the amount of polymer obtained, when a known quantity of MMA was copolymerized with a known quantity of styrene and reprecipitated in methanol. The percentage conversions of the copolymers were calculated after assuming that 100% conversion of styrene had taken place, in order to determine the extent of conversion of MMA.

The results show a large variation in the overall conversions obtained which is thought to be attributable to the different conditions employed for each of the copolymerizations. CP2 showed that very little MMA had been polymerized, which is thought to be because the polystyryl lithium was left for a period of 24 hours before it was used to initiate the polymerization of MMA. After a period the colour of the polystyryl lithium had deepened; this may be attributed to a change in the nature of the propagating ends to a more inactive form. Amass *et al* [88] studied the stability of living polystyryl lithium in cyclohexane using UV/visible spectrophotometry. They reported that the living ends were subject to decay in activity over a long period of time by elimination of lithium hydride from the monomeric form of the species.

There is no obvious relationship between the extent of conversion and the temperature at which copolymerization was carried out. However, it has been reported that in the anionic polymerization of MMA, higher percentage conversions are achieved when polymerization is carried out at low temperature. CP3 was carried out at -78°C and obtained only a 30% conversion, whereas a 99% conversion was obtained from CP4 which was carried out at 60°C. The low percentage conversion obtained in CP3, could also be attributed to the fact that a low concentration of MMA was used; this may cause termination since the concentration of impurities in the system are proportionately greater than the concentration of reagents used.

The higher percentage conversions obtained for CP4 and CP5 can be explained by the length of time allowed for the polymerization of styrene. From the results it would appear that 24 hours is too long for this reaction since it may lead to the decay of the living

polystyryl ends to an inactive form, whereas 20 minutes does not allow enough time for complete consumption of styrene or may give rise to inefficient initiation, owing to the presence of polystyryl aggregates at the beginning of polymerization. Amass *et al*[88] reported that the decay in absorbance of polystyryl lithium occured most rapidly in the first 100 minutes and was thought to be governed by the dissociation of any associated propagating species in solution. The subsequent decay in the absorbance then proceeded at a constant rate which was dependent on the concentration of species present. The decay in activity of polystyryl lithium was thought to be associated with the formation of monomeric propagating species and hence the prevention of decay may be achieved by causing such species to become associated.

The ratio of [Al]/[Li] was increased from 3, for CP1-CP3 to 5, for CP4 and CP5; this may also have been the cause of the higher percentage yields obtained from the latter polymerizations but would be in contrast to the results obtained from the homopolymerization of MMA were this the case.

5.3.1 SEC Analysis

Appendices 22 and 23 show the SEC traces obtained from both the copolymer and the respective polystyrene for CP4. These traces are typical of the traces obtained for the copolymerizations which all exhibited broad bimodal (or multimodal in the case of CP5) behaviour. For the bimodal molecular weight distributions; the higher molecular weight curve corresponds to the copolymer and the lower molecular weight curve corresponds to unreacted polystyryl lithium.

The existence of copolymer was verified from the response given by the UV detector. The UV detector responds to chromophoric groups which are either attached to, or are a part of the polymer backbone e.g. polystyrene. The response this detector gives is proportional to the concentration of solute present in the solution and the molar extinction coefficient of the solute at the set wavelength. The wavelength was set at 254 nm, which was the maximium absorbance for polystyrene. A deflection on the chart recorder which corresponds to the UV detector, appears at the same point as the deflection corresponding

to the RI detector, for both the unreacted polystyryl lithium and the copolymer. The presence of the UV signal at the point where the copolymer is eluted, indicates that the copolymer contains polystyrene. However, the height of the peak obtained from the UV signal, is small compared with the height obtained from the RI signal, indicating that only a small amount of polystyrene is present. Appendices 2 and 3 show the UV absorbances at 254 nm of pure poly(styrene) and pure poly(methyl methacrylate) respectively. Although there is a UV signal from PMMA, the deflection is small and PMMA can be assumed to absorb negligibly since the factor is approximately 1/200 th of that of polystyrene. It is therefore assumed that any UV deflection that is observed in the copolymer corresponds to that of polystyrene.

A UV signal was not observed for the higher molecular weight curve in CP2 (see appendix 24) ; this suggests that this curve corresponds to homopolymethyl methacrylate, whereby MMA had been initiated by some other mechanism. The analysis confirms the percentage conversion for CP2, which indicated that only a small amount of MMA had been polymerized. The SEC trace of CP2 shows the presence of a large quantity of unreacted polystyryl lithium.

The molecular weights and molecular weight distributions obtained from CP1-CP5 are shown in tables 5.2 and 5.3 :

Table 5.2 Molecular Weight Distributions for the Copolymers Obtained and the Percentage Initiation Efficiency of Polystyryl Lithium, from the Anionic Block Copolymerization of Styrene and Methyl Methacrylate in the Presence of $Al(^iBu)_3$.

Block Copolymer	$\overline{M}_n$ / gmol^{-1} (copolymer)	$\overline{M}_w$ / gmol^{-1} (copolymer)	Polydispersity (copolymer)	Initiator Efficiency (%)
CP1	2900	9000	3.1	372
CP2	59100	98000	1.65	4
CP3	42500	77200	1.81	7
CP4	40200	65200	1.62	49
CP5	4200	28000	6.66	476

Table 5.3 Molecular Weight Distributions for the Polystyrene from CP1-CP5 in the Anionic Block Copolymerization of Styrene and Methyl Methacrylate in the Presence of $Al(^iBu)_3$.

Block Copolymer	$\overline{M}_n$ / gmol^{-1} (polystyrene)	$\overline{M}_w$ / gmol^{-1} (polystyrene)	Polydispersity (polystyrene)
CP1	1900	3000	1.58
CP2	2300	4100	1.78
CP3	3300	5400	1.64
CP4	3500	5800	1.66
CP5	2600	4200	1.62

The results show that CP4 produced a copolymer of narrower molecular weight distribution than all the other copolymerizations. CP4 was carried out at 25°C, whereby the time allowed for the polystyrene polymerization was 1 hour. Contrary to the results obtained from the homopolymerization of MMA in the presence of $Al(^iBu)_3$, the polydispersity index is narrow even though CP4 was carried out by premixing the MMA with $Al(^iBu)_3$ before addition of the initiator. This suggests that the molecular weight distributions and percentage conversions of the copolymers obtained are largely governed

by the initiation efficiency of polystyryl lithium, and not by the mode of addition of reagents. The copolymer obtained from CP5 exhibits a broad, multimodal molecular weight distribution. The broadening may be caused by the occurence of side reactions because of the high temperature employed.

The molecular weight distributions of the polystyrene obtained from the copolymerizations were found to lie between 1.5 and 1.8. The polydispersity of the polystyrene from CP2 appears to be slightly higher than the others, which may be attributed to the greater length of time allowed for the polystyrene polymerization. The initiator efficiency, appears to be extremely high for both CP1 and CP5, when the length of time allowed for the polymerization of styrene was 25 minutes and 40 minutes respectively.

5.3.2 NMR Analysis

5.3.2.1 ^{1}H NMR

Appendix 25 shows the ^{1}H NMR spectrum of the block copolymer of styrene and methyl methacrylate obtained for CP4. Table 5.4 assigns the chemical shifts δ, of the peaks corresponding to the ^{1}H NMR spectrum of the copolymer.

Table 5.4 ^{1}H NMR Analysis of Polystyrene-*b*-PMMA for CP4 in the Presence of [Al(^{i}Bu)$_3$]

Chemical Shift (ppm)	Assignment	Area
0.82	syndiotactic -CH_3 (rr)	159.8
0.99	heterotactic -CH_3 (mr)	61.3
1.18	isotactic -CH_3 (mm) from PMMA	26.3
1.39	-CH_2 from PMMA backbone	22.4
1.57		77.2
1.86		54
2.14	-CH_2 from polystyrene backbone	4.5
2.32		24.4
3.57	-CH_3O from PMMA	223.9
7.15	aromatic protons from polystyrene	22.6
7.23		19.2

The spectrum indicates the presence of both polystyrene and PMMA peaks. The spectrum is typical of the spectra obtained from all the other copolymerizations with the exception of CP2. The spectrum of CP2 resembles that of polystyrene, with an additional peak indicating the presence of -CH_3O groups from the small amount of MMA which was polymerized. The spectrum for the copolymer of CP2 (appendix 26) is compared with that of the respective poly(styrene) from CP2 (appendix 27) .

The tacticitiy of the copolymer obtained from CP4 was determined. Analysis of the relevent areas corresponding to the -CH_3 peaks on the spectrum for CP4 showed that σ = 0.2. This corresponds to an isotactic content of 4%, syndiotactic 64% and heterotactic 32%.

5.3.2.2 ^{13}C NMR

Appendix 28 shows the ^{13}C NMR spectrum of the block copolymer of styrene and methyl methacrylate obtained for CP4. Table 5.5 assigns the chemical shifts δ, of the peaks corresponding to the ^{13}C NMR spectrum of the copolymer.

Table 5.5 ^{13}C NMR Analysis of Polystyrene-*b*-PMMA for CP4 in the Presence of [Al(^{i}Bu)$_3$]

Chemical Shift (ppm)	Assignment
16.42	syndiotactic -CH_3 (rr)
18.85	heterotactic -CH_3 (mr)
21.42	isotactic -CH_3 (mm)
	from PMMA
44.48	syndiotactic -CH_2 (rr)
44.82	heterotactic -CH_2 (mr)
	from PMMA
51.7	-CH_3O from PMMA
54.36	quaternary carbon from PMMA
125.25	aromatic carbons from polystyrene
128.18	
128.99	
176.96	-C=O syndiotactic (rrrr)
177.78	heterotactic (rrrm)
178.08	heterotactic (rrmm)
	from PMMA

The peaks on the spectrum indicate the presence of both polystyrene and PMMA.

5.4 Discussion

The purpose of the work carried out in this chapter was to determine the effect of aluminium alkyls on block copolymer formation of styrene and methyl methacrylate. The previous work involving the homopolymerization of MMA indicated that $Al(^{i}Bu)_3$ was the best aluminium alkyl to use of the three that were investigated. The experiments conducted in the investigation showed that block copolymers of relatively narrow molecular weight distribution and high percentage conversions were successfully synthesized; regardless of whether the monomer was premixed with the aluminium alkyl before initiation, or the aluminium alkyl was premixed with the initiator before addition of the monomer.

Further work needs to be carried out to ascertain the optimum conditions required to produce copolymers of unimodal molecular weight distribution. It is believed that this can be obtained by improving the initiation efficiency of the polystyryl lithium, since the SEC traces showed that a large proportion of the polystyryl lithium had remained unreacted, producing copolymers of bimodal molecular weight distribution. The initiator efficiency can be improved by controlling the time interval allowed for the styrene polymerization to be completed before addition of MMA.

The colour of the polystyryl lithium disappears on addition of the aluminium alkyl which indicates the possibility of complex formation between the two species. Addition of MMA to this complex initially forms a yellow solution, which indicates that the aluminium alkyl is also complexed to the carbonyl group of the methyl methacrylate. The conclusions drawn from this work, in conjunction with the kinetic studies carried out on the homopolymerization of MMA, suggest that the aluminium alkyl is coordinated to the initiator, with any excess coordinating to the carbonyl groups of both the monomer and polymer.

CHAPTER SIX

THE CHARACTERISATION OF STYRENE-*b*-4-VINYL PYRIDINE DIBLOCK COPOLYMER MICELLES USING STATIC LIGHT SCATTERING

6.1 Introduction

6.1.1 Block Copolymer Micelles

The solution properties of ionic block copolymers have revealed their ability to form micelles in both water and organic solvents[89-92]. The formation of aggregates occurs above a critical micelle concentration (cmc) and the behaviour of block copolymers in solution is in many respects similar to that of soap and surfactants in water, in that they are able to "solubilize" otherwise insoluble substances and "compatibilize" otherwise incompatible substances. The combination of high aggregate stability, low cmc values and a large range of aggregate sizes give ionic block copolymers a large range of potential applications, for instance, they can be used in drug delivery systems.

Block copolymers are known to undergo micellization when placed in a selective solvent i.e. one which is a thermodynamically good solvent for one of the constituent blocks and simultaneously a nonsolvent, or precipitant for the other[93] . In such solvents, the copolymers are known to form spherical aggregates via a mechanism known as closed association, which is characterised by a dynamic equilibrium between micelles having narrow molar mass and size distribution. The structure of micelles are typically compact cores of insoluble blocks surrounded by soluble coronae.

The system studied in this investigation was the styrene-*b*-4-vinylpyridine diblock copolymers (PS-*b*-P4VP) in both quaternised and unquaternised forms. These block copolymers are known to form "star" micelles when placed in a selective solvent[94] . Star micelles are spherical in shape, with small cores and expanded coronae since the length of

the soluble block is considerably longer than the length of the insoluble block (see figure 6.1). Halperin's model for "star" micelles predicts that the radius of the core (R_{core}) is independent of the soluble block length and scales as $N_B^{3/5}$, where N_B is the number of units in the insoluble block[95] .

Figure 6.1 Structure of Star-Shaped Micelle.

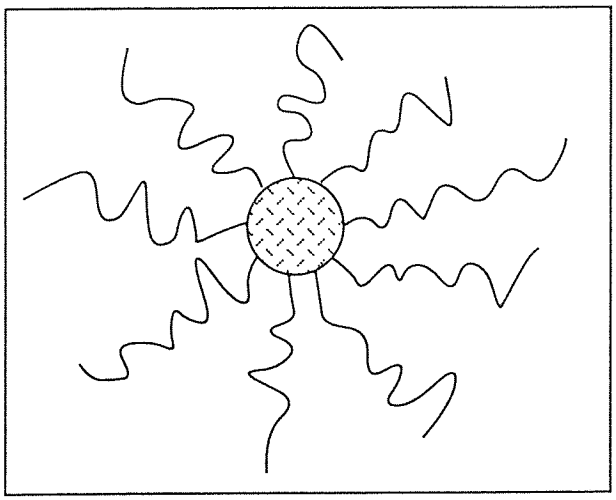

The phenomenon of critical micelle concentration has been addressed by a number of theoretical treatments[96-98]. It was only recently, however, that the polydispersity of the insoluble blocks was properly considered. Gao and Eisenberg[99] refined the model proposed by Holland and Rubingh[100,101], in order to account for the effect of polydispersity of the insoluble block on the cmc. The model also suggests that the insoluble blocks collapse into colloidal spheres below the cmc; the driving force of micellization is therefore considered to be van der Waals interactions between spherical particles. A plot of single chain concentration as a function of total block copolymer concentration for a polystyrene-*b* -polyisoprene system in n-hexadecane, shows that for an average insoluble block length of 67 styrene units, the cmc decreases and becomes less distinct with increase in polydispersity. There appears to be a sharp pseudo-phase transition for the cmc values of polydispersity indices which are greater than 1.

There has been much interest shown in the colloidal bahaviour of ionic block copolymers over the last few years. These copolymers possess both ionic blocks of ionic repeat units

and hydrophobic blocks of nonionic units which are covalently linked together. There is a high degree of incompatability between the ionic and nonionic blocks which leads to very low cmc's[102,103] and high aggregate stability[91,92] when these block copolymers are placed in a selective solvent.

There are two main categories of ionic block copolymers: block polyelectrolytes and block ionomers. Eisenberg and Rinaudo[104] proposed that the properties of block polyelectrolytes are governed by electrostatic interactions over relatively large distances within the corona and between micelles, whereas the properties of block ionomers are governed by short range interactions within the core of the micelle.

Ionic block copolymers are said to be either block polyelectrolytes or block ionomers depending on the nature of the solvent in which they are dissolved. When placed in water, they behave as polyelectrolytes, forming micelles with nonionic cores and coronae consisting of soluble ionic blocks. In organic solvents, however, they behave as block ionomers, forming micelles with ionic cores which are surrounded by insoluble coronae consisting of nonionic blocks. Block ionomers in solution are sometimes referred to as "reverse" micelles which is derived from the terminology used to describe surfactants in non-aqueous solvents. Block ionomers generally have long nonionic blocks and short ionic blocks, whereas block polyelectrolytes have long ionic blocks and short nonionic blocks. Contrary to this, the so-called "crew-cut"[105,106] polyelectrolytes have fairly short ionic blocks surrounding a large nonionic core (see figure 6.2).

Figure 6.2 Structure of Crew-Cut Micelle.

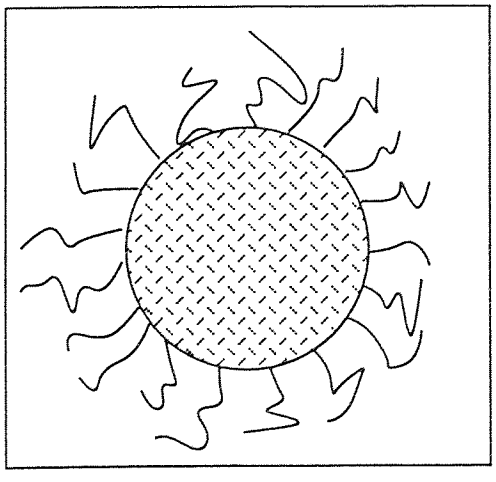

During the rest of this investigation the "reverse" micelles, formed when placing block ionomers in organic solvents will be considered in greater detail. The styrene-*b*-4-vinylpyridine system was studied by placing the diblocks in toluene and characterising the micelles produced using static light scattering. The solution properties of these block copolymers in toluene showed that they form micelles consisting of insoluble cores of 4VP blocks, surrounded by soluble coronae of PS blocks, both when the 4VP is unquaternised and also when quaternised by addition of methyl iodide.

6.1.2 Styrene-*b*-Vinylpyridine Systems

Block and graft copolymers of vinylpyridine monomers are important as emulsifying agents, thermoplastics and membranes[107] . Quaternisation of the vinylpyridine segment with methyl iodide results in the polymers exhibiting emulsifying properties. Polymers of isomeric vinylpyridinium salts have been employed commercially as flocculating agents in water treatment, in photography and also in ion exchange resins .

The polystyrene based diblock ionomers are the most extensive group of ionic block copolymers studied in organic solvents. These generally consist of a long polystyrene block joined to a relatively short ionic block e.g. quaternised poly (4-vinylpyridine).

A wide range of methods or combination of methods have been used to enable complete characterisation of these systems, for instance: static light scattering (SLS), dynamic light scattering (DLS), small-angle x-ray scattering (SAXS), transmission electron microscopy (TEM), size exclusion chromatography (SEC) and viscometry[93] .

Antonetti *et al* [94] reported that dilute solutions of styrene-*b*-4-vinylpyridine diblocks exhibit aggregation numbers in excess of 800 when placed in toluene. This was attributed to a cylindrical morphology being present when the percentage of 4VP block which constitutes the micelle core was found to be 33%. When the percentage of the core block is much lower i.e.~15%, it is generally believed that spherical micelles exist which exhibit characteristically lower aggregation numbers, found typically in the region of 60-200. Antonetti *et al*, however, showed that spherical block copolymer micelles can exist with aggregation numbers being as high as 500. They concluded that for spherical block

copolymer micelles, the aggregation number follows the length of the insoluble block (or core content) and the interfacial energy between the insoluble block and the solvent. They also reported that the better the solvent quality for the corona, the smaller the micelles and that stretching of corona chains can occur, owing to osmotic repulsions of the solvating chains. This results in a destabilisation of the spherical shape, which is characterised by a high aggregation number and cylindrical morphology. This type of morphology is only exhibited in the case of small polymer chains or under bad solvent conditions for the solvating chain.

Studies carried out by Tuzar and Sikora[108] on poly(styrene)-*b*-poly(2-vinylpyridine) in toluene showed that the phenomenon of anomalous micellization was observed within a certain temperature interval where unusually large particles were formed. Moller and Kunz[109] also reported the presence of "defect structures" in cylindrical and lamellar morphologies of well defined poly(styrene)-*b*-poly(2-vinylpyridine) samples, which they studied using electron spectroscopic imaging. Samples of high poly(2-vinylpyridine) content showed the presence of poly(2-vinylpyridine) cylinders embedded in a poly(styrene) matrix. The electron micrographs indicated regions where the microdomains were highly ordered and regions where they appeared to be packed loosely and were in disarray. In these regions the poly(styrene) matrix was filled with small sphere-type domains and the poly(2-vinylpyridine) cylinders were missing.

Nguyen and Eisenberg[110], investigated the effect of ionic chain polydispersity on the morphology of spherical ionic microdomains using small-angle X-ray scattering and transmission electron microscopy for poly(styrene)-*b*-poly(4-vinylpyridinium iodide). Samples were prepared by mixing diblock ionomers of constant polystyrene chain lengths and different ionic block lengths. The samples were prepared using either conditions close to thermodynamic equilibrium or non-equilibrium conditions. They reported that the radii of the ionic microdomains varied linearly with ionic chain polydispersity when the samples were prepared under conditions close to thermodynamic equilibrium. However, if the samples were prepared under non-equilibrium conditions the polydispersity had no effect on the sizes of the domains. Transmission electron micrographs of the blends

showed the presence of spherical ionic microdomains and dual morphology was not observed even for the binary blends, in which two very different ionic block lengths were mixed together.

Schwab and Hellwell[111,112] utilized diblock copolymers of styrene and 2-vinylalkylpyridinium halides as model systems, in order to study the effects of block structure in the areas of thickening ability and shear and brine sensitivity. They reported that further quaternisation of these 2-vinylalkylpyridinium halides with methyl iodide improved the solubility of the previously quaternised materials with long-chained alkyl halides, but their thickening ability was considerably lower than the same polymer quaternised with methyl iodide only.

6.1.3 Static Light Scattering (SLS) from Large Particles

Static Light Scattering is a convenient method of characterising polymers in solution from which the morphology of the polymers can be obtained. Studies of polymer solutions using SLS yield information about the weight average molecular weight, radius of gyration and second virial coefficient. When the particle size is greater than approximately $\lambda/20$, it has been shown that[113]

$$\frac{Kc}{R(\theta)} = \frac{1}{P(\theta)M_w} + 2A_2c + \ldots \qquad (1)$$

where K is the optical constant, $(2\pi^2(n_o\ dn/dc)^2\lambda_o^{-4}N_{AV}^{-1})$, n_o is the refractive index of the solvent at the incident radiation wavelength in vacuum, dn/dc is the specific refractive index increment, λ_o is the wavelength in vacuum, N_{AV} is the Avagadros number, c is the concentration, $R(\theta)$ is the Rayleigh ratio at the angle of measurement, $P(\theta)$ is the particle scattering function, $\overline{M}_w$ is the weight average molecular weight, and A_2 is the second virial coefficient; the higher order virial coefficients can be neglected for sufficiently dilute solutions.

The particle scattering function describes the angular variation of the scattered intensity and accounts for the intraparticle interference. It can be expressed in the form of a power series in $\sin(\theta/2)$:

$$P(\theta) = 1-\alpha_1 \sin^2(\theta/2) + \alpha_2 \sin^4(\theta/2) -... \qquad (2)$$

For small angles of observation the reciprocal scattering function is given by :

$$P(\theta)^{-1} = 1 + \frac{16\pi^2}{3\lambda^2} <Rg^2>z \sin^2(\theta/2) \qquad (3)$$

where $<Rg^2>z$ is the square z-average radius of gyration. Therefore, the particle size can be evaluated independently of the particle shape from the initial slope of the inverse particle scattering function as a function of $\sin^2(\theta/2)$.

A graphical method used to solve eq.1 with the particle scattering scattering function given by eq.3 was developed by Zimm[114]. By plotting (Kc/R(θ) for different angles and concentrations as a function of $\sin^2(\theta/2)$ + kc (where k is the scaling factor) and extrapolating to zero concentration, information on the particle size can be obtained from the initial linear slope (eq.3). Similarly, in the limit of θ approaching 0, the particle scattering function is equal to unity and the slope of the line is proportional to the second virial coefficient. The intercepts from the zero concentration and zero angle lines yield the inverse weight average molecular weight. This double linear extrapolation method is referred to as a Zimm plot[114].

For particles of very high molecular weight (e.g.>10^6 g/mol) the dependence of (Kc)/R(θ) exhibits significant curvature in the angular dependence. It should be noted that for these high molecular weights, small errors in the extrapolations can result in a relatively large error, when the reciprocal is computed in the Zimm plot for the evaluation of molecular weight[115]. Similarly, there would be a large error in the radius of gyration which depends on $\overline{M}_w$. In these cases the Debye plot can be used, which is similar to a Zimm plot, except that the ordinate is plotted as R(θ)/Kc.

Another problem in the analysis of large particles is the evaluation of the radius of gyration from the angular dependence of scattered light intensity. The Zimm method is based on linear extrapolations of the concentrations and angles. For large particles, however, the angular dependence is non-linear at high angles. Hence, the data which depart significantly from linearity should be omitted in the analysis[115]. The advantage of

the instrument used in this study is the accessability of a wide range of angles. Thus, it is possible to fit the angular dependence with a polynomial expansion of the particle scattering function in which the term linear in $\sin^2(\theta/2)$, would yield the radius of gyration (Rg).

The dissymmetry in the light scattered from large particles can be evaluated from the dissymmetry ratio, Zd. This is defined as the ratio of the scattered light of two angles which are symmetrical about 90°. The angles used most frequently are 45° and 135°,

$$Zd = P(45)/P(135) = R(45)/R(135)$$

This is a measure of the particle size, since for large particles the scattering at low angles will be larger, owing to constructive interference of the scattered light from the particle. Also, the scattering at large angles will be reduced, owing to destructive interference of the scattered light. These dyssymmetry ratios can be correlated to different particle shapes, as well as serve as an indication of the particle size.

Before $\overline{M}_w$ can be calculated from light scattering measurements, the specific refractive index increment, dn/dc, must be known for the particular polymer and solvent system under examination. It is defined as (n-no)/c where n and no are the refractive indices of the solution and the solvent respectively and c is the concentration. Measurements of dn are made using a differential refractometer employing the same wavelength of light as used in the light scattering study.

It should also be noted that for block copolymers, the $\overline{M}_w$, Rg and A_2 values refer to apparent values because of the compositional heterogeneity of the systems[113].

6.2 Experimental

The characterisation of poly(styrene)-*b*-poly(4-vinylpyridine) reverse micelles and their quaternised analogues was carried out in toluene using static light scattering

6.2.1 Synthesis of Block Copolymers

The syntheses of diblock copolymers of poly(styrene)-*b*-poly(4-vinylpyridine) (PS-*b*-P4VP) were carried out by sequential anionic polymerization of styrene followed by 4-vinylpyridine, using butyllithium as the initiator[110] (see scheme 6.1). The polymerizations were performed in tetrahydrofuran (THF) at -78°C under an atmosphere of nitrogen. The apparatus used for the polymerizations allowed for the withdrawal of the reaction mixture during the course of the reaction. Thus, for a given constant poly(styrene) block length, a series of diblocks was obtained, with the lengths of poly(4-vinylpyridine) segments varying from 10 to 100 units. Aliquots of the reaction mixtures were withdrawn for characterisation after the polystyrene block had been formed and also after the 4-vinylpyridine was added. The PS-*b*-P4VP diblock copolymers were then recovered and purified by repeated precipitation in hexanes. The poly(4-vinylpyridine) content of the diblocks was determined by nonaqueous titration of the vinylpyridine segments with perchloric acid.

The quaternisation of the poly(4-vinylpyridine) was carried out by dissolving the block copolymers in a 5% solution of dried THF, followed by the addition of freshly distilled methyl iodide in 10-fold excess. The reaction mixture was then refluxed under nitrogen for 3-4 hours to achieve full quaternisation. The disappearence of the 1414cm^{-1} 4VP IR band was evidence of complete quaternisation. The copolymers were then recovered by precipitation in a 10-fold volume excess of 2-propanol and dried in a vacuum oven at 60°C.

Scheme 6.1 Synthesis of Poly(styrene)-*b*-Poly (4-vinyl pyridine) Diblock Copolymers

Initiation of Styrene

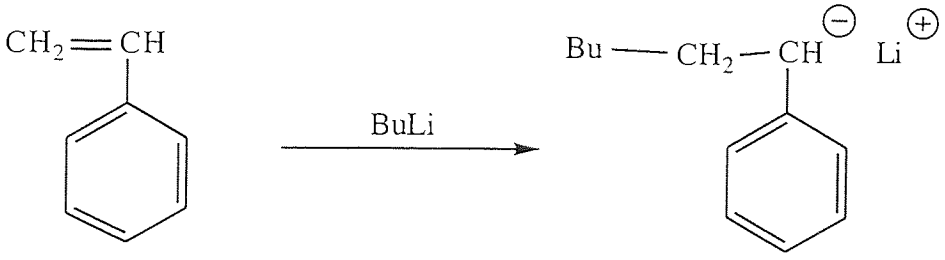

Initiation of 4-Vinylpyridine

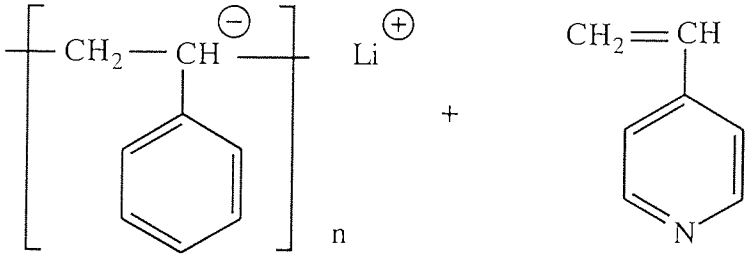

polystyryl lithium

4-vinylpyridine

CH_3I

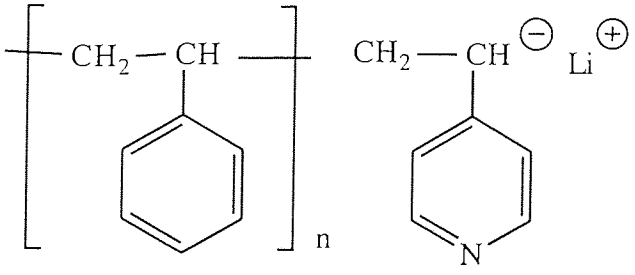

unquaternised diblock copolymer
PS -*b*- P-4VP

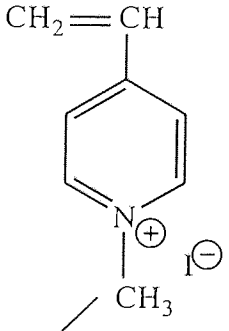

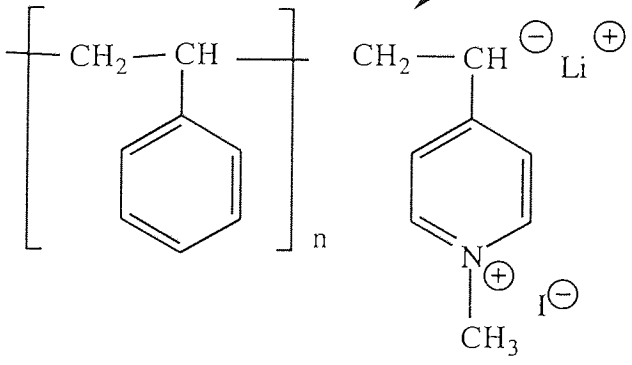

quaternised diblock copolymer
PS-*b*-P-4VPMeI

The molecular weight of the poly(styrene) block was determined using size exclusion chromatography (SEC) in THF, calibrated using poly(styrene) standards. The polydispersity indices of the poly(styrene) blocks were approximately 1.1 and those of the diblocks, were found to vary between 1.1 and 1.3. Two series of samples were prepared corresponding to quaternised and unquaternised forms of poly(4-vinylpyridine). For each series the molecular weight of the poly(styrene) block was kept constant for a given set of samples, whereas, that of the poly(4-vinylpyridine) was varied between 7 and 94 units. The sample notation used indicates the copolymer composition; for example, PS(473)-*b*-4PVP(94) represents a poly(styrene) chain of 473 units joined to a poly(4-vinylpyridine) chain of 94 units. The quaternised form is denoted by using the suffix MeI.

The preparation of all samples of block copolymers used in this investigation was carried out by Dr. Xing-Fu Zhong.

6.2.2 Sample Preparation for Static Light Scattering (SLS)

The polymer samples used for SLS measurement were dissolved in filtered, spectrophotometric grade toluene and stirred overnight. The concentrations of the stock solutions prepared, ranged from 5×10^{-5} to 3×10^{-2} g/ml. Static light scattering measurements were performed on these stock solutions which were then diluted with toluene to make up 5 different concentrations in total. SLS measurements were performed after each dilution in order to collect enough data to produce a Zimm plot.

The filters used were always rinsed first with 10ml of toluene in order to remove any possible contaminants. The toluene was filtered through filters of pore size 0.22μm and the polymer solutions were filtered through filters of pore size 0.45μm. The pore sizes for the filters were chosen on the basis that there would be no change in concentration of the polymer solution after filtration. Filtration was carried out slowly and care was taken to exclude any dust particles which would give an inaccurate reading.

One of the quaternised block copolymer samples was prepared using the technique described by Nguyen *et al* [110]. The sample was cast as a film from N, N-dimethylformamide (DMF) and the solvent was evaporated slowly, enabling the micelles to be prepared under conditions closer to those of thermodynamic equilibrium. PS-*b*-P4VPMeI block copolymer micelles were dissolved in DMF (a good solvent for both blocks), whereby single chains were obtained. The films were cast by placing the polymer solution into indentations or "holes" on a metal base, which had previously been covered by a teflon sheet. Finally, the tray was placed in a desiccator under vacuum to enable the DMF to evaporate slowly and re-form micelles under equilibrium conditions. The micelles were dissolved in filtered HPLC grade THF before SLS measurements were performed.

The effect of temperature on the micellization of poly(styrene)-*b*-poly(4-vinylpyridine) diblocks in quaternised and unquaternised forms was also investigated. Stock solutions of the samples were prepared and diluted to cover a range of concentrations which varied in composition from 85%, to 15% of the stock solutions. Initially, SLS measurements were taken for all the concentrations at room temperature in order to formulate an adequate Zimm plot. The samples were then placed in a thermostatically controlled water bath and SLS measurements were taken for each concentration at different temperatures; the temperatures being varied between 40°C and 80°C. A time interval of approximately half an hour was allowed between the measurements, to enable thermal equilibrium to be reached.

6.2.3 SLS Measurement

Light scattering experiments were performed using a DAWN-F multiangle laser photometer (Wyatt Technology, Santa Barbara, CA) at 25°C, which operates at 15 angles, from 26° to 137°, and is equipped with a He-Ne laser (632.8nm). The instrument used is shown in figure 6.3. Data acquisition and analysis utilised the Dawn software package. The polymer solutions were filtered directly into scintillation vials, which were used for the light scattering measurements. Care was taken to ensure that the vials were free from

scratches and fingerprints since this could severely distort the measurements. The measurement was performed by dilution of a stock solution which had an approximate concentration in the range of 5×10^{-5} to 3×10^{-2} g/ml, depending on the molecular weight of the sample; the concentrations were always larger than the cmc values. A minimum of four concentrations were used to determine the weight average molecular weight, radius of gyration and second virial coefficient with the aid of a Zimm plot, which was processed with the Aurora software.

For the SLS experiments involving a change in temperature, the sample cell was set to the required temperature and left for 10 minutes until that temperature had been reached.

6.2.4 Specific Refractive Index Increment Measurement (dn/dc)

The specific refractive index increment (dn/dc) for the polymer and solvent system was determined using the Wyatt/Optilab 903 interferometric refractometer and accompanying software (Dndc 2.01) at a wavelength of 630nm. The monochromatic beam (selected by filter) from a mercury vapour lamp was directed through a differential cell, which consisted of a solution and solvent compartment separated by a diagonal glass wall. The deflection of the light beam was measured, firstly with solvent in the forward compartment and polymer solution in the rear, giving deflection d_1; the position was reversed and deflection d_2 was measured. Since similar readings for solvent, d_1^o and d_2^o were obtained, then the total displacement Δd was determined as :

$$\Delta d = (d_1 - d_2) - (d_1^o - d_2^o)$$

The cell constant was determined by calibration with solutions of different concentrations of sodium chloride (99.99%, Aldrich solutions), of known Dn. Each dn/dc determination was obtained using eight to ten different concentrations. Hence :

$$Dn = c' \Delta d,$$

was obtained where c' is the calibration constant. By measuring Δd for a number of concentrations of polymer, dn was obtained from a knowledge of c', and (dn/dc) obtained from the slope of the plot of dn as a function of c.

Figure 6.3 Diagram of Dawn-F Laser Photometer

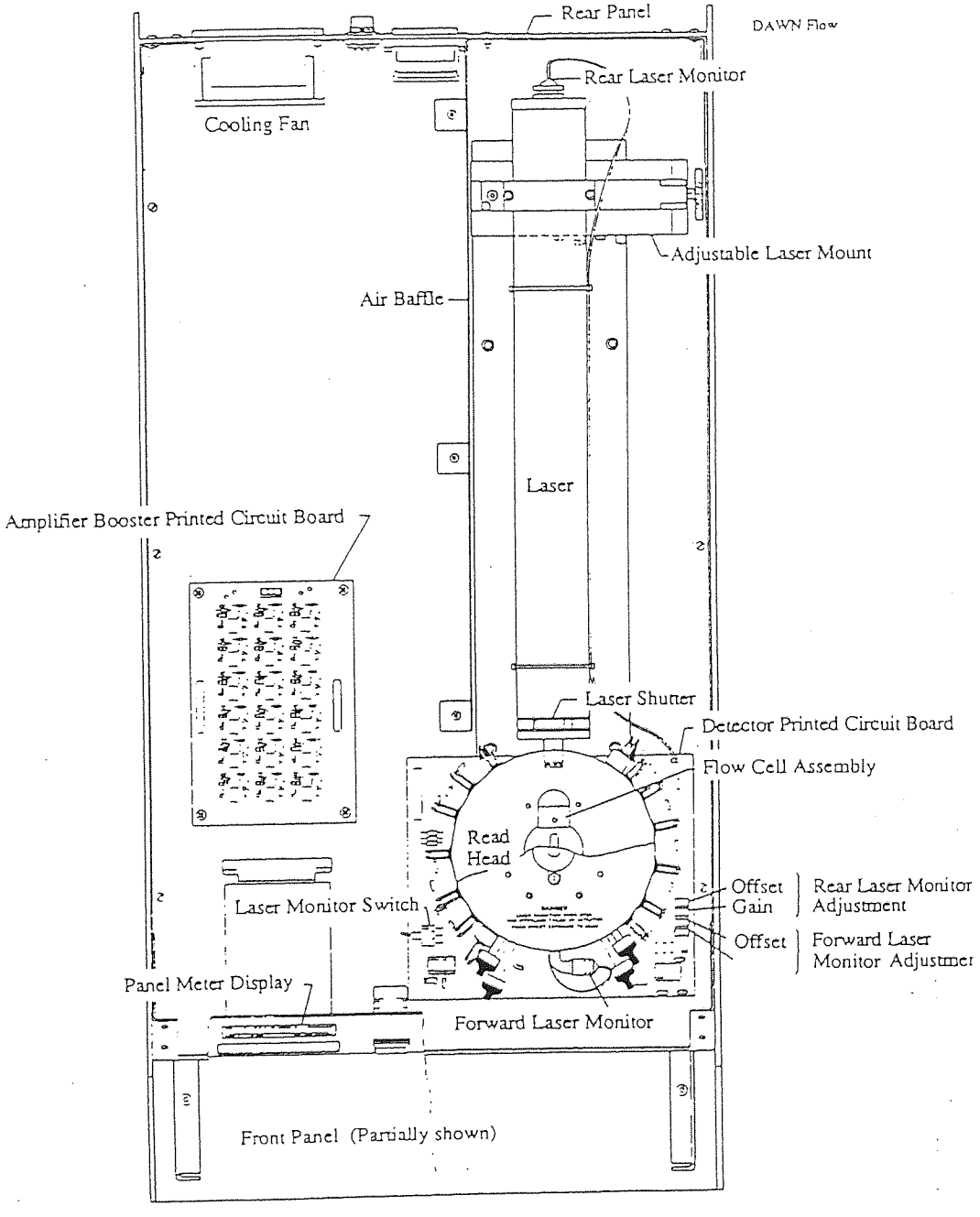

6.3 Results and Discussion

The results and discussion will be divided into three sections. In the first section the data from the SLS measurements on the PS-*b*-P4VPMeI system in toluene will be analysed and discussed. The effect on the aggregation number has been investigated when these micelles are formed under equilibrium conditions by casting them as films from DMF, followed by dissolving in THF. Secondly, the data from the SLS measurements on the PS-*b*-P4VP system in toluene will be analysed and discussed. The final section will address the effect of temperature on the micelle formation for both the quaternised and unquaternised block copolymers which are under investigation.

6.3.1 SLS Measurements for PS-*b*-P4VPMeI

Table 6.1 summarises the results obtained from SLS measurements performed on the PS-*b*-P4VPMeI system in toluene. The data was obtained from the Zimm plots which employ the double extrapolation method to determine the weight average molecular weight ($\overline{M}_w$), the radius of gyration (Rg), and the second virial coefficient (A_2). The percentage of the ionic block relates to the percentage of the P4VPMeI as a function of the block copolymer. The aggregation number (N_{agg}), relates to the number of block copolymer chains per micelle and was calculated using the relationship:

$$N_{agg} = \overline{M}_w \text{ (micelle)} / \overline{M}_w \text{ (single chain)}$$

Figures 6.4 and 6.5 show typical Zimm plots of some of the samples measured for the PS-*b*-P4VPMeI system in toluene. The plots shown exhibit a non-linear angular dependence at high angles, owing to the larger size of the particles and therefore, a second order fit was found to be more appropriate for these samples.

Table 6.1 SLS Data for PS-*b*-P4VPMeI Block Copolymer Samples.

PS-*b*-P4VPMeI	% Ionic	$\overline{M}_w$ (g/mol^{-1})	R_g (nm)	A_2 (mol ml/g)	N_{agg}
600-12	1.96	2.78 x 10^6	27.4	4.11 x 10^{-5}	42
473-94	16.58	1.68 x 10^7	40.1	3.2 x 10^{-6}	231
473-71	13.05	1.28 x 10^7	48.6	8.35 x 10^{-6}	191
473-52	9.9	1.79 x 10^7	34.2	2.85x 10^{-6}	287
473-26	5.2	3.51 x 10^6	22.1	4.41 x 10^{-5}	63
473-17	3.47	3.71 x 10^6	18.3	2.27 x 10^{-5}	69
473-7	1.46	1.61 x 10^6	18.9	6.27 x 10^{-5}	31
380-68	15.18	3.52 x 10^7	68.7	2.09 x 10^{-5}	623
380-37	8.87	2.57 x 10^7	61	3.55 x 10^{-5}	526
195-35	15.2	3.54 x 10^7	92.2	7.48 x 10^{-6}	1220
195-18	8.45	3.94 x 10^6	29.8	5.48 x 10^{-5}	159

The results show a general trend in that, for a constant poly(styrene) block length, there is a decrease in aggregation number,with a decrease of ionic block length. There also appears to be an increase in aggregation number corresponding to a decrease in poly(styrene) block length for a constant ionic block length. These results suggest that aggregation increases with an increase in percentage composition of the ionic (insoluble) block, and decreases (to a lesser extent) with percentage composition of the poly(styrene) (soluble) block.

Figure 6.4 Zimm Plot of PS(473)-*b*-P4VPMeI(71) in Toluene

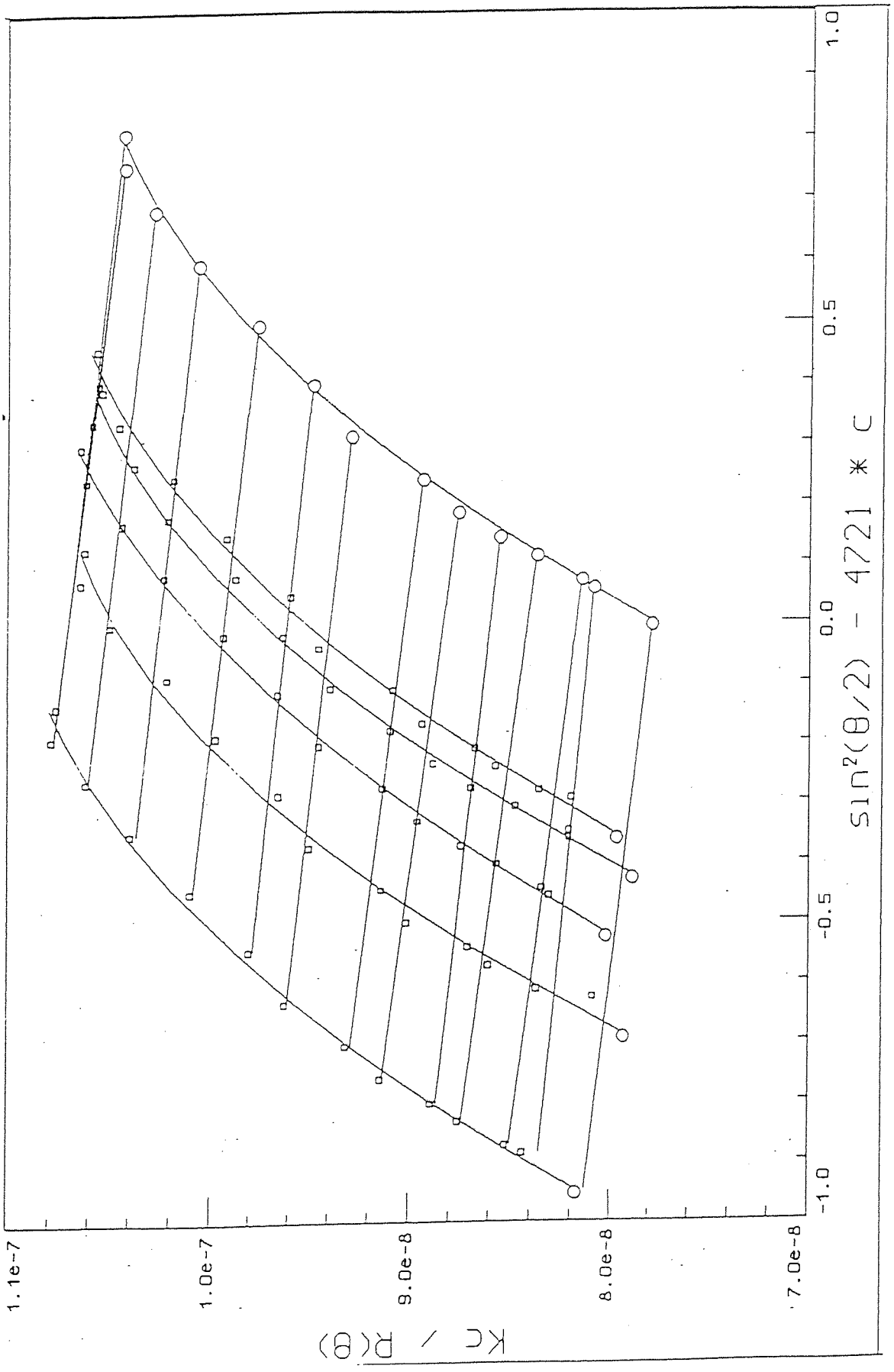

Figure 6.5 Zimm Plot of PS(380)-*b*-P4VPMeI(68) in Toluene

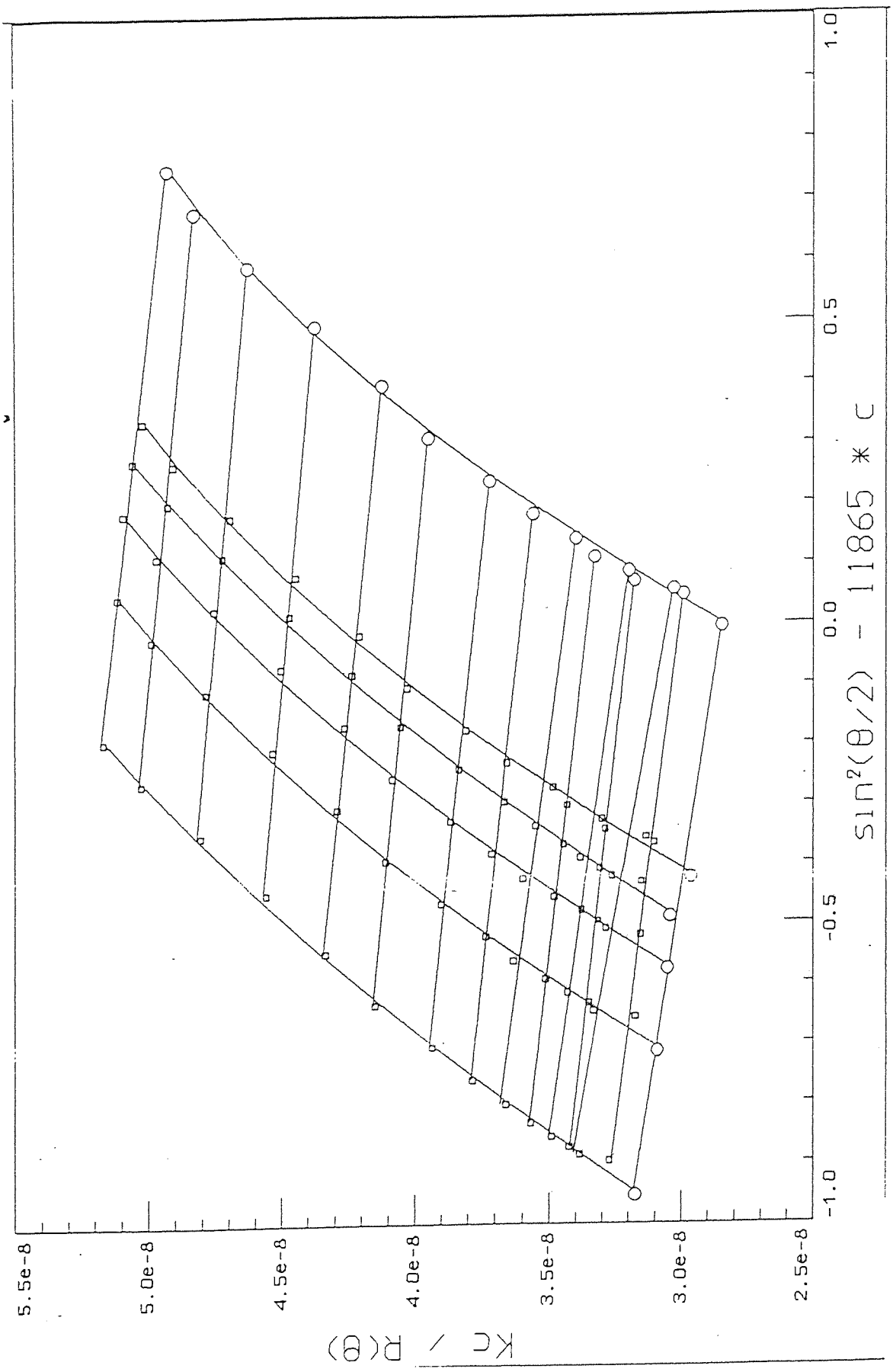

There are, however, some unusually high aggregation numbers associated with some of the samples; particularly PS (195)-*b*-P4VPMeI (35), which exhibits an aggregation number of 1220, compared to a much smaller value of 159 for the PS (195)-*b*-P4VPMeI (18) copolymer. Measurements were repeated for this sample and the readings were found to give consistently high aggregation numbers; molecular weights from these determinations agreed to within +/-10%. This anomalous behaviour for the PS (195)-*b*-P4VPMeI (35) sample suggests that a different morphology exists, probably one of cylinders or rods, which would also be consistent with the extremely large radius of gyration obtained for this sample. Verification of this morphology can be achieved by carrying out transmission electron microscopy (TEM) studies on the sample. Nguyen *et al* [110] have previously studied transmission electron micrographs of copolymer blends with a polystyrene block length of 473 units. Spherical ionic microdomains were found to be present, but dual morphology was not observed even for the binary blends, in which two very different ionic block lengths were mixed together.

The fairly large aggregation numbers associated with the samples of a poly(styrene) block length of 380 units could still cause these particles to have spherical morphology. This would be in agreement with the findings of Antonetti *et al* [94], who reported that spherical block copolymer micelles can exist with aggregation numbers being as high as 500. They also stated that stretching of corona chains can occur, owing to osmotic repulsions of the solvating chains, which results in a cylindrical morphology. This type of morphology is only exhibited in the case of small polymer chains or under bad solvent conditions for the solvating chain. The poly(styrene) chain in this instance consists of 380 units and is considerably longer than for the PS (195)-*b*-P4VPMeI (35) sample, which would imply that the PS(380)-*b*-P4VPMeI (68) and PS(380)-*b*-P4VPMeI (37) samples probably exhibit spherical morphology, characterised by slightly lower aggregation numbers.

The following graph (see figure 6.6), shows the changes in aggregation numbers as a function of the percentage of ionic block length, for a series of PS-*b*-P4VPMeI copolymers of three different poly(styrene) block lengths.

Figure 6.6 Changes in Aggregation Number as a Function of % Ionic Block Length for PS-*b*-P4VPMeI Samples

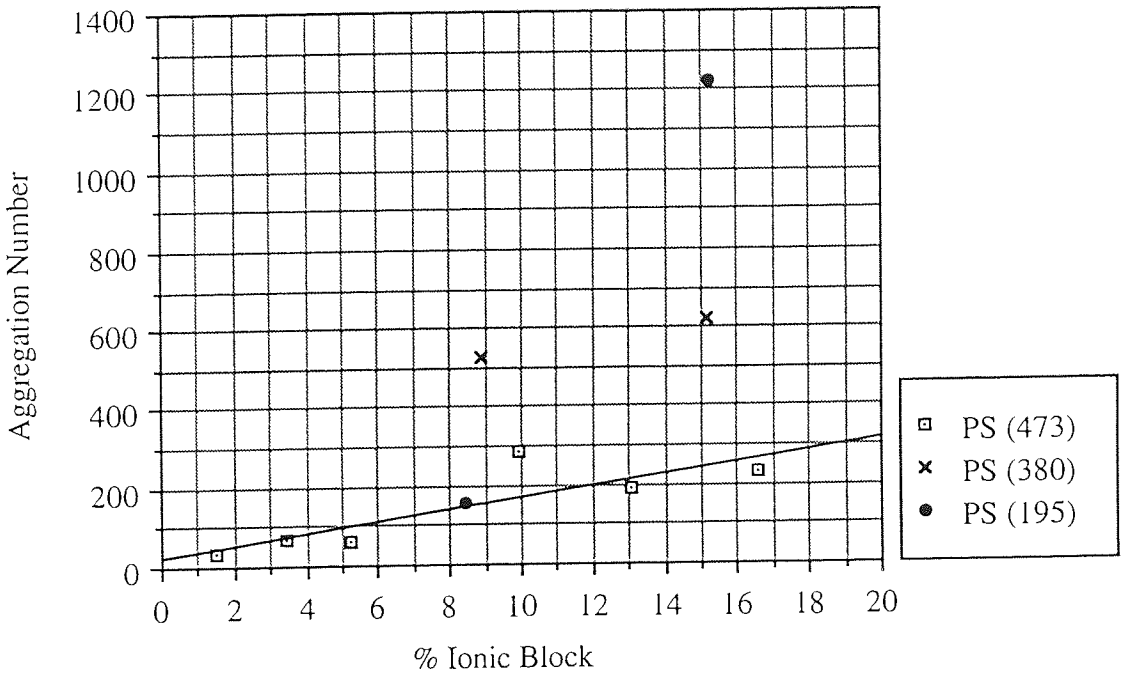

The sample PS(473)-*b*-P4VPMeI(71) was also analysed, when cast as a film from DMF under conditions close to thermodynamic equilibrium. The sample was then dissolved in THF for the purposes of obtaining SLS data, since it was found to be more soluble in THF than in toluene. The data obtained showed that the micelles formed had an aggregation number of 945; this was considerably higher than when the sample had been prepared under non-equilibrium conditions by dissolving in toluene.

6.3.2 SLS Measurements for PS-*b*-P4VP

Table 6.2 summarises the results obtained from SLS measurements performed on the PS-*b*-P4VP system in toluene. The data was obtained from the Zimm plots, some of which can be seen in figures 6.7 and 6.8.

Table 6.2 SLS Data for PS-*b*-P4VP Block Copolymer Samples.

PS-*b*-P4VP	% P4VP	$\overline{M}_w$ (g/mol^{-1})	R_g (nm)	A_2 (mol ml/g)	N_{agg}
600-12	1.96	9.08×10^4	0	4.54×10^{-4}	1.5
473-94	16.58	1.73×10^7	35.6	-3.07×10^{-7}	291
473-71	13.05	4.46×10^6	23.3	5.27×10^{-6}	78
380-68	15.18	4.97×10^6	17.5	-3.87×10^{-6}	106
380-37	8.87	8.91×10^5	16.8	3.47×10^{-5}	20
195-18	8.45	3.78×10^4	23.1	-8.95×10^{-5}	1.7

The data shows that the aggregation numbers are considerably lower than those obtained for the corresponding quaternised samples. This can be explained by the fact that the interfacial tension between the P4VP and toluene is smaller than between P4VPMeI and toluene, i.e. toluene is a better solvent for P4VP than for P4VPMeI. Hence, the solubilities of PS and P4VP are more closely related than those of PS and P4VPMeI, which would lead to lower aggregation numbers for the former. It is to be noted that those copolymers of very small P4VP content exhibited little or no aggregation at all, which suggests that these block copolymers exist as single chains with no micellization occurring.

Figure 6.7 Zimm Plot of PS(473)-*b*-P4VP(94) in Toluene

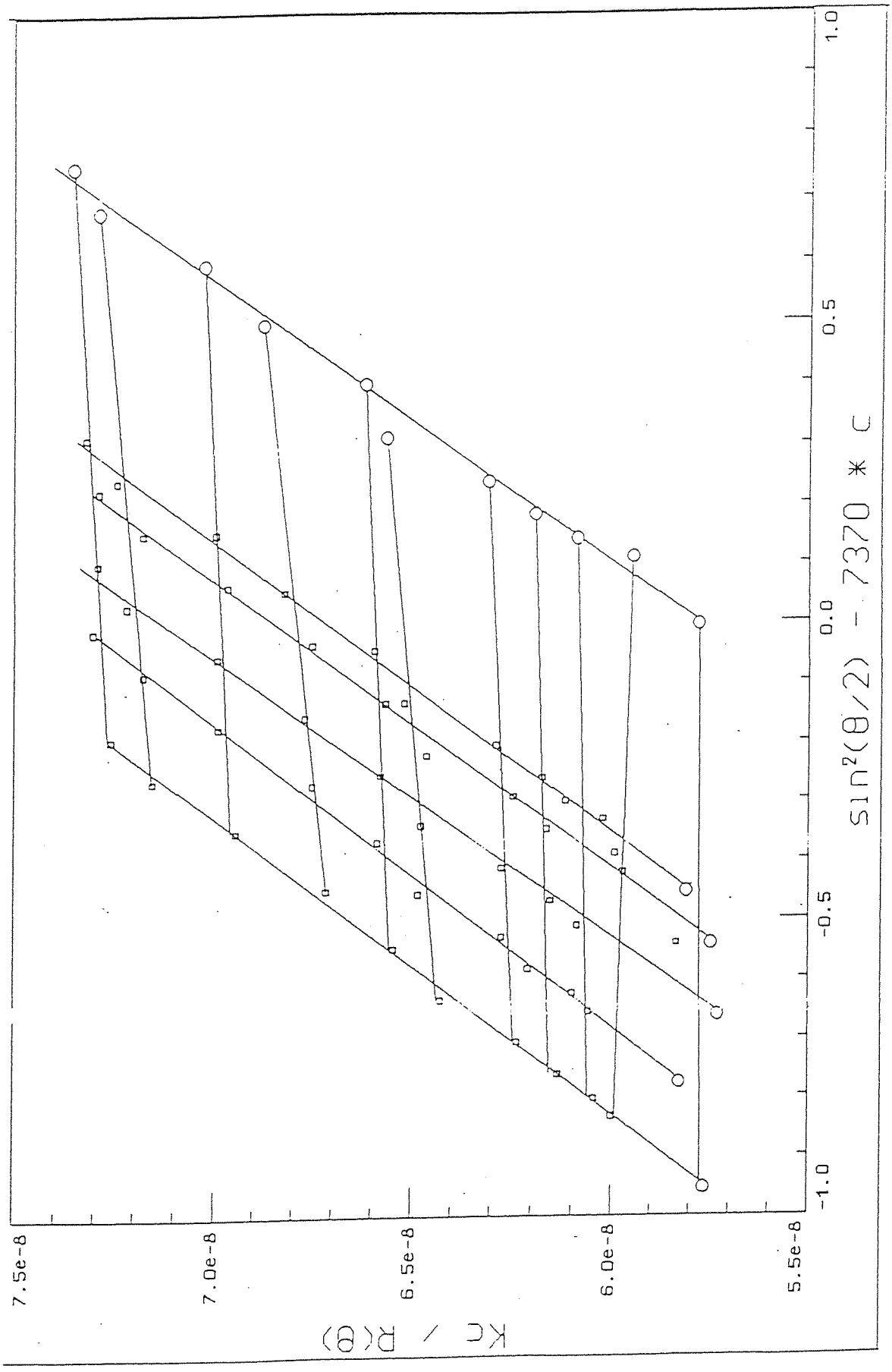

Figure 6.8 Zimm Plot of PS(473)-*b*-P4VP(71) in Toluene

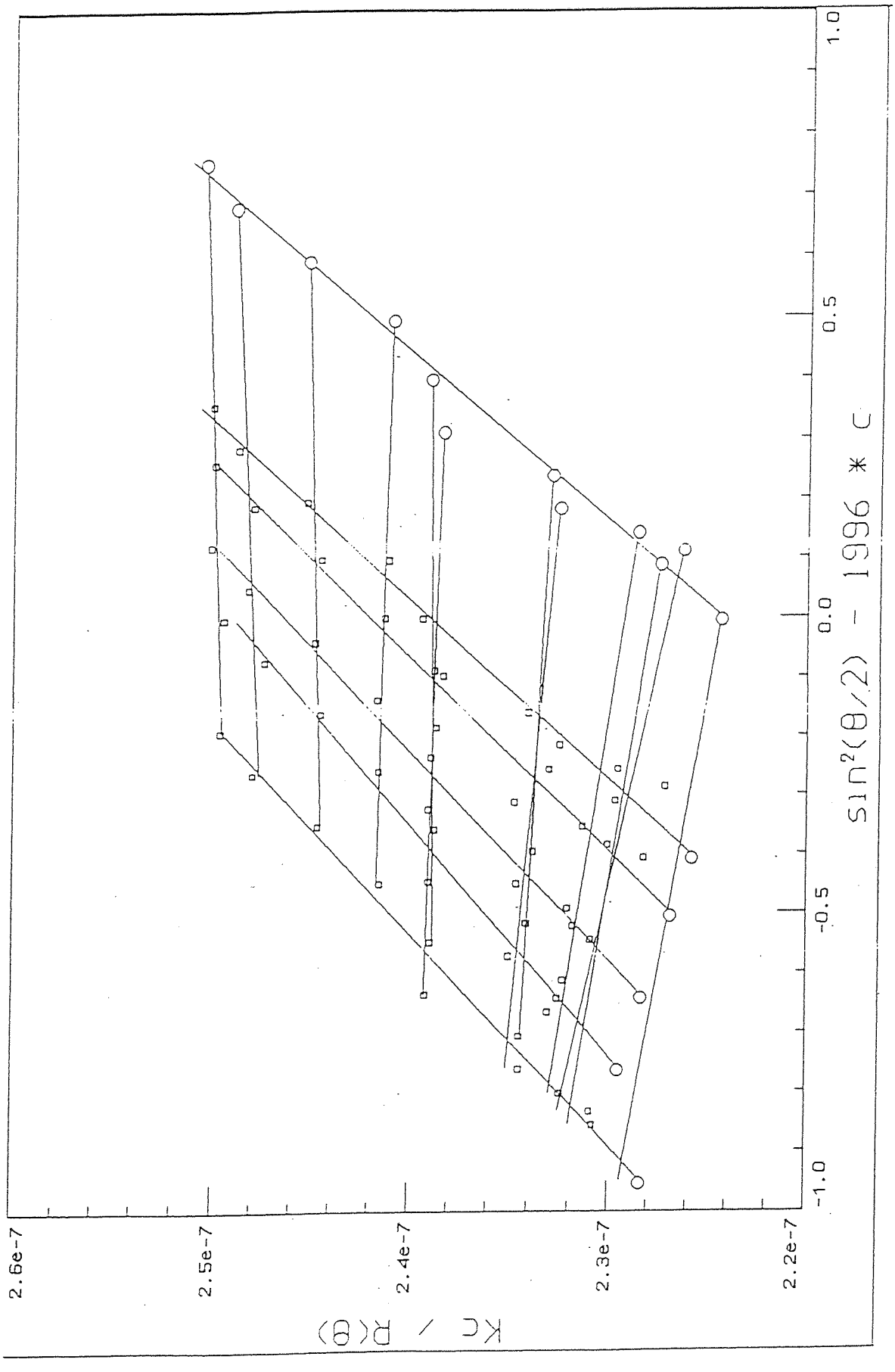

It is also interesting to note that some of these block copolymer samples exhibit negative A_2 values, which suggests that they are fairly unstable in the particular solvent environment. The reasons for this are as yet uncertain and further work needs to be carried out on these samples before any conclusions can be drawn.

6.3.3 Temperature Effects on Micellization Behaviour of PS(473)-*b*-P4VP(71) and PS(473)-*b*-P4VPMeI(71)

The effect of temperature on the micellization behaviour was investigated. SLS measurements were carried out on both the quaternised and unquaternised block copolymers of poly(styrene)(473)-*b*-poly(4-vinylpyridine)(71) over a temperature range from 25-80°C, as described in section 6.2.2. The results obtained from the static light scattering data are summarised in tables 6.3 and 6.4.

Table 6.3 SLS Data from Temperature Effects for PS(473)-*b*-P4VPMeI(71)

Temperature /°C	$\overline{M}_w$ (g/mol^{-1})	R_g (nm)	A_2 (mol ml/g)	N_{agg}
25	2.09 x 10^7	57.3	2.79 x 10^{-5}	312
40	2.07 x 10^7	47.6	7.58 x 10^{-6}	309
60	2.45 x 10^7	64.5	2.28 x 10^{-5}	366
80	2.34 x 10^7	66.1	3.24 x 10^{-5}	349

Table 6.4 SLS Data from Temperature Effects for PS(473)-*b*-P4VP(71)

Temperature /°C	$\overline{M}_w$ (g/mol^{-1})	R_g (nm)	A_2 (mol ml/g)	N_{agg}
25	5.45 x 10^6	22	1.84 x 10^{-5}	96
39.2	4.68 x 10^6	19.3	1.1 x 10^{-5}	82
54.2	4.08 x 10^6	16.3	5.13 x 10^{-6}	72
80.4	4.17 x 10^6	14.9	8.18 x 10^{-5}	73

The results show that micellization behaviour is affected by temperature in the unquaternised samples but no such temperature effect was observed in the quaternised samples. The unquaternised samples exhibit a decrease in aggregation number as the temperature is increased, which implies that this causes greater dissociation of micelles to from single chains. Although there appears to be a change in aggregation number as a function of temperature for the quaternised samples, there is no significant trend and so this can be attributed to experimental error. These trends are illustrated more clearly in the graphs shown in figures 6.9 and 6.11. The plots show the average scattering intensity as a function of temperature for the five different concentrations of both the quaternised and unquaternised samples. The average intensities, taken as direct readings from SLS measurements, are proportional to the molecular weights and, therefore, also proportional to the aggregation numbers.

Figure 6.9 Changes in Scattering Intensity as a Function of Temperature for PS-*b*-P4VP

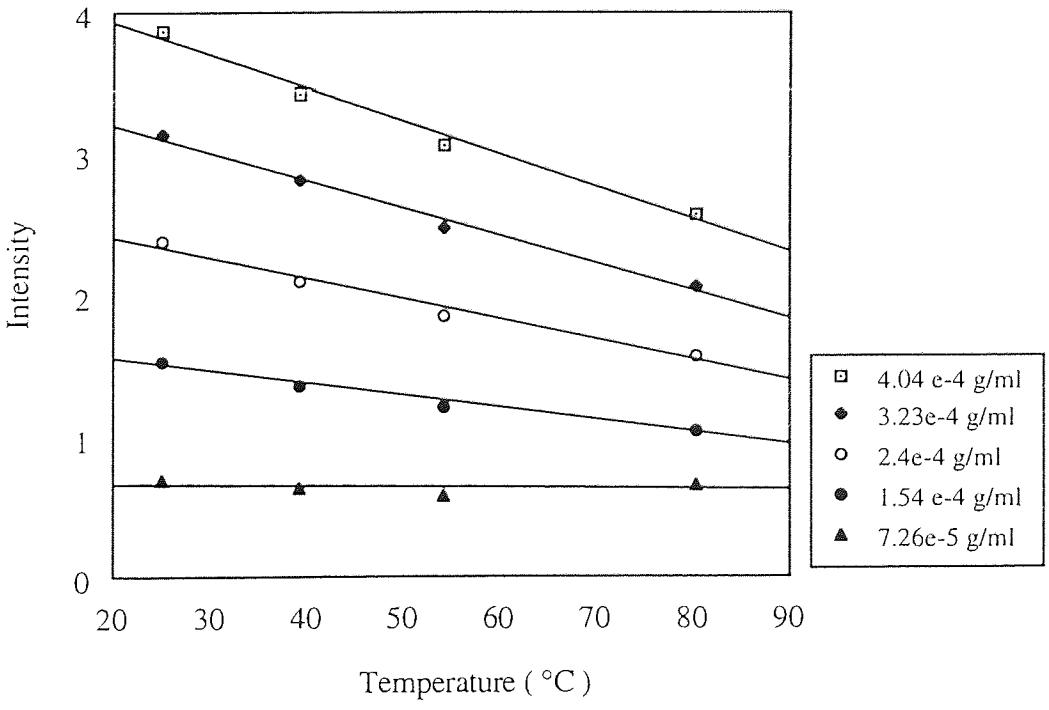

It should be noted that the extent of dissociation decreases with decrease in concentration. Figure 6.9 shows that dissociation does not appear to be exhibited at the lowest concentration. The gradient of each line corresponds to the different concentrations and decreases in a logarithmic fashion as a function of decrease in concentration. This can be attributable to the fact that the cmc value is approached as the concentration decreases, therefore, a greater proportion of single chains exist at the lower concentrations. This is illustrated in the graph shown in figure 6.10 which is a plot of the gradient of each of the lines as a function of concentration.

Figure 6.10 Changes in Gradient as a Function of Concentration for Intensity-Temperature Graph of PS(473)-*b*-P4VP(71)

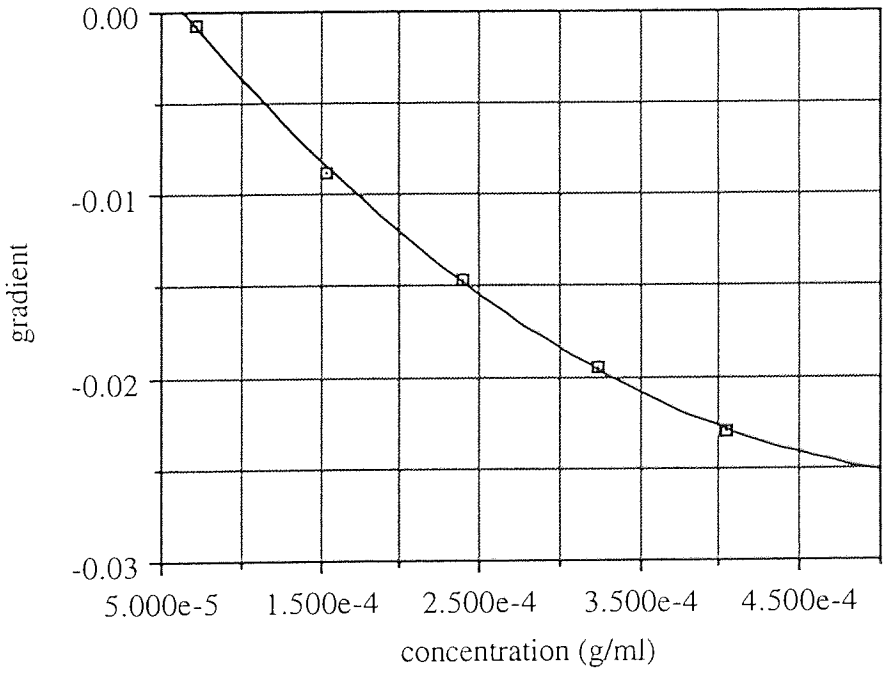

Figure 6.11 Changes in Scattering Intensity as a Function of Temperature for PS-*b*-P4VPMeI

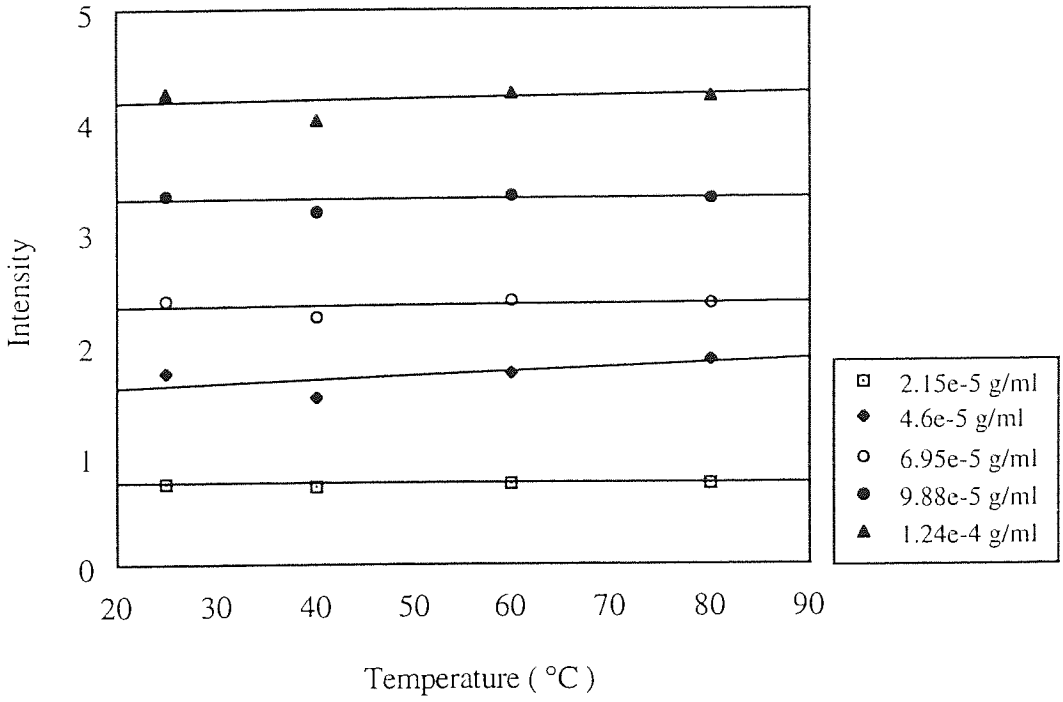

6.4 Discussion

The static light scattering studies carried out in this investigation have shown that block copolymers of poly(styrene)-*b*-poly(4-vinylpyridine) and poly(styrene)-*b*-poly(4-vinylpyridine methyl iodide) form reverse micelles when placed in toluene. These micelles are star-shaped, in that short poly(4 vinylpyridine) blocks form the insoluble core and the relatively long poly(styrene) blocks form the soluble corona.

Most of the samples analysed are thought to exhibit spherical morphology but some of the quaternised samples with a larger insoluble block length may be in the form of rods or spheres. The aggregation numbers for the quaternised samples are charateristically higher than their corresponding unquaternised counterparts. This can be explained in terms of the degree of solubility of the insoluble block for the two sets of samples. Increases in the insoluble block length, correspond to increases in aggregation number and greater micelle stability for both the quaternised and unquaternised samples.

The effect of temperature on micellization behaviour of the unquaternised samples showed that the micelles dissociate to form single chains with an increase in temperature. The greater stability of the quaternised micelles meant that the effect of temperature on their dissociation was much less marked.

The morphologies of these samples can only be fully understood by carrying out transmission electron microscopy studies. Characterisation of these micelles can also be conducted using dynamic light scattering in order to obtain information about the hydrodynamic volume and, hence, gain a further understanding of the nature of these polymers in solution.

CHAPTER SEVEN

CONCLUSIONS AND SUGGESTIONS FOR FURTHER WORK

The main aims of this project were to synthesise and characterise methyl methacrylate polymers and block copolymers of narrow molecular weight distribution via living anionic polymerization. Living anionic polymerization is an important technique for the formation of block copolymers, which are of paramount importance as industrial products. Polymerizations were carried out using different techniques in order to ascertain the optimum conditions for obtaining polymers of narrow molecular weight distribution.

Two different systems were investigated for the synthesis of living polymers of methyl methacrylate: polymerizations initiated by polystyryl lithium in the presence of lithium chloride, and those initiated by butyllithium or polystyryl lithium in the presence of different structural isomers of aluminium alkyls. A comparison can be made of the two systems involving initiation using polystyryl lithium. It was found that the molecular weight distributions for the copolymers of both systems exhibited broad multimodal behaviour. Most of the copolymers showed bimodal molecular weight distributions in both systems; the lower molecular weight curve corresponding to polystyrene and the higher molecular weight curve being copolymer. This behaviour can be attributed to the occurrence of side reactions on the carbonyl moiety of MMA, particularly in the case of the aluminium alkyl system since these polymerizations were conducted at higher temperatures than are normally used for anionic polymerization. The polymerizations carried out in the presence of lithium chloride appeared to exhibit very low initiation efficiency, resulting in large quantities of homopoly(styrene) being produced. The initiator efficiencies were found to be considerably higher for the polymerizations carried out in the presence of aluminium alkyls and for these polymerizations some of the values exceeded the theoretical value of 100%. This suggests that a greater number of monomer molecules were initiated then were theoretically expected, or that the molecular weights obtained were lower than the expected values owing to the occurrence of termination

reactions. Addition of 1,1, diphenyl ethylene to the polystyryl lithium appeared to have no effect on the initiator efficiency in the lithium chloride system. Future work could include carrying out the polymerizations on the aluminium alkyl system by addition of a capping agent, in order to see if there is further improvement in the initiation efficiency. The effect of using different structural isomers of butyllithium on the molecular weight distributions of the polymers obtained in the lithium chloride system, can also be investigated.

The work conducted on the homopolymerization of methyl methacrylate in the presence of aluminium alkyls, conclusively showed that the *t*-butyllithium/triisobutylaluminium system was the most efficient initiating system of the three different aluminium alkyl systems investigated. This system exhibited high initiator efficiency and 100% conversion of monomer to polymer. The results of the investigation into the three different systems showed that the efficiency of the initiator is thought to be solely dependent on the size of the alkyl group on the aluminium component of the initiating system, whereas the molecular weight distributions of the polymers obtained are thought to be solely dependent on the size of the alkyl group on the lithium component. The aluminum alkyl is thought to be coordinated to the initiator, as well as the carbonyl groups of both the monomer units and polymer chains, whereby it sterically hinders the attack on the carbonyl group by the initiator and prevents the occurrence of termination reactions. Studies of the kinetics of polymerization have revealed the possibility that there is a decrease in the rate of propagation at a critical degree of polymerization; this is thought to be because of a decrease in concentration of aluminium alkyl coordinated or 'activated' monomer, as a result of an increase in concentration of aluminuim alkyl coordinated polymer. The kinetics of polymerization were investigated by withdrawing samples from the polymerization mixture at known time intervals, hence the polymerization was disturbed and was not allowed to proceed smoothly. This "crude" technique allowed for the possibility of contamination of the polymerization system with impurities, although every precaution was taken to prevent this occurrence. Further work needs to be carried out using a more reliable technique to monitor the kinetics of polymerization in order to confirm the validity of the results obtained from this investigation. An appropriate

at regular time intervals without disturbing the reaction mixture. Further experiments can also be carried out on this system at lower temperatures, typically -78°C, in order to see the effect on the molecular weight distributions of the polymers produced. A detailed investigation into the effect of changing the mode of addition of reagents on the efficiency of initiation and the molecular weight distributions of the polymers, would also be a further step towards deducing the mechanistic role of the aluminium alkyl in the polymerization.

The static light scattering studies carried out on block copolymers of styrene-*b* -4 vinyl pyridine and styrene-*b* -4 vinyl pyridine methyl iodide, have shown that they form star-shaped "reverse" micelles when placed in toluene. Most of the copolymer samples were found to exhibit spherical morphology, however, some of the quaternised samples with a longer insoluble block length may be in the form of rods or cylinders. The aggregation numbers of the quaternised samples were found to be characteristically higher than their corresponding unquaternised counterparts. An increase in temperature caused a dissociation of micelles into single chains in the unquaternised samples; this dissociation behaviour is much less pronounced as the critical micelle concentration approaches. The greater micelle stability of the quaternised samples meant that the effect of temperature on their dissociation was much less marked. The morphologies of these samples can be more fully understood by carrying out transmission electron microscopy studies and characterisation can also be carried out using dynamic light scattering. The studies can be extended to characterise the poly(styrene)-*b*-poly(methyl methacrylate) block copolymers synthesised in the earlier part of this project. The behaviour of this block copolymer in solution and its ability to form micelles can be investigated once a suitable selective solvent for the system has been found.

REFERENCES

1 **Szwarc, M.,** Living Polymers and Mechanisms of Anionic Polymerization, *Advances in Polymer Science,* Springer-Verlag, Berlin, Heidelberg and New York, (1983), **49,** 1

2 **Szwarc, M. and Van Beylen, M.,** Ionic Polymerization and Living Polymers, *Chapman and Hall :* London, New York, (1993)

3 **Szwarc, M.,** Carbanions, Living Polymers and Electron Transfer Processes, *Interscience Publishers Inc.* : London, (1968)

4 **Szwarc, M.,** 'Living' Polymers, *Nature,* (1956), **178,** 1168-1169

5 **Szwarc, M.,** Ions and Ion Pairs in Organic Reactions, Szwarc, M. (Ed)*Wiley-Interscience* : New York, London, Sydney, Toronto, (1972), **1**

6 **Szwarc, M.,** Ions and Ion Pairs in Organic Reactions - Role of Ions and Ion Pairs in Chemical Reactions, Szwarc, M. (Ed)*Wiley-Interscience* : New York, London, Sydney, Toronto, (1974), **2**

7 **Kroschwitz, J.I.**(Ed.), Encyclopedia of Polymer Science and Engineering - Anionic to Cationic Polymerization, **2,** *Wiley-Interscience* : New York, Chichester, Brisbane, Toronto, Singapore, (1985)

8 **Fontanille, M.,** Comprehensive Polymer Science - The Synthesis, Characterization, Reactions and Applications of Polymers. ***Pergamon Press ;*** Oxford, New York, Beijing, Frankfurt, Sao Paulo, Sydney, Tokyo, Toronto, (1989), **3,** Chapter 25, Carbanionic Polymerization: General Aspects and Initiation, 365-385

9 **Muller, A.H.E.,** Comprehensive Polymer Science - The Synthesis, Characterization, Reactions and Applications of Polymers. ***Pergamon Press ;*** Oxford, New York, Beijing, Frankfurt, Sao Paulo, Sydney, Tokyo, Toronto, (1989), **3,** Chapter 26, Carbanionic Polymerization:Kinetics and Thermodynamics, 387-423

10 **Mulvaney, J.E., Overberger, C.G. and Schiller A.M.,** Anionic Polymerization, *Advances in Polymer Science*, Springer-Verlag, Berlin, Heidelberg and New York, (1961), **3,** 106-138

11 **Beylen, M.V., Bywater, S., Smets G., Szwarc, M. and Worsfold, D.J.,** Developments in Anionic Polymerization - A Critical Review, *Advances in Polymer Science,* (1988), **86**, 87-143

12 **McGrath, J.E.**(Ed), Anionic Polymerization - Kinetics, Mechanisms and Synthesis, *American Chemical Society Symposium Series* (1981), **166,** *(Am. Chem. Soc., Div. Polym.Chem-179th Meeting, 1980)*

13 **Staudinger, H.,** Polymerization, *Berichte der Deutschen Chemischen Geselleschaft.,* (1920), **53,** 1073-1085

14 **Cowie, J.M.G.,** Polymers : Chemistry and Physics of Modern Materials - 2nd Edition, *Blackie* : Glasgow and London (1991)

15 **Ziegler, K.,** The importance of Alkali Metallo-organic compounds for synthesis, *Angew.Chem.*, (1936), **49,** 499-502

16 **Szwarc, M.,** Shelftime of Living Polymers - Some Comments on Living Cationic Polymerization of Vinyl Monomers, *Makromol. Chem. Rapid Commun.* (1992), **13,** 141-145 .

17 **Penczek, S., Kubisa, P. and Szymanski, R.,** On the Diagnostic Criteria of the Livingness of Polymerizations, *Makromol. Chem, Rapid Commun.,* (1991), **12,** 77-80

18 **Muller, A.H.E. and Jeuck, H.,** Kinetics of the Anionic Polymerization of Methyl Methacrylate in Tetrahydrofuran Using Lithium and Potassium as Counterions, *Makromol. Chem Rapid. Commun.,* (1982), **3**, 121-125

19 **Margerison, D. and Newport, J.P.,** Degree of Association of n-Butyl Lithium in Hydrocarbon Media, *Trans Faraday Soc.* (1963), **59**, 2058-2063

20 **Wittig, G., Meyer, F.J., and Lange,G.,** Uber das Verhalten von Diphenylmetallen als Komplexbildner, *Justus Liebigs Ann. Chem.,* (1950), **571**, 167-200

21 **Brown, T.L. and Rogers, M.T.,** The Preparation and Properties of Crystalline Lithium Alkyls,*J. Am. Chem. Soc.,* (1957), **79**, 1859-1861

22 **Weiner, M., Vogel, G and West, R.,** The Physical Properties and Structure of *t*-Butyllithium, *Inorg. Chem.,* (1962), **1**, 654-658

23 **Worsfold, D.J., Bywater, S.,** Anionic Polymerization of Styrene, *Can. J. Chem.,* (1960), **38**, 1891-1900

24 **Weiss, E. and Hencken, G.,** Uber Metall-Alkyl Verbindungen. 7 Verfeinerung der Kristallstruktur der Methyl-lithiums *J. Organomet. Chem.* (1970), **21**, 265-268

25 **Duck, E., in Saltman, W.M. (Ed),** The Stereo Rubbers, *John Wiley and Sons, Inc,* New York, (1977), Chapt. 4

26 **Worsfold, D.J. and Bywater, S.,** Alkyllithium Anionic Polymerization Initiators in Hydrocarbon Solvents, *J. Organomet. Chem.* (1967),**10,** 1-6

27 **Hsieh, H.L.,** Kinetics of Polymerization of Butadiene, Isoprene and Styrene with Alkyllithiums. Part 2. Rate of Initiation, *Journal of Polymer Science,* (1965), **A3,** 163-172

28 **Roovers, J.E.L. and Bywater, S.** The Polymerization of Isoprene with *sec*-Butyllithium in Hexane, *Macromolecules.*, (1968), **1**, 328-331

29 **Roovers, J.E.L. and Bywater, S.,** The Reaction of *tert*-Butyllithium with Styrene and Isoprene. A Comparison of Chain Initiation with the Isomers of Butyllithium, *Macromol.ecules*, (1975), **8**, 251-254

30 **Morton, M., Bostick, E.E. and Livigni, R,** Advances in Anionic Polymerization, *Rubber Plastics Age,* (1961),**42**,397-401

31 **Geacintov, G., Smid, J. and Szwarc, M.,** The Absolute Rate Constant of Propagation of Anionic Polymerization of Styrene, *J. Americ. Chem Soc.,* (1961), **83,** 1253-1254

32 **Geacintov, G., Smid, J. and Szwarc, M.,** Kinetics of Anionic Polymerization of Styrene in Tetrahydrofuran, *J. Americ. Chem Soc.,* (1962), **84,** 2508-2514

33 **Bhattacharyya, D.N., Lee, C.L., Smid, J. and Szwarc, M.,** The Absolute Rate Constants of Anionic Propagation by Free Ions and Ion-Pairs of Living Polystyrene, *Polymer*, (1964), **5**, 54-56

34 **Hostaika, V.H., Figini, R.V.and Schuiz, G.M.,** On the Anionic Polymerization of Styrene in Tetrahydrofuran, *Makromol. Chem.,* (1964), **71,** 198-202

35 **Bhattacharyya, D.N., Lee, C.L., Smid, J. and Szwarc, M.,** Reactivities and Conductivities of Ions and Ion Pairs in Polymerization Processes, *Journal of Physical Chemistry,* (1965), **69**, 612-627

36 **Allen, G., Gee, G., Stretch, C.,** Anionic Polymerization of Styrene by Sodium Naphthalene, ***Journal of Polymer Science,*** (1960), **48,** 189-193

37 **Stretch, C. and Allen, G.,** Anionic Polymerization of Styrene, ***Polymer,*** (1961), **2**, 151-160

38 **Dainton, F.S., East G.C., Harpell, G.A., Hurtworth, N.R., Ivin, K.J., LaFlair, R.T., Pallen, R.H. and Hui, K.M.,** The Kinetics of Anionic Polymerization of Styrene and α-Methylstyrene, ***Makromol Chem,*** (1965), **89**, 257-262

39 **Komiyama, J., Bohm, L.L. and Schulz, G.V.,** Kinetik der anionischen Polymerisation von Styrol in Dioxan mit Polystyryl-Natrium als Reactiontrager, ***Makromol Chem,*** (1971), **148**, 297-304

40 **Muller, A.H.E.,** Kinetics of the Anionic Polymerization of *tert*-Butyl Methacrylate in Tetrahydrofuran, ***Makromol. Chem.,*** (1981), **182**, 2863-2871

41 **Schreiber, H.,** Uber die Abbruchsreaktionen bei der anionischen Polymerisation von Methylmethacrylat, ***Makromol. Chem.,*** (1960), **36**, 86-90

42 **Wiles, D.M. and Bywater, S.,** Methoxide Ions in the Anionic Polymerization of Methyl Methacrylate,***Chemistry and Industry:*** London, (1963), 1209

43 **Mita, I., Watanabe, Y., Akatsu, T. and Kambe, H.,** Anionic Polymerization of Methyl Methacrylate in Tetrahydrofuran, ***Polymer Journal*** , (1973), **4**, 3, 271-278

44 **Kawabata, N. and Tsuruta, T.,** Elementary Reactions of Metal Alkyl in Anionic Polymerization. 1. Reaction Mode of *n*-Butyllithium in the Initiation Step of Methyl Acrylate and Methyl Methacrylate Polymerization, ***Makromol. Chem.,*** (1965), **86**, 231-252

45 **Hatada, K., Kitayama, T., Fujikawa, K., Ohta, K. and Yuki, H.,** Studies on the Anionic Polymerizaion of Methyl Methacrylate with Butyllithium by Using Perdeuterated Monomer, ***Polymer Bulletin*** , (1978), **1**, 103-108

46 **Hatada, K., Kitayama, T., Fujikawa, K., Ohta, K. and Yuki, H., in McGrath, J.E.(Ed),** Anionic Polymerization - Kinetics, Mechanisms and Synthesis, ***American Chemical Society Symposium Series*** (1981), **166,** Chapter 23, *(Am. Chem. Soc., Div. Polym.Chem-179th Meeting, 1980)*

47 **Szwarc, M. and Rembaum, A.,** Polymerization of Methyl Methacrylate Initiated by an Electron Transfer to the Monomer, ***Journal of Polymer Science*** , (1956), **22**, 189-191

48 **Lohr, G. and Schulz. G.V.,** On the Kinetics of the Anionic Polymerization of Methyl Methacrylate in Tetrahydrofuran at -75°C, ***Makromol. Chem.,*** (1973), **172,** 137-149

49 **Lohr, G. and Schulz. G.V.,** Kinetics of Anionic Polymerization of Methyl Methacrylate with Caesium and Sodium as Counterions in THF, ***Eur. Polym. Jourmal,*** (1974), **10,** 121-130

50 **Warzelhan, V. and Schulz, G.V.,** On a New Active Species in the Anionic Polymerization of Methyl Methacrylate in Tetrahydrofuran Using a Bifunctional Initiator with Sodium as Gegenion, ***Makromol. Chem,*** (1976), **177**, 2185-2190

51 **Warzelhan, V. and Schulz, G.V.,** The Anionic Polymerization of Methyl Methacrylate with a Bifunctional Initiator, ***Makromol. Chem,*** (1980), **181**, 149-163

52 **Kraft, R., Muller, A.H.E., Warzelhan, V., Hocker, H. and Schulz, G.V.,** On the Structure of the Propagating Species in the Anionic Polymerization of Methyl Methacrylate. Kinetic Investigations in Tetrahydrofuran Using Monofunctional Initiators, ***Macromolecules,*** (1978), **11**, 1093-1096

53 **Warzelhan, V., Hocker, H. and Schulz, G.V.,** Kinetic Studies of the Anionic Polymerization of Methyl Methacrylate in Tetrahydrofuran with Na^+ as Counterion, Using Monofunctional Initiators, ***Makromol. Chem,*** (1978), **179**, 2221-2240

54 **Muller, A.H.E., Hocker, H. and Schulz, G.V.,** Rate Constants of the Tactic Monomer Addition in the Anionic Polymerization of Methyl Methacrylate in THF with Caesium as Coumterion, ***Macromolecules,*** (1977), **10**, 1086-1089

55 **Warzelhan, V., Lohr, G., Hocker, H. and Schulz, G.V.,** A n Automatically Controlled Reaction Vessel Suitable for the Kinetic Investigation of Polymerization Proceses with Half Life Periods of 2 Seconds and Greater, ***Makromol. Chem,*** (1978), **179**, 2211-2219

56 **Muller A.H.E, in McGrath, J.E.(Ed),** Anionic Polymerization - Kinetics, Mechanisms and Synthesis, ***American Chemical Society Symposium Series*** (1981), **166,** Chapter 8, *(Am. Chem. Soc., Div. Polym.Chem-179th Meeting, 1980)*

57 **Kraft, R., Muller, A.H.E., Hocker, H. and Schulz, G.V.,** Kinetics of the Anionic Polymerization of Methyl Methacrylate in 1,2-Dimethoxyethane, *Makromol. Chem Rapid. Commun.,* (1980), **1**, 363-368

58 **Yuki, H. and Hatada, K.,** Stereospecific Polymerization of Alpha-Substituted Acrylic Acid Esters, *Advances in Polymer Science,* Springer-Verlag, Berlin, Heidelberg and New York, (1979), **31**, 1-26

59 **Jerome, R., Forte, R., Varshney, S.K., Fayt, R. and Teyssie, Ph.,** The Anionic Polymerization of Alkyl Acrylates : A Challenge, *Eur. Pat. Appl ,.Fontanille, M., Guyot, A. (Eds.), Recent Advances in Mechanistic and Synthetic Aspects of Polymerization,* Reidel Publishing Company, (1987), 101-117

60 **Forte, R., Ouhadi, T., Fayt, R., Jerome, R. and Teyssie, Ph.,** Anionic Block Copolymerization of Methyl Methacrylate in the Presence of Alkali and Alkali-Earth Metal Salts, *Journal of Polymer Science* , (1990), **28,** 2233-2236.

61 **Fayt, R., Forte, R., Jacobs, C., Jerome, R., Ouhadi, T., Teyssie, Ph. and Varshney, S.K.,** New Initiator System for the "Living" Anionic Polymerization of *tert*-Butyl Acrylates,*Macromolecules,* (1987), **20**, 1442-1444

62 **Varshney, S.K., Hautekeer, J.P., Fayt, R., Jerome, R. and Teyssie, Ph.,** Anionic Polymerization of Acrylic Monomers. 5. Synthesis, Characterization, and Modification of Polystyrene-Poly(*tert* -butyl acrylate) Di- and Triblock Copolymers, *Macromolecules,* (1990), **23,** 3893-3898 .

63 **Varshney, S.K., Jacobs, C.,Hautekeer, J.P., Bayard, P., Jerome, R., Fayt, R. and Teyssie, Ph.,** Anionic Polymerization of Acrylic Monomers. 6. Synthesis, Characterization, and Modification of Poly(methyl methacrylate)-Poly(*tert* -butyl acrylate) Di- and Triblock Copolymers, *Macromolecules,* (1991), **24,** 4997-5000

64 **Varshney, S.K., Hautekeer, J.P., Fayt, R., Jerome, R. and Teyssie, Ph.,** Anionic Polymerization of (Meth)acrylic Monomers. 4. Effect of Lithium Salts as Ligands on the "Living" Polymerization of Methyl Methacrylate Using Monofunctional Initiators, *Macromolecules,* (1990), **23,** 2618-2622 .

65 **Varshney, S.K., Gao, Z., Zhong, X.F. and Eisenberg, A.,** Effect of Lithium Chloride on the "Living" Polymerization of *tert* - Butyl Methacrylate and Polymer Microstructure Using Monofunctional Initiators, *Macromolecules,* (1994), **27,** 1076-1082

66 **Muller, A.H.E., Kunkel, D., Lochmann, L. and Janata, M.,** Effect of Lithium Chloride on the Kinetics and MWD in the Anionic Polymerization of (Meth)acrylates, ***Polymer Preprints,*** *(Am. Chem. Soc., Div. Polym. Chem.)* , (1991), **32**, 1, 301-302

67 **Muller, A.H.E., Lochmann, L. and Trekoval, J.,** Equilibria in the Anionic Polymerization of Methyl Methacrylate, 1 ; Chain-Length Dependence of the Rate and Equilibrium Constants [a], ***Makromol. Chem.,*** (1986), **187** , 1473-1482

68 **Muller, A.H.E. and Lochmann, L.,** Equilibria in the Anionic Polymerization of Methyl Methacrylate, 2[a] ; Effect of Lithium *tert* -butoxide on rate and equilibrium constants, ***Makromol. Chem.,*** (1990), **191** , 1657-1664

69 **Kitayama, T., Shinozaki, T., Sakamoto, T., Yamamoto, M.and Hatada, K.,** Living and Highly Syndiotactic Polymerization of Methyl Methacrylate and other Methacrylates by *tert*-butyllithium-trialkylaluminium in Toluene, ***Makromolekulare Chemie, Supplement*** , (1989), **15**, 167-185

70 **Kitayama, T., Ute, K. and Hatada, K.,** Synthesis of Stereoregular Polymers and Copolymers of Methacrylate by Living Polymerization and their Characterization by NMR Spectroscopy, ***British Polymer Journal*** , (1990), **23**, 5-17

71 **Hatada., K., Kitayama, T.,Ute, K., Masuda, E. and Shinozaki, T.,** Formation of Living PMMA's with High Stereoregularity and their Utilization to Block and Graft Copolymer Synthesis, ***Polymer Preprints*** *(Am. Chem. Soc., Div. Polym. Chem.)* , (1988), **29**, 2, 54-55

72 **Kitayama, T., Shinozaki, T., Masuda, E., Yamamoto, M.and Hatada, K.,** Highly Syndiotactic Poly(methyl methacrylate) with Narrow Molecular Weight Distribution Formed by *tert*-butyllithium-trialkylaluminium in Toluene, ***Polymer Bulletin,*** (1988), **20**, 505-510

73 **Ballard, D.G.H., Bowles, R.J., Haddleton, D.M., Richards, S.N., Sellens, R. and Twose, D.L.,** Controlled Polymerization of Methyl Methacrylate using Lithium Aluminium Alkyls, ***Macromolecules*** , (1992), **25**, 5907-5913

74 **Haddleton, D.M. and Hunt, K.,** Living Polymerization of Methacrylates using Aluminium and Lithium alkyls, ***Polymer Preprints*** *(Am. Chem. Soc., Div. Polym. Chem.)* , (1994), **35**, 2, 599-600

75 **Schlaad, H. and Muller, A.H.E.,** Mechanism of Anionic Polymerization of Methyl Methacrylate in the presence of aluminium alkyls, ***Polymer Preprints*** *(Am. Chem. Soc., Div. Polym.Chem.)* , (1994), **35**, 2, 597-598

76 **Schlaad, H., Muller, A.H.E. and Kolshorn, H.,** Mechanism of Anionic Polymerization of (Meth)acrylates in the Presence of Aluminium Alkyls, **1-** ^{13}C NMR Studies of Model Compounds in Toluene, ***Macromol. Rapid Communications*** , (1994), **15**, 517-525

77 **Morton, M. and Fetters, L.J.** , Homogeneous Anionic Polymerization of Unsaturated Monomers, ***Macromolecular Reviews,*** (1967), **2**, 98, ***Wiley-Interscience,*** New York

78 **Klein J.W., Lamps J.P., Gnanou Y, Rempp P,** Synthesis and Characterization of Block Copolymers containing Poly (tert.Butyl Acrylate) Blocks, ***Polymer***, (1991), **32**, 12, 2278-2282

79 **Glusker, D.L., Gallucio, R.A. and Evans, R.A.,** The Mechanism of the Anionic Polymerization of Methyl Methacrylate. 3. Effects of Solvents on Stereoregularity and Rates in Fluorenyllithium-Initiated Polymerizations, ***J. Am. Chem. Soc.,*** (1964), **86** , 187-196.

80 **Lochmann, L., Kolarik, J., Doskocilova, D., Vozka, S. and Trekoval, J.,** Metallo Esters. 7. Stabilising Effect of Sodium *tert*-Butoxide on the Growth Centre in the Anionic Polymerization of Methacrylic Esters, ***Journal of Polymer Science*** , (1979), **17**, 1727-1737

81 **Evans, D.C., Barrie, J.A. and George, M.H.,** Synthesis and Characterization of a cis-1,4-Polyisoprene-*b*-Poly(methyl methacrylate) Copolymer, ***Polymer,*** (1975), **16**, 151-152.

82 **Flory, P.J.,** Principles of Polymer Chemistry, ***Cornell University Press,*** Ithaca, New York, (1953)

83 **Allen, R.D., Long, T.E.and McGrath, J.E.,** Preparation of High Purity, Anionic Polymerization Grade Alkyl Methacrylate Monomers, ***Polymer Bulletin***, (1986),**15**,127-134

84 **Plesch, P.H.,** Dilatometry and Dilatometers for Kinetic Studies, ***International Laboratory-Chemical Analysis***, (October 1986), 18-27

85 **Harwood, J.M. and Moody, C.J.,** Experimental Organic Chemistry - Principles and Practice,.***Blackwell Scientific Publications :*** Oxford, London, Edinburgh, Boston, Melbourne, (1990)

86 **Ingram, G.**,Some Further Deliberations on the Rapid Combustion Procedure, *Mikrochim. Acta* ,**1-6**, (1956), 885-893

87 **Adachi, T., Sugimoto, H., Aida, T. and Inoue, S.**, Aluminium Thiolate Complexes of Porphyrin as Excellent Initiators for Lewis-Acid Assisted High-Speed Living Polymerization of Methyl Methacrylate, ***Macromolecules,*** (1993), **26**, 1238-1243

88 **Amass, A.J., Amass W and Desai, H.,** Anionic Polymerization of Styrene; A Study of the Stability of Living Systems, ***Polymer Preprints*** *(Am. Chem. Soc., Div. Polym. Chem.)* , (1994), **35**, 2, 568-569

89 **Selb, J. and Gallot, Y**, Polymeric Amines and Ammonium Salts, ***Goethals, E. J. Ed.***, Pergamon Press : New York, (1980), 205

90 **Selb, J. and Gallot, Y.**, Development in Block Copolymers, ***Goodman, I., Ed;*** Elsevier Applied Science : London, U.K., (1985), **2**, 27-96

91 **Desjardins, A. and Eisenberg, A.,** Colloidal Properties of Block Ionomers. 1. Characterization of Reverse Micelles of Styrene-*b*-Metal Methacrylate Diblocks by Size Exclusion Chromatography, ***Macromolecules***, (1991), **24**, 5779-5790

92 **Desjardins, A., van de Ven, T.G.M. and Eisenberg, A.**,Colloidal Properties of Block Ionomers. 2. Characterization of Reverse Micelles of Styrene-*b*-Methacrylic Acid and Styrene-*b*-Metal Methacrylate Diblocks by Dynamic Light Scattering, ***Macromolecules,*** (1992), **25**, 2412-2421

93 **Tuzar, Z. and Kratochvil, P.**, Micelles of Block and Graft Copolymers in Solutions, ***Adv.Surface and Colloid Science,*** (1993),**15**, 1, Matijevic, E., Ed., Plenum Press: New York

94 **Antonetti, M., Heinz, S., Schmidt, M. and Rosenauer, C.,** Determination of the Micelle Architecture of Polystyrene/Poly (4-vinylpyridine) Block Copolymers in Dilute Solution, ***Macromolecules,*** (1994), **27**, 3276-3281

95 **Halperin, A.,** Starlike Micelles: Their Growth in Homopolymer Solutions, ***Macromolecules,*** (1989), **22**, 3806-3807

96 **Noolandi, J. and Hong, K.M.,** Interfacial Properties of Immiscible Homopolymer Blends in the Presence of Block Copolymers, ***Macromolecules,*** (1982), **15**, 482-491

97 **Marko, J.F.and Rabin, Y.,** Microphase Separation of Charged Diblock Copolymers: Melts and Solutions, ***Macromolecules,*** (1992), **25**, 1503-1509

98 **Yuan, X.F., Masters, A.J. and Price, C.,** Self-Consistent Field Theory of Micelle Formation by Block Copolymers, ***Macromolecules,*** (1992), **25**, 6876-6884

99 **Gao, Z. and Eisenberg, A.,** A Model of Micellization for Block Copolymers in Solutions, ***Macromolecules,*** (1993), **26**, 7353-7360

100 **Holland, P.M. and Rubingh, D.N.,** Nonideal Multicomponent Mixed Micelle Model, ***Journal of Physical Chemistry***, (1983), **87**, 1984-1990

101 **Holland, P.M.,** Nonideal Mixed Micellar Solutions, ***Advances in Colloid and Interface Science,*** (1986), **26**, 111-129

102 **Astafieva, I., Zhong, X.F. and Eisenberg, A.,** Critical Micellization Phenomena in Block Polyelectrolyte Solutions. ***Macromolecules***, (1993), **26**, 7339-7352

103 **Khougaz, K., Gao, Z. and Eisenberg, A.,** Determination of the Critical Micelle Concentration of Block Copolymer Micelles by Static Light Scattering, ***Macromolecules,*** (1994), **27**, 6341-6346

104 **Eisenberg, A. and Rinaudo, M.,** Polyelectrolytes and Ionomers, ***Polymer Bulletin,*** (1990), **24**, 671

105 **Nagarajan, R., Barry, M. and Ruckenstein E.,** Unusual Selectivity in Solubilization by Block Copolymer Micelles, ***Langmuir***, (1986), **2**, 210-215

106 **Nagarajan, R. and Ganesh C.,** Block Copolymer Self-Assembly in Selective Solvents: Theory of Solubilization in Spherical Micelles, ***Macromolecules,*** (1989), **22**, 4312-4325

107 **Salamone, J.C. and Rice, W.C.,** Vinylpyridine Polymers, ***Encyclopedia of Polymer Science,*** 2nd Ed., **17**, 567-588

108 **Tuzar, T. and Sikora, A.,** Association of Two-Block Copolymer Polystyrene-*b*-poly (2-vinylpyridine) in Toluene, ***die Makromolekulare Chemie,*** (1983), **184**, 2049-2059

109 **Moller, M. and Kunz, M.** Electron-Spectroscopic Imaging on Polystyrene-Poly-2-Vinylpyridine Block Copolymers. ***Polymer Preprints,*** *(Am. Chem. Soc., Div. Polym. Chem.)* ,(1988), **29,** 1, 446-447

110 **Nguyen, D., Zhong, X., Williams, C.E. and Eisenberg, A.**, Effect of Ionic Chain Polydispersity on the Size of Spherical Ionic Microdomains in Diblock Ionomers, *Macromolecules,* (1994), **27**, 5173-5181

111 **Schwab, F.C. and Heilweil, I.J.**, Synthesis and Solution Properties of Styrene-Vinyl-N-Alkylpyridinium Halide Block Polymers, ***Polymer Preprints,*** *(Am. Chem. Soc., Div. Polym. Chem.)* , (1989), **24,** 2, 65-66

112 **Schwab, F.C. and Heilweil, I.J.**, Synthesis and Solution Properties of Styrene-Vinyl-N-Alkylpyridinium Halide Block Polymers, *American Chemical Society, Ind. Eng. Chem. Prod. Res. Dev.,* (1984), **23,** 435-437

113 **Huglin, M.B.** (Ed), Light Scattering from Polymer Solutions, *Academic Press :* London and New York, (1972).

114 **Zimm, B.H.,** Apparatus and Methods for Measurement and Interpretation of the Angular Variation of Light Scattering; Preliminary Results on Polystyrene Solutions, *J. Chem . Phys.* (1948), **16,** 1099-1116

115 **Wyatt, P.J.**, Light Scattering and the Absolute Characterization of Macromolecules, *Anal. Chim. Acta,* (1993), **272**, 1-40

APPENDICES

Appendix 1. SEC Chromatogram of PS-*b*-PMMA from CP1, in the Anionic Block Copolymerization of Styrene and Methyl Methacrylate in the Presence of Lithium Chloride

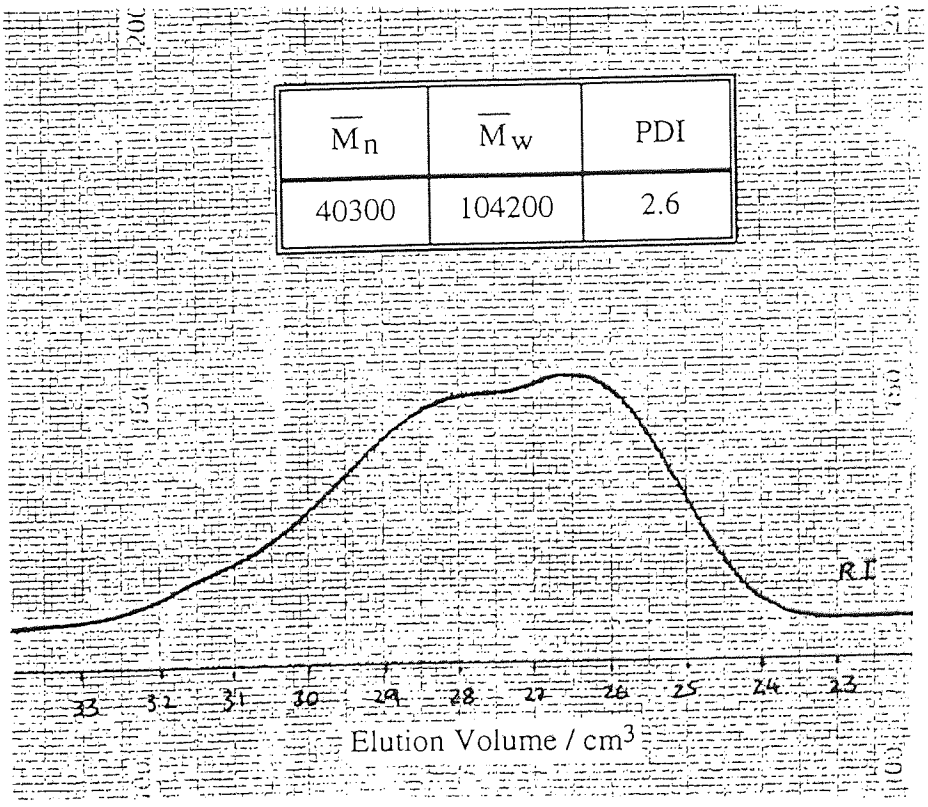

Appendix 2. SEC Chromatogram Showing UV absorbance at 254 nm for Pure Poly(styrene)

Mn= 15342 Polydispersity= 1.182

Mw= 18001 Peak Area = 683867

Mp= 26825

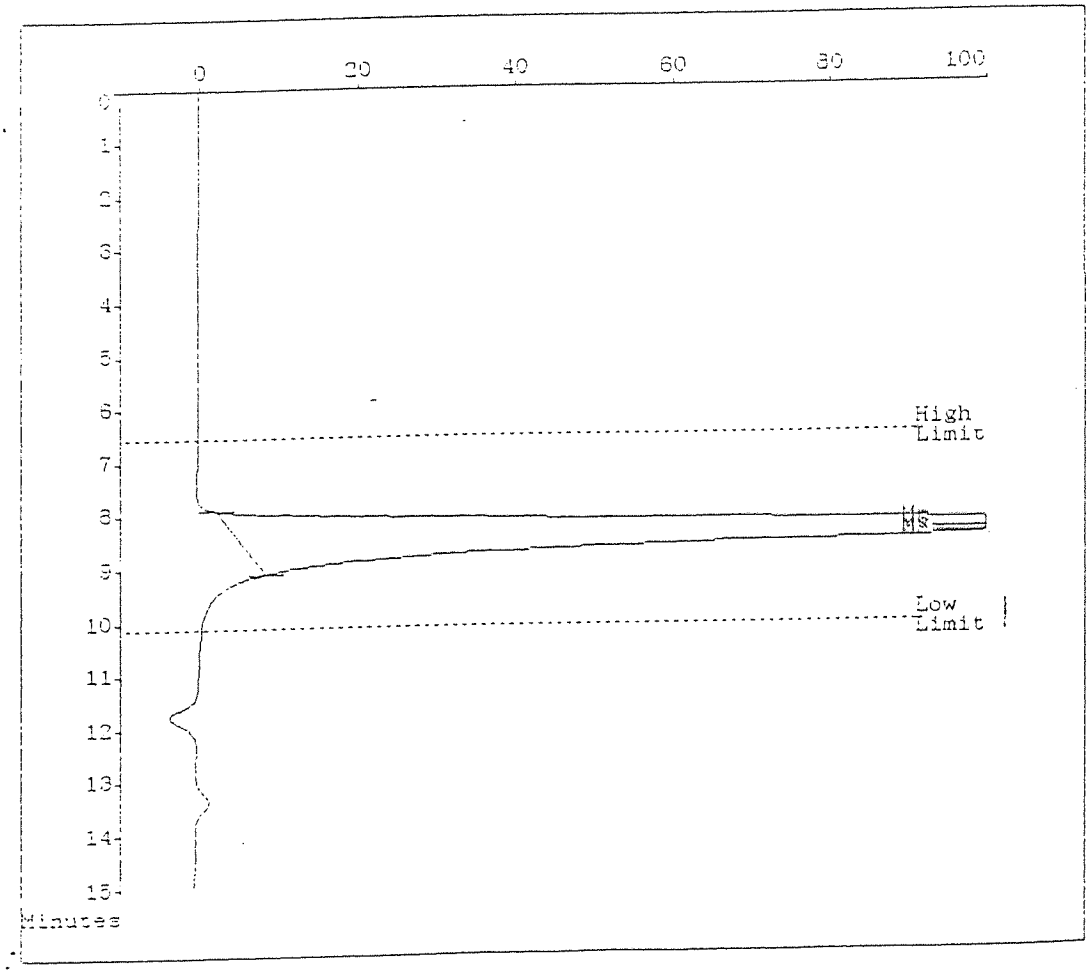

Appendix 3. SEC Chromatogram Showing UV absorbance at 254 nm for Pure Poly(Methyl Methacrylate)

Mn= 16284 Polydispersity= 1.496

Mw= 24356 Peak Area = 2115

Mp= 24548

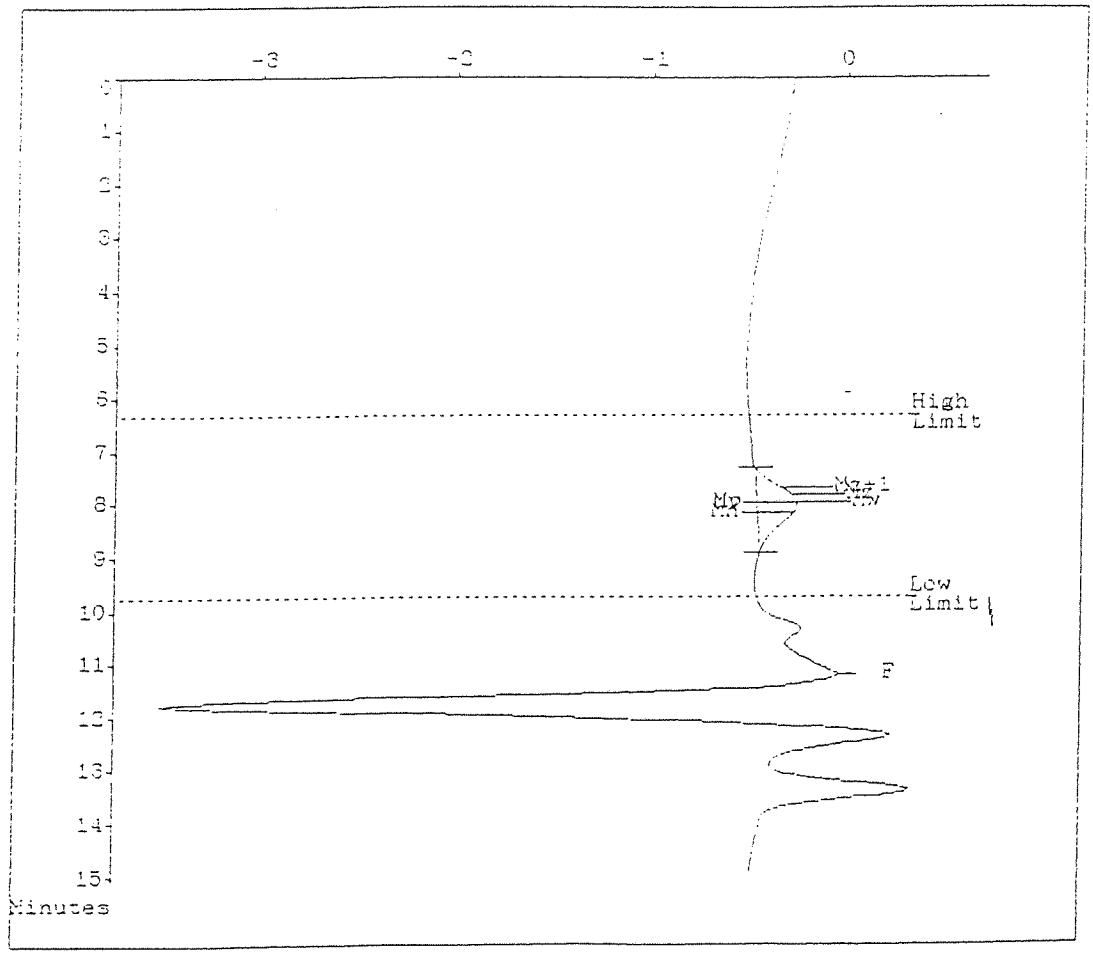

Appendix 4. FTIR Spectrum of PS-*b*-PMMA from CP5, in the Anionic Block Copolymerization of Styrene and Methyl Methacrylate in the Presence of Lithium Chloride

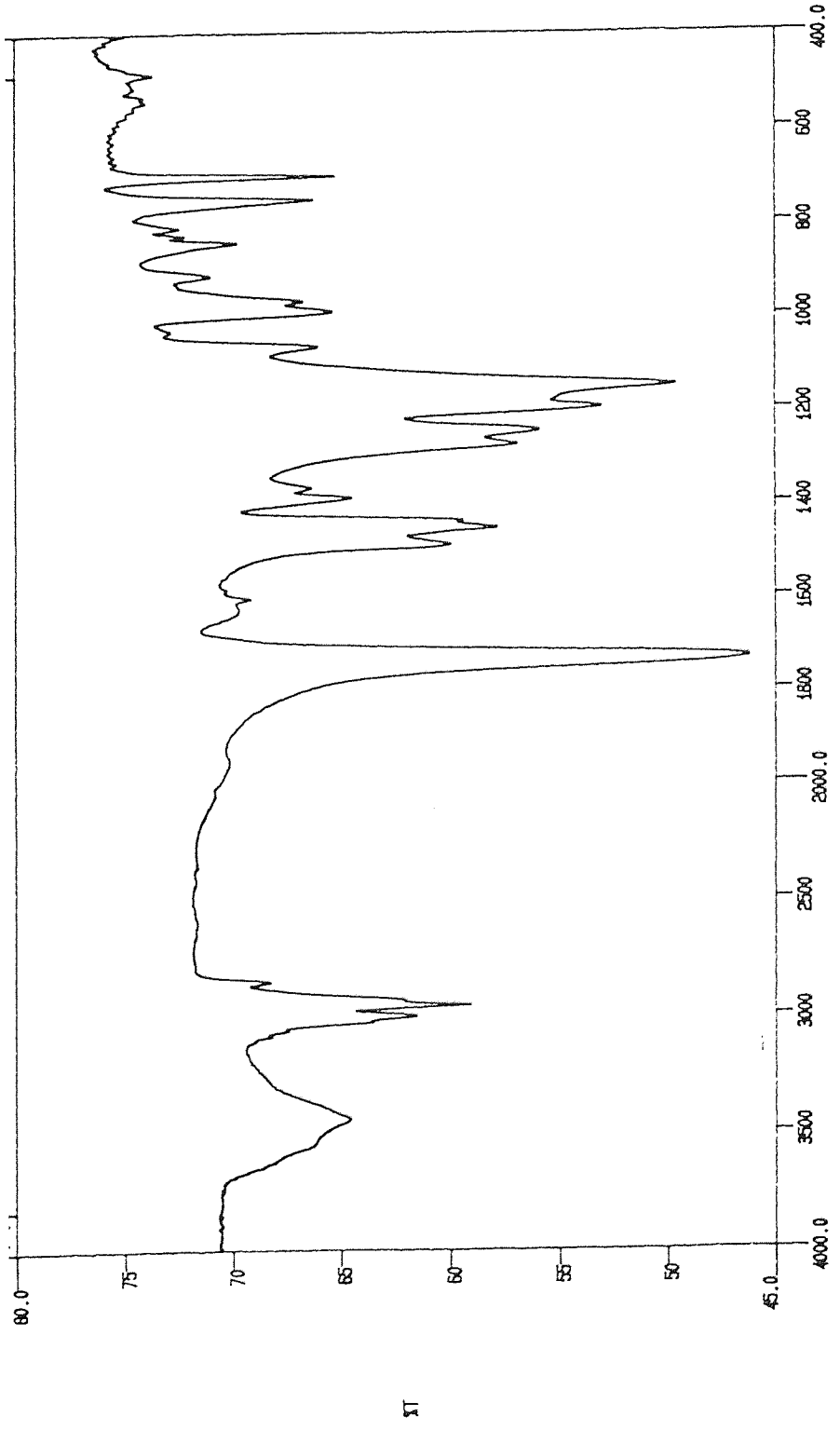

Appendix 5. FTIR Spectrum of PS-*b*-PMMA from CP6, in the Anionic Block Copolymerization of Styrene and Methyl Methacrylate in the Presence of Lithium Chloride

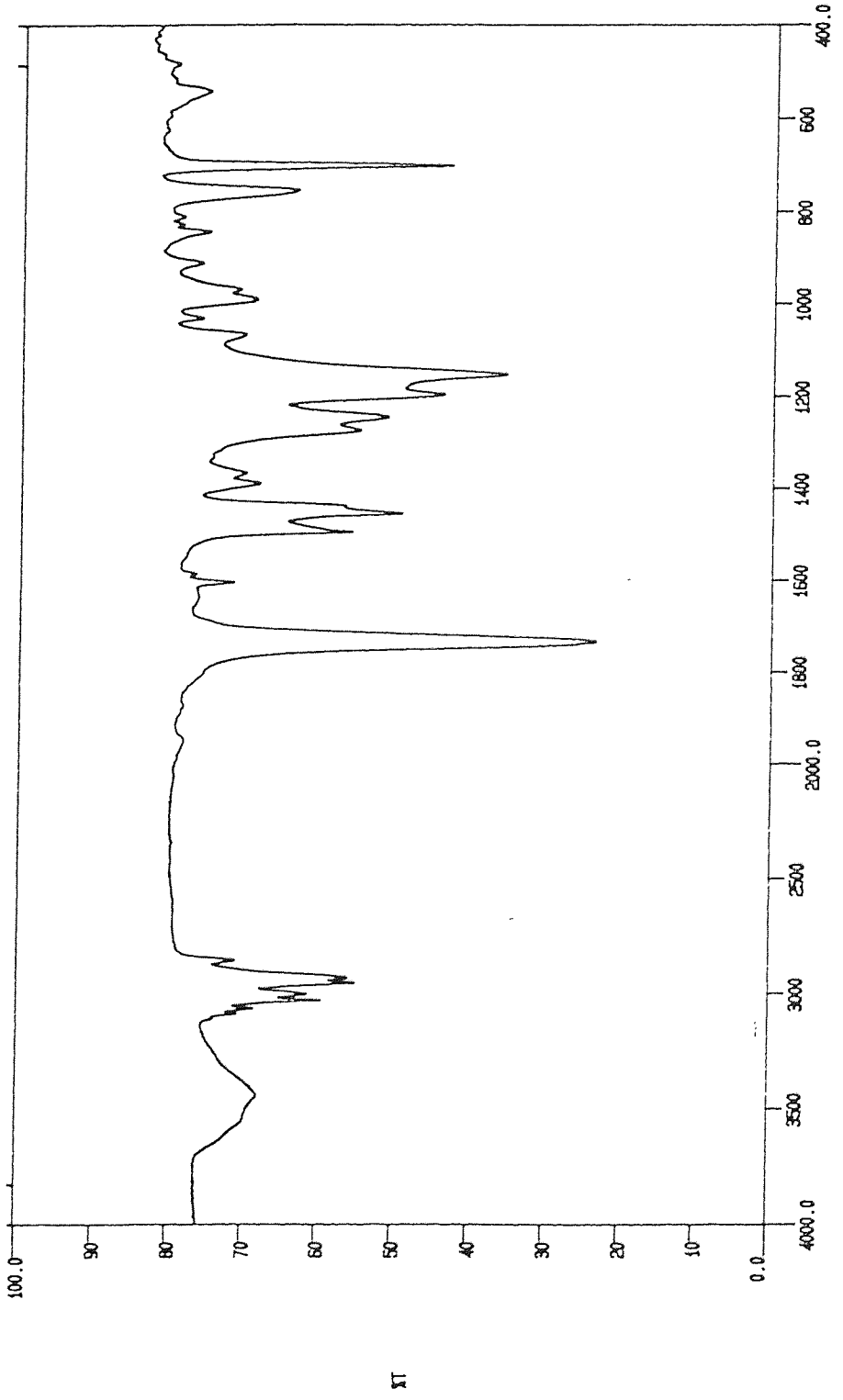

Appendix 6. ^{1}H NMR Spectrum of PS-*b*-PMMA from CP6, in the Anionic Block Copolymerization of Styrene and Methyl Methacrylate in the Presence of Lithium Chloride

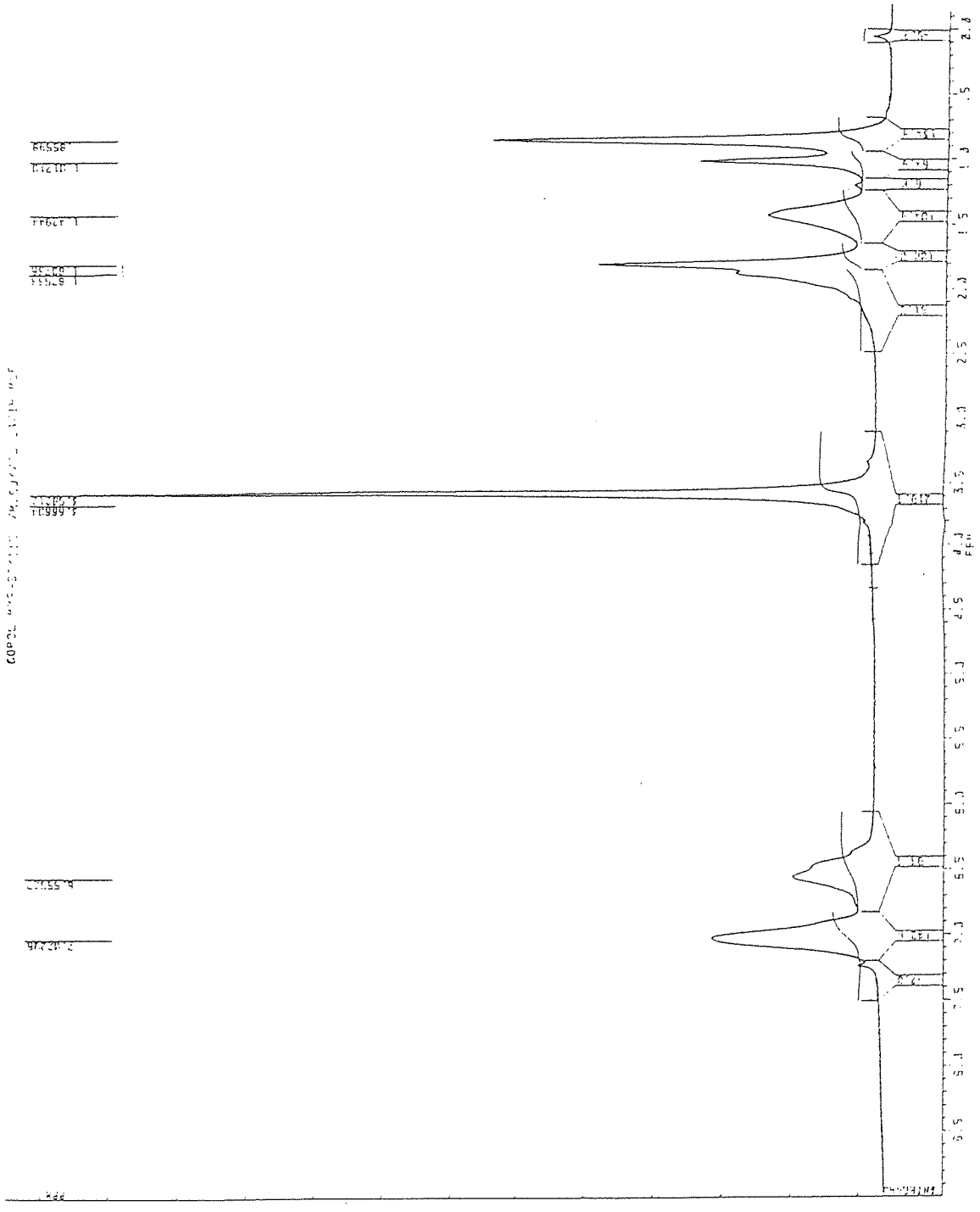

Appendix 7. ^{13}C NMR Spectrum of PS-*b*-PMMA from CP6, in the Anionic Block Copolymerization of Styrene and Methyl Methacrylate in the Presence of Lithium Chloride

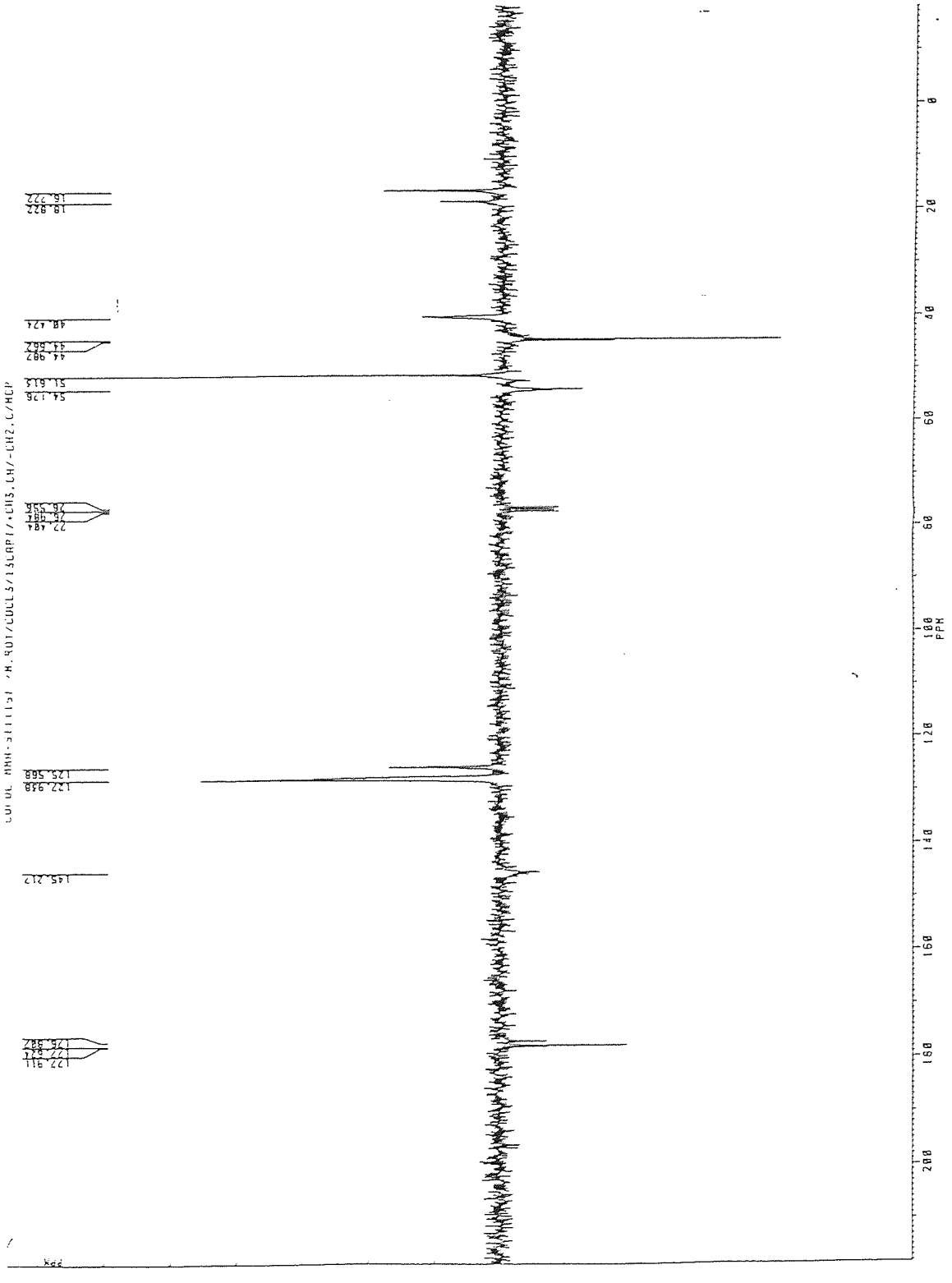

Appendix 8. ^{1}H NMR Spectrum of PMMA, in the Anionic Polymerization of Methyl Methacrylate Initiated by BuLi/$AlEt_3$ Using Cyclohexane as Solvent

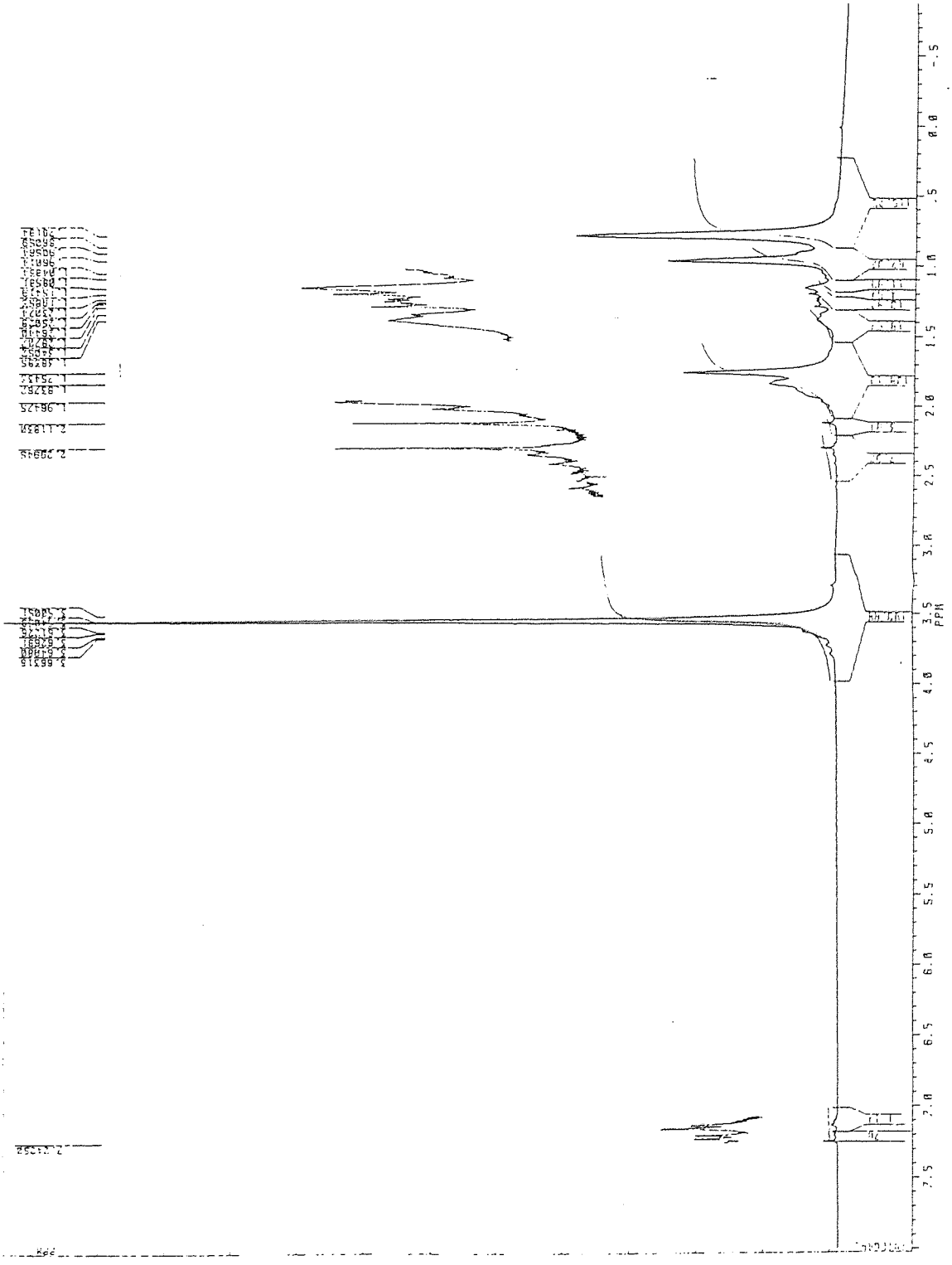

Appendix 9. ^{13}C NMR Spectrum of PMMA, in the Anionic Polymerization of Methyl Methacrylate Initiated by BuLi/$AlEt_3$ Using Cyclohexane as Solvent

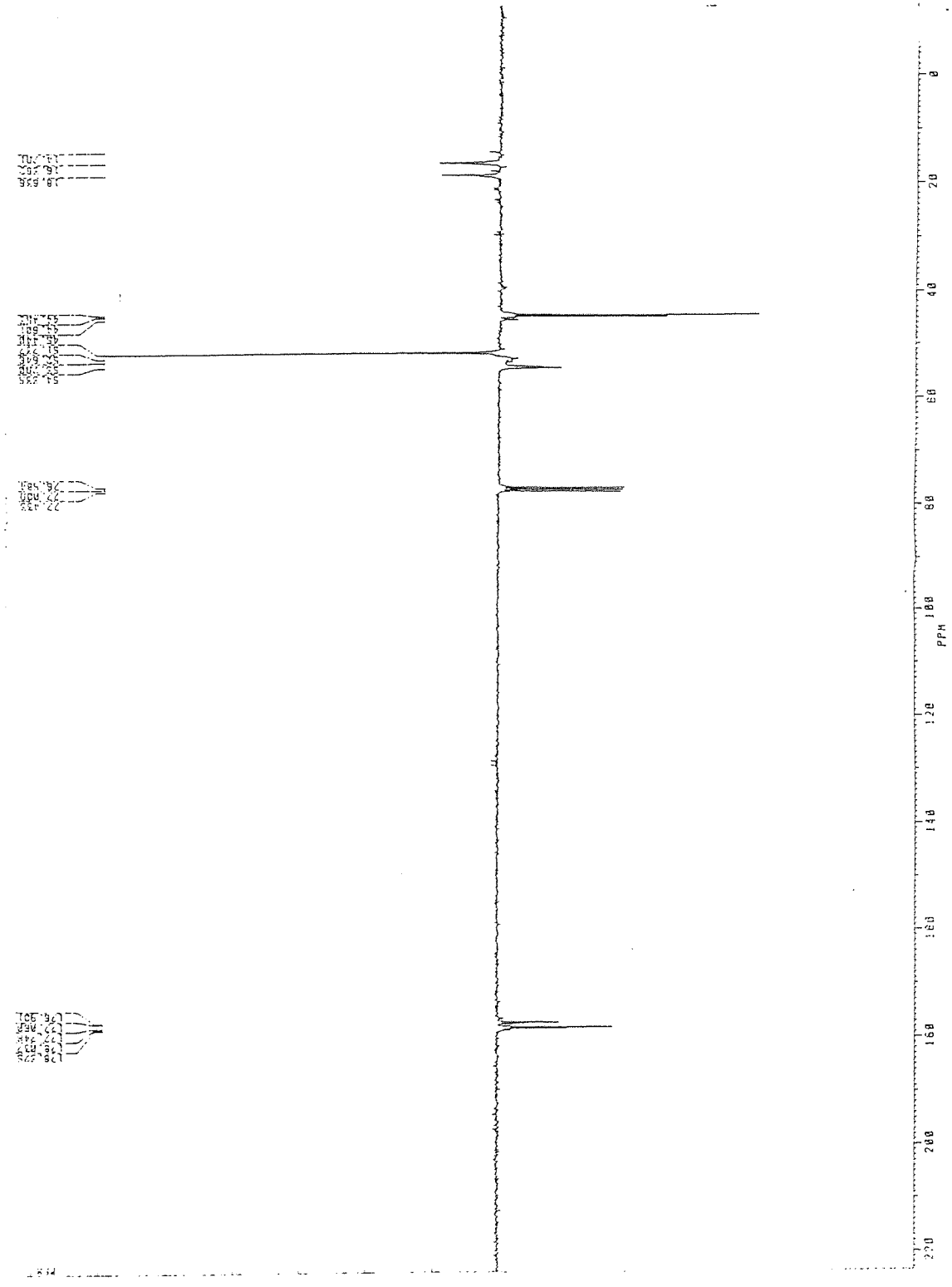

Appendix 10. SEC Chromatogram of PMMA , in the Anionic Polymerization of Methyl Methacrylate Initiated by BuLi/$AlEt_3$ Using Cyclohexane as Solvent

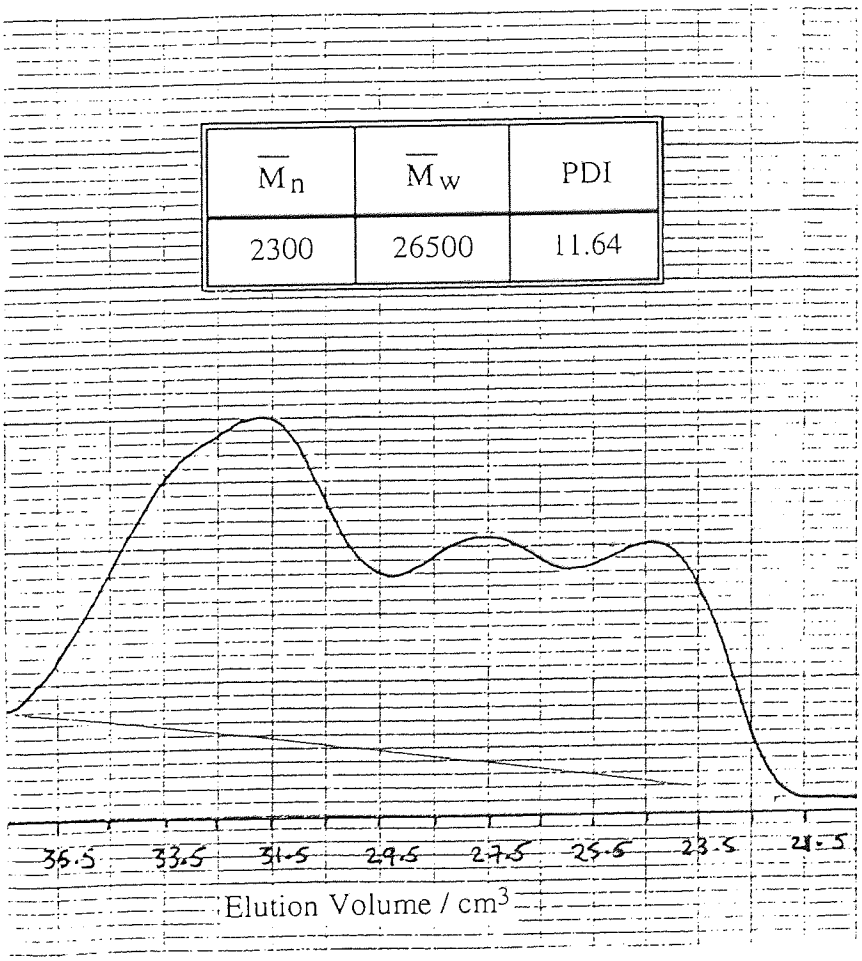

Appendix 11. SEC Chromatogram of PMMA for P3 at 19% Conversion, in the Anionic Polymerization of Methyl Methacrylate Initiated by BuLi/$AlEt_3$

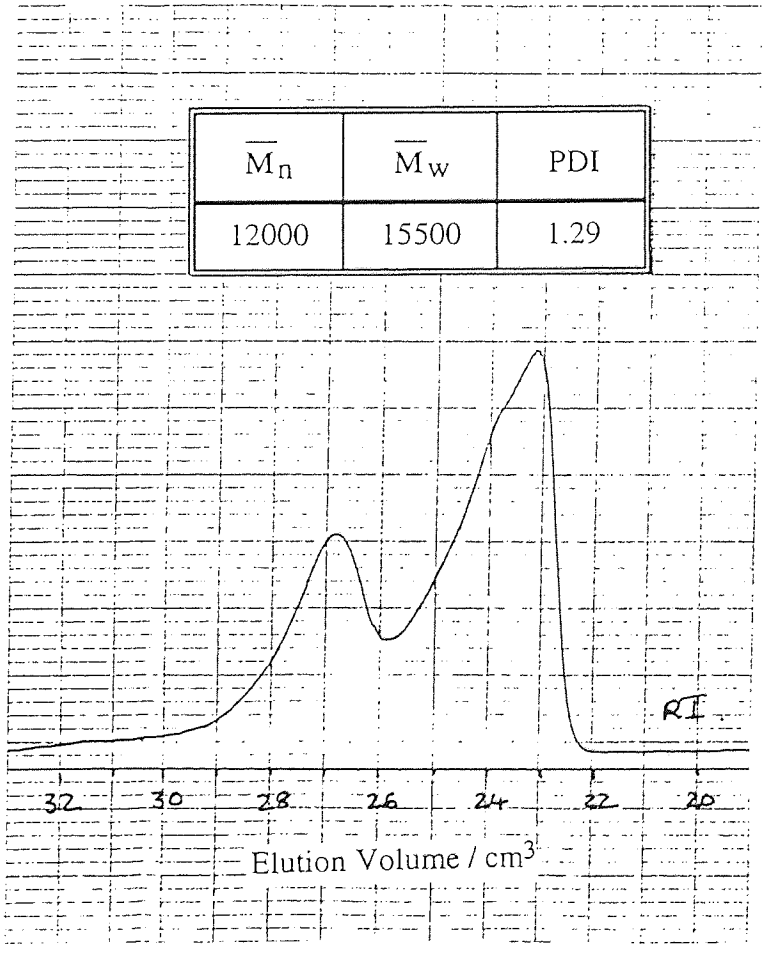

Appendix 12. SEC Chromatogram of PMMA for P3 at 75% Conversion, in the Anionic Polymerization of Methyl Methacrylate Initiated by $BuLi/AlEt_3$

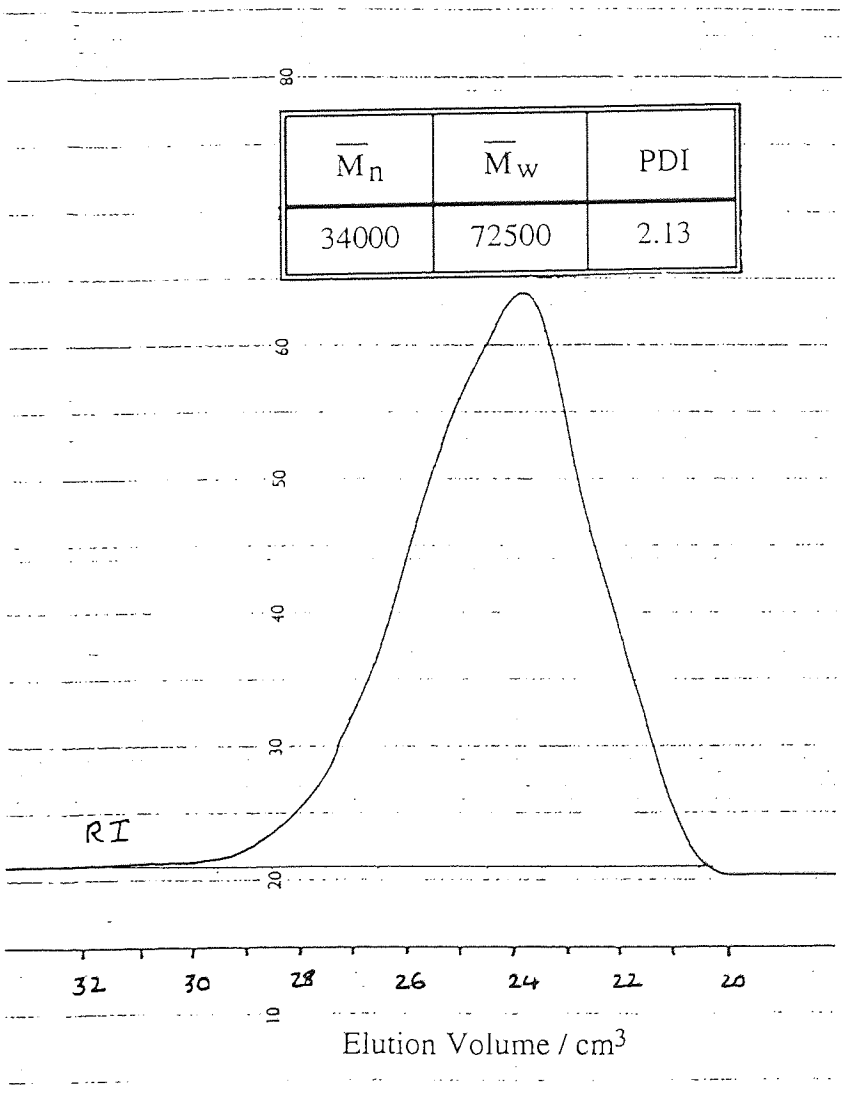

Appendix 13. ^{1}H NMR Spectrum of PMMA for P3, in the Anionic Polymerization of Methyl Methacrylate Initiated by BuLi/$AlEt_3$

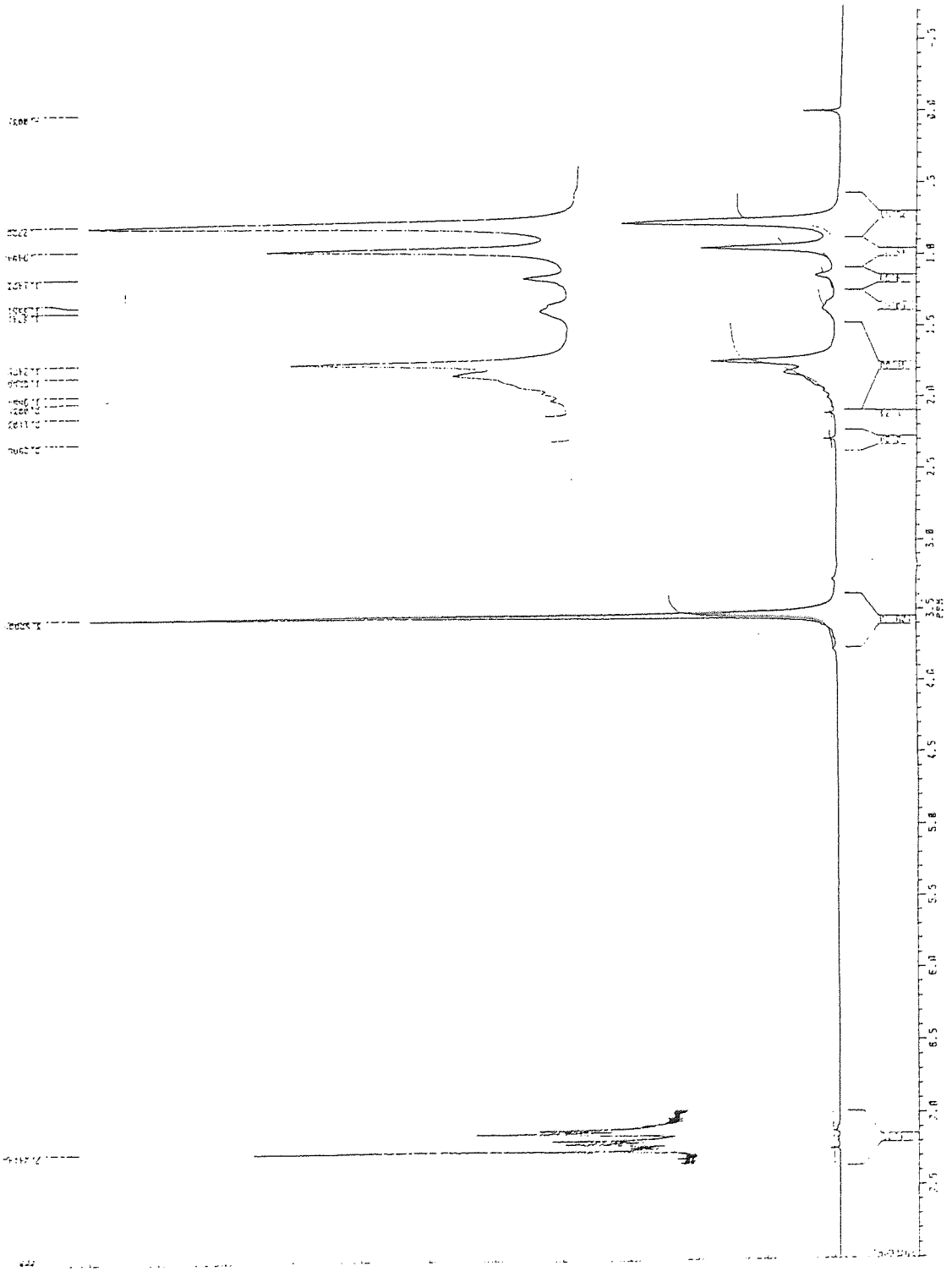

Appendix 14. ^{13}C NMR Spectrum of PMMA for P3, in the Anionic Polymerization of Methyl Methacrylate Initiated by BuLi/$AlEt_3$

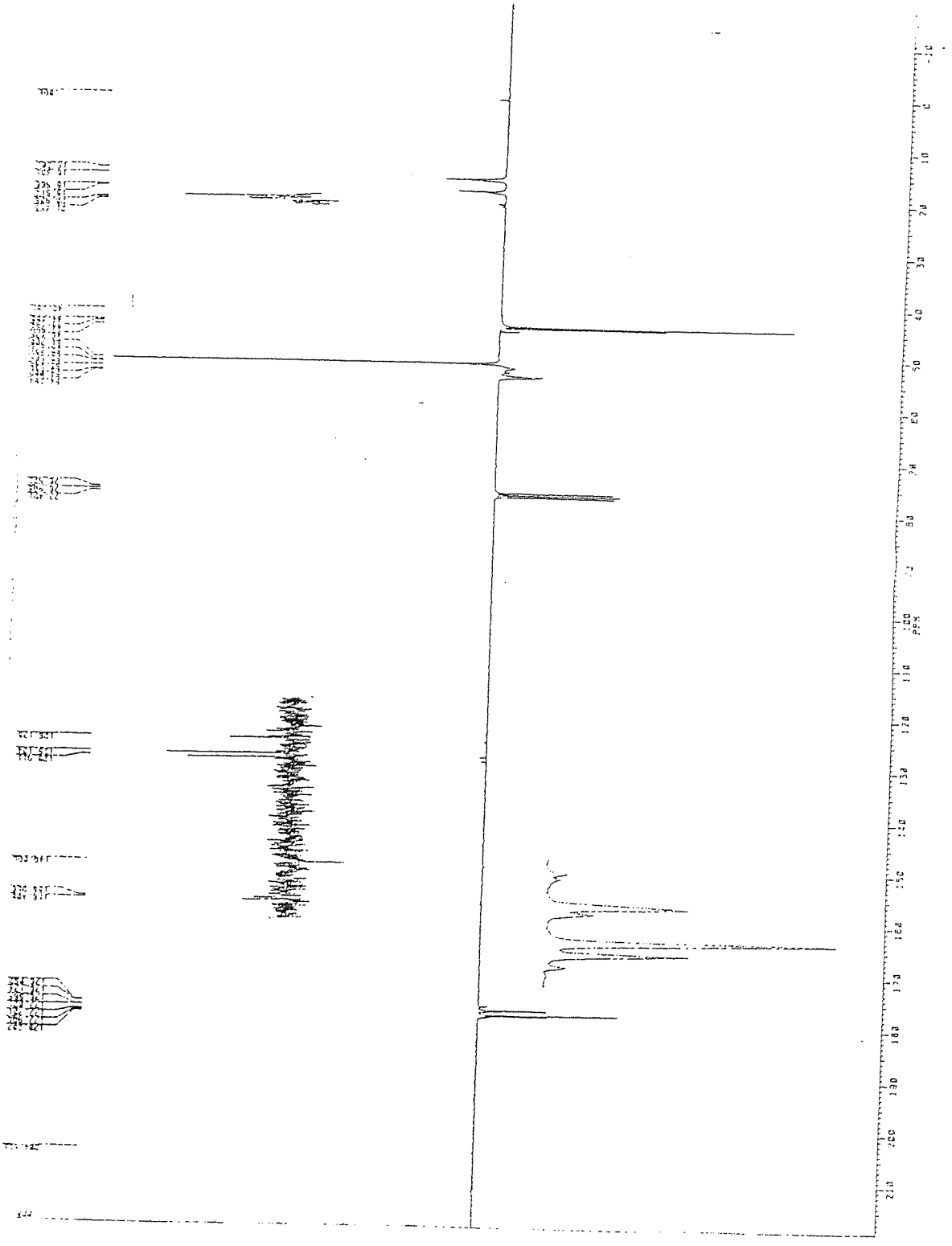

Appendix 15. SEC Chromatogram of PMMA for P9 at 45% Conversion, in the Anionic Polymerization of Methyl Methacrylate Initiated by *t*-BuLi/$AlEt_3$

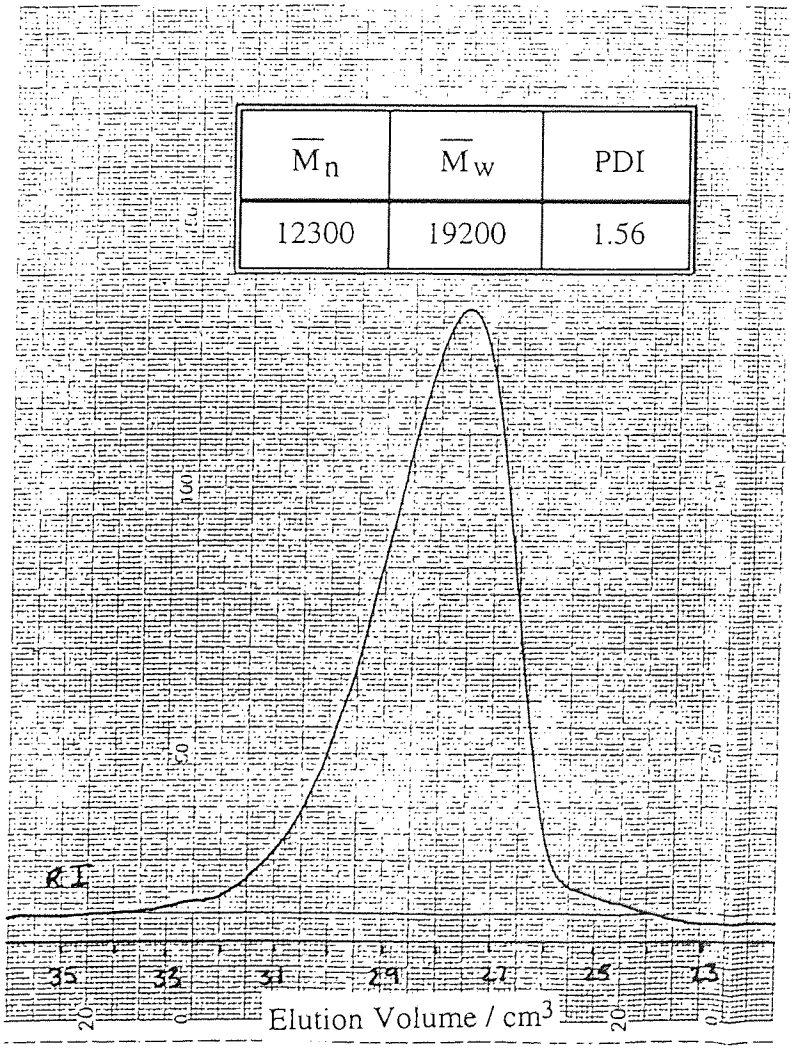

Appendix 16. SEC Chromatogram of PMMA for P10 at 40% Conversion, in the Anionic Polymerization of Methyl Methacrylate Initiated by *t*-BuLi/$AlEt_3$

$\overline{M}_n$	$\overline{M}_w$	PDI
14300	21200	1.48

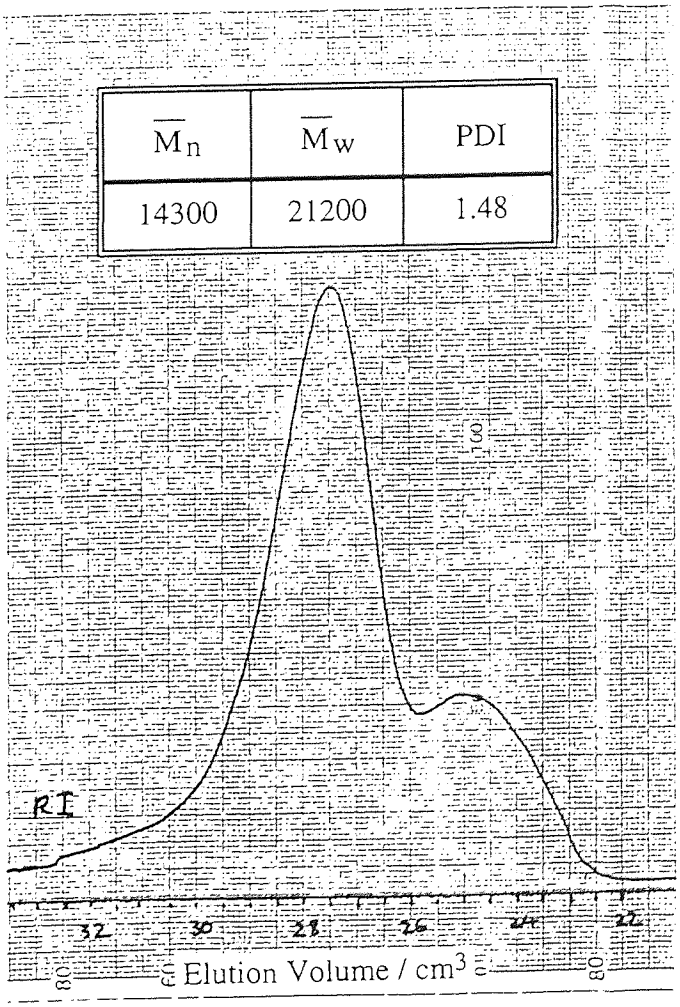

Appendix 17. ^{1}H NMR Spectrum of PMMA for P9, in the Anionic Polymerization of Methyl Methacrylate Initiated by *t*-BuLi/$AlEt_3$

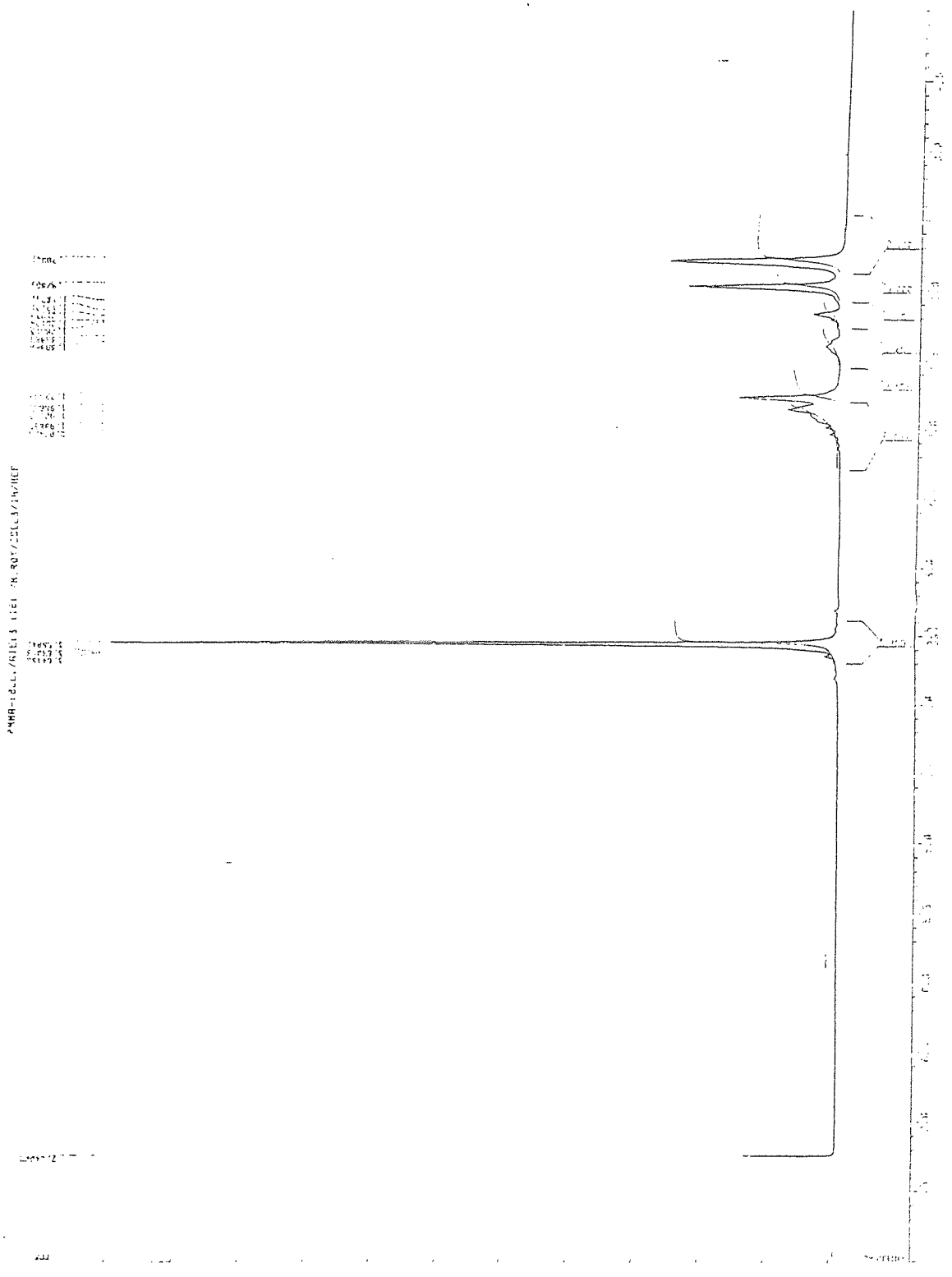

Appendix 18. ^{13}C NMR Spectrum of PMMA for P9, in the Anionic Polymerization of Methyl Methacrylate Initiated by *t*-BuLi/$AlEt_3$

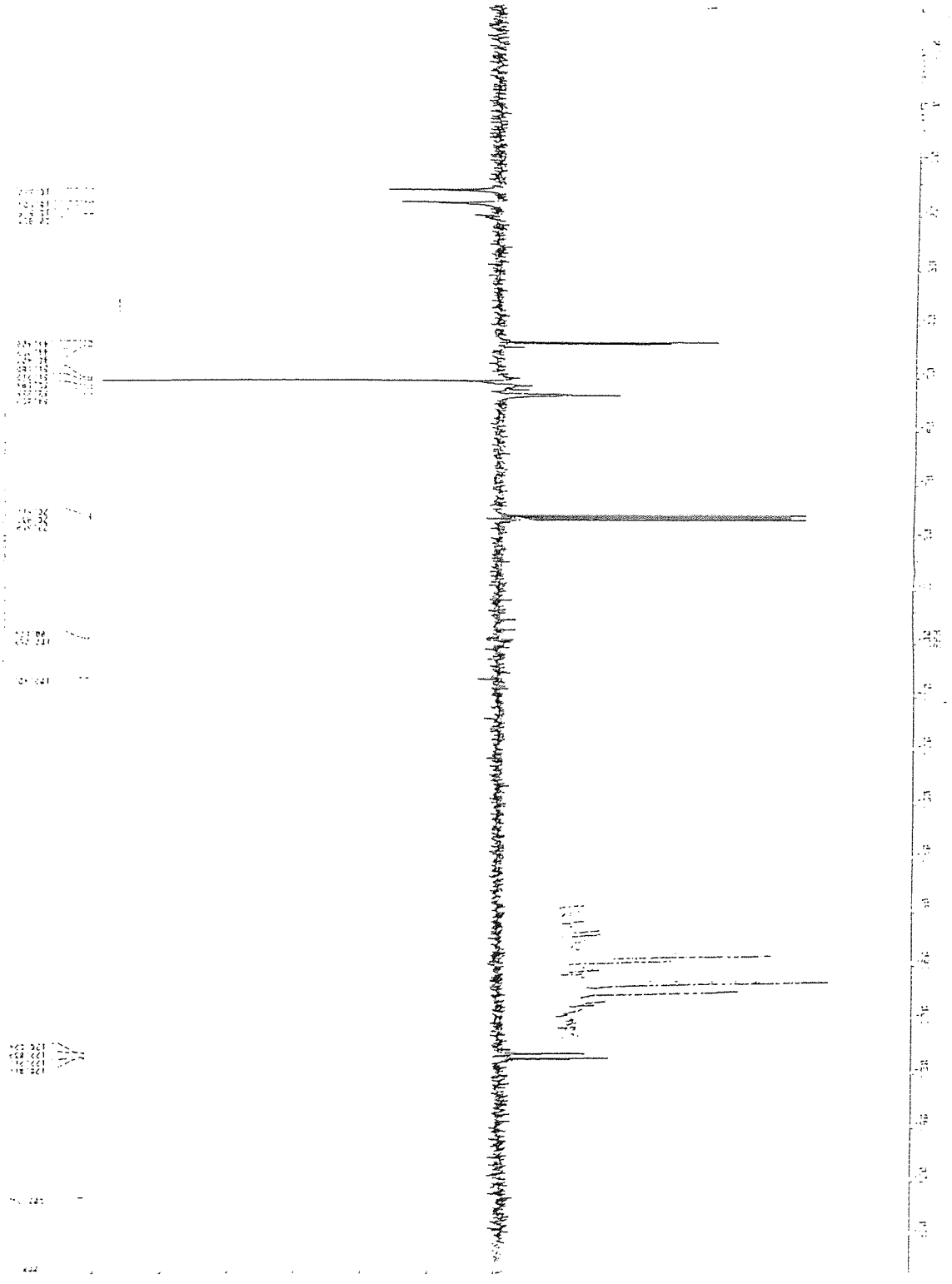

Appendix 19. SEC Chromatogram of PMMA for P12 at 50% Conversion, in the Anionic Polymerization of Methyl Methacrylate Initiated by *t*-BuLi/Al(^{i}Bu)$_3$

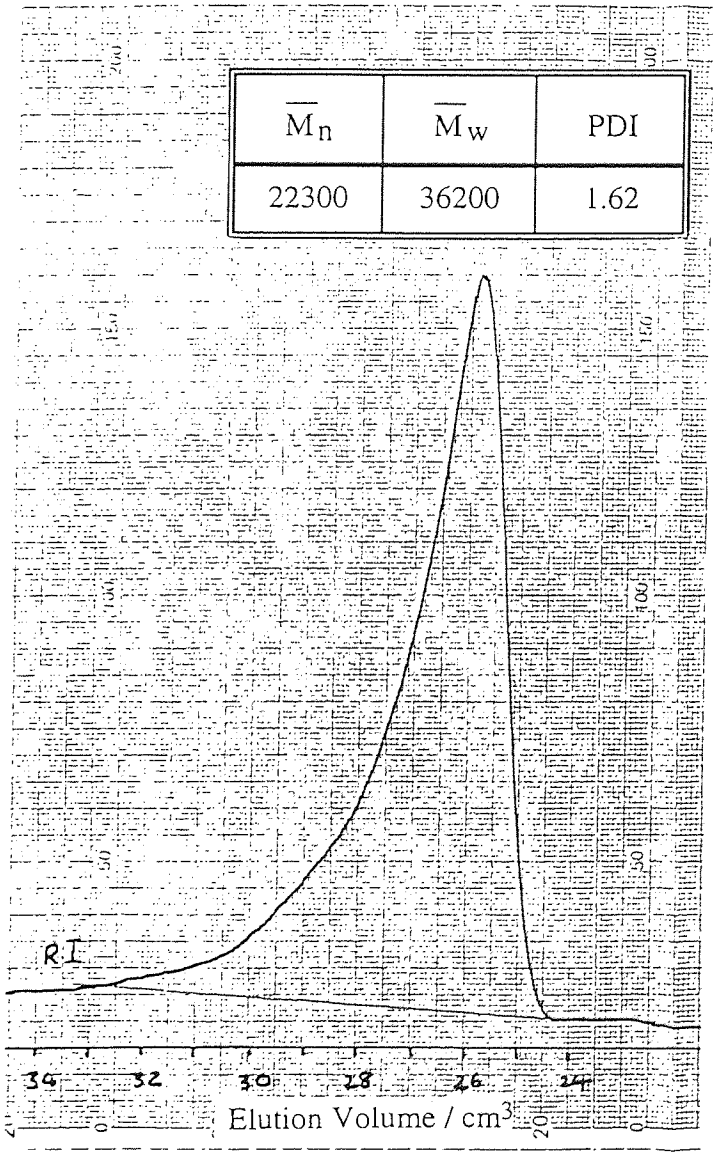

Appendix 20. ^{1}H NMR Spectrum of PMMA for P12, in the Anionic Polymerization of Methyl Methacrylate Initiated by *t*-BuLi/Al(^{i}Bu)$_3$

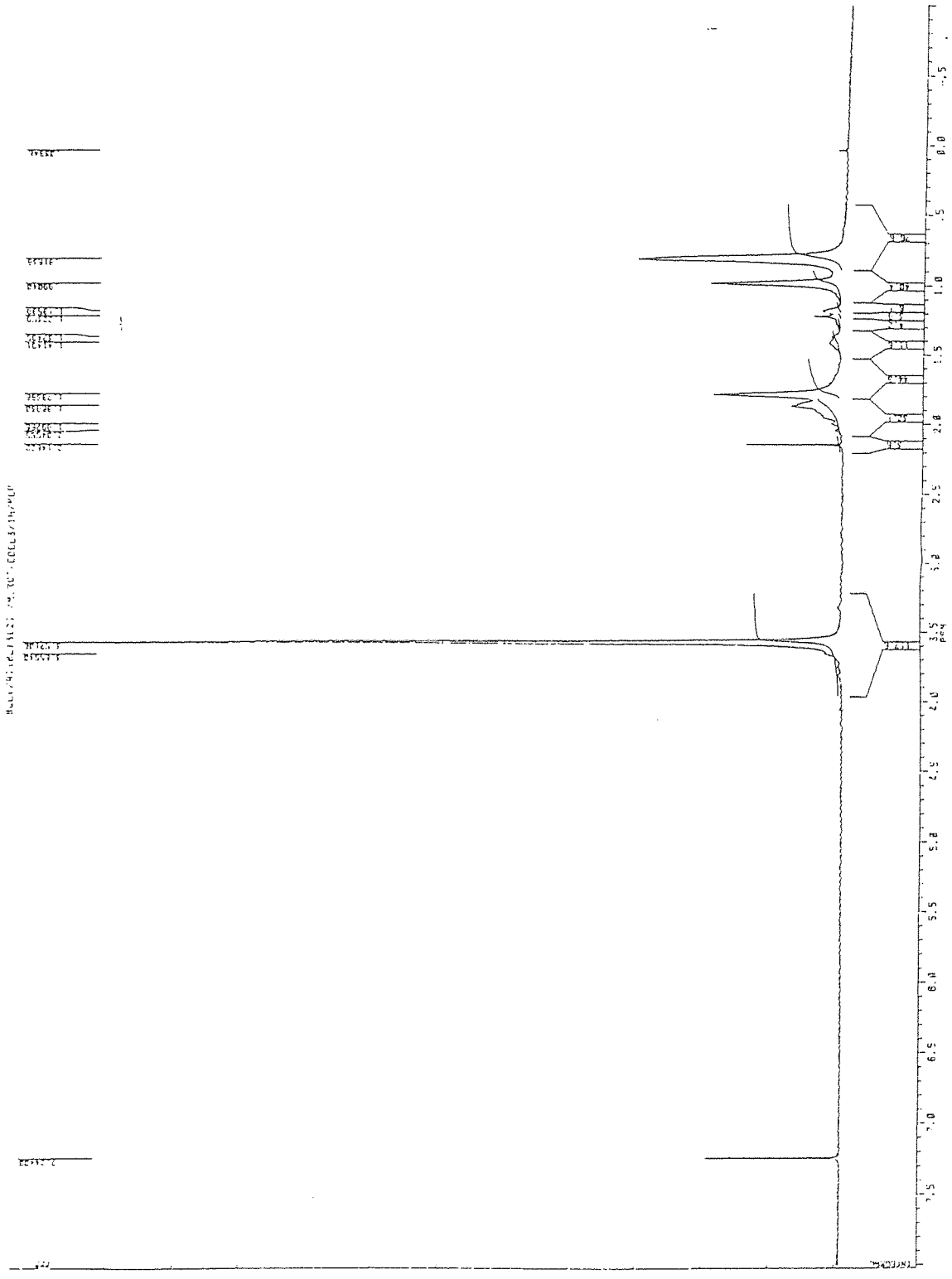

Appendix 21. ^{13}C NMR Spectrum of PMMA for P12, in the Anionic Polymerization of Methyl Methacrylate Initiated by *t*-BuLi/Al(^{i}Bu)$_3$

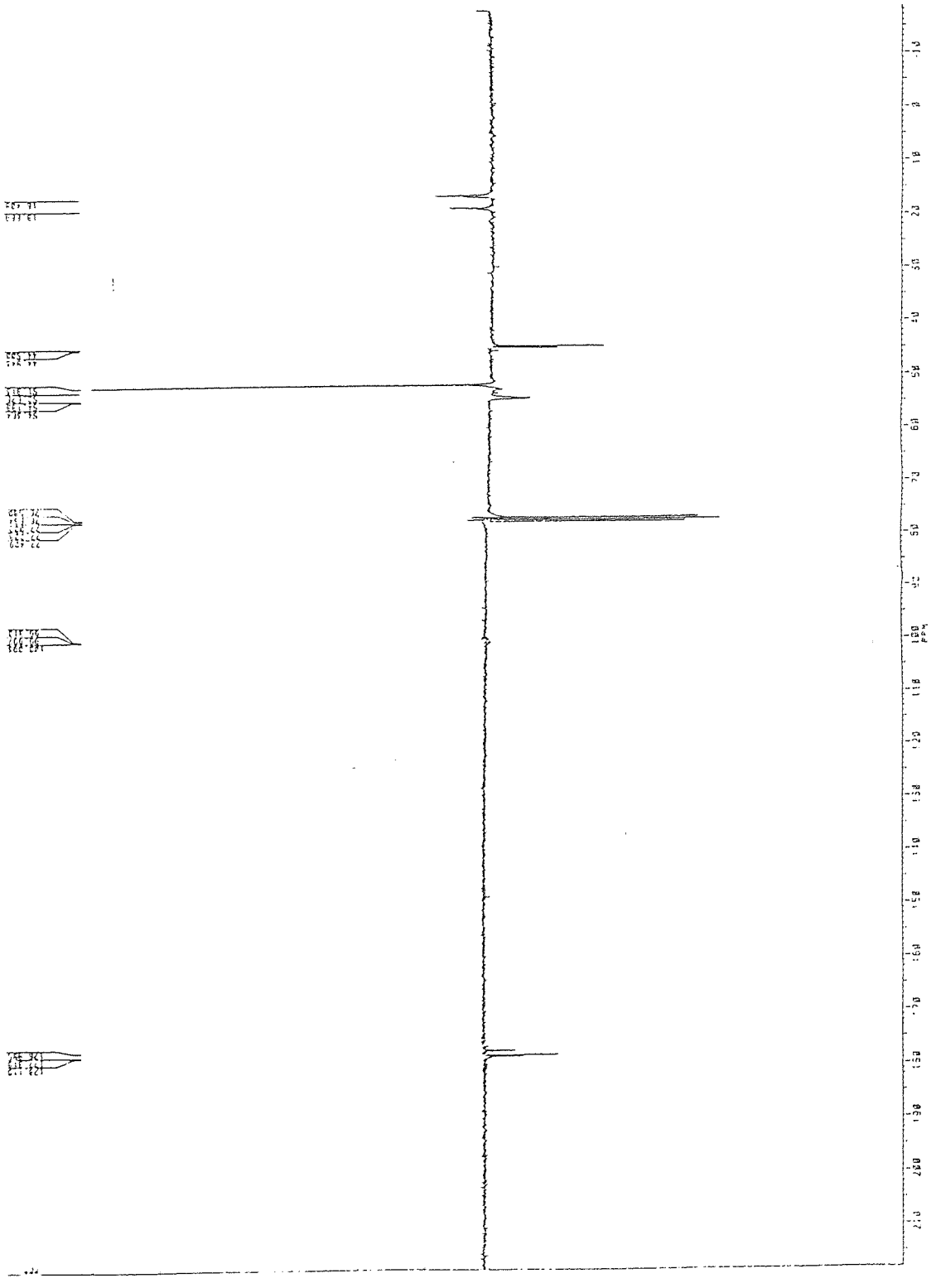

Appendix 22. SEC Chromatogram of PS-*b*-PMMA for CP4, in the Anionic Block Copolymerization of Styrene and Methyl Methacrylate in the Presence of $Al(^{i}Bu)_3$

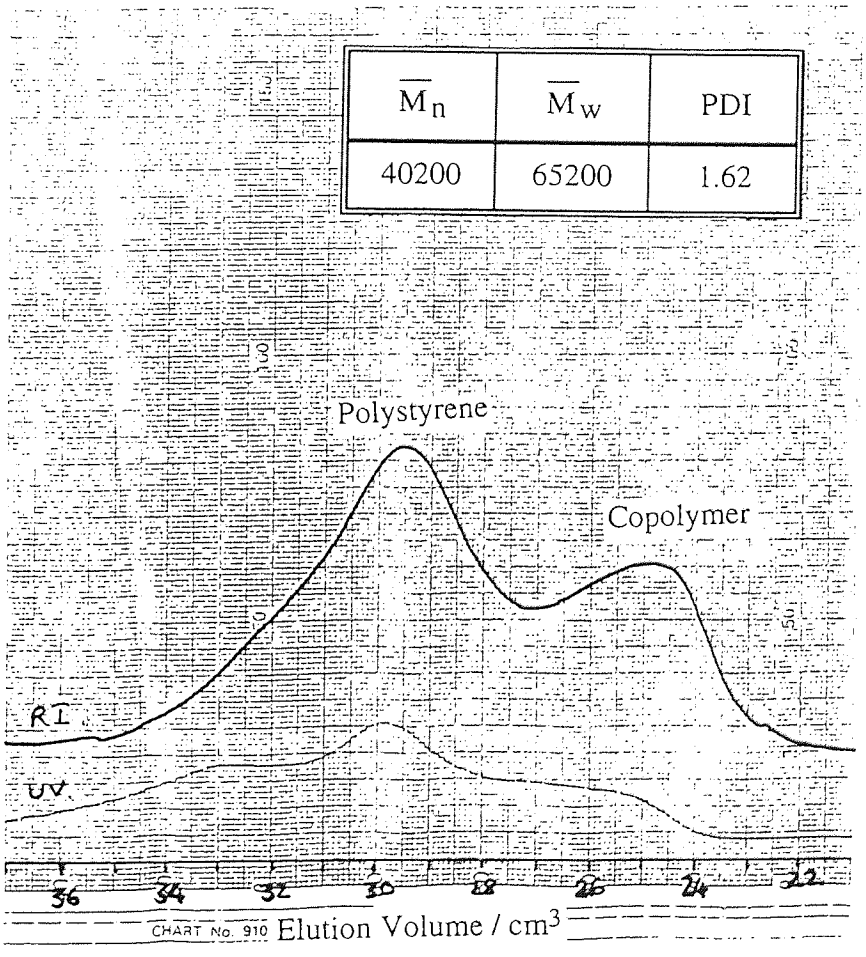

$\overline{M}_n$	$\overline{M}_w$	PDI
40200	65200	1.62

Appendix 23. SEC Chromatogram of Poly(styrene) Obtained From CP4, in the Anionic Block Copolymerization of Styrene and Methyl Methacrylate in the Presence of $Al(^iBu)_3$

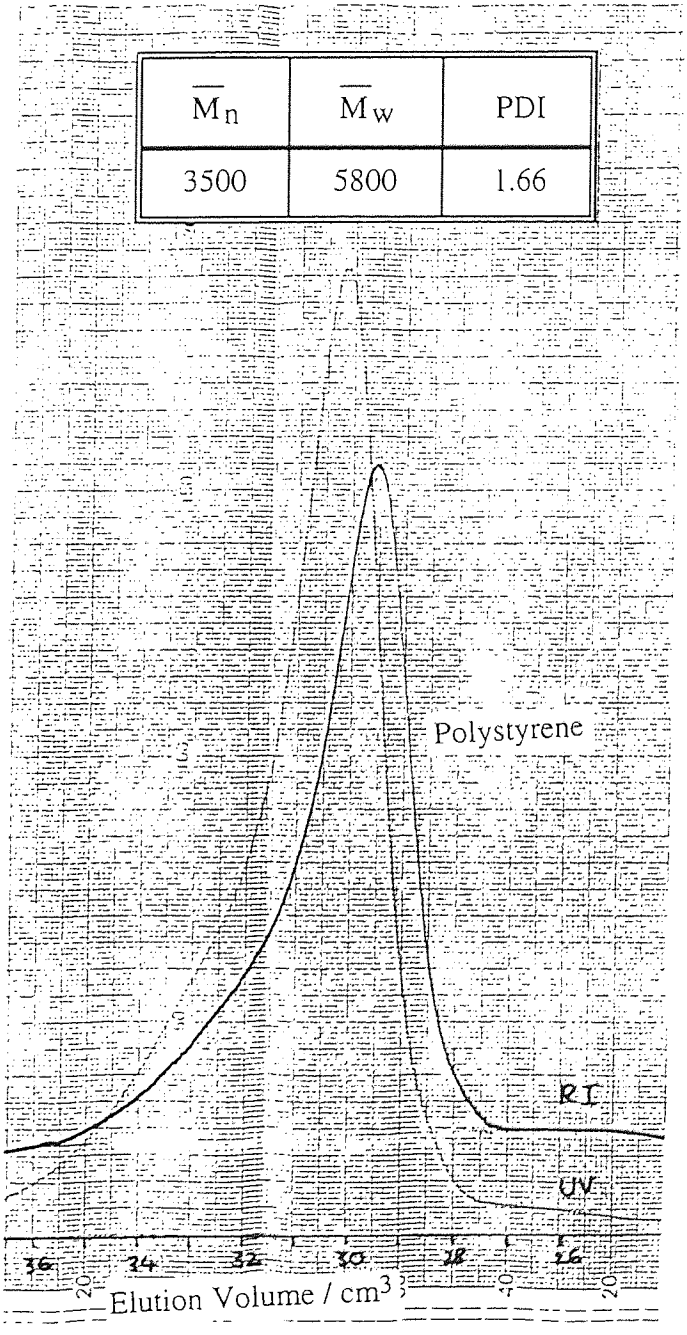

$\overline{M}_n$	$\overline{M}_w$	PDI
3500	5800	1.66

Appendix 24. SEC Chromatogram of PS-*b*-PMMA for CP2, in the Anionic Block Copolymerization of Styrene and Methyl Methacrylate in the Presence of $Al(^iBu)_3$

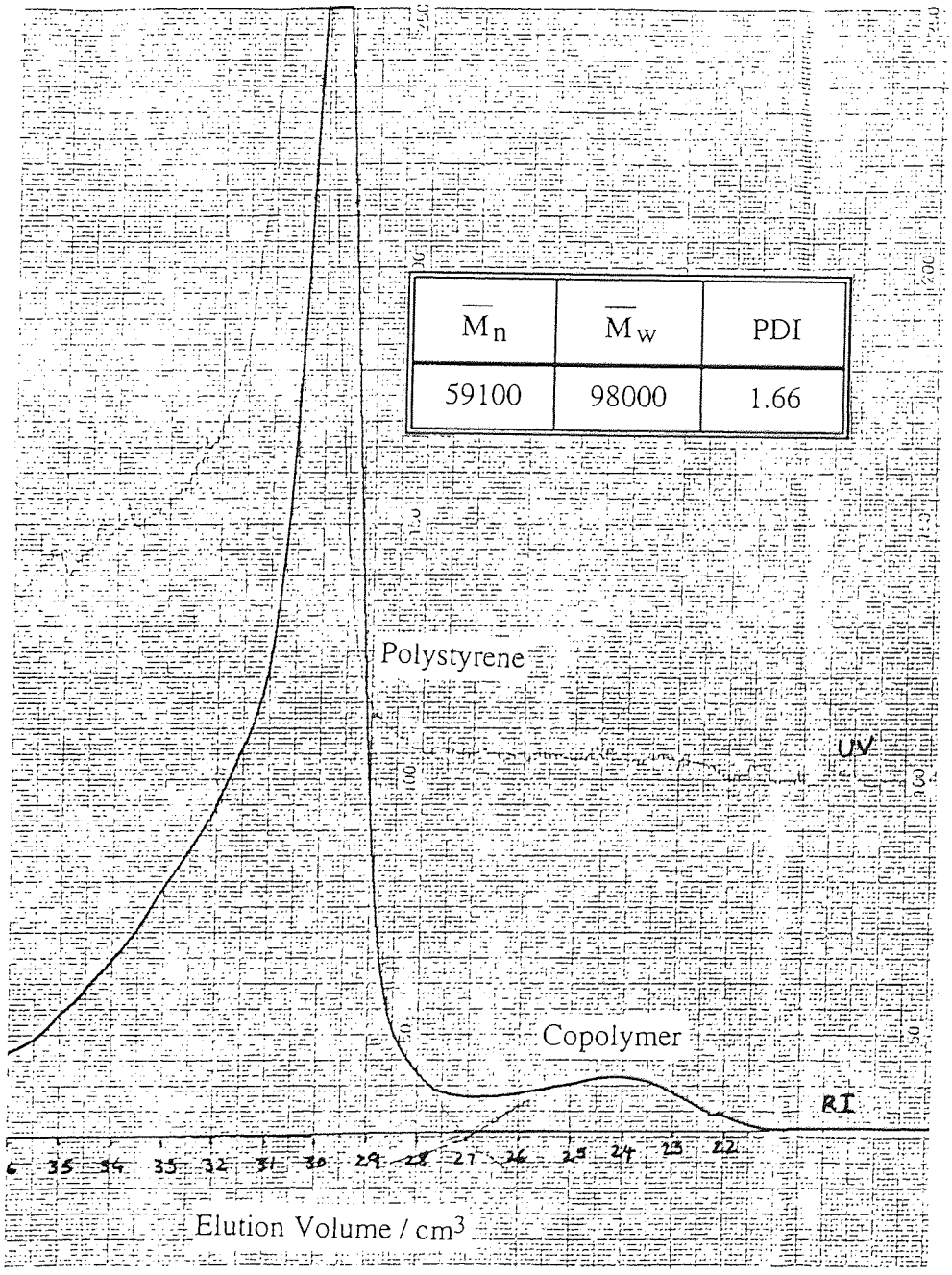

Appendix 25. ^{1}H NMR Spectrum of PS-*b*-PMMA for CP4, in the Anionic Block Copolymerization of Styrene and Methyl Methacrylate in the Presence of Al(^{i}Bu)$_3$

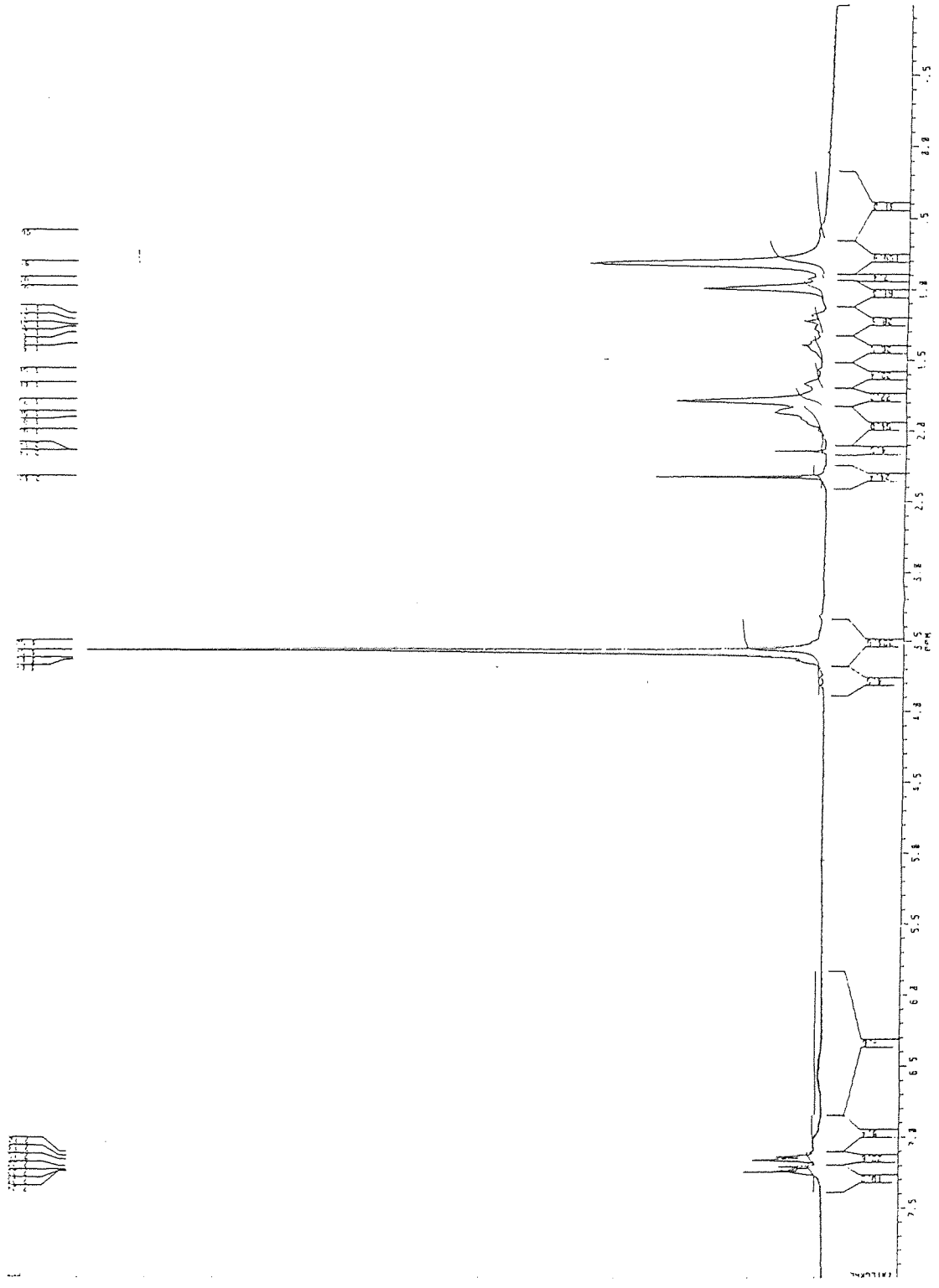

Appendix 26. ^{1}H NMR Spectrum of PS-*b*-PMMA for CP2, in the Anionic Block Copolymerization of Styrene and Methyl Methacrylate in the Presence of Al(^{i}Bu)$_3$

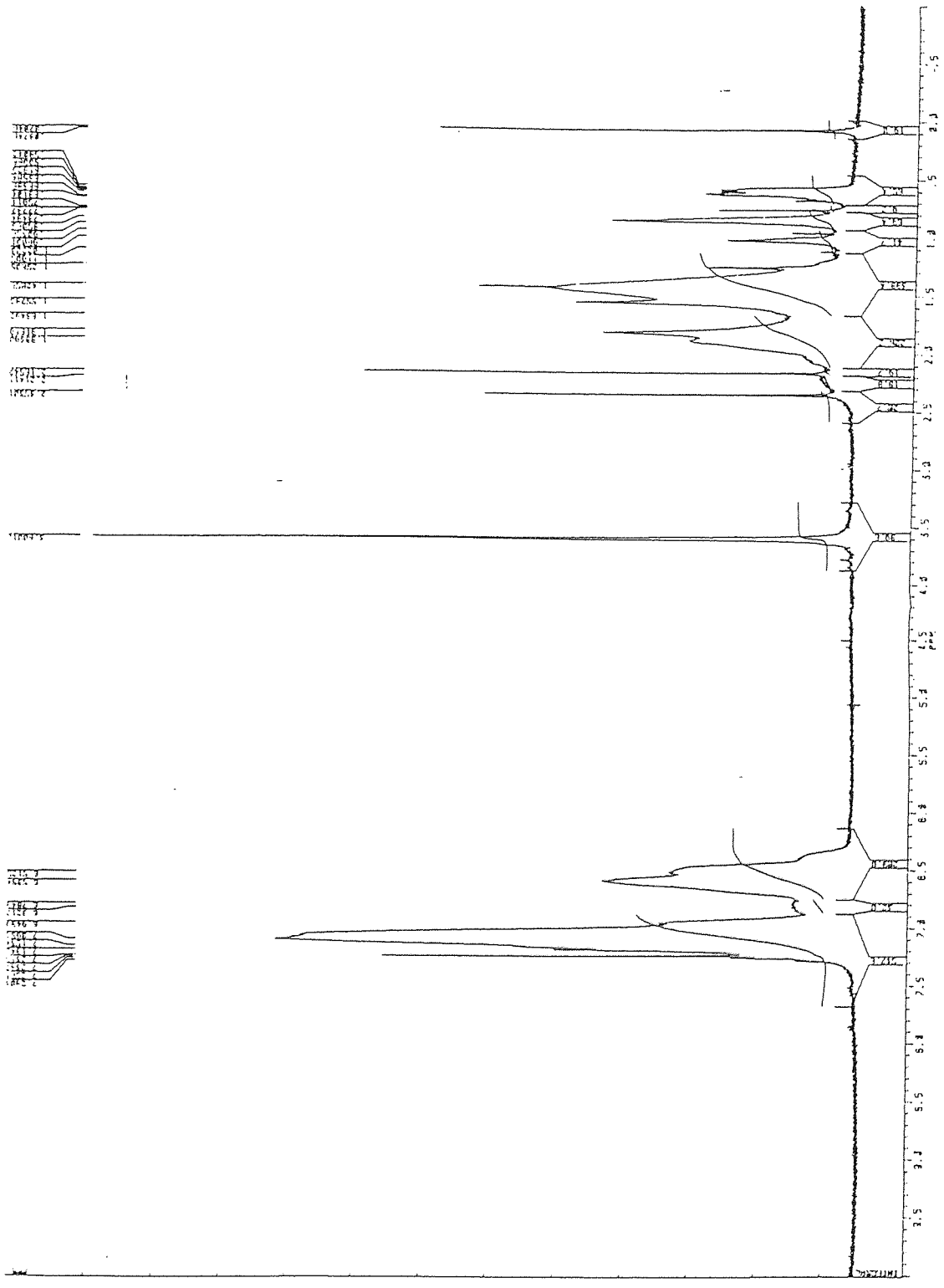

Appendix 27. ^{1}H NMR Spectrum of Poly(styrene) Obtained From CP2, in the Anionic Block Copolymerization of Styrene and Methyl Methacrylate in the Presence of $Al(^{i}Bu)_3$

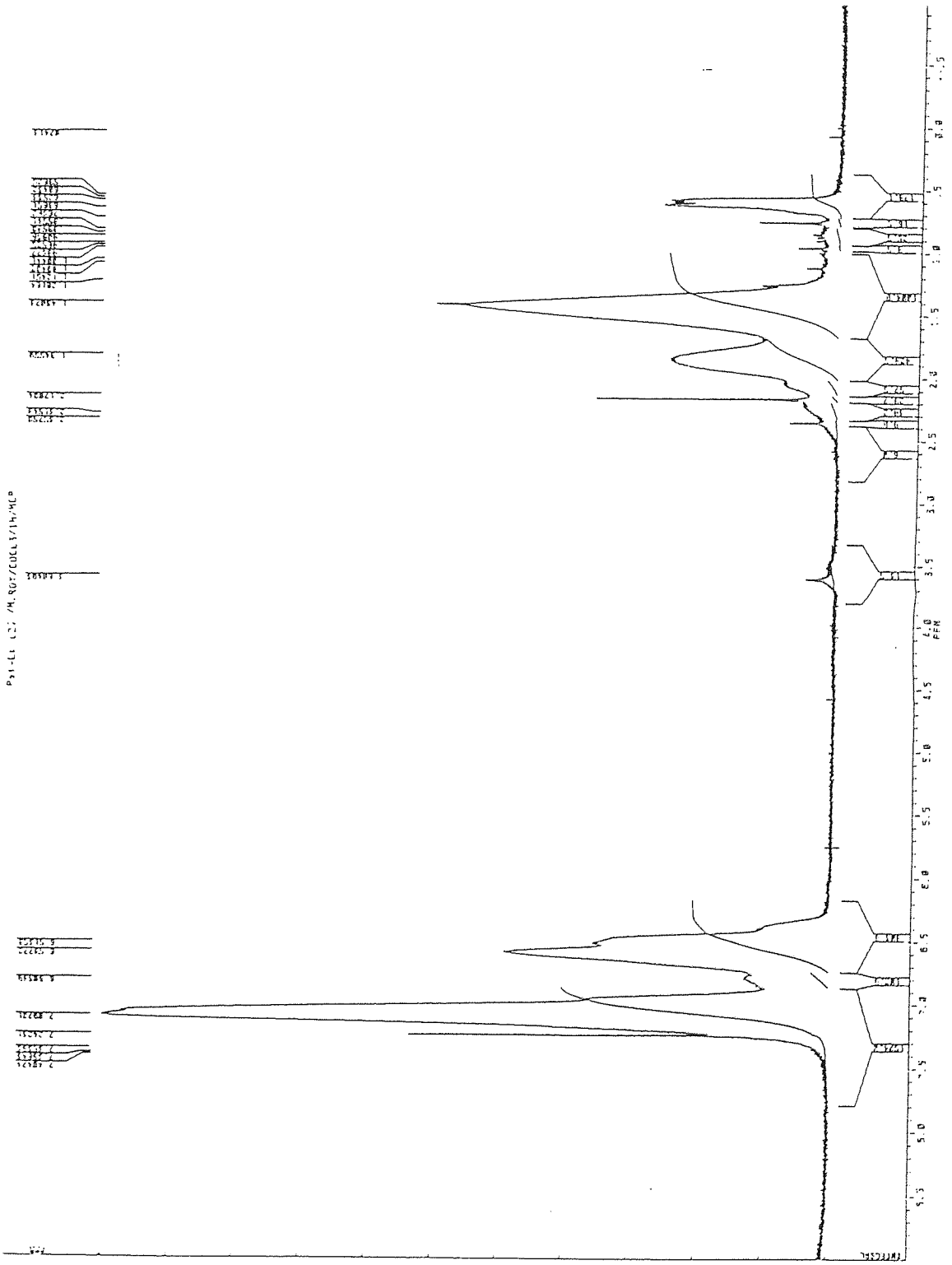

Appendix 28. ^{13}C NMR Spectrum of PS-*b*-PMMA for CP4, in the Anionic Block Copolymerization of Styrene and Methyl Methacrylate in the Presence of Al(^{i}Bu)$_3$